

**UNIVERSIDADE DE SÃO PAULO
INSTITUTO DE QUÍMICA**

Programa de Pós-Graduação em Ciências Biológicas (Bioquímica)

TALITA GLASER

Modulação da diferenciação neural de células tronco embrionárias por transientes de cálcio intracelulares: papéis dos receptores purinérgicos e de canais de cálcio voltagem-dependentes

Versão original da Tese corrigida

São Paulo

Data do depósito na SPG:

13/10/2015

TALITA GLASER

**Modulação da diferenciação neural de células tronco
embrionárias por transientes de cálcio
intracelulares: papéis dos receptores purinérgicos e
de canais de cálcio voltagem-dependentes**

*Tese apresentada ao Instituto de Química da
Universidade de São Paulo para obtenção do Título de
Doutor em Ciências (Bioquímica)*

Orientador: Prof. Dr. Alexander Henning Ulrich

São Paulo
2015

Ficha Catalográfica

Elaborada pela Divisão de Biblioteca e
Documentação do Conjunto das Químicas da USP.

Glaser, Talita

G548m Modulação da diferenciação neural de células tronco embrionárias por transientes de cálcio intracelulares: papéis dos receptores purinérgicos e de canais de cálcio voltagem-dependentes / Talita Glaser. -- São Paulo, 2015.

130p.

Tese (doutorado) - Instituto de Química da Universidade de São Paulo. Departamento de Bioquímica
Orientador: Ulrich, Alexander Henning

1. Diferenciação celular : Fisiologia I. T. II. Ulrich, Alexander Henning, orientador.

574.87612 CDD



UNIVERSIDADE DE SÃO PAULO
INSTITUTO DE QUÍMICA

“Modulação da diferenciação neural de células tronco embrionárias por transientes de cálcio intracelulares: papéis dos receptores purinérgicos e de canais de cálcio voltagem-dependentes”

TALITA GLASER

Tese de Doutorado submetida ao Instituto de Química da Universidade de São Paulo como parte dos requisitos necessários à obtenção do grau de Doutora em Ciências no Programa de Ciências Biológicas (Bioquímica) - Área de Concentração: Bioquímica.

Aprovado (a) por:

Prof. Dr. Alexander Henning Ulrich
(Orientador e Presidente)

Profa. Dra. Bettina Malnic
IQ - USP

Prof. Dr. Eduardo Moraes Rego Reis
IQ - USP

Profa. Dra. Chao Yun Irene Yan
ICB - USP

Prof. Dr. Antonio Carlos Cassola
ICB - USP

SÃO PAULO
24 de novembro de 2015

Dedicatórias

Eu dedico essa tese ao meu marido Leonardo e à minha família, que tanto me apoiou nesses anos, dando-me forças para que mesmo nos momentos de desânimo eu tivesse fôlego para completar essa tarefa.

AGRADECIMENTOS

Aos meus familiares, especialmente meus pais Susi e Bernardo que sempre me incentivaram a estudar e escolher como profissão o que me alegra. A determinação e foco que posso são apenas reflexos da educação dada por vocês. Obrigada!

Ao Prof. Dr. Alexander Henning Ulrich, orientador e amigo, pelo apoio dado em momentos tão complicados da vida acadêmica e pela confiança e incentivos confiado a mim, proporcionando amadurecimento científico. Obrigada!

Ao Leonardo Koji Ito, pelo apoio e incentivo nos momentos mais difíceis, ajudando-me a tomar decisões e confortando-me até do outro lado do mundo. Graças a você tudo se tornou mais fácil e leve.

À Dra. Hiromi Shimojo, por ter me ensinado tantas técnicas e pesquisa de altíssima qualidade. Além disso, mostrou-me que a amizade transcende as barreiras da língua, da cultura e da distância. Muito obrigada!

Agradeço a todos os amigos do Laboratório de Neurociências da IQ-USP, em especial a Cláudia, Maynara, Ana Paula, Ágatha, Denise, Laura, Juliana e Zilda. O dia-a-dia do laboratório se tornou mais estimulante e agradável com vocês.

Agradeço aos amigos japoneses e brasileiros que me ajudaram tanto a viver no Japão e a superar o choque cultural. Muito obrigada!

Aos amigos, Gustavo Battesini, Edson Takeshi e Mariana Longhi, pelos estudos e discussões durante as disciplinas da Pós-Graduação. Sem vocês as aulas e estudos seriam chatos.

Às alunas de Iniciação Científica, Patrícia Martins, Renata Beco, Suzan Miranda e Ana Regina Castillo, pela confiança na minha orientação e por acreditarem nas minhas idéias. Assim como vocês, eu aprendi muito nesse período adquirindo experiências enriquecedoras e que me conferiram maior maturidade acadêmica.

Ao Instituto de Química da USP, pelo suporte, em especial aos Docentes por cederem equipamentos, reagentes ou tempo.

Ao Prof. Dr. Ryoichiro Kageyama, pela oportunidade de desenvolver parte deste trabalho em seu laboratório (Universidade de Quioto, Japão).

Aos Dr. Arthur e Dra. Isis pela amizade e na adaptação ao novo ambiente de trabalho.

À FAPESP e CNPQ pelo auxílio financeiro.

A todos que de alguma forma contribuíram para a realização deste trabalho.

“Um cientista em seu laboratório não é um mero técnico: é também uma criança que confronta os fenômenos naturais que o impressionam como faziam os contos de fada.”

Marie Curie

“Seu trabalho vai ocupar uma grande parte da sua vida. A única maneira de estar verdadeiramente satisfeito é fazendo aquilo que você acredita ser um ótimo trabalho. E o único jeito de fazer um ótimo trabalho é fazendo algo que você ama. ”

Steve Jobs

RESUMO

Glaser, T. Modulação da diferenciação neural de células tronco embrionárias por transientes de cálcio intracelulares: papéis dos receptores purinérgicos e de canais de cálcio voltagem-dependentes. 2015. 130p. Tese de Doutorado – Programa de Pós-Graduação em Ciências Biológicas (Bioquímica). Instituto de Química, Universidade de São Paulo, São Paulo.

Receptores purinérgicos e canais de cálcio voltagem-dependentes estão envolvidos em diversos processos biológicos como na gastrulação, durante o desenvolvimento embrionário, e na diferenciação neural. Quando ativados, canais de cálcio voltagem-dependentes e receptores purinérgicos do tipo P2, ativados por nucleotídeos, desencadeiam transientes de cálcio intracelulares controlando diversos processos biológicos. Neste trabalho, nós estudamos a participação de canais de cálcio voltagem-dependentes e receptores do tipo P2 na geração de transientes de cálcio espontâneos e sua regulação na expressão de fatores de transcrição relacionados com a neurogênese utilizando como modelo células tronco (CTE) induzidas à diferenciação em células tronco neurais (NSC) com ácido retinóico.

Descrevemos que CTE indiferenciadas podem ter a proliferação acelerada pela ativação de receptores P2X7, enquanto que a expressão e a atividade desse receptor precisam ser inibidas para o progresso da diferenciação em neuroblasto. Além disso, ao longo da diferenciação neural, por análise em tempo real dos níveis de cálcio intracelular livre identificamos 3 padrões de oscilações espontâneas de cálcio (onda, pico e unique), e mostramos que ondas e picos tiveram a frequência e amplitude aumentadas conforme o andamento da diferenciação. Células tratadas com o inibidor do receptor de inositol 1,4,5-trifosfato (IP3R), Xestospongin C, apresentaram picos mas não ondas, indicando que ondas dependem exclusivamente de cálcio oriundo do retículo endoplasmático pela ativação de IP3R.

NSC de telencéfalo de embrião de camundongos transgênicos ou pré-diferenciadas de CTE tratadas com Bz-ATP, o agonista do receptor P2X7, e com 2SUTP, agonista de P2Y2 e P2Y4, aumentaram a frequência e a amplitude das oscilações espontâneas de cálcio do tipo pico. Dados, obtidos por microscopia de luminescência, da expressão em tempo real de gene repórter luciferase fusionado à Mash1 e Ngn2 revelou que a ativação dos receptores P2Y2/P2Y4 aumentou a expressão estável de Mash1 enquanto que ativação do receptor P2X7 levou ao aumento de Ngn2. Além disso, células na presença do quelante de cálcio extracelular (EGTA) ou do depletor dos estoques intracelulares de cálcio do retículo endoplasmático (thapsigargin) apresentaram redução na expressão de Mash1 e Ngn2, indicando que ambos são regulados pela sinalização de cálcio.

A investigação dos canais de cálcio voltagem-dependentes demonstrou que o influxo de cálcio gerado por despolarização da membrana de NSC diferenciadas de CTE é decorrente da ativação de canais de cálcio voltagem-dependentes do tipo L. Além disso, esse influxo pode controlar o destino celular por estabilizar expressão de Mash1 e induzir a diferenciação neuronal por fosforilação e translocação do fator de transcrição CREB.

Esses dados sugerem que os receptores P2X7, P2Y2, P2Y4 e canais de cálcio voltagem-dependentes do tipo L podem modular as oscilações espontâneas de cálcio durante a diferenciação neural e consequentemente alteram o padrão de expressão de Mash1 e Ngn2 favorecendo a decisão do destino celular neuronal.

Palavras-chave: fatores de transcrição, oscilações espontâneas de cálcio, sinalização do cálcio, decisão do destino celular, canais de cálcio voltagem-dependentes, receptores purinérgicos do tipo P2.

ABSTRACT

Glaser, T. Modulation of neural embryonic stem cell differentiation by intracellular Ca²⁺ oscillations. Roles of purinergic receptors and voltage gated Ca²⁺ channels. 2015. 130p. PhD Thesis – Graduate Program in Biochemistry. Instituto de Química, Universidade de São Paulo, São Paulo.

Purinergic receptors and voltage gated Ca²⁺ channels have been attributed with developmental functions including gastrulation and neural differentiation. Upon activation, nucleotide-activated P2 purinergic receptor and voltage-gated Ca²⁺ channel subtypes trigger intracellular calcium transients controlling cellular processes. Here, we studied the participation of voltage-gated calcium channels and P2 receptor activity in spontaneous calcium transients and consequent regulation expression of transcription factors related to retinoic acid-induced neurogenesis of mouse neural stem and embryonic stem cells (ESC).

In embryonic pluripotent stem cells, proliferation is accelerated by P2X7 receptor activation, while receptor expression / activity needs to be down-regulated for the progress of neuroblast differentiation. Moreover, along neural differentiation time lapse imaging with means of a cytosolic calcium-sensitive fluorescent probe provided different patterns of spontaneous calcium transients (waves and spikes) showing that both, frequency and amplitude increased along differentiation. Cells treated with the inositol 1,4,5-trisphosphate receptor (IP3R) inhibitor Xestospongin C showed spikes but not waves, indicating that waves exclusively depended on calcium release from endoplasmic reticulum by IP3R activation. Cells treated with the P2X7 receptor subtype agonist Bz-ATP and the P2Y2 and P2Y4 receptor 2-S-UTP increased frequency and amplitudes of calcium transients, mainly spikes, in embryonic telencephalon neural stem cells (NSC) and NSC pre-differentiated from ESC. Data obtained by luminescence time lapse imaging of stable transfected cells with Mash1

or Ngn2 promoter-protein fusion to luciferase reporter construct revealed increased Mash1 expression due to activation of P2Y2/P2Y4 receptor subtypes, while increased expression of Ngn2 was observed following P2X7 receptor activation. In addition, cells imaged in presence of the extracellular calcium chelator EGTA or following endoplasmic reticulum calcium store depletion by thapsigargin showed a decrease in Mash1 and Ngn2 expression, indicating that both are regulated by calcium signaling.

Investigation of the roles of voltage gated Ca^{2+} channels in neural differentiation showed that Ca^{2+} influx in NSC pre-differentiated from ESC is due to membrane depolarization and L-type voltage gated Ca^{2+} channel activation, thereby controlling cell fate decision, by stabilizing the expression of MASH1 and inducing differentiation, by phosphorylation of the transcription factor CREB. Altogether these data suggest that P2X7, P2Y2, P2Y4 receptors and L-type voltage gated Ca^{2+} channels can modulate spontaneous calcium oscillations during neural differentiation and consequently change the Mash1 and Ngn2 expression patterns, thus favoring the cell fate decision to the neuronal phenotype.

Keywords: transcription factors, spontaneous Ca^{2+} oscillations, Ca^{2+} signaling, cell fate decision, L-type voltage gated calcium channels, P2 purinergic receptors.

LISTA DE ABREVIATURAS E SIGLAS

Ca²⁺- cálcio

[Ca²⁺]i - concentração de cálcio intracelular livre

Δ[Ca²⁺]i - transientes da concentração de cálcio intracelular livre

ADP- adenosina difosfato

AR ácido retinóico

ATP- Adenosina 5'-trifosfato

bFGF, fibroblast growth basic; fator de crescimento de fibroblasto básico

bHLH (basic helix-loop-helix)

BrdU - 5-bromo-2-deoxiuridina

BSA - bovine serum albumine; albumina de soro bovino

Bz-ATP - 3'-O-(4-benzoil)benzoiladenosine 5'-trifosfato

cADPR- ADPribose cíclico

CaM - calmodulina

CaMKII - Ca²⁺/calmodulin-dependent protein kinase

Cav1 - VGCC do tipo L

Cav 2.1 - VGCC do tipo P/Q

Cav 2.2 - VGCC do tipo N

Cav 3- VGCC do tipo T

CBP - CREB-binding protein

cDNA - DNA complementar

CNS - central nervous system; sistema nervoso central

CREB - cAMP response element-binding; elemento ligante responsivo ao cAMP

EB- corpos embriôides de células tronco embrionárias (CTE)

DAG - 1,2-diacilglicerol

DMEM - Dulbecco's modified Eagle's medium; meio de Eagle Dulbecco-modificado

DNA - deoxyribonucleicacid, ácido deoxirribonucleico

EB - Embryoid bodies, corpos embriôides

EGTA - etilenogilcol-bis-(beta-amino-etil éter) N,N,N',N'-ácido tetraacético, etilenoglicol-bis-(beta-amino-etil éter)

FBS - fetal bovine serum, soro fetal bovino

Fluo 3-AM - 4-éster de (6-Acetoximetoxi-2,7-dicloro-3-oxo-9-xantenil)-4'metil-2,2' (etilenedioxi)dianilina-N,N,N',N'-ácido tetraacéticoquaiis (acetoximetil)

Fmax - fluorescência máxima

Fmin - fluorescência mínima

HEPES, N-(2-hydroxyethyl)-piperazine-N'-2-ethanesulfonic acid;

hMSC - células tronco mesequimais de medula óssea

heterogeneous nuclear ribonucleoprotein K - hnRNP K

IP3 - inositol-1,4,5- trifosfato

IP3R - receptor de inositol-1,4,5- trifosfato

IPTG - isopropil-β-D-thiogalactopyranoside

IRBIT - proteína ligante do IP3R liberada com IP3

Kd - constante de dissociação

LB-ágar - meio Luria-Bertani ágar

LIF - fator inibitório da leucemia

MAPK - Mitogen-activated protein kinases

NAADP - nicotinic acid adenine dinucleotide phosphate

NCX - permease presente na membrana plasmática Na+/Ca²⁺

NFAT - Nuclear factor of activated T-cells

NF-κB - fator nuclear kappa B

Ngn 1 - neurogenina 1

Ngn 2 - neurogenina 2

NSC - células tronco neurais

p300 - E1A binding protein p300

PCAF - P300/CBP-associated factor

pCREB - CREB fosforilada

PFA Paraformaldeído

PIP2 - fosfatidilinositol 4,5-bisfosfato

PLC-β fosfolipase c b

PKC - proteína quinase C

PMCA - bomba de Ca²⁺ da membrana plasmática

RE/RS - retículo endoplasmático ou sarcoplasmático

ROCs - canais iônicos dependentes de ligantes

ROS - espécies reativas de oxigênio

RYR - receptor de rianodina

SERCA - a Ca²⁺-ATPase do retículo endoplasmático ou sarcoplasmático

Shh - Sonic Hedgehog

SOCE - influxo de cálcio controlado pelo estoque intracelular

SSEA-1 - stage-specific embryonic antigen-1

UDP - uridina difosfato

UTP - uridina trifosfato

VGCC - canais de Ca²⁺ dependentes de voltagem

XeC - Xestospongin C

SUMÁRIO

1. INTRODUÇÃO.....	19
1.1. Bases teóricas.....	20
1.1.1. A homeostase do cálcio.....	20
1.1.2. Receptores Purinérgicos.....	26
1.1.3. Células tronco embrionárias e o desenvolvimento.....	31
1.1.4. Expressão gênica modulada por $\Delta[Ca^{2+}]_i$ na diferenciação neural.....	34
2. OBJETIVOS.....	38
2.1 Objetivo geral.....	39
2.2 Objetivos específicos.....	39
3. MATERIAIS E MÉTODOS	41
3.1. Cultivo e diferenciação de CTE E14-Tg2a.....	41
3.2. Medidas das $\Delta[Ca^{2+}]_i$ por microscopia	43
3.3. Medidas das $\Delta[Ca^{2+}]_i$ por microfluorimetria.....	46
3.4. Curva de crescimento celular.....	47
3.5. Extração de RNA total e síntese de cDNA.....	47
3.6. PCR em tempo real.....	48
3.7. RT-PCR.....	48
3.8. Ensaio de Western Blotting.....	51
3.9. Imunocitoquímica e microscopia de fluorescência.....	52
3.10. Microscopia eletrônica de varredura.....	53

3.11. Ensaio de incorporação de BrdU.....	53
3.12. Proliferação celular por Ki67.....	54
3.13. Análise de citometria de fluxo.....	54
3.14. Medidas nas variações no potencial de membrana celular por microfluorimetria.....	55
3.15. Estabelecimento de linhagens celulares para verificação de alterações da expressão do gene repórter bioluminescente em tempo real.....	56
3.15.1. Mash1-Luc NSC.....	56
3.15.2. Ngn2-Luc E14Tg2a.....	57
3.16. Verificação de alterações na expressão em tempo real do gene repórter bioluminescente.....	61
3.17. Detecção indireta da concentração de ATP extracelular por bioluminescência.....	62
3.18. Análise estatística.....	63
4. RESULTADOS E DISCUSSÃO.....	64
4.1. Diferenciação neural.....	65
4.1.1. Estabelecimento e caracterização do protocolo de diferenciação neural.....	65
4.1.2. Conclusão da diferenciação neural.....	74
4.2. Eventos espontâneos na $\Delta[\text{Ca}^{2+}]_i$	74
4.2.1. Caracterização dos eventos espontâneos na $\Delta[\text{Ca}^{2+}]_i$	74
4.2.2. Conclusão parcial.....	80
4.3. Canais para Ca^{2+} voltagem-dependentes.....	80

4.3.1. Canais para Ca ²⁺ voltagem-dependentes no controle das Δ[Ca ²⁺] _i espontâneas e da diferenciação neural.....	80
4.3.2. Conclusão sobre a participação de canais de Ca ²⁺ voltagem-dependentes na indução da diferenciação neuronal.....	92
4.4. Receptores purinérgicos.....	92
4.4.1. Caracterização do sistema purinérgico na diferenciação neural.....	92
4.4.2. Papéis do receptor P2X7 em CTE.....	95
4.4.3. Envolvimento dos receptores purinérgicos nas Δ[Ca ²⁺] _i espontâneas e na expressão de fatores de transcrição pró-neurais.....	104
4.4.4. Conclusão parcial sobre receptores puinérgicos.....	108
4.5. Δ[Ca ²⁺] _i espontâneas regulando o destino neural.....	108
4.5.1 Convergência entre os sinais gerados por receptores purinérgicos e VGCC.....	108
4.5.2. Conclusão parcial.....	111
5. CONCLUSÕES FINAIS	112
6. REFERÊNCIAS.....	116
7.LISTA DE ANEXOS.....	130
7.1. SÚMULA CURRICULAR	
7.2. ARTIGO 1	
7.3 ARTIGO 2	
7.4 ARTIGO 3	
7.5. ARTIGO 4	
7.6. ARTIGO 5	
7.7. ARTIGO 6	

INTRODUÇÃO

1. INTRODUÇÃO

1.1 BASES TEÓRICAS

1.1.1 A homeostase do cálcio

Altas concentrações de cálcio (Ca^{2+}) dentro das células podem acarretar à formação de sais pouco solúveis em reações metabólicas que produzem fosfato inorgânico, portanto, evolutivamente houve a necessidade da existência de sistemas transportadores desse íon para o meio extracelular (Xia et al. 1998), que consequentemente levou à formação de um gradiente eletroquímico com concentrações na escala de 10^{-3}M (extracelular) vs 10^{-8} - 10^{-7} M (citosólico). Esse gradiente é aproveitado como um sistema de sinalização pela célula sendo que o Ca^{2+} participa de várias funções importantes nos organismos vivos, tais como: contrações musculares, secreção hormonal, locomoção celular, transmissão neuronal, fertilização, expressão gênica para apoptose, dentre outros papéis (Carafoli et al. 2001). A participação do Ca^{2+} nas cascadas de sinalização intracelulares é uma das mais importantes participações desse íon, pois é o mensageiro biológico mais ubíquo que se conhece. Mudanças rápidas na concentração intracelular de Ca^{2+} , os chamados transientes da concentração de cálcio intracelular livre ($\Delta[\text{Ca}^{2+}]_i$), são suficientes para desencadear várias respostas (Berridge et al. 2003; Cheng & Lederer 2008).

A $[\text{Ca}^{2+}]_i$ é mantida em níveis bem baixos, cerca de 10 - 100nM, por mecanismos homeostáticos (Figura 1) que incluem: o trocador presente na membrana plasmática $\text{Na}^+/\text{Ca}^{2+}$ (NCX) (Sharma & O'Halloran 2014), que troca Ca^{2+} intracelular por Na^+ extracelular; a bomba de Ca^{2+} da membrana plasmática (PMCA) (Brini et al. 2013) para a extrusão do Ca^{2+} ; a Ca^{2+} -ATPase do retículo endoplasmático ou

sarcoplasmático (RE/RS) (SERCA) (Carafoli & Brini 2000); e por uma série de moléculas tamponantes de Ca^{2+} que diferem em suas propriedades cinéticas de se ligar ao Ca^{2+} (Marenholz et al. 2004), pois a manutenção de altos níveis de $[\text{Ca}^{2+}]_i$ é tóxico. Na mitocôndria, pode haver captação de Ca^{2+} pelo canal uniporte mitocondrial (Collins et al. 2001), já no complexo de Golgi a recaptação do Ca^{2+} é mediada pelo transportador Ca^{2+} -ATPase do tipo P.

O cálcio que origina os transientes de $[\text{Ca}^{2+}]_i$ pode ser de origem extracelular, que é mediada por canais para Ca^{2+} , que podem sofrer diferentes modulações na abertura que incluem: voltagem, ligantes, força mecânica, mudança de temperatura, pH, espécies reativas de oxigênio (ROS), ou o próprio estoque intracelular de Ca^{2+} (SOCE), também conhecido como entrada de Ca^{2+} operada por estoque (Feske et al. 2006; Hardingham et al. 2001; Ong et al. 2014; Parekh 2003).

Compartimentos membranares intracelulares também podem originar os transientes de $[\text{Ca}^{2+}]_i$, por liberação de cálcio principalmente do RE/RS, que é mediado por duas famílias de canais, o receptor de rianodina (RYR) e o receptor de inositol-1,4,5-trifosfato (IP3R) (Fill & Copello 2002; Franzini-Armstrong & Protasi 1997; Meissner 1994), mas que podem ser ativados por uma variedade de mensageiros como: o IP3, ADPribose cíclico (cADPR), nicotinic acid adenine dinucleotide phosphate (NAADP) e outros (Berridge et al. 2003).

Em resposta a ativação de receptores na superfície membranar, o IP3 é gerado por estimulação de fosfolipase C β (PLC- β), que hidrolisa o fosfolipídeo de membrana fosfatidilinositol 4,5-bisfosfato (PIP2) gerando IP3 e diacilglicerol (DAG). Então, IP3 pode levar à liberação de Ca^{2+} do RE após a ligação com o receptor de IP3 (Furuichi et al. 1989; Streb et al. 1983; Maeda et al. 1990).

Em mamíferos, existem 3 genes que codificam para IP3R, o qual fica ancorado na membrana do RE por 6 domínios transmembrânicos formando homo- ou hetero tetrâmeros de 1.2 MDa. O IP3R também funciona como uma proteína andaime, pois interage com diversas proteínas como: proteína ligante do IP3R liberada com IP3 (IRBIT), calmodulina (CaM), proteína ligante de FK506 (FKBP12) dentre outras que podem modular a função de IP3R (Ando et al. 2003). A função de IP3R também pode ser modulada por fosforilação/defosforilação por quinases e fosfatases (Vanderheyden et al. 2009).

Alguns estudos estruturais revelaram um domínio de ligação ao IP3, e um domínio supressor na região N-terminal do IP3R (Bosanac et al. 2002) que possuem papel importante no acoplamento entre a interação do ligante e a abertura do canal.

Mesmo que o IP3R seja largamente expresso, e que as isoformas compartilhem de 60-80% de homologia, a sua diversidade e distribuição celular é significante. O IP3R tipo 1 é expresso principalmente nas células cerebelares de Purkinje, o tipo 2 em cardiomiócitos, e o tipo3 em células secretórias de insulina (Krebs et al. 2015).

Diversos trabalhos detalharam a destacada complexidade funcional e estrutural do IP3R, a diversidade na regulação, abertura, distribuição em tecidos e no desenvolvimento (Mikoshiba 2007; Foskett et al. 2007). Além disso, já foi descrito que doenças cardíacas e neurais estão correlacionadas com disfunção de IP3R (Berridge 2012), como Alzheimer, transtorno bipolar e Huntington (Berridge 2013).

Apesar de o influxo de Ca^{2+} pela membrana plasmática ser o sinal primário por vários estímulos extracelulares, os sinais de Ca^{2+} podem ser amplificados por liberações subsequentes de Ca^{2+} de estoques internos, chamado de liberação de Ca^{2+} induzida por Ca^{2+} (Kostyuk & Verkhratsky 1994), que normalmente é associado com a atividade dos RYR. Essa sensibilidade por aumento da $[\text{Ca}^{2+}]_i$ desses dois

receptores pode ser influenciada por vários fatores, incluindo outros mensageiros (ex. inositol trifosfato e difosfato de adenosina cíclica- ribose) ou pelo grau de armazenamento de carga elétrica.

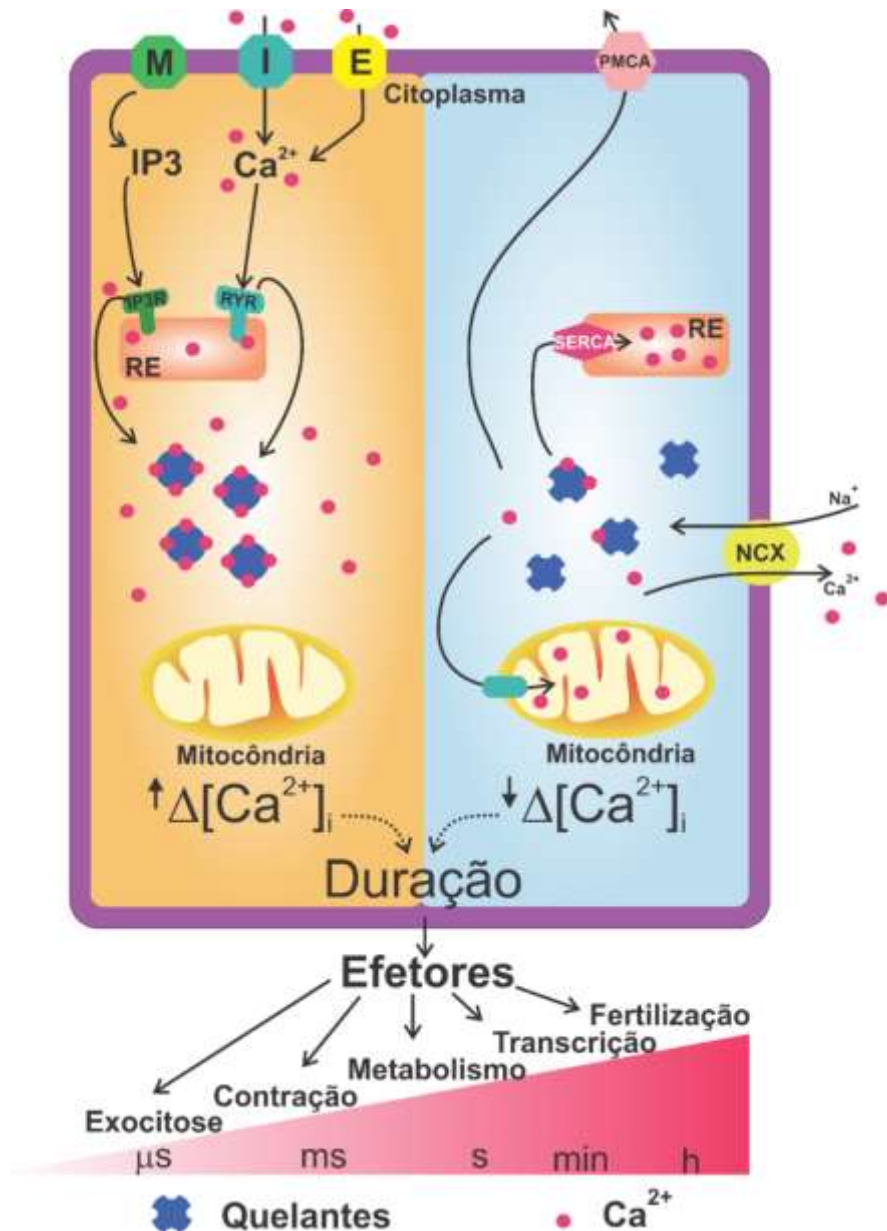


Figura 1: Dinâmica e homeostase da sinalização por cálcio. Durante as reações de entrada de cálcio há formação de mensageiros secundários, que liberam o cálcio presente no retículo endoplasmático (RE), que então liga-se aos efetores para ativação de vários processos celulares. Nas reações do re-sequestro de cálcio, este não mais está ligado aos efetores e é removido do citoplasma por translocadores e bombas (NCX, PMCA, SERCA). IP3R, receptor de inositol-1,4,5-trifosfato; RYR, receptor de rianodina. Receptor metabotrópico (M), canal iônico (I), canal iônico controlado por estoques de Ca^{2+} intracelulares (E), proteínas quelantes de Ca^{2+} (quelantes). Modificado de (Berridge et al. 2003).

O cálcio opera como um importante regulador numa grande variedade de processos neuronais. Neurônios usam ambos os estoques extra- e intracelulares de cálcio, sendo que este último é muito desenvolvido em neurônios, evidenciado pela diferente e especializada estruturação do RE nesse tipo celular, que possui especializações regionais para a sinalização por Ca^{2+} participando na formação de ondas globais ou locais de cálcio que desencadeiam respostas diferentes na célula (McGraw et al. 1980; Westrum & Gray 1986). O RE de neurônios é tão desenvolvido que se estende por toda a célula, inicia-se no corpo celular do neurônio e alcança até os dendritos e os axônios, chegando a ficar bem próximo da membrana plasmática (Stutzmann & Mattson 2011).

Íons Ca^{2+} difundem-se muito lentamente pelo citoplasma dos neurônios, pois há abundância de proteínas citoplasmáticas ligantes de Ca^{2+} , gerando um coeficiente de difusão de $10\mu\text{m}^2\text{s}^{-1}$. Portanto, ondas globais ocorrem por liberação substancial de estoques intracelulares, enquanto que as locais são geradas por liberação limitada de estoques intracelulares e de canais da membrana plasmática (Sala & Hernandez-Cruz 1990).

Em neurônios, o RE possui IP3R e RYR, que podem variar na proporção de suas concentrações de acordo com a região do cérebro em que estão presentes. Como por exemplo, nas espinhas dendríticas (extensões dendríticas especializadas que aumentam a área disponível nos neurônios para contato sinápticos) dos neurônios de Purkinje que contém IP3Rs mas não apresentam RYRs (Walton et al. 1991). O arranjo oposto é observado em espinhas dendríticas de células da região CA1 do hipocampo onde os RYRs estão presentes numa concentração maior do que IP3Rs (Sharp et al. 1993).

A dinâmica de produção de IP₃ pode diferir muito de acordo com o tipo de receptor, existem evidências de que os receptores metabotrópicos para Glutamato 1 e 5 (mGluR1 e mGluR5), ambos receptores para glutamato, possam gerar padrões de transientes de cálcio totalmente diferentes, o primeiro produz um único transiente de cálcio enquanto que o segundo gera um padrão oscilatório (Berridge 2009).

Sabe-se que oscilações na concentração intracelular de cálcio induzem mudanças no perfil de expressão e atividade de várias proteínas (Spitzer 2002; Gomez & Spitzer 1999). Como exemplo, oscilações espontâneas na [Ca²⁺]_i modificam o perfil de expressão de neurotransmissores em neurônios espinhais embriônicos (Spitzer et al. 2004). Existem basicamente 2 tipos de Δ[Ca²⁺]_i espontâneas: ondas e picos. A primeira é mediada por IP3Re/ou RYR, relacionada com a sensibilidade às [Ca²⁺]_i. Essa Δ[Ca²⁺]_i é ativada durante o potencial de repouso e atinge [Ca²⁺]_i menor que picos. Se houver junções comunicantes conectando as células, essas ondas podem difundir para as células vizinhas, coordenando a atividade neural e processos fisiológicos de muitas células (Spitzer et al. 2000; Ulrich et al. 2012). Comparada aos picos, as ondas revelam uma frequência de disparos menor com uma duração média de 30s, assim como observado nos cones de crescimento; e são independentes de potenciais de ação. Normalmente ocorrem localmente e decaem com a distância do sitio de iniciação.

Os picos dependem de Ca²⁺ oriundo do meio extracelular, e ocorre normalmente por canais para Ca²⁺ dependentes de voltagem (VGCC), por canais iônicos dependentes de ligantes (ROCs) e por liberação de Ca²⁺ induzida por Ca²⁺ via ativação de RYR. Podem alcançar [Ca²⁺]_i de 500nM, uma duração de aproximadamente 10s e ocorrem por toda a células excitável, já que dependem de potenciais de ação (Spitzer et al. 2004).

A frequência de $\Delta[\text{Ca}^{2+}]_i$ espontâneas do tipo pico em neurônios em cultura variam de 1-10/h. Similarmente, a atividade de picos foi descrita em estágios do tubo neural in vivo (Berridge et al. 2000; Spitzer et al. 2004) e durante a diferenciação neuronal de células pluripotentes de carcinoma embrionário e em células tronco mesenquimais de medula óssea (hMSC) (Resende et al. 2009; Resende et al. 2010). Essas baixas frequências podem regular a transcrição de genes e sugerem ser essenciais para o progresso da diferenciação neural e da especificação fenotípica (Berridge et al. 2000; Lipp et al. 1997; Spitzer 2002; Tonelli et al. 2012). Em corpos embrióides de células tronco embrionárias (CTE), oscilações espontâneas de cálcio induzem a diferenciação para tecido endodérmico (Sauer et al. 1998).

Os padrões oscilatórios específicos são interpretados por efetores que ativam processos celulares, e são dependentes da frequência e da amplitude, como um sinal de rádio. Os efetores sensíveis ao Ca^{2+} são normalmente enzimas com múltiplos sítios de ligação ao Ca^{2+} que podem regular sua fosforilação total, exemplos desses efetores sensíveis à frequência são: *Nuclear factor of activated T-cells* (NFAT), fator nuclear kappa B (NF- κ B), *Ca2+/calmodulin-dependent protein kinase* (CaMKII), *Mitogen-activated protein kinases* (MAPK) e calpain (Smedler & Uhlen 2014; Pinto et al. 2015). Isso nos leva a crer que a interferência nas oscilações dos transientes de cálcio possa modificar o perfil de expressão e atividade de alguns grupos proteicos.

1.1.2 Receptores purinérgicos

O sistema purinérgico foi descrito pela primeira vez por Geoffrey Burnstock em 1970 (Burnstock et al. 1970), desde então muitos estudos foram realizados caracterizando o sistema e suas funções.

A Adenosina 5'-trifosfato (ATP) ativa receptores de membrana denominados de receptores purinérgicos, este foi o primeiro mensageiro do sistema purinérgico a ser descrito, mas não é o único, pois adenosina difosfato (ADP), uridina trifosfato (UTP), uridina difosfato (UDP) e UDP-glicose também podem modular a atividade de alguns subtipos de receptores purinérgicos (Abbracchio et al. 2006). O ATP pode ser liberado pelas células em condições fisiológicas por exocitose, por transportadores, poros ou até mesmo por lisossomos. No caso do ATP ser liberado de uma maneira descontrolada por células danificadas, este pode induzir a morte celular (Miras-Portugal et al. 2015).

O ATP no espaço extracelular é rapidamente hidrolisado por ectonucleotidas que acabam por produzir outras moléculas sinalizadoras do sistema purinérgico, como: ADP, adenosina monofosfato e adenosina (Verkhratsky et al. 2009) (Figura 2).

Com base nas propriedades farmacológicas e estruturais, os receptores purinérgicos podem ser divididos em metabotrópicos (P1 e P2Y) e ionotrópicos (P2X).

Os receptores do tipo P1 são seletivos para adenosina e são receptores de 7 passagens transmembrânicas estando acoplados a proteínas Gi, Go e Gs. Podem ainda ser subdivididos em A1 (AdoRA1), A2A (AdoRA2A), A2B (AdoRA2B) e A3 (AdoRA3), e diferem entre si pela farmacologia e funcionalidade (Di Virgilio 2012), por exemplo os receptores do tipo A1, A2A e A3 apresentam alta afinidade à adenosina, e os do tipo A2B, apresentam baixa afinidade para este agonista (Ciruela et al. 2010) (Figura 2).

Os subtipos A1 e A3 exercem papéis inibitórios na enzima adenilil ciclase e também podem promover a atividade de PLC-β e consequentemente a formação de IP3 (Verkhratsky et al. 2009). A adenosina formada a partir do catabolismo dos

nucleotídeos de adenina (ATP) parece ativar preferencialmente nos receptores A2a, enquanto que a adenosina liberada através do transportador de nucleosídeo específico parece agir preferencialmente nos receptores A1 (Cunha et al. 1996).

Já os receptores P2, podem ser ativados por ATP, ADP, UTP, UDP ou UDP-glicose, e são divididos em subclasses P2X e P2Y (Burnstock 1997). Os receptores do tipo P2X são canais para cátions ($\text{Na}^+/\text{K}^+/\text{Ca}^{2+}$) ativados por ATP (Burnstock 1997; North 1996), que se complexam na membrana plasmática nas formas homo ou heterotriméricas dependendo da combinação de subunidades, que variam de 1-7 (P2X1-P2X7). Diferentes combinações de expressão dos receptores purinérgicos, P2X1, P2X2, P2X3, P2X4, P2X2/3, P2X2/6, P2X4/6, P2X1/5 e P2X7 mostraram-se permeáveis ao Ca^{2+} (North 1996) (Figura 2). Eles são majoritariamente expressos por células excitáveis, e caso haja uma entrada abrupta de Ca^{2+} pode ocorrer durante processos patológicos, como a morte celular, neuroinflamação e toxicidade durante um surto epiléptico (Burnstock 2006; Dona et al. 2009; Glaser et al. 2013).

Os receptores P2Y são expressos pelo sistema nervoso central e autônomo, e por células não excitatórias, exercendo efeitos de longa duração como proliferação e diferenciação (Verkhratsky et al. 2009). O tipo P2Y é o mais heterogêneo na possibilidade de ligantes, pois pode ser ativado por ATP, ADP, UTP, UDP ou UDP-glicose e são divididos em P2Y_{1,2,4,6,11,12,13,14} baseados na similaridade filogenética (Verkhratsky et al. 2009)(Figura 2). Os subtipos P2Y_{1,2,4,6,11} são acoplados a proteínas Gq/G11 que levam a ativação de PLC-β, que acaba por induzir a liberação de Ca^{2+} por IP3 no RE (Verkhratsky et al. 2009; Burnstock 1997; Dubyak & el-Moatassim 1993). P2Y_{12,13,14} inibem a adenilil ciclase via Gi/o e também podem alterar $[\text{Ca}^{2+}]_i$. Esses receptores são expressos na maioria dos tipos celulares e os

primeiros receptores de neurotransmissores a serem presente durante o desenvolvimento (Burnstock & Ulrich 2011).

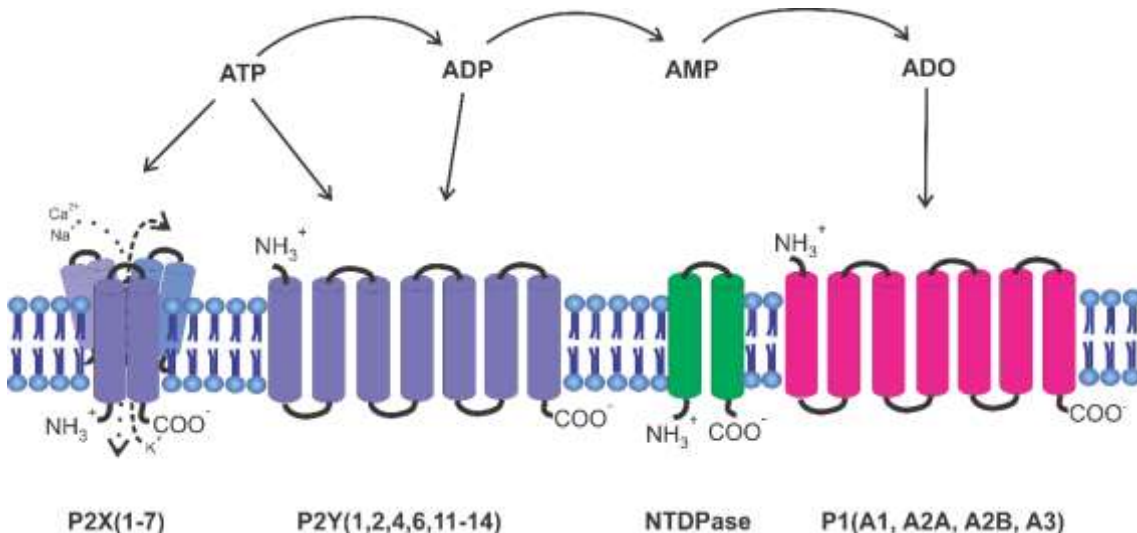


Figura 2. Sistema purinérgico. ATP é secretado pelas células e pode se ligar aos receptores P2 (P2X e P2Y) ou ser convertido em ADP, que pode se ligar a P2Y1, P2Y12 e P2Y13 ou ser convertido em AMP e adenosina (ADO), esta pode se ligar aos receptores P1. As sucessivas conversões de ATP até o estado de ADO são catalisadas por ectoenzimas, chamadas ectonucleotidases (NTPDase). Modificado de (Burnstock 2006).

Na literatura existem trabalhos demonstrando que a ativação dos receptores purinérgicos induzem $\Delta[\text{Ca}^{2+}]_i$ em processos do desenvolvimento embrionário (Mironov 1994; Salter & Hicks 1995), e que também possuem papel na diferenciação neuronal (Resende et al. 2007; Resende et al. 2010). Os receptores P2X2 e P2X6 são mais expressos conforme ocorre a neurogênese no telencéfalo de ratos (Schwindt et al. 2010), assim como a atividade de P2X já foi descrita como indutor da proliferação de progenitores do hipocampo (Shukla et al. 2005). O receptor P2X7, apesar de participar no processo de formação de poro e morte celular, também é amplamente expresso nas estruturas sinápticas, indicando um possível papel na plasticidade neuronal (Burnstock 2007).

O receptor P2X2 em condições de silenciamento com RNA de interferência ao longo da diferenciação neural de células P19 de carcinoma embrionário resultou numa redução da neurogênese, enquanto que o silenciamento de P2X7 inibiu a proliferação e a gliogênese. Em nosso laboratório, no mesmo modelo de estudo, já foi descrito que a forma truncada da subunidade P2X6 é mais expressa nas células indiferenciadas (da Silva et al. 2007) sugerindo um mecanismo de splicing alternativo para regular a expressão de P2X6.

O papel do receptor P2Y1 talvez seja o melhor descrito na indução de $\Delta[\text{Ca}^{2+}]_i$, que se propaga em forma de onda por várias células vizinhas por junções comunicantes e hemicanais de connexin43, resultando na sincronização dos progenitores neurais em fase de migração na região subventricular (Ulrich et al. 2012), assim como a ativação de CaMKII seguida de fosforilação de cAMP/Ca²⁺ response element binding protein (CREB) em neurônios cerebelares, modulando a transcrição gênica (Leon et al. 2006). A baixa frequência de $\Delta[\text{Ca}^{2+}]_i$ globais e locais induzidas por receptores purinérgicos, durante estágios precoces da diferenciação neural, promoveu o crescimento de neuritos e especificação para neurônios GABAérgicos (Ciccolini et al. 2003).

Em células tronco neurais, Lin e colaboradores (Lin et al. 2007) descreveram que as células liberam ATP, ativando receptores P2Y para a manutenção da proliferação. De acordo com esse estudo, a proliferação de células P19 de carcinoma embrionário indiferenciadas foi acelerado por ATP via subtipos P2Y1 e P2Y2 (Resende et al. 2008; Resende et al. 2007).

1.1.3 Células tronco embrionárias e o desenvolvimento

Células tronco são células com capacidade de diferenciar em outros tipos celulares e que proliferam indefinidamente, além de serem importantes em processos biológicos na embriogênese, no crescimento dos órgãos e na renovação celular do organismo adulto. Podem ser classificadas quanto à sua fonte de obtenção e quanto à sua potência de diferenciação.

No início do desenvolvimento, o zigoto sofre clivagens e alcança o estágio de mórula, ambos os estágios possuem apenas células tronco totipotentes, ou seja, células que podem originar o indivíduo e os anexos extra-embrionários, como a placenta. Após mais clivagens a mórula alcança o estágio de blástula, no qual ocorre o primeiro evento de diferenciação celular no indivíduo. As células da camada externa compõem a trofectoderme, que originará o trofoblasto, que é importante para a formação da placenta e correta implantação do embrião no útero. As células do interior são denominadas massa celular interna do blastocisto e por sua vez são capazes de originar o indivíduo completo (Hall et al. 2013). As CTE são derivadas da massa celular interna de blastocisto de 3,5 dias (Martin 1981; Evans & Kaufman 1981) e são pluripotentes, pois podem diferenciar em células dos três folhetos embrionários (ectoderma, endoderma e mesoderma) (Figura 3).

Mesmo durante a vida adulta, o organismo ainda possui células tronco com capacidades de diferenciação, porém mais restrita se comparada às CTE e são chamadas de multipotentes. Células tronco multipotentes são capazes de originar células dos tecidos que são provenientes e estão envolvidas na renovação celular que ocorre nos órgãos. Alguns exemplos de células tronco multipotentes são as células

da medula-óssea (hematopoiéticas), células tronco neurais e células tronco mesenquimais (Peltier & Schaffer 2010).

CTE murinas podem ser mantidas no estado indiferenciado *in vitro* com a adição de LIF (fator inibitório da leucemia) ao meio de cultura. Em suspensão formam estruturas tridimensionais chamadas de corpos embriôides (EB), que dão origem espontaneamente a uma grande variedade de tipos celulares. EBs são ótimos modelos *in vitro* do desenvolvimento embrionário, visto que formam estruturas com os três folhetos embrionários e possuem orientação de eixos definidos pela sinalização de WNT (ten Berge et al. 2008).

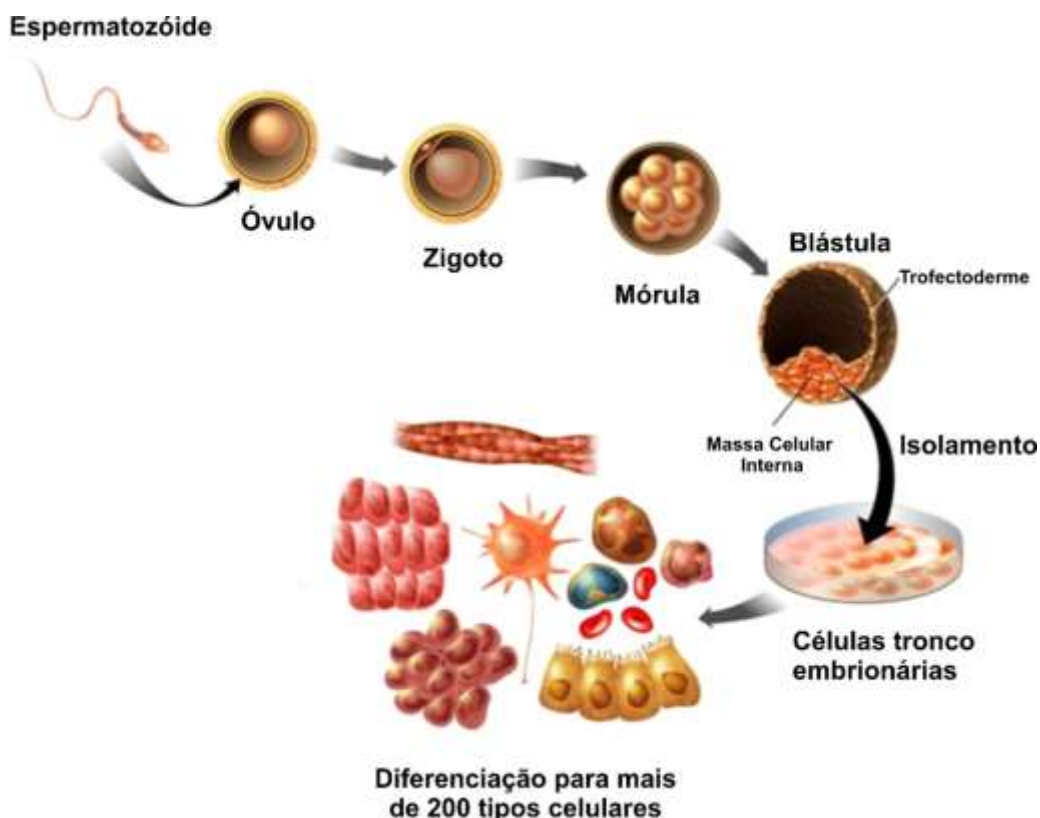


Figura 3. Início do desenvolvimento embrionário e origem de CTE. Após a fecundação do óvulo pelo espermatozoide, há a formação do zigoto (embrião de 1 célula) que então sofre sucessivas clivagens, passando pelo estado de mórula (8-16 células) e chegando ao estágio de blástula/blastocisto (64-200 células). Neste estágio ocorre o primeiro evento de diferenciação celular, gerando 2 tipos celulares que se dividem na massa celular interna do blastocisto e na trofetoderme. As células isoladas da massa celular interna e cultivadas *in vitro* são chamadas de células tronco embrionárias e podem diferenciar-se em mais dos 200 tipos celulares do organismo adulto, como células cardíacas, músculos esqueléticos, neurônios, células do sangue, pancreáticas, etc. Modificado de <http://sgugenetics.pbworks.com/w/page/38198357/Embryonic%20Stem%20Cells>.

Já foram descritos diversos trabalhos modulando a diferenciação de CTE para determinados tipos celulares *in vitro* como: em neurônios motores (Wu et al. 2012), GABAérgicos (Ma et al. 2012), serotoninérgicos (Yamasaki et al. 2015), precursores de fotorreceptores (Gonzalez-Cordero et al. 2013), dopaminérgicos (Daadi et al. 2012), cardiovasculares (Ohtani et al. 2013), rins (Takasato et al. 2013), progenitores pancreáticos (Rezania et al. 2012), dentre outros.

A facilidade de manipulação das CTE aliada à possibilidade de diferenciar estas células em tipos celulares específicos, dependendo apenas da forma que são cultivadas, as torna uma importante ferramenta para o estudo de eventos fundamentais que ocorrem durante o processo de diferenciação celular.

Ulrich e Majumder descreveram a importância das CTE como modelo para o entendimento da cinética de expressão gênica e secreção de fatores extrínsecos necessários à diferenciação neuronal (Ulrich & Majumder 2006). Elas oferecem um sistema *in vitro* capaz de recapitular as vias de sinalização envolvidas na determinação do fenótipo neural a partir de células embrionárias, durante o desenvolvimento do sistema nervoso central (SNC).

O desenvolvimento do SNC ocorre a partir da placa neural, nos eventos que decorrem na neurulação e geram o tubo neural, cujo é inicialmente uma única camada de células pseudo-estratificadas que proliferam rapidamente e dão origem os diversos tipos neurais (Wilson & Maden 2005). Um mesmo precursor pode dar origem às células gliais e neuronais, o que diferencia é o tipo de divisão celular. Na neurogênese a proliferação dá-se por divisão assimétrica, ou seja, com divisão desigual do conteúdo citoplasmático, enquanto que para a gliogênese há um retorno dos precursores em dividir-se simetricamente (Guillemot 2007; Trujillo et al. 2009).

Embora os processos morfogenéticos que ocorrem na formação do SNC possam ser facilmente visualizados *in vivo*, os passos intermediários nos quais as células tronco neurais (NSC) se diferenciam não foram completamente elucidados, pois há vários fatores que atuam neste processo, tais como moléculas de matriz extracelular, moléculas de adesão celular, fatores solúveis, interações célula-célula, neurotransmissores e seus respectivos receptores (Kim et al. 2009; Abranhes et al. 2009; Yan et al. 2015; Sobeih & Corfas 2002). Apesar da função diferenciadora de vários fatores de crescimento e que seus receptores já tenham sido estudados intensamente, pouco se sabe ainda sobre a ação de neuropeptídeos e neurotransmissores e seus receptores que, em muitos casos, já são funcionais antes mesmo do término da diferenciação.

1.1.4 Expressão gênica modulada por $\Delta[\text{Ca}^{2+}]_i$ na diferenciação neural

Mudanças na $[\text{Ca}^{2+}]_i$ livre, resultantes de eventos espontâneos ou regulados por sinais extracelulares, iniciam programas celulares específicos, que culminam, por exemplo, na diferenciação celular em células musculares e neuronais (Buonanno & Fields 1999).

Uma variedade de fatores de transcrição é sequencialmente expressa durante a neurogênese, sugerindo a existência de um complexo conjunto de eventos transcricionais que controlam o destino celular e os fenótipos específicos das células diferenciadas resultantes deste processo. Entre estes fatores, proteínas da classe bHLH (basic helix-loop-helix) desempenham um papel central não somente na aquisição do destino neural e determinação da linhagem neuronal, mas também da especificação dos fenótipos nos neurônios (Nieto et al. 2001). Para as células que seguirão o destino neural, a transição da proliferação à neurogênese envolve o

aumento coordenado da ativação de fatores pró-neurais, como os fatores bHLH, em camundongos. Esta classe de reguladores transpcionais iniciam um processo irreversível que culmina na diferenciação neuronal terminal (Ross et al. 2003). Assim, a neurogênese é mediada por duas amplas categorias de fatores bHLH: 1) fatores bHLH pró-neurais (ex: neurogeninas e Mash), que estão envolvidos na iniciação da neurogênese, e 2) fatores bHLH envolvidos na mediação da diferenciação neuronal terminal (ex: neuroD) que determina qual tipo de neurônio será formado.

Em camundongos, e de forma geral em mamíferos, fatores bHLH pró-neurais e fatores bHLH da diferenciação neuronal terminal são transativadores transpcionais. Estes fatores se ligam ao DNA como complexos heterodiméricos juntamente com proteínas E (E12, E47, E2-2, HEB), e o domínio básico destes fatores medeia a interação com sequências de DNA que contêm o motivo composto de 6 nucleotídeos CANNTG conhecido como Ebox. A transativação é mediada pela interação dos heterodímeros bHLH com co-ativadores, tais como p300 (*E1A binding protein p300*)/CBP (CREB-binding protein) e PCAF (*P300/CBP-associated factor*). Estes co-ativadores, além de recrutar um grande complexo que inclui a maquinaria de transcrição basal, facilitam a transcrição pela acetilação de histonas, tornando o DNA mais acessível à maquinaria de transcrição (Bertrand et al. 2002).

Durante o desenvolvimento, os fatores bHLH Ngn 1 (neurogenina 1), Ngn 2 (neurogenina 2) e MASH 1 são expressos em níveis baixos enquanto as células progenitoras estão sendo especificadas; já na iniciação da neurogênese, há um aumento transitório na expressão destes genes (Imayoshi & Kageyama 2014).

Corroborando este fato, fatores pró-neurais bHLH são expressos na zona ventricular, onde células progenitoras iniciam a diferenciação, mas não são expressos

na placa cortical, onde encontram-se neurônios totalmente diferenciados. De acordo com o modelo prevalente da neurogênese, a expressão transiente de fatores pró-neurais bHLH induzem uma segunda onda de expressão de genes bHLH de diferenciação terminal. Estes genes são membros da família NeuroD/Nex que incluem NeuroD/NeuroD2, e Nex (também chamado de Math2). Semelhantemente aos fatores pró-neurais, as proteínas bHLH da diferenciação neuronal são ativadores transpcionais que se ligam a Ebox e quando são super expressos são suficientes para induzir a parada do ciclo celular e consequente diferenciação neuronal (Bertrand et al. 2002).

A expressão gênica também pode ser ativada pelo gene NFAT durante o desenvolvimento (Hogan et al. 2003). NFAT na forma fosforilada é inativa, quando desfosforilada por calcineurina, expõe a sua sequência de localização nuclear e transloca para o núcleo (Muller & Rao 2010) (Figura 4). A calcineurina é ativada por aumentos locais e temporais na $[Ca^{2+}]$ durante a ativação de VGCC.

$\Delta[Ca^{2+}]_i$ também podem induzir cascatas de fosforilação, que culminam na ativação de NF- κ B pela atividade de CaMK (tipos I, II ou III) (Theatre et al. 2009), ou por proteínas quinases C (PKC) (Mellstrom et al. 2008; Moscat et al. 2003), que por sua vez ativam a transcrição de genes relacionados com a sobrevivência e a proliferação (Chafouleas et al. 1982).

Curiosamente, a ativação de IP3Rs e RYRs em células tronco neurais, geram $\Delta[Ca^{2+}]_i$ espontâneas na transição do ciclo celular da fase G1 para S (Tonelli et al. 2012; Resende et al. 2009). Nessas células a duração de G1 e a frequência de disparos de $\Delta[Ca^{2+}]_i$ estão conectadas pela diminuição da expressão de p27kip1, um inibidor do ciclo celular (Resende et al. 2009).

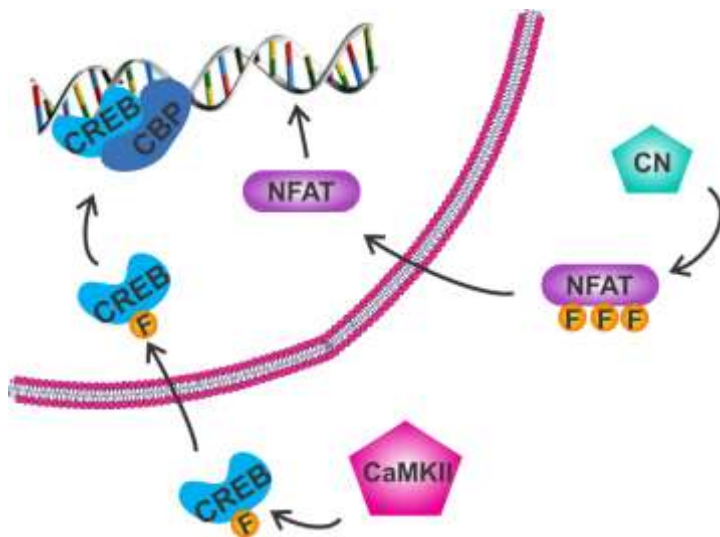


Figura 4. Mecanismos moleculares da transcrição dependente de Ca^{2+} . Representação das principais redes transcricionais reguladas por proteína fosfatase dependente de Ca^{2+} /calmodulina (calcineurina) e por proteína quinase dependente de Ca^{2+} /calmodulina (CaMKII) e regulação de NFAT e CREB. Retirado de (Mellstrom et al. 2008).

O fator de transcrição CREB também já foi descrito como participante da plasticidade neuronal no cérebro (Dolmetsch et al. 2001; Hardingham et al. 2001; Greer & Greenberg 2008), pois controla a expressão de vários genes como c-fos e fator neurotrófico derivado do cérebro (BDNF). A ativação de CREB ocorre quando é fosforilada por proteínas quinases A e C, CaMK ou mitogen-activated kinases (MAPK; ERK e p38). Wheeler e colaboradores já demonstraram que a ativação de VGGC do tipo L causa um aumento local de Ca^{2+} e ativação de CaMKII levando à transdução da via CREB, no entanto a magnitude das $\Delta[\text{Ca}^{2+}]_i$ não mostrou influência na atividade e fosforilação de CREB (Wheeler et al. 2008) (Figura 4).

A complexidade e o grande número de vias de sinalização celular até hoje descritas, necessariamente conduzem a uma abordagem reducionista, onde algumas moléculas específicas devem ser selecionadas como alvo de estudo. Neste trabalho focamos nos efeitos dos transientes de cálcio intracelulares na diferenciação neuronal.

OBJETIVOS

2.OBJETIVOS

Objetivo geral

Elucidar o papel dos transientes de cálcio intracelulares e a ativação de receptores purinérgicos e de canais para Ca^{2+} dependentes de voltagem na diferenciação neuronal de células tronco embrionárias.

Objetivos específicos

Padronizar a cultura celular com um protocolo de diferenciação neuronal que origine populações mais homogêneas ao longo do processo.

Caracterizar o padrão dos transientes de cálcio intracelulares em células cultivadas em condições normais ao longo da diferenciação neuronal.

Esclarecer a função de canais para Ca^{2+} voltagem dependentes no padrão de transientes de cálcio intracelulares espontâneos e no destino celular

Avaliar a expressão gênica ao nível do RNA e de proteína dos diferentes receptores purinérgicos e sua funcionalidade ao longo da diferenciação neuronal.

Avaliar o papel de receptores purinérgicos ao longo da diferenciação neuronal, no padrão de transientes de cálcio intracelulares espontâneos e no destino celular.

MATERIAIS E MÉTODOS

3. MATERIAIS E MÉTODOS

3.1 Cultivo e diferenciação de CTE E14-Tg2a

Neste trabalho utilizamos a linhagem murina de células tronco embrionárias ES-E14TG2a (ATCC® CRL-1821™) doadas pela Prof.a Dr.a Deborah Schechtman do Instituto de Química USP, e que diferentemente de outras linhagens, não necessita de uma camada de fibroblastos inativados (*feeder layer*), sendo cultivadas apenas sobre gelatina na presença de LIF (fator inibitório da leucemia, do inglês leukemia inhibitory factor) (Smith et al. 1988). As CTE foram expandidas e mantidas em cultivo em meio que consiste em DMEM High glucose, com 15% de SFB (soro fetal bovino), 1% de aminoácidos não-essenciais, 2mM de L-glutamina, 50 µg/ml de penicilina e estreptomicina, 2mM de piruvato de sódio, e 10³U ESGRO/LIF.

Para o protocolo de indução de E14TG2a em fenótipos neurais, formamos corpos embrioides (EBs) e utilizamos ácido retinóico como indutor, pois quando aplicado em CTE de camundongos em altas concentrações (10⁻⁶ a 10⁻⁷ M) induz a diferenciação neuronal em estágios precoces do desenvolvimento (Rohwedel et al. 1999; Wobus et al. 1994; Bain et al. 1996; Fraichard et al. 1995; Strubing et al. 1995) originando neurônios GABAérgicos, glutamatérgicos e dopaminérgicos, com potenciais de ação e expressão de marcadores de sinapses (Strubing et al. 1995; Rohwedel et al. 1999). Sabe-se que a diferenciação neural se dá por etapas, sendo o neurônio e a glia obtidos a partir de um precursor celular comum que expressa nestina (Bazan et al. 2004). Portanto, também optamos por uma seleção das linhagens neurais seguindo os estudos de Okabe e colaboradores (Okabe et al. 1996), que utilizam fatores de crescimento para especificação e seleção da linhagem neuronal,

como o fator básico de crescimento de fibroblasto (bFGF), fator de crescimento epidermal (EGF; (Okabe et al. 1996), FGF8, e Sonic Hedgehog (Lee et al. 2000); resultando em neurônios dopaminérgicos, GABAérgicos, glutamatérgicos e serotoninérgicos, além de células gliais (Lee et al. 2000; Okabe et al. 1996; Rolletschek et al. 2001). Como também nos baseamos no trabalho de Stavridis no qual o cultivo de precursores neurais em meio DMEM/F12 suplementado com meio N2 numa superfície tratada com laminina favorecem a aderência e crescimento de células neuronais (Stavridis & Smith 2003).

Portanto, CTE após terem atingido 80% de confluência no estado indiferenciado, foram dissociadas com tripsina por 2 min (Tryple, GIBCO), centrifugadas a 1000 RPM por 4min e ressuspensas em meio EB. Neste cultivo, 6×10^5 células permanecem em suspensão em placas de petri não aderentes, para que haja formação de EB. A constituição do meio EB é DMEM High-glucose, contendo 20% de SFB, 1 % de aminoácidos não-essenciais, 2 mM de L-glutamina, 1% de meio condicionado, contendo antibióticos, e 2mM de piruvato de sódio. Após dois dias nós induzimos a diferenciação neural com o 2 μ M de AR pelo intervalo de 4 dias. Posteriormente as células foram semeadas em garrafas de cultura celular previamente tratadas com 1 μ g/ml laminina em meio seletivo, composto por DMEM-F12, acrescido de 20 ng/ml bFGF para expansão de precursores neurais e 1% de suplemento N2 (GIBCO) para diferenciação neural. A maioria dos tipos celulares não sobrevivem a essas condições de cultura, e a porção restante fica enriquecida em células progenitoras neurais, assim como descrito em (Stavridis & Smith 2003), pois não possui soro que é rico em diversos fatores de crescimento. Células precursoras neurais estavam presentes do 6º ao 12º dia, enquanto que neurônios jovens já

surgiam a partir do 7º dia, com maturação iniciando ao 16º dia. A gliogênese decorreu do 14º ao 16 dia.

Tratamento farmacológicos durante a diferenciação para modulação de receptores purinérgicos ou VGCC foram realizados desde o 6º dia de diferenciação.

3.2 *Medidas das $\Delta[\text{Ca}^{2+}]_i$ por microscopia*

Células ao longo do processo de diferenciação foram transferidas para placas de cultura de 35 mm (Nalgene Nunc international). Antes de iniciar as medidas, as células foram incubadas a 37°C por 30 minutos, com 5 μM de Fluo-3AM (Invitrogen), 0,5% Me2SO e 0,1% do surfactante plurônico F-127 em meio DMEM/F12. O grupo acetoximetil (AM) está ligado ao indicador por uma ligação éster, ele permite que o indicador permeie a membrana plasmática, no entanto para que o indicador não retorne para o meio extracelular, esterase intracelulares desesterificam separando o indicador do grupo AM. Após incubação com Fluo-3AM, as células foram lavadas e mantidas em meio extracelular (140 mM de NaCl, 3 mM de KCl, 1 mM de MgCl₂, 2 mM de CaCl₂, 10 mM de HEPES, 10 mM de glicose, pH 7,4) por 20min para garantir uma completa desesterificação do grupo acetoximetil (AM) do indicador.

Células ao longo do processo de diferenciação tiveram seus transientes na concentração de cálcio livre intracelular ($\Delta[\text{Ca}^{2+}]_i$) espontâneos acompanhados e caracterizados através de microscopia de fluorescência e analisado pelo programa Nis elements AR (Nikon, Japão).

A determinação de $\Delta[\text{Ca}^{2+}]_i$ espontâneos foi realizada por captação na variação da intensidade de fluorescência emitida (F), que indica a $\Delta[\text{Ca}^{2+}]_i$, observada em

imagens sequenciais (inicialmente com intervalos de 1s) utilizando microscópio invertido de fluorescência ECLIPSE-TiS (Nikon) equipado com uma câmera CCD (Charge Coupled Device) de alta resolução de 14 bit CoolSNAP HQ2. Seguido da adição de 5 μ M ionóforo de cálcio (ionomicina ou 4-Br-A23187) para aquisição da fluorescência máxima (F_{max}) por formar vários poros na membrana celular específicos para esse íon, e então pela adição de 10mM EGTA como quelante para aquisição da fluorescência mínima possível (F_{min}). O Fluo-3AM foi excitado com uma lâmpada de xenônio no comprimento de onda de 488nm, a fluorescência emitida foi detectada usando um filtro de long-pass acima de 510 nm (Figura 5).

A $[Ca^{2+}]_i$ foi calculada pela equação:

$$[Ca^{2+}]_i = K_d \cdot (F - F_{min}) / (F_{max} - F)$$

K_d é a constante de dissociação do fluoróforo de cálcio que pode variar de acordo com a temperatura e o pH (K_d Fluo-3AM= 450 nM a 37°C e pH=7); F_{min} é a fluorescência mínima obtida após adição de 10mM de EGTA, e F_{max} é a fluorescência máxima obtida após aplicação de 5 μ M de ionóforo, e F é a fluorescência medida na célula, nesse caso sem adição de estímulo (Hallett et al. 1990).

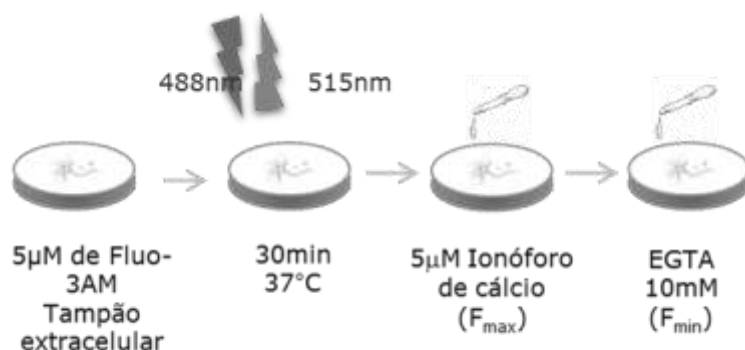


Figura 5. Ilustração dos passos para aquisição da $\Delta[Ca^{2+}]_i$. F_{max} , fluorescência máxima obtida com ionomicina e F_{min} , fluorescência mínima obtida na presença de quelante de Ca^{2+} .

Uma curva de calibração foi feita utilizando tampões com diferentes $[Ca^{2+}]$ livre com as mesmas condições do kit comercial (Calcium Calibration Buffer Kit da Life Technologies/Thermofisher) para confirmação do K_d nas nossas condições experimentais. A fluorescência emitida por Fluo-3AM é diretamente proporcional à $[Ca^{2+}]$ livre no intervalo de 10nM à 1 μ M, como demonstrado na figura 6.

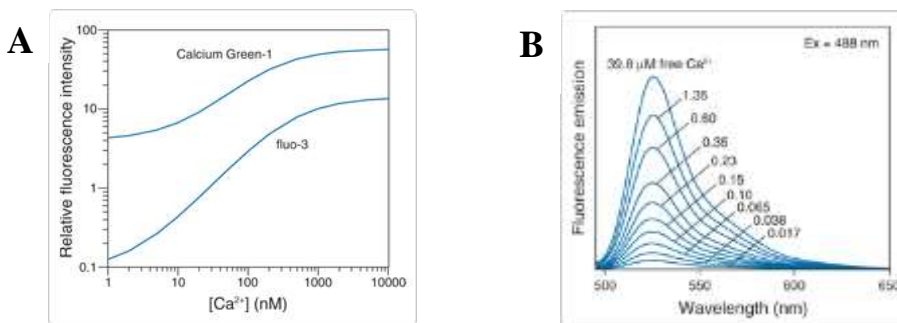


Figura 6. A. Comparação da intensidade de fluorescência para indicadores de Ca^{2+} , Fluo-3 e Calcium Green-1 em diferentes $[Ca^{2+}]$ livre. **B.** Fluo-3 não possui deslocamento do pico de emissão quando complexado ao cálcio. Retirado do manual do fabricante Life Technologies/Thermofisher.

No caso de células que em seguida foi analisada a luminescência do gene repórter, utilizou-se meio DMEM/F12 livre de vermelho de fenol e foi utilizada uma câmera de alta resolução CCD (iKon-M DU934P-BV, Andor) em objetiva de 40X e 5segundos entre quadros para aquisição.

Nos testes funcionais para a atividade de alguns receptores que utilizam Ca^{2+} como segundo mensageiro, mensuramos a $\Delta[Ca^{2+}]_i$ após aplicação de agonistas como glutamato (para receptores de glutamato, 100 μ M), carbachol (para receptores de acetilcolina, 50 μ M), e ATP (receptores purinérgicos 100 μ M).

Para tratamentos anteriores às aquisições das $\Delta[Ca^{2+}]_i$ espontâneas foram utilizados: 500nM Xestospongin C, que é inibidor de receptor de IP3 (XeC), 2mM de um quelante de Ca^{2+} (EGTA), 1 μ M Isradipina (ISR), inibidores do receptor P2X7 (10 μ M de KN-62 e 1 μ M de A438079), 10 μ M de 2'(3')-O-(4-Benzoilbenzol)adenosina-

5'-trifosfato (Bz-ATP, agonista do receptor P2X7), 1 μ M de 2-Tiouridina-5'-Trifosfato (2SUTP, agonista de P2Y2), 1 μ M de Tapsigargina (depletor dos estoques de Ca²⁺ do retículo endoplasmático).

3.3 Medidas das $\Delta[Ca^{2+}]_i$ por microfluorimetria

$\Delta[Ca^{2+}]_i$ foram determinadas por microfluorimetria utilizando o equipamento FlexStation III (Molecular Devices Corp., Sunny Valley, CA), segundo as instruções do fabricante. Basicamente, 3-5x10⁴ células/poço de CTE indiferenciadas foram semeadas no dia anterior à aquisição das medidas, enquanto que para células diferenciadas por 8,16 e 20 dias, 2 EBs/poço foram semeados em placas de 96poços pretas de fundo transparente, pré-tratadas com lamina (1 μ g/ml), com 100 μ l de meio de cultura por poço. As células foram incubadas por 60 min a 37°C com o FlexStation Calcium Assay Kit (Molecular Devices Corp.) contendo 2.5mM de probenecid num volume final de 200 μ l/poço. A fluorescência das amostras foi excitada a 485nm, e a fluorescência emitida detectada a 525nm.

As amostras foram lidas a intervalos de 1.52 segundos com um total de 200segundos. Após 20 segundos de monitoramento de fluorescência basal para os níveis da [Ca²⁺]i em células sem estímulo, aplicou-se ATP, Bz-ATP, (S)-(-)-Bay K 8644 (ativador de canais para Ca²⁺ do tipo L) ou KCl e as $\Delta[Ca^{2+}]_i$, foram monitoradas até 200 segundos. As respostas à adição de agonistas foram determinadas através da subtração da intensidade da fluorescência basal do valor adquirido no pico da fluorescência durante a resposta utilizando o software SoftMax2Pro software (Molecular Devices Corp.). Foram realizadas triplicatas para cada medida. Dados foram plotados com a media \pm erro padrão.

3.4 Curva de crescimento celular

Para análise da curva de crescimento na presença de inibidores do receptor P2X7, 30×10^4 CTE indiferenciadas foram semeadas em placas p35mm previamente gelatinizadas com 0,1% gelatina em PBS. Células foram removidas em duplicatas com tripsina e ressuspendidas em 1ml de solução salina de Hanks contendo 0.5% PFA para fixar após 8, 12, 24, 36, 48 e 60 h. Número celular foi determinado com uma câmera de Neubauer (0.100 mm profundidade, 0.0025 mm² área) em um microscópio invertido Axiovert 200 (Zeiss).

3.5 Extração de RNA total e síntese de cDNA.

O RNA total foi isolado de células indiferenciadas e diferenciadas com o reagente Trizol de acordo com protocolo do fabricante (Invitrogen) e a quantificação das amostras foi feita por espectrofotometria nas absorbâncias 260 e 280 nm. A integridade das amostras foi verificada através da análise da integridade dos rRNA por eletroforese em gel de agarose 1% (Huggett et al. 2005). Amostras de RNA total foram utilizadas como molde para a síntese de cDNA em uma reação de transcrição reversa.

Foram utilizados para a síntese de cDNA 2 μ g de RNA total, previamente tratados com DNase I (Ambion) para eliminação de contaminantes, utilizando a enzima transcriptase reversa segundo protocolo do fabricante (Invitrogen). Para isso, foi utilizado 1 μ l de dNTP (10 mM cada), 2 μ l de MgCl₂ (25 mM), 1 μ l oligodT (50ng/ml), 200 U transcriptase reversa, 40 U de inibidor de RNase, 2 μ l de tampão (10x), em um volume total de 20 μ l. As reações foram incubadas a 20° C por 10 minutos, 42° C por 45 minutos, 95° C por 5 minutos e 4° C por 10 minutos. A quantificação das amostras

foi feita através do ensaio de PCR em tempo real utilizando primers específicos (Tabela1).

3.6 PCR em tempo real.

PCR em tempo real foi realizado com equipamento ABI Step One Plus (Life Technologies) utilizando SYBR®-Green Dye como sistema de detecção. Cada reação foi feita em triplicata com um volume final de 15 µl. Para o PCR em tempo real foram utilizados 1 µl de cDNA, 3µl de primer Forward e Reverse e 6µl de SYBR®-Green cDye. As amplificações foram realizadas em termociclador ABI Step One Plus nas seguintes condições: 40 ciclos de 95°C por 2 minutos, 95°C por 30 segundos, 60°C por 30 segundos, 72°C por 30 segundos, seguido de curva de dissociação.

Após esse processo, foi empregada a técnica comparativa de 2- $\Delta\Delta CT$ para quantificação relativa da expressão gênica (Pal et al. 2013) utilizando a expressão de gliceraldeído-3-fosfato desidrogenase (GAPDH) como controle interno para normalização.

3.7 RT-PCR.

O RNA total de células indiferenciadas e diferenciadas por 8 dias foi extraído e o cDNA sintetizado como descrito no item 3.5 A amplificação foi realizada utilizando 5 pmol de primers específicos (Tabela 2), 20 µl de tampão de reação com 2µg cDNA, 1µl de Maxima Hot Start Taq DNA Polymerase (Thermo Scientific Fermentas). As condições da amplificação foram: desnaturação por 10 min a 95 °C seguido por 40 ciclos de desnaturação por 15 s a 95 °C, e anelamento por 30 s a 60°C e extensão por 1 min a 70 °C, seguido da extensão final de 10min a 72°C. Uma alíquota de 10µl

da reação de PCR foi analisada em gel de agarose 1,5% contendo brometo de etídeo sob luz ultravioleta. As bandas resultantes foram submetidas a análise de densitometria com o software Image J. As expressões foram normalizadas pela expressão de GAPDH.

Tabela 1. Sequencias de primers utilizados nas reações de RT-PCR e PCR em tempo real e tamanho esperado do produto em pares de base.

Gene	Forward (5'-3')	Reverse (5'-3')	(pb)
GAPDH	TGCACCACCAACTGCTTAG	GGATGCAGGGATGATGTTC	177
SSEA-1	CGGACCGACTCGGATGTCT	TTGGATCGCTCCTGGAATAGA	58
Oct-4	ATG CCG TGA AGT TGG AGA AG	TGT ACC CCA AGG TGA TCC TC	123
S100β	GAGCAGGAAGTGGTGGACAA	CACTCCCCATCCCCATCTT	59
TH	CCTTCCGTGTGTTCAGTGC	TCAGCCAACATGGGTACGTG	112
ChAT	CCCAACCAAGCCAAGCAATC	GGATAGGGGAGCAGCAACAA	113
GAD65	CACCGAGCTGATGGCATCTT	GGGCGCAGGTTGGTAGTATT	84
NMDAR	TGGGAAGTGTACGGTGCTTC	CGATCTGACCGCTCCAAATGC	86
V-Glut2	GACCCTGAGGAAACAAGCGA	TCCTGTGAGGTAGCACCGTA	131
5-HT	CAAAGGGGACCTTCCTCTGC	CATCTTGCCTTGCCTCAG	103
Dcx	GAGTGGGGCTTCGAGTGAT	AAAGAAAGCCGTGTGCCCTG	78
MAP-2	TCCTCCAAAGTCCCAGCTA	CCGGCAGTGGTTGGTTAATA	245
TUJ1	AGA CCT ACT GCA TCG ACA ATG AAG	GCT CAT GGT AGC AGA CAC AAG G	110
Nestin	GAG AGT CGC TTA GAG GTG CA	CCA CTT CCA GAC TCC GGG AC	241
NGN2	TCGGCTTAACTGGAGTGCC	GTGTGTTGTCGTTCTCGTGC	94
GFAP	AAGAGTGGTATCGGTCCAAGTTG	CAGTTGGCGGCGATAGTCAT	107
P2X2	TCCCTCCCCCACCTAGTCAC	CACCACCTGCTCAGTCAGAGC	149
P2X3	CTGCCTAACCTCACCGACAAG	AATACCCAGAACGCCACCC	150
P2X4	CCCTTGCCTGCCAGATAT	CCGTACGCCTGGTGAGTGT	149
P2X5	GGATGCCAATGTTGAGGTTGA	TCCTGACGAACCCCTCTCCAGT	81
P2X6	CCCAGAGCATCCTCTGTTCC	GGCACCAAGCTCCAGATCTCA	152

P2X7	GCACGAATTATGGCACCGTC	CCCCACCCTCTGTGACATTCT	171
IsoA	TGAGACAAACAAAGTCACCCG	TCAGTAGGGATACTTGAAGCC	1750
IsoB	TGCTCTTCTGACCGGCGTTG	TCAGGTGCGCATAACATACATG	945
IsoC	TGCTCTTCTGACCGGCGTTG	GAAACAAGTATCTAGGTTGG	923
Isok	GCCC GTGAGGCCACTTATGC	TCAGTAGGGATACTTGAAG	1774
P2Y1	GAGACACGAGTTCTGAAGGC	CAGGGATGTCTTGTGACCATGT	70
P2Y2	CTGATCAGGTCCAGGGCAAT	GTATCCCAGTTCGTCCCCCT	87
P2Y4	AAGGGTGGTGGTGGTACTCC	AGGAGCACCATCTTAGTTCCAG	100
P2Y6	TTGCATGAGACAGACTCTCCG	ATGGTGCCATTGTCCTGCTC	70
P2Y12	GTGCAAGGGGTGGCATCTAC	CCAAACTGGAAAAACAGGGGT	70
P2Y13	AACAAAGCTGATGCTCGGGA	CAGCTGTGTCATCCGAGTGT	94
P2Y14	TTCGTCCGGCAGCTGTAGT	ACATTGCCAGAACATCCCACAC	61
cav1.1	CGTCATCGGCAGCATCATTG	ATCTGGGTCAACGTTCCCG	109
cav1.2	CCTCATCGTCATTGGGAGCA	TCCTCTGCACTCATAGAGGGA	248
cav1.3	CGCAACACGATACTGGGCTA	TAGTTCCCTGCAGAAAGCCCC	119
cav1.4	TGGCAACTACATCCTGCTGAAC	GAGGGTTCCCTCACTGCTCT	116
cav 2.1	GAGGGTTCCCTCACTGCTCT	TCGATCATCTTGATCACCATCTCA	102
cav 2.2	TGCGTTCTCGAGCTTCATGG	CCGCTTGATGGTCTTGAGGG	103
cav2.3	CCAGCAACAGATTGAGCGAG	CGAACGACTTCCAAGGCTGA	117
cav3.1	TTCCAGGCAGAGGAAATCGG	CTGACTCAGACTTGGTGGCA	106
cav3.2	ACTGTGGTTCAAGCTCTGCC	TATCCTCGCTGCATTCTAGCC	118
cav3.3	ATGGCTGACAGCAACTTACCA	CCGGCTGCTCAGTGATTCC	73

3.8 *Ensaio de Western blotting*

Células tronco embrionárias submetidas à diferenciação neuronal tiveram suas proteínas extraídas. Estas células foram tripsinizadas, centrifugadas por 10min a 400g, lavadas com PBS e centrifugadas novamente. Depois o sobrenadante foi descartado e as células homogeneizadas em tampão de lise contendo 10 mM de Tris-HCl (pH 7,5), 150 mM NaCl, 20 mM de EDTA, 1% de Triton X-100, 8 M de uréia, inibidores de protease (Thermo Life Sciences) e inibidores de fosfatase (2 mM ortovanadato e 5 mM fluoreto de sódio, Thermo Life Sciences), as amostras foram então incubadas por 15 min no gelo e centrifugadas por 25min a 2000g a 4°C. O mesmo procedimento foi feito com os lisados totais de cérebro de camundongos knockout para o receptor P2X7. A concentração proteica foi determinada pelo método de Bradford utilizando albumina sérica bovina como padrão (Kruger 1994). Os extratos celulares (60 μ g) foram separados em SDS-PAGE (gel de separação 10%) numa voltagem constante de 120V e transferidos para membranas de nitrocelulose (Thermo-scientific) num sistema úmido por 1 h e amperagem constante de 400mA.

As membranas foram bloqueadas com TBS-Tween (Tris-buffered saline-Tween) contendo 5% de leite desnatado por 30min a temperatura ambiente. Após o bloqueio, as membranas foram incubadas com anticorpos primários diluídos na concentração recomendada pelo fabricante em TBST com 1% de BSA e incubados “overnight” a 4°C. A membrana foi lavada 3 vezes com TBST, e incubada com anticorpo secundário Alexa Fluor 488 ou 647 (Invitrogen, Life Technologies), por 1h sob agitação. Ambos os anticorpos primários e secundários foram diluídos em TBS-T com 1% de BSA. As membranas foram lavadas com TBS-T e escaneadas com o

scanner Typhoon (GE Healthcare). As bandas resultantes foram submetidas a densitometria com o software Image J. Os dados foram normalizados pela expressão de β-actin.

Os anticorpos primários utilizados foram: Oct-4 (policlonal de coelho 1:1000 Millipore), receptor P2X7 epítopo extracelular (monoclonal coelho 1:2000 AbCam), receptor P2X7 epítopo C-terminal (policlonal de coelho 1:1000 Alomone), monoclonal de coelho Anti-CREB (phospho S133) (1:500, Abcam) e β-actin (1:1000 Sigma-Aldrich).

3.9 Imunocitoquímica e microscopia de fluorescência

Para os ensaios de imunofluorescência, as células E14Tg2A foram cultivadas e diferenciadas em lamínulas redondas de vidro (1cm diâmetro), fixadas em 4% PFA e permeabilizadas com 0,05% Triton X-100 em PBS por 15 minutos. Após a permeabilização, as células foram incubadas com soro de cabra 2% por 30min a temperatura ambiente para o bloqueio de sítios inespecíficos. Na sequência, foi feita uma incubação dessas células com anticorpos primários “overnight” a 4°C. Após lavagens com PBS, as células foram bloqueadas por 30 minutos com PBS contendo 0,5% soro de cabra, 0,1% Triton X-100 e incubadas com anticorpos secundários Alexa Fluor 488 ou 555 goat anti-mouse ou rabbit (1:1000, Life Technologies/Thermofischer) por 1 hora em presença de 0.1% DAPI (4',6-diamidino-2-phenylindole) para evidenciar os núcleos. As lâminas foram lavadas e cobertas com lamínulas utilizando o meio vectashield (Vector Laboratories). As lâminas foram fotografadas no microscópio invertido epifluorescente Axiovert 200 (Zeiss) equipado com uma câmera Nikon DMX1200F e adquiridas com o software ACT-1 (Nikon). Para microscopia confocal

utilizamos o equipamento Zeiss LSM 780-NLO Multiphoton e analisamos com software LSMib software (Zeiss).

Os anticorpos primários utilizados foram: monoclonal de camundongo anti stage-specific embryonic antigen-1 (SSEA-1) (1:200, Chemicon, Bioscience Research Reagents), policlonal de coelho anti-TUJ1 (1:200, Millipore), policlonal de coelho Oct-4 (1:1000 Millipore), policlonal de coelho anti-MAP-2 (1:500 Cell Signaling), policlonal de coelho anti- GFAP (1:1000, Dako Systems), monoclonal de coelho anti-P2X7R (1:2000 AbCam), monoclonal de camundongo anti-nestina (1:1000 Millipore), monoclonal de camundongo anti-Synaptophysin (AXYLL, 1:50), policlonal de coelho anti-ISL1 (GeneTex, 1:200), policlonal de coelho anti-Pax6 (GeneTex, 1:200).

3.10 Microscopia eletrônica de varredura

Os EBs foram cultivados em lamínulas de vidro, lavados com PBS e fixados em PFA10%, seguido de uma desidratação por trocas consecutivas de soluções aquosas contendo concentrações crescentes de etanol (25, 50, 70, 90, 95 e 100%) por 10 min cada, e finalmente liofilizados. Posteriormente realizamos a análise de microscopia eletrônica de varredura em um microscópio Jeol FEG7401F equipado com um Field-Emission Gun. A superfície resultante foi analisada depois de uma cobertura de ouro ser aplicada.

3.11 Ensaio de incorporação de BrdU

A proliferação celular foi mensurada após incubação com 20 μ M de 5-bromo-2-deoxiuridina (BrdU; Sigma-Aldrich) por 1 hora. As células foram então fixadas com 75% de etanol no gelo por 10min, lavadas com PBS, incubadas por 30min em 2M de HCl e neutralizado com 0,1M tetraborato de sódio. As células foram bloqueadas com

2% de soro fetal bovino, 0,1% Triton-X100 em PBS por 30 min. Depois de lavadas com PBS, foram incubadas por 2horas com anticorpo policlonal de rato anti-BrdU (Abcam; 1:200). Então foram lavadas com PBS e incubadas com anticorpo Alexa Fluor 488 (1:1000, Life Technologies). Após mais um passo de lavagem, adicionou-se iodeto de propídeo (Life Technologies) a 50 μ g/ml com RNase A (SIGMA Aldrich) para corar o DNA. Células que não foram coradas com iodeto de propídeo ou marcadas com anticorpo primário, foram utilizadas como controle negativo. Os dados foram adquiridos com o citômetro de fluxo Attune (Life Technologies). Ambos os fluoróforos foram excitados com o laser azul 488nm. A emissão de Alexa Fluor 488 foi capturada com um filtro 530/30 nm e do iodeto de propídeo com um filtro de 574/26 nm.

3.12 Proliferação celular por Ki67

Após fixação das células com 75% de etanol por 10 minutos, as células foram lavadas com PBS, bloqueadas com 2% de soro fetal bovino, 0,1% Triton-X100 em PBS por 30 min. Células foram incubadas por 1 h com anticorpo policlonal de coelho anti-Ki67 (Millipore, 1:500), no qual marca células proliferativas. O anticorpo secundário Alexa Fluor 488 (Life Technologies) foi diluído 1:1000 e excitado a 488nm com um laser azul e a emissão capturada por um filtro de 530/30 nm.

3.13 Análise de citometria de fluxo

As células foram fixadas com 4% de paraformaldeído por 30min, lavadas em PBS e bloqueadas com 2% de soro fetal bovino, 0,1% Triton-X100 em PBS por 30min. As células foram então incubadas com anticorpos primários por 1h. Posteriormente as células foram incubadas por 45min com Alexa Fluor 488 anti-rabbit e Alexa Fluor 647 anti-mouse (Life Technologies, 1:1000). Célula que não foram imunomarcadas foram utilizadas como controle negativo. As populações foram mensuradas no citômetro de

fluxo Attune (Life Technologies, CA). Alexa Fluor 488 foi excitado com um laser de azul a 488nm e as emissão capturada com um filtro de 530/30. Alexa Fluor 647 foi excitado com um laser vermelho 638nm e sua emissão capturada com um filtro de 660/20.

Os anticorpos primários utilizados foram: monoclonal de camundongo anti-SSEA-1 (Millipore, 1:500), policlonal de coelho anti-TUJ1 (Sigma, 1:700).

3.14 Medidas nas variações no potencial de membrana celular por microfluorimetria

Mudanças no potencial de membrana foram determinados por microfluorimetria usando o leitor de placa FlexStation III e o kit FLIPR Membrane Potential Assay Kit Segundo as instruções do fabricante, pois o kit é 10 vezes mais rápido e mais estável que os corantes tradicionais e tem ótima correlação com ensaios manuais de patch clamp (Molecular Devices). O FLIPR Membrane Potential Assay Kit detecta a modulação de canais iônicos por aumentar ou diminuir o sinal de fluorescência conforme o potencial da membrana celular muda. O aumento na intensidade de fluorescência ocorre durante a depolarização da membrana, pois o indicador segue os íons positivamente carregados para dentro das células. Durante a hiperpolarização, o sinal fluorescente decai já que o indicador solta-se da célula juntamente com os íons carregados positivamente.

Os EBs foram coletados e semeados no 6º dia de diferenciação em placas de 96 poços pretas de fundo transparente previamente tratadas com laminina, foram colocados 2 EBs por poço em 100 µL de meio de cultura. Células em diferentes momentos da diferenciação foram incubadas por 60min a 37 °C com o corante do kit

FlexStation membrane potential Assay Kit (Molecular Devices Corp., USA) contendo 2.5 mM probenecid num volume final de 200 µL por poço. A fluorescência foi excitada a 488nm e emitida e detectada por um filtro band pass de 540-590 nm FLIPR Filter.

As amostras foram lidas em intervalos de 1s por 120 s. Após 30 s de monitoramento de atividade basal, um agente despolarizante foi aplicado (KCl, concentrações de 10-100mM finais). As respostas à adição do agente foram determinadas como a fluorescência basal subtraída da fluorescência máxima. A intensidade de fluorescência foi analisada utilizando o software SoftMax2Pro (Molecular Devices Corp., USA). Dados são expressos como média± erro padrão (S.E.).

3.15 Estabelecimento de linhagens celulares para verificação de alterações da expressão do gene repórter bioluminescente em tempo real.

3.15.1 MASH1-LUC NSC

Para as análises da expressão de Mash1 nós utilizamos a linhagem já estabelecida por Imayoshi (Imayoshi et al, 2013) de células tronco neurais (NSC) de telencéfalo de embriões de camundongos transgênicos por microinjeção nuclear de um cromossomo bacteriano (BAC DNA) contendo o inserto composto de região promotora de Mash1, os éxons de Mash1 fusionados à luciferase 2 (Figura7).

As células eram mantidas em DMEM/F12 suplementado com 1% meio suplemento N2 e 10ng/ml de FGF-2 e repicadas quando atingissem 80% de confluência com accutase (GIBCO).

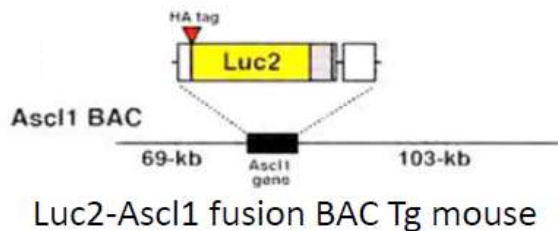


Figura 7. BAC DNA com MASH1 fusionado a luciferase 2 em camundongos transgênicos originados por microinjeção nuclear (Imayoshi, 2014).

3.15.2 *Ngn2-LUC E14-Tg2a*

Para estabelecimentos das CTE E14TG2a transgênicas, nós subclonamos o inserto presente em um BAC DNA correspondente ao promotor e proteína de Ngn2 fusionados à Luciferase (Figura 8), seguida da Região codificante de proteína Ngn2 e pela porção 3' UTR (regiões não traduzidas do mRNA), em um vetor plasmidial contendo sistema tol2 (que utiliza transposase para inserir a sequência de DNA no genoma eucarionte) por recombinação homóloga. Para tanto desenhamos os primers para os braços 5' e 3' de recombinação homóloga (HA): 5'HA forward 5'gtcgac CTAATTAGACAGATCTGAGTGC GG3', 5'HA reverse gcgccccgc; 3'HA forward TGCTAACCATGAAGACCAGAGG, 3'HA reverse gcggccgc; CTGGGAACACAGGGCTATGC, 3'HA reverse gaattc; CCATCTAGAAGAACAGAACAGGG. Os braços foram amplificados por PCR utilizando 1µg de BAC DNA, 2,5mM de dNTP mix, 10µM Primer forward e reverse e enzima KODFX_Neo (Nacalai tesque) segundo as instruções do fabricante.



Figura 8. Ilustração do constructo utilizado no estabelecimento da linhagem de CTE transgênica Ngn2-LUC. Região promotora do gene Ngn2 (pNgn2), exons 1 e 2 (Ex1 e Ex2), luciferase 2 (LUC), sequência da região codificante de Ngn2 (Ngn2 CDS), sequência não

traduzida da região 3' (3'UTR), promotor da quinase de fosfoglicerato 1 (PGK), proteína vermelha fluorescente (mCherry), região interna de entrada do ribossomo (IRES), gene de resistência a Puromicina (PURO).

Os produtos da PCR foram aplicados em gel de agarose 0,8% corados com Midori green (intercalante de DNA), as bandas com tamanho correto (~500pb) foram excisadas do gel e purificados com o kit Accuprep gel purification (Bioneer corporation). Os HA foram ligados ao plasmídeo comercial pT7blue vector (Novagen) utilizando 5µl do produto de PCR, 1µl pT7blue vector e 6 µl do reagente Mighty mix (ligation mix da Nacalai tesqe) por 18horas a 16°C.

Posteriormente, bactérias competentes de E.coli, cepa DH5α foram transformadas com o mix de ligação com os HA por choque térmico segundo os seguintes passos: incubar no gelo por 20min, aquecer por 45seg a 42°C, incubar novamente no gelo por 2 min, adicionar 200µl de LB, incubar a 37°C por 40min, centrifugar a 8000rpm por 1 min. Então foram semeadas em placas com meio Luria-Bertani ágar (LB-ágar- triptona 1%, extrato de levedura 1%, cloreto de sódio 0,5%, pH 7,5) com 100µg/ml ampicilina, 20µg/ml de X-Gal (5-bromo-4-cloro-3-indolil-β-D-galactosidase), 1,0mM de IPTG (isopropil-β-D-thiogalactopyranoside) e cultivadas por 18horas à 32°C. As colônias brancas contendo o inserto do DNA desejado foram isoladas e inoculadas em 2ml de LB com 100µg/ml ampicilina.

Obtivemos o DNA plasmidial das bactérias isoladas anteriormente utilizando o kit Accuprep plasmid extraction kit (Bioneer) e as amostras foram purificadas usando o kit CleanSEQ segundo as instruções do fabricante e checadas por sequenciamento utilizando o kit BigDye Terminator v3.1 cycle sequencing kit com o sequenciador ABI PRISM 3100 Genetic Analyzer.

Os plasmídeos que não possuíam mutações foram digeridos com as enzimas de restrição (SALI, BamHI). A reação final foi aplicada e separada em gel de agarose

0,8%. Os HAs (3'HA e 5'HA) foram excisados do gel e purificados como descrito anteriormente. O mesmo foi feito com o plasmídeo T2a-mCherry-Puro-vector linearizado, que possui o promotor PGK (Mouse phosphoglycerate kinase 1 promoter) que leva a alta expressão de genes repórter, regulando a expressão constitutiva da proteína fluorescente mCherry, seguida de IRES (internal ribosome entry site) que permite a iniciação da tradução no meio do RNAm e o gene de resistência a puromicina para seleção da linhagem (Figura 8), e então misturados com o reagente Mighty mix e incubados por 16horas a 16°C.

Após ligação dos HAs ao vetor, transformamos bactérias XL1blue por choque térmico, assim como descrito acima, com a diferença de que as bactérias foram incubadas a 30°C por 18hs. Então as colônias foram isoladas e crescidas em 2ml de LB por mais 12hs. Então os plasmídeos foram isolados por miniprep e as sequencias checadas por sequenciamento.

O plasmídeo oriundo do clone que não possuía mutações, foi escolhido para a reação de recombinação homóloga. Para tanto o plasmídeo foi linearizado e por eletroporação foi inserido nas bactérias contendo o BAC DNA com o constructo de Ngn2-LUC.

Para a eletroporação, 50 ml da cepa de bactéria contendo o BAC DNA, foi cultivada por 15 min a 42°C sob agitação para ativação da enzima de recombinação homóloga, depois foi mantida a 0°C, lavada 10X vezes com água, centrifugada a 5000rpm por 5min a 0°C e ressuspendida em 50μl de agua com 5-10μg do plasmídeo T2a-mCherry-Purovector- HAs e transferida para a cubeta. Foram eletroporadas com o eletroporador da (BioRad) 1.8kV, 5ms. Imediatamente depois foi adicionado 1 ml de LB gelado e então transferido para tubo de ensaio com mais 1ml de LB e incubado 1h

a 32°C sob agitação, então semeou-se as bactérias em placas de petri com LB agar com ampicilina por 18hs a 30°C.

Posteriormente as colônias foram isoladas e expandidas para extração por mini prep e checagem por sequenciamento. Os seguintes primers foram utilizados: 1- luc2_5F: GTGGACATTACCTACGCCGAG, 2- luc2_5R: CTTCATAGCTTCTGCCAGCCG, 3- Seq7_luc2: TGCTCATGTACCGCTTCGAGG, 4- luc2_3F: TGTGTTCGTGGACGAGGTGCC, 5- luc2_3R: GTCCAACTTGCCGGTCAGTCC, 6- Ngn2_check2Fv2: ATCAAGAACCGCGCAGGCTC, 7- Ngn2_check2Rv2: CTCTAGATACAGTCCCTGGCG. O plasmídeo foi utilizado para transformar novamente a bactéria XL1blue, as colônias isoladas e expandidas para extração por Midi Prep kit (TaKaRa Bio company) seguido de checagem das sequencias por digestão com enzima de restrição. Este plasmídeo (Ngn2-LUC-t2a-mCherry-Puro) com ~15Kb foi transfectado conjuntamente com o vetor contendo a sequência codificador apenas para Transposase nas células com o reagente viafect (Thermofischer) e as eficiências medidas. As células foram selecionadas por 7 dias com puromicina 1ug/ml e depois selecionadas duas vezes por FACS sorting, no equipamento FACS Calibur, utilizando a fluorescência emitida por mCherry (Figura 9).

Depois disso as células foram incubadas com Fluo3-AM como descrito acima, luciferina adicionada ao meio e filmadas em microscópio de fluorescência com uma câmera de alta resolução CCD (iKon-M DU934P-BV, Andor hipersensível. Para a verificação de alterações $\Delta[\text{Ca}^{2+}]_i$ nós adquirimos 1quadro a cada 5segundos e para bioluminescência nós adquirimos 1quadro a cada 10minutos.

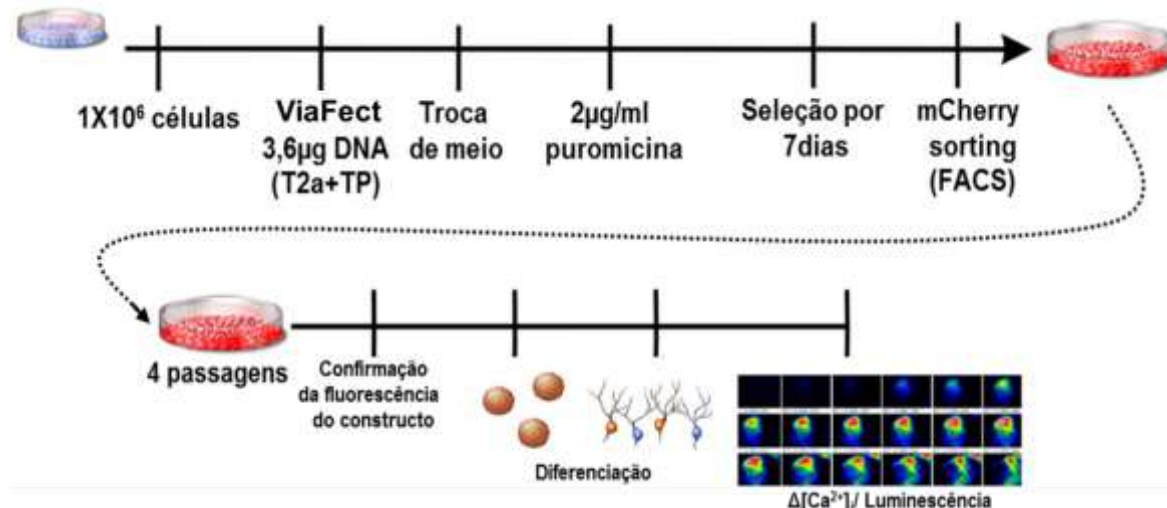


Figura 9. Ilustração dos passos para o estabelecimento da linhagem de CTE transgênica Ngn2-LUC. T2a, plasmídeo contendo o inserto Ngn2-LUC, e TP, vetor com a sequência para transposase.

3.16 Verificação de alterações na expressão em tempo real do gene repórter bioluminescente.

A linhagem Ngn2-LUC-E14 Tg2a, que possui fusionada à proteína Ngn2 a enzima luciferase, foram diferenciadas em placas de 35mm com fundo de vidro ($\varnothing 12\text{-mm glass}$, IWAKI 3911-035) e colocadas em um microscópio invertido (Olympus IX81) com 1 ml do meio acrescido de 1 mM de luciferina (Nacalai Tesque) por 2 dias a 37°C em 5% CO₂, e a luminescência capturada pela câmera de alta resolução CCD (iKon-M DU934P-BV, Andor) em objetiva de 40X e 10-min de exposição para aquisição (Masamizu et al. 2006).

3.17 Detecção indireta da concentração de ATP extracelular por bioluminescência.

Para a quantificação dos níveis de ATP secretado no meio extracelular, as células foram semeadas em placas de 96 poços pretas e com fundo transparente. Para mensuração as células foram incubadas por 5 min com tampão extracelular livre de fosfato e então adicionado o tampão do *Adenosine 5'-triphosphate Bioluminescent Somatic Cell assay kit* (Sigma-Aldrich) sem adição do *ATP releasing buffer*, pois este promove a lise celular. O tampão do kit possui tanto luciferina como luciferase e utiliza o ATP liberado pelas células na reação. Também foi feita uma curva padrão com concentrações conhecidas de ATP. A luminescência emitida detectada com o leitor de placa *FlexStation III* (Molecular Devices Corp., Sunny Valley, CA).

3.18 Análise estatística

As análises estatísticas foram feitas com ANOVA de uma ou duas vias seguido de post hoc test Bonferroni com o software GraphPad Prism 5.0 (GraphPad Software Inc., San Diego, CA). O critério estatístico para p valor significativo é $p < 0.05$ (*), $p < 0.01$ (**), ou $p < 0.001$ (***)

RESULTADOS E DISCUSSÃO

4.RESULTADOS E DISCUSSÃO

4.1 Diferenciação neural.

4.1.1 Estabelecimento e caracterização do protocolo de diferenciação neural.

O intuito deste trabalho foi estudar como a sinalização mediada por Ca^{2+} , por receptores purinérgicos e por canais para Ca^{2+} voltagem dependentes poderiam influenciar na diferenciação neuronal de células tronco embrionárias. Com esta finalidade, foi indispensável o tratamento crônico das células com diferentes fármacos. Para que os tratamentos fossem mais eficazes, necessitávamos desenvolver e caracterizar um protocolo de diferenciação neural que demonstrasse uma maior homogeneidade celular em diferentes momentos da diferenciação e que se assemelhasse ao desenvolvimento embrionário do sistema nervoso sem restringir a diferenciação para apenas um tipo neuronal.

A definição de um protocolo para indução da diferenciação de CTE E14TG2a em fenótipos neurais foi baseada em vários protocolos descritos na literatura que estão melhor detalhados na metodologia (seção 3.1). Basicamente, escolhemos usar ácido retinóico (AR, 2×10^{-6} M) como indutor de diferenciação neural (Bain et al. 1996; Fraichard et al. 1995; Rohwedel et al. 1999; Strubing et al. 1995; Wobus et al. 1994) e subsequente cultivo de células precursoras em meio seletivo livre de soro, composto por bFGF para expansão de precursores neurais (Okabe et al. 1996) e meio N2 para seleção neuronal e eliminação de células não-neurais (Stavridis & Smith 2003) sobre uma superfície pré-tratada com laminina (Figura 10). A figura 10 traz uma linha do tempo com as diferentes etapas do protocolo estabelecido e exemplos da morfologia celular obtida em cada etapa.

Para o estabelecimento do protocolo, primeiramente verificamos a pluripotência das CTE através da expressão de proteínas típicas de CTE indiferenciadas, como o fator de transcrição Oct4 e o trissacarídeo de membrana SSEA-1 por imunofluorescência (Figura 11A). Pudemos observar que a maioria das células submetidas a primeira etapa do protocolo expressam Oct4 e SSEA-1 e, portanto, estão no estado indiferenciado. A análise da expressão gênica do marcador de pluripotência Oct4 por PCR em tempo real durante a diferenciação demonstrou que a expressão de Oct4 diminui ao longo do processo, caindo pela metade 2 dias após o início da diferenciação (FIGURA 11B). Esse resultado valida o protocolo por indicar que as células estão perdendo a pluripotência e se comprometendo a um tipo celular, como o esperado.

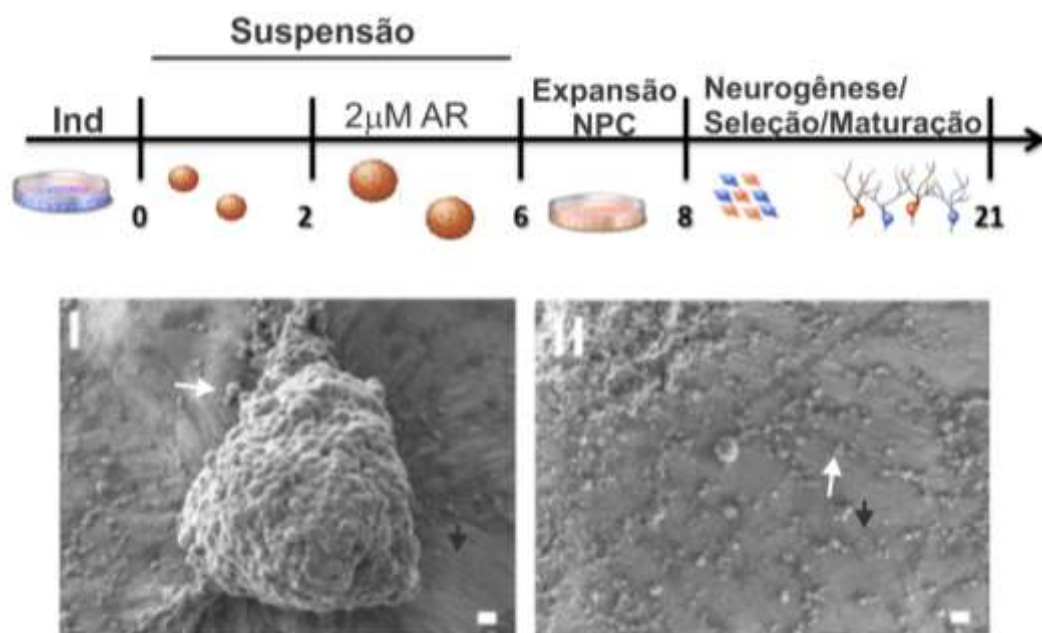


Figura 10. Caracterização da diferenciação neural. A. Linha do tempo com as principais etapas do protocolo de diferenciação e microscopia eletrônica de varredura de EBs com 14 dias de diferenciação destacando o corpo embriônico aderido (I) e as células neurais migrando a partir desse (II). Setas pretas indicam os prolongamentos celulares e as setas brancas os corpos celulares.

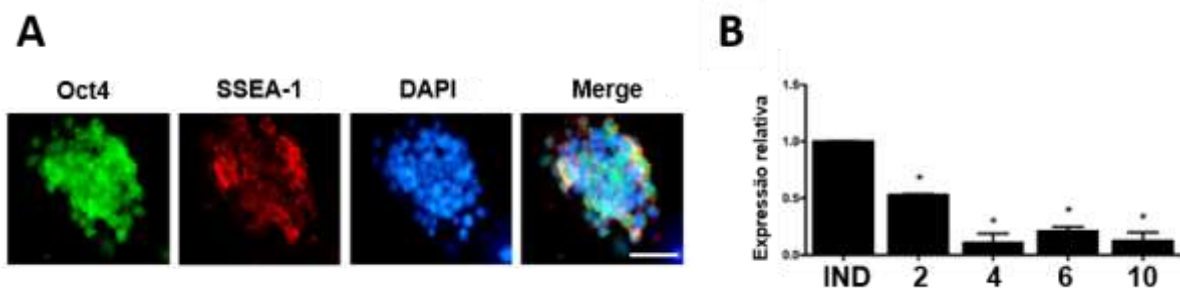


Figura 11. CTE no estado indiferenciado. **A.** Estado de indiferenciado CTE E14 Tg2a. Células foram imunomarcadas para expressão de Oct4 e SSEA-1. Escala 50µm, cromatina (DAPI) em azul. Experimento representativo de 3 experimentos independentes. **B.** Análise da expressão gênica de Oct4 ao longo da diferenciação. Níveis de expressão normalizadas pela expressão do gene endógeno GAPDH. *P≤0,05 de 3 experimentos independentes. Após 2 dias a expressão diminuiu em 50%.

O processo de diferenciação com este protocolo resultou em 79±2% de neurônios totais após 14 dias de diferenciação, evidenciado pela expressão de TUJ1 para neurônios e MAP-2 para neurônios maduros (Figura 12A), sendo que 41±10% das células ainda possuem potencial proliferativo (Figura 12A), evidenciado pela expressão de Ki67, uma proteína expressa em células não quiescentes.

Além disso, o protocolo gerou neurônios que passíveis de despolarização por estímulo com KCl, sendo 40mM a concentração necessária para atingir metade da despolarização máxima (Figura 12B). Esses dados foram reforçados pelo fato desses neurônios expressarem a proteína de sinapse *synaptophysin*, indicando a presença de vesículas sinápticas (Figura 12C).

Ao verificamos a expressão de fatores de transcrição expressos por neurônios motores e sensoriais observamos que o protocolo origina os 2 tipos celulares, uma vez que encontramos células que apresentam tanto ISL1 (Liang et al. 2011) como PAX6 (Martinez-Monedero et al. 2008) (Figura 12D).

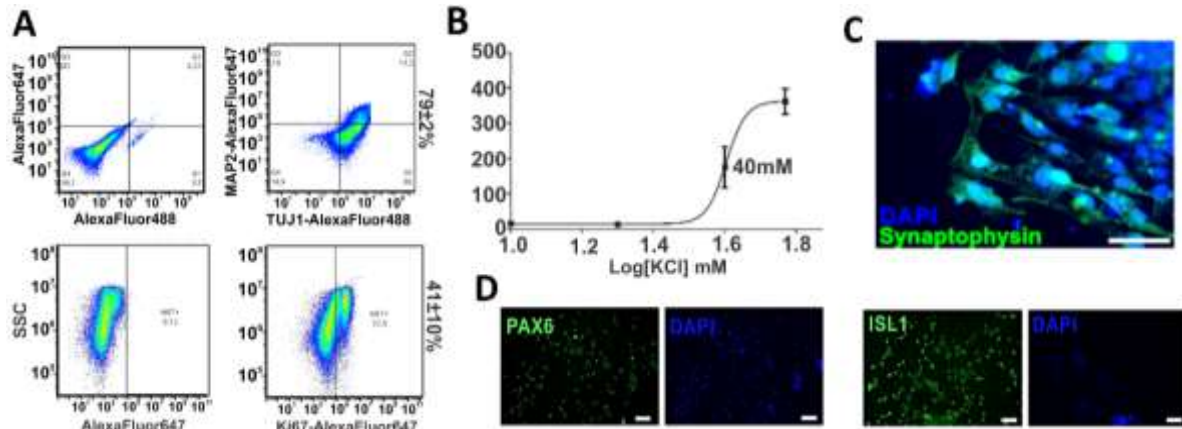


Figura 12. Caracterização da diferenciação neural. **A.** EBs com 14 dias de diferenciação e imunomarcados para TUJ1 (componente do citoesqueleto de neurônios jovens), MAP-2 (proteína do citoesqueleto expresso em neurônios maduros, pois auxilia a formação de neuritos), e Ki67 (proteína expressa em células proliferativas) analisadas por citometria de fluxo. Experimento representativo de 5 experimentos independentes. **B.** Curva dose resposta de variação no potencial de membrana após aplicação de KCl por microfluorimetria. 3 experimentos independentes em triplicata. **C.** Células diferenciadas por 16 dias e imunomarcadas para *Synaptophysin* (glicoproteína de vesículas sinápticas). Escala 50µm, cromatina (DAPI) em azul. Experimento representativo de 3 experimentos independentes. **D.** Células diferenciadas por 14 dias e imunomarcadas para *Pax-6* (fator de transcrição relacionado com a diferenciação de neurônios sensoriais) e para *ISL1* (fator de transcrição relacionado com diferenciação de motoneurônios). Escala 50µm, cromatina (DAPI) em azul. Experimento representativo de 3 experimentos independentes.

Caracterizamos os tipos celulares obtidos em cada momento do processo para definir o momento da diferenciação que apresenta células precursoras neurais ainda não comprometidas e poder modular a neurogênese. Para tanto, realizamos ensaios de imunofluorescência e PCR em tempo real para alguns marcadores clássicos de diferenciação neural, como: TUJ1 (neurônio jovem), Nestina (precursor/progenitor neural), GFAP (célula da glia ou progenitora) e MAP-2 (neurônio maduro) (Figura 13).

Obtivemos células expressando a proteína TUJ1 desde o 8º dia de diferenciação, com destaque para o 12º dia quando podemos observar a marcação por todo o corpo embrióide (Figura 13A e). No entanto, diferente da expressão proteica, a expressão gênica apresentou um pico no 6º dia, indicando atraso ou

mesmo alguma regulação pós-transcricional de TUJ1, possivelmente decorrentes de um mecanismo celular de decisão do destino neuronal.

No 8º dia de diferenciação pudemos observar um aumento na marcação de células expressando em relação a todos os outros dias do protocolo, indicando ser o dia chave para a neurogênese. O 16º dia não apresenta células com marcação para nestina (Figura 13B e F). A ausência de precursores neurais indica completa diferenciação e comprometimento celular.

Sequencialmente, também analisamos outros marcadores como MAP-2 (expresso em neurônio maduro) e GFAP (expresso em células gliais). Acompanhamos a diferenciação até o 21º dia, momento no qual observamos uma predominância de células marcadas para MAP-2 e GFAP tanto por imunofluorescência como por PCR em tempo real (Figura 13C-D, G-H). Esses dados sugerem que a diferenciação para células gliais é mais tardia e ocorre paralelamente ao amadurecimento dos neurônios.

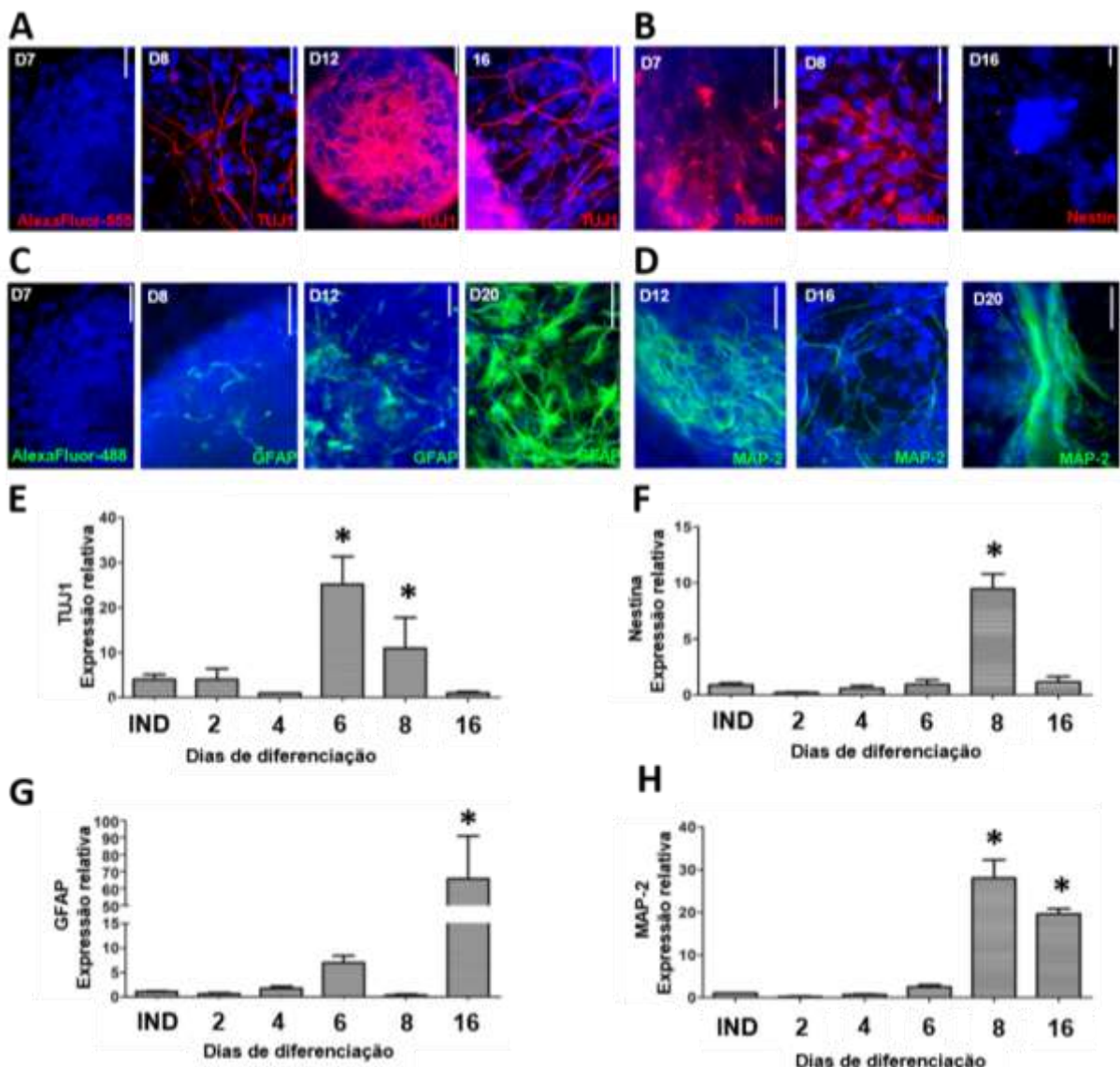


Figura 13. Caracterização da diferenciação neural. Células em diferentes momentos da diferenciação neural imunomarcadas para TUJ1 (A), Nestina (B), GFAP (C) e MAP-2 (D) e fotografadas por microscopia de fluorescência. Escala 50µm, cromatina (DAPI) em azul. Experimento representativo de 3 experimentos independentes. Análise da expressão gênica de TUJ1 (E), Nestin (F), GFAP (G) e MAP-2 (H) ao longo da diferenciação. Expressão normalizada pela expressão do gene endógeno GAPDH. ANOVA de uma via * P≤0,05. 3 experimentos independentes.

Sabe-se que o sistema nervoso central possui uma organização funcional composta por neurônios que liberam diferentes tipos de neurotransmissores, baseada na liberação de neurotransmissores por neurônios pré-sinápticos que atuarão em neurônios responsivos pós-sinápticos. A fim de determinarmos quais subtipos neuronais foram obtidos com esse protocolo de diferenciação, averiguamos a

expressão de marcadores típicos dos diferentes fenótipos neuronais como: tirosina hidroxilase para neurônios dopaminérgicos, GABA e GAD65 para neurônios GABAérgicos, *Colina acetiltransferase* (ChAT) para neurônios colinérgicos, receptor de 5-hidroxitriptamina (5-HT) para serotoninérgicos e ambos *transportador vesicular de glutamato* (Vglut) e receptor de *N-Metil-D-aspartato* (NMDAR) para neurônios Glutamatérgicos (Figura 14).

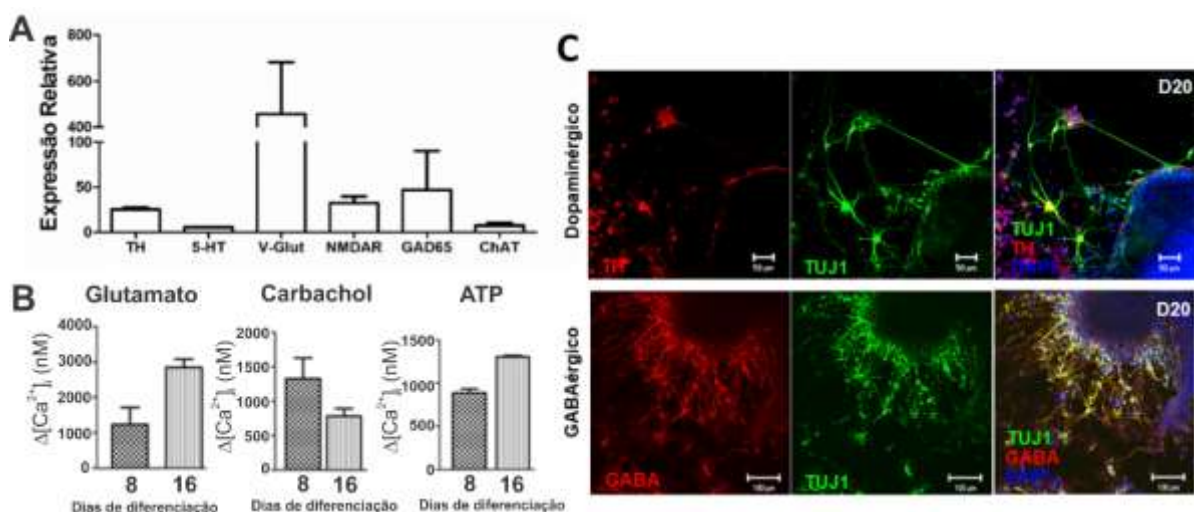


Figura 14. Caracterização da diferenciação neural/ tipos neuronais. A. Análise dos níveis de expressão gênica de Tirosina Hidroxilase (TH; dopaminérgicos), Receptor de 5-HT (5-HT; serotoninérgico), vesicular glutamate transporter (V-Glut; glutamatérgico), receptor de NMDA (NMDAR; glutamatérgico), glutamato descarboxilase (GAD65; GABAérgico), choline O-acetyltransferase (ChAT; colinérgico) após 16 dias de diferenciação. Expressão normalizada pela expressão do gene endógeno α-actina e relativa à célula na condição indiferenciada. 3 experimentos independentes. B. Variação na concentração de Ca²⁺ intracelular livre ($\Delta[\text{Ca}^{2+}]_i$) após estimulação com glutamato, carbachol e ATP em células diferenciadas. 3 experimentos independentes. C. Células diferenciadas por 20 dias e imunomarcadas para TUJ1 (em verde), TH e GABA (ambos em vermelho), e cromatina (DAPI) em azul. Imagens adquiridas por microscopia confocal. Escala 50μm. Experimento representativo de 3 experimentos independentes.

Por PCR em tempo real, observou-se uma maior expressão de V-Glut, NMDAR e GAD65), e uma menor expressão de 5-HT (Figura 14A). Esses dados indicam que a população obtida consiste principalmente de neurônios glutamatérgicos e GABAérgicos, com uma menor quantidade de neurônios serotoninérgicos.

Uma análise de microscopia confocal de EBs imunomarcados para TH e GABA indicam que a diferenciação *in vitro* também pode originar muitos neurônios GABAérgicos e alguns dopaminérgicos, corroborando os dados de PCR em tempo real (Figura 14C).

Além dos testes de expressão, nós também realizamos testes funcionais para avaliar a atividade de alguns receptores que utilizam Ca²⁺ como segundo mensageiro. Mensuramos a Δ[Ca²⁺]_i após aplicação de agonistas como glutamato (para receptores de glutamato, 100μM), carbachol (para receptores muscarínicos e nicotínicos de acetilcolina, 50μM), e ATP (receptores purinérgicos 100μM). Os dados indicam que há neurônios responsivos para esses neurotransmissores e que conforme a diferenciação decorre, as respostas ao glutamato e ao ATP aumentam enquanto que para o carbachol diminuem (Figura 14B).

Alguns grupos de pesquisa já demonstraram que a adesão de EBs em placas de cultura após a indução com ácido retinóico é capaz de originar neurônios GABAérgicos, glutamatérgicos e dopaminérgicos, com potenciais de ação e expressão de marcadores de sinapses (Strubing et al. 1995; Rohwedel et al. 1999). Sabe-se que a diferenciação neural se dá por etapas, sendo o neurônio e a glia obtidos a partir de um precursor celular comum que expressa uma proteína de citoesqueleto chamada nestina (Bazan et al. 2004), e que fatores como Sonic Hedgehog (Shh) e FGF-8 induzem as células que expressam nestina a diferenciarem em, além de células gliais, neurônios dopaminérgicos, GABAérgicos, glutamatérgicos e serotoninérgicos (Rolletschek et al. 2001; Okabe et al. 1996; Lee et al. 2000).

O conjunto desses dados indicam que esse protocolo pode originar uma grande proporção de precursores neurais após 8 dias de diferenciação e de neurônios funcionais após 16 dias, enquanto que a gliogênese é mais tardia e coincide com a maturação dos neurônios. Portanto, o intervalo ideal para modularmos a neurogênese farmacologicamente seria do 7º ao 12º dia. Além disso obtivemos vários fenótipos neuronais, indicando uma pan-diferenciação neuronal, assim como observado no desenvolvimento embrionário.

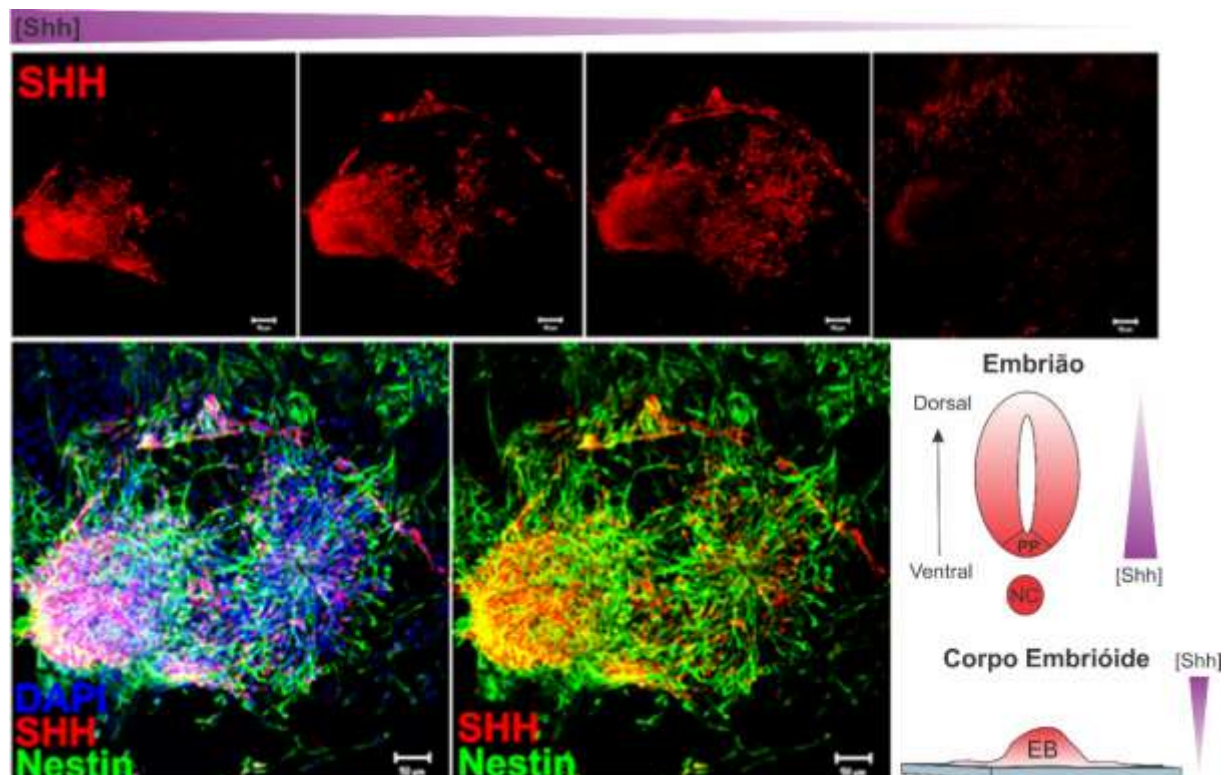


Figura 15. Expressão de Sonic Hedgehog nos corpos embrióides na fase de precursores neurais. Células diferenciadas por 12 dias e imunomarcadas para Shh (em vermelho), Nestina (em verde) e DAPI para cromatina (em azul) e analisadas por microscopia confocal. Escala 50µm. O painel superior mostra fatias da região do topo do EB para a base (da esquerda para a direita) expressando SHH. No painel inferior à esquerda, o mesmo corpo embrióide e imunomarcado para expressão de nestina (precursor neural). À direita esquema ilustra a distribuição do gradiente de Shh no embrião e no EB. No embrião Shh é liberado pela notocorda (NC) e inibe a proliferação da placa do piso do tubo neural (PP). Experimento representativo de 3 experimentos independentes.

Durante o desenvolvimento embrionário, existe um gradiente de moléculas sinalizadoras no tubo neural como o Shh, que regula a ventralização dos neurônios (Briscoe & Ericson 2001). Altas concentrações dessa proteína resultam em uma

inibição local da proliferação celular, deixando a placa do piso neural fina se comparada às regiões laterais do tubo neural em que a proliferação celular não foi alterada. Em contrapartida, baixas concentrações estimulam a proliferação e indução de diferenciação de vários tipos neurais ventrais e, após o estabelecimento da placa do piso, esta secreta SHH independentemente da notocorda.

A expressão dessa proteína pode ser induzida durante a diferenciação de CTE *in vitro* a partir da indução com AR (Renoncourt et al. 1998). Outros genes neurais específicos para diferenciação numa determinada linhagem também podem ser induzidos por AR, como fatores de transcrição Pax6 (Renoncourt et al. 1998; Gajovic et al. 1997) e Mash-1, e outra molécula sinalizadora como WNT-1 (Bain et al. 1995). Tendo em vista essas informações, nós analisamos a expressão de SHH por imunomarcação e microscopia confocal em EBs com 12 dias de diferenciação e observamos que, coincidentemente ao que ocorre no embrião, há um gradiente de concentração com uma maior concentração de SHH na parte superior do EB no momento em que temos a prevalência de precursores neurais (Figura 15). Esses dados indicam, portanto, que desenvolvemos um protocolo que assemelha-se ao desenvolvimento embrionário, pois assim como no desenvolvimento do tubo neural que possui células seguindo eixos radiais para migração e com informações de eixo distinguindo ventral e dorsal, o gradiente de Shh indica que as células migram a partir do EB aderido e possuem eixo dorso-ventral.

4.1.2 Conclusão da Diferenciação Neuronal.

Nossos dados sugerem que o protocolo estabelecido para a indução da diferenciação neural de células tronco embrionárias gerou um sistema que

assemelha-se ao encontrado no embrião em desenvolvimento, pois obtivemos vários tipos de neurônios como: motores, sensoriais, dopaminérgicos, colinérgicos, glutamatérgicos e GABAérgicos, sendo que o corpo embrióide apresenta um gradiente de SHH produzido por ele mesmo assim como observado no embrião. Além disso, as etapas da diferenciação são bem determinadas, sendo facilmente distinguível entre a neurogênese, a gliogênese e a maturação neuronal. A definição acurada das etapas da diferenciação celular permite a escolha do momento certo para aplicação dos tratamentos farmacológicos para a investigação das oscilações de $[Ca^{2+}]_i$ e os receptores purinérgicos na neurogênese.

4.2 EVENTOS ESPONTÂNEOS NA $\Delta[Ca^{2+}]_i$

4.2.1 Caracterização dos eventos espontâneos na $\Delta[Ca^{2+}]_i$

Como descrito anteriormente na introdução, o íon cálcio participa de várias funções importantes nos organismos vivos. Neurônios em desenvolvimento geram transientes de cálcio espontâneos em *Xenopus laevis* como descrito por Spitzer (Spitzer 2002). Portanto investigamos os padrões de oscilações espontâneas na $\Delta[Ca^{2+}]_i$ durante a diferenciação neural induzida por AR 5 μM e seguida de seleção de precursores neurais, além de quais os mecanismos envolvidos e seus efeitos na diferenciação neural.

Corpos embriôides de células tronco embrionárias E14 Tg2A em diferentes dias da diferenciação tiveram suas $\Delta[Ca^{2+}]_i$ acompanhadas indiretamente por registros da intensidade de fluorescência do corante Fluo3-AM (Figura 16A) por 20 minutos. Em seguida, foram adicionados o ionóforo de cálcio (ionomicina) para obtenção da fluorescência máxima e EGTA para fluorescência mínima e confirmação de células viáveis.

Desta maneira, identificarmos 3 tipos de oscilações espontâneas classificadas de acordo com a sua duração e frequência (Figura 16B). O primeiro perfil de oscilação é chamado de pico e tem duração média de 15s e amplitude média de 500nM. O segundo é chamado de onda e possui duração média de 30s e amplitude média de 250nM. Tanto picos como ondas foram determinados seguindo o padrão determinado por Spitzer e colaboradores (Spitzer et al. 2000). O terceiro perfil de oscilação, que foi denominado por nós como “unique” e que apresenta duração maior que 60s e amplitude em torno de 200nM, não está descrito na literatura.

Ao longo da diferenciação neuronal, oscilações do tipo pico tiveram sua frequência aumentada de aproximadamente 10 picos/hora no 8º dia para 32 picos/hora no 20º dia, sendo a amplitude média da $\Delta[\text{Ca}^{2+}]_i$ aumentada de 300nM ± 21 no 8º dia para 800nM±253 no 16º dia (Figuras 16C-D).

Para as oscilações do tipo onda, a frequência aumentou de 8 picos/hora no 8º dia para 17picos/hora no 20º, e a amplitude média da $\Delta[\text{Ca}^{2+}]_i$ variou de 250nM± 23 no 8º dia para 400nM± 33 no 20º dia (Figuras 16C-D).

Com relação às oscilações do tipo unique, a frequência não aumentou ao longo da diferenciação (Figuras 16C-D), enquanto a amplitude média da $\Delta[\text{Ca}^{2+}]_i$ variou de 258nM± 34 no 8º dia para 717nM± 468 no 20º dia (Figuras 16C-D). Investigamos ao longo desse estudo os fatores que originam essas oscilações e as modulamos para analisar a influência das mesmas durante todo o processo de diferenciação.

Esses dados, em conjunto com os dados obtidos sobre expressão de marcadores na diferenciação, indicam que durante a fase de precursores neurais no dia 8 (Figura 13B) picos e ondas possuem menor amplitude e frequência. Além disso, concomitantemente ao comprometimento, diferenciação e maturação de neurônios (Figura 16), há um aumento na frequência de disparos e na amplitude. Dessa forma,

a distribuição das $\Delta[\text{Ca}^{2+}]_i$ parece alterar-se no decorrer da diferenciação, sugerindo um possível papel dessas oscilações na manutenção do desenvolvimento do sistema nervoso.

Spitzer e colaboradores (Spitzer 2002; Spitzer et al. 2004) demonstraram em neurônios embrionários espinhais de *Xenopus* que a frequência de picos diminui no desenvolvimento e que o aumento na frequência de picos pode inibir a expressão do neurotransmissor glutamato. Todavia, em nosso estudo vimos um aumento na frequência até o dia 20, indicando que temos um sistema ainda mais precoce quando comparado ao estudado por Spitzer.

Spitzer e colaboradores também demonstraram que ondas possuem uma frequência constante ao longo do desenvolvimento, enquanto nós observamos um leve aumento no 20º dia no nosso modelo experimental, momento no qual acontece a maturação dos neurônios. Possivelmente as ondas estão aumentadas no nosso modelo devido à sua capacidade de regular a extensão de neuritos no cone de crescimento através da ativação de calcineurina, como descrito em *Xenopus laevis*.

A fim de compreender melhor como essas oscilações são desencadeadas, acompanhamos as $\Delta[\text{Ca}^{2+}]_i$ no 8º dia de diferenciação em corpos embrioides tratados com Xestospongin C (XeC), um inibidor de receptor de IP3 que está localizado no retículo endoplasmático, ou com um quelante de cálcio (EGTA, 2mM) para simular a condição sem $[\text{Ca}^{2+}]$ extracelular livre.

Poucas células permaneceram aderidas após tratamento com EGTA, uma vez que o Ca^{2+} posiciona as proteínas extracelulares que medeiam a adesão célula-célula, as caderinas, que impedem que mudem de conformação e sejam degradadas. Além disso, foi possível observar a abolição das oscilações do tipo pico e uma diminuição nas amplitudes de unique (Figura 16E-F).

As células com 8 dias de diferenciação (precursores neurais) tratadas com XeC (500nM) deixaram de apresentar oscilações do tipo onda e apresentaram um aumento significativo da frequência de picos (Figuras 16E-F), mostrando que há algum mecanismo de regulação entre esses dois tipos de oscilações. Ondas são conhecidas por serem desencadeadas por liberação de Ca^{2+} oriundo de estoques do retículo endoplasmático, e como vimos é completamente dependente de efeitos mediados por IP3. Dessa forma, a inibição dos receptores de IP3 leva à diminuição da liberação dos estoques de Ca^{2+} e menor ativação de oscilações do tipo onda. Houve também uma diminuição na frequência de oscilações do tipo unique e um concomitante aumento na amplitude, evidenciando uma dependência parcial de IP3 nesse momento da diferenciação (Figuras 16E-F). Portanto, ondas são desencadeadas por IP3 e a ausência delas induz disparos do tipo pico, causados por entrada de cálcio extracelular. Oscilações unique são dependentes de efeitos mediados por IP3 para controle dos disparos, mas inibição de receptores de IP3 aumenta a amplitude de unique.

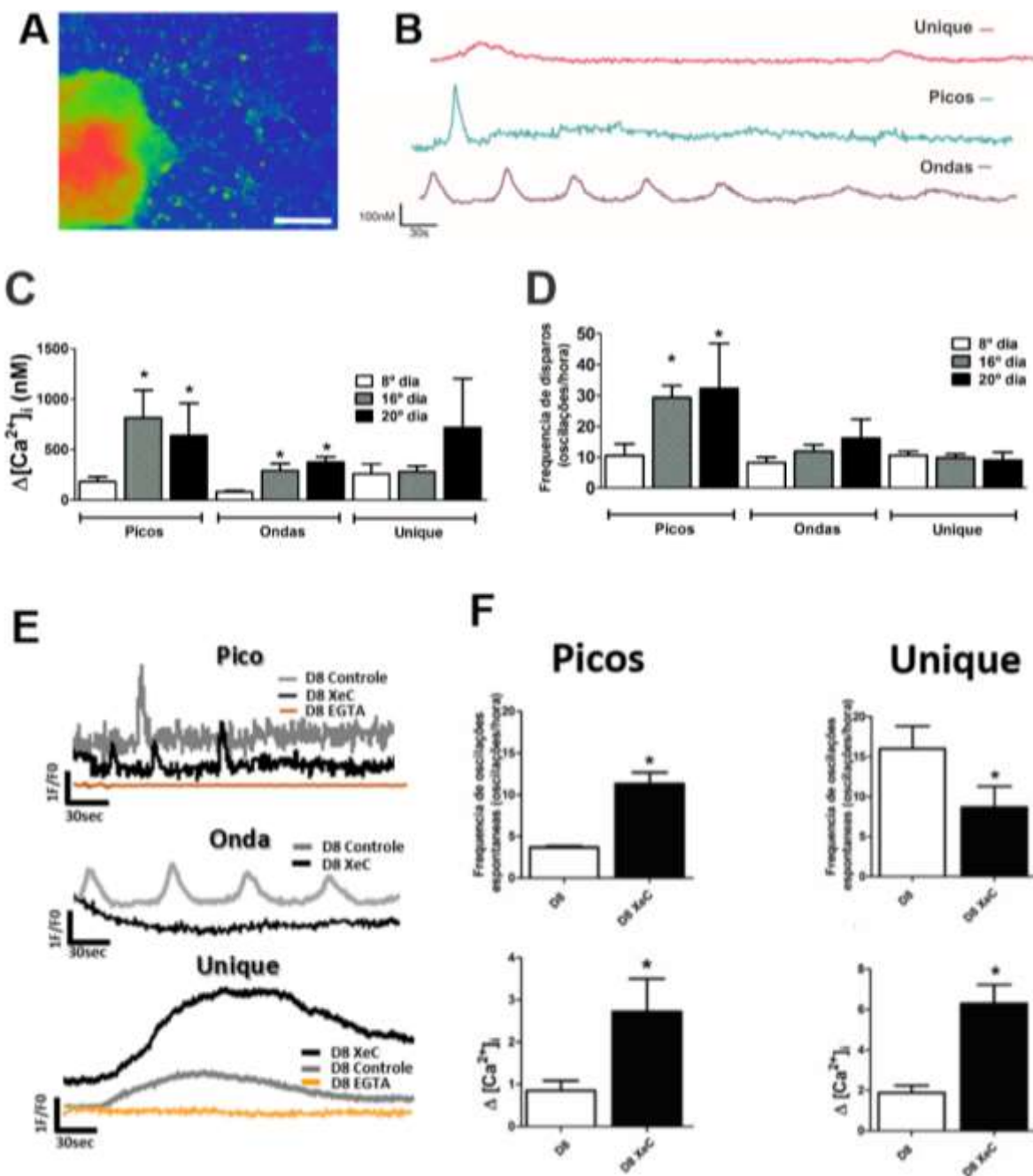


Figura 16. Caracterização da $\Delta[\text{Ca}^{2+}]_i$ espontânea na diferenciação de CTE em neurônios. **A.** EBs incubados com o indicador fluorescente de Ca^{2+} Fluo3-AM foram filmados por 20min com 500ms/frame e **B.** foram caracterizados 3 padrões de oscilações, Unique, Pico e Onda. Experimento representativo de 3 experimentos independentes. **C.** Quantificação da amplitude da $\Delta[\text{Ca}^{2+}]_i$ dos diferentes padrões ao longo da diferenciação. Dias 8,16 e 20 de diferenciação. 3 experimentos independentes. **D.** Frequência de disparos de cada padrão da $\Delta[\text{Ca}^{2+}]_i$ espontânea ao longo da diferenciação. Dias 8,16 e 20 de diferenciação. 3 experimentos independentes. **E.** Perfilis da $\Delta[\text{Ca}^{2+}]_i$ espontânea de células tratadas com 500nM Xestospongin C, que é inibidor de receptor de IP3 (XeC, preto) e com 2mM de um quelante de Ca^{2+} extracelular (EGTA, laranja). Experimento representativo de 3 experimentos independentes. **F.** Quantificação da amplitude e da frequência de disparos da $\Delta[\text{Ca}^{2+}]_i$ espontâneas de pico e unique no 8º dia de diferenciação em células tratadas com XeC. *P≤0,05 de 3 experimentos independentes.

4.2.2 Conclusão parcial

Com base nos nossos dados, podemos concluir que assim como já conhecido em *Xenopus*, a diferenciação neural de células murinas também apresentam oscilações espontâneas na $[Ca^{2+}]_i$ do tipo pico e onda. Além desses padrões já descritos na literatura, identificamos um novo padrão que chamamos de unique e que possui uma duração longa (~3min). Os dados também indicam que ondas são desencadeadas por IP3 e sua liberação de Ca^{2+} intracelular e que picos são por Ca^{2+} de origem extracelular, enquanto que unique depende da modulação dos dois tipos de Ca^{2+} .

4.3 CANAIS PARA Ca^{2+} DEPENDENTES DE VOLTAGEM

4.3.1 Canais para Ca^{2+} voltagem-dependentes no controle das $\Delta[Ca^{2+}]_i$ espontâneas e da diferenciação neural.

Ao diminuir o potencial de membrana de uma célula excitável (despolarização), é possível aumentar o influxo de Ca^{2+} no citosol através da abertura de VGCC. Malmersjö utilizando precursores neurais derivados de CTE (Malmersjo et al. 2013) descreveu a presença de oscilações rítmicas na $\Delta[Ca^{2+}]_i$ induzidas por VGCC. Além disso descrevemos que a amplitude e frequência de $\Delta[Ca^{2+}]_i$ do tipo pico, dependente de Ca^{2+} extracelular, aumentam ao longo do processo de diferenciação.

A fim de averiguar se os canais para cálcio voltagem dependentes possuem alguma relação com a diferenciação neuronal de CTE, primeiramente determinamos os padrões de expressão genética destes canais em células indiferenciadas e com 8 e 16 dias de diferenciação para todos os subtipos de canais (Figura 17). Foi possível observar que os canais do tipo L possuem um pico de expressão nas células com 8 dias de diferenciação quando as células se apresentam como precursores neurais,

indicando um possível papel desses canais na neurogênese (Figura 17A-D). Os canais do tipo L, normalmente encontrado em músculos e retina, são sensíveis as dihidropiridinas –DHP, como por exemplo, o ativador (S)-(-) Bay K 8644 e bloqueador Isradipina, e são ativados por uma forte despolarização que tem pouco efeito sobre a sua inativação.

Os canais do tipo P/Q (Cav 2.1) possuem expressão diminuída em células com 16 dias de diferenciação (Figura 17E), enquanto que a dos tipos N (Cav 2.2) e T (Cav 3) estão aumentadas no 8º dia e assim se mantém durante o restante da diferenciação (Figura 17F, H-J). É possível que os canais do tipo R (Cav 2.3) possam desempenhar o mesmo papel que os do tipo L, já que possuem o mesmo padrão de expressão durante a diferenciação (Figura 17G).

Os subtipos de Cav2 acoplam os potenciais de ação à liberação de neurotransmissores na fenda sináptica, processo que requer $[Ca^{2+}]_i$ entre 10 e 100 μM . Cav2 interagem com a maquinaria molecular de exocitose do terminal pré-sináptico, sendo responsável pela ativação da sintaxina 1, que medeia a ancoragem e fusão das vesículas com a membrana pré-sináptica.

Destes seis tipos de VGCC, apenas Cav3 são ativados por uma despolarização de baixo limiar (Wang & Lewin 2011). Os canais para Ca^{2+} tipo T foram inicialmente denominados canais ativados por baixa voltagem por poderem ser ativados por pequenas despolarizações da membrana plasmática, participando dos potenciais de ação rítmicos das células musculares cardíacas e neurônios (Elmslie 2004).

A despolarização da membrana causada pela adição de KCl pode abrir VGCC aumentando os níveis citosólicos de Ca^{2+} . A fim de elucidarmos um possível papel de VGCC na diferenciação e no controle das oscilações do tipo pico, primeiramente averiguamos a variação no potencial de membrana celular ($\Delta\Psi$) de EBs após a

aplicação de 60mM KCl utilizando o kit de detecção indireta FLIPR, e pudemos observar que no estágio de precursores neurais (dia 8) já existem células excitáveis (Figura 18A). Com o decorrer da neurogênese (dia16) e da maturação neuronal (dia 20) a amplitude de $\Delta\Psi$ aumenta chegando a dobrar quando comparado com o 8º dia (Figura 18A), provavelmente pelo fato de que com o estabelecimento de sinapses, mais células são potencialmente excitáveis. A despolarização com KCl nessas células também resultou num influxo de Ca^{2+} em todos os momentos da diferenciação, indicando a participação de VGCC.

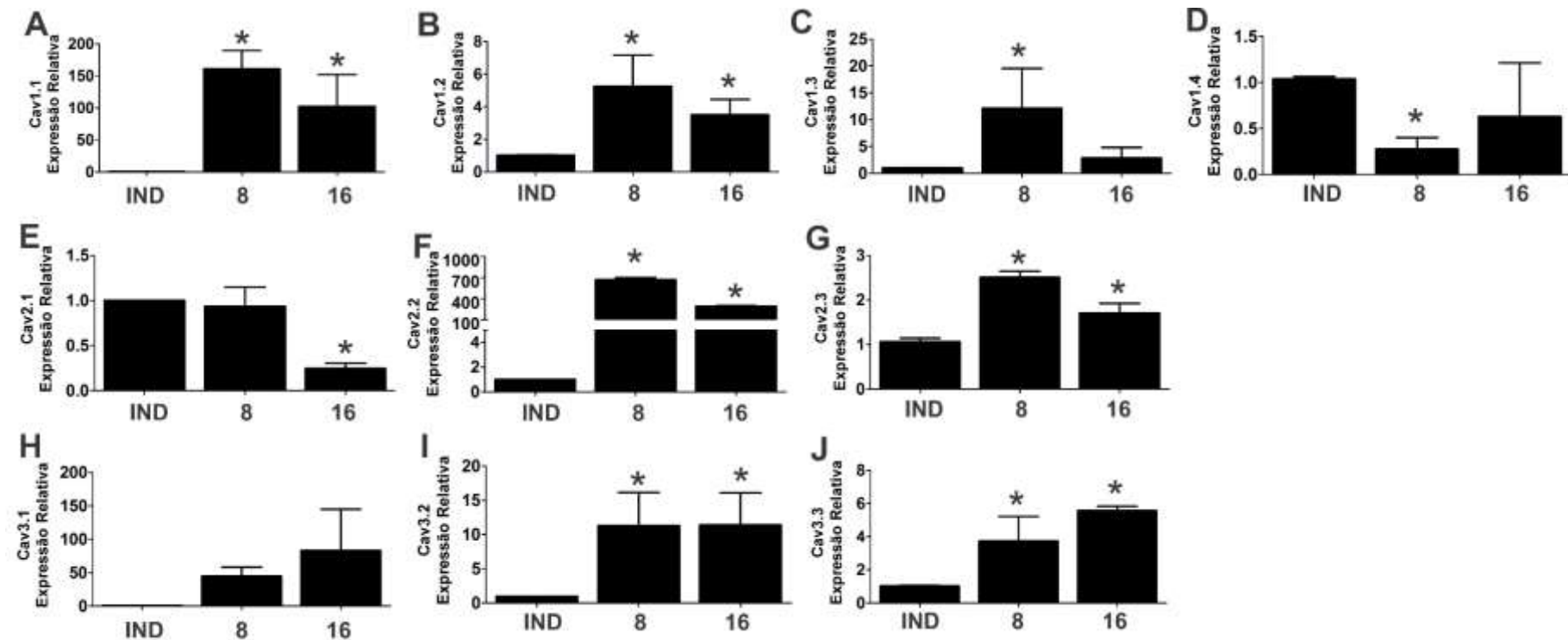


Figura 17. Expressão gênica relativa de VGCC ao longo da diferenciação neural induzida por ácido retinóico. Células indiferenciadas e diferenciadas por 8 e 16 dias foram analisadas por PCR em tempo real para a expressão de VGCC do tipo L (A-D), P/Q (E), N (F), R (G) e T (H-J). Os valores de CT foram normalizados pela expressão do gene endógeno GAPDH. Células indiferenciadas (IND), 8 e 16 dias de diferenciação. Anova * $p \leq 0.05$, 3 experimentos independentes.

O influxo de Ca²⁺ por VGCC, especialmente pelos do tipo L (Cav1), pode ativar vias de sinalização que afetam a expressão gênica em diversos tipos celulares como descrito na introdução. Neste sentido, tratamos as células por 5min com 1µM de Isradipina, um bloqueador específico de Cav1, e analisamos a Δ[Ca²⁺]_i após estímulo com KCl. Supreendentemente, ao longo de todo o processo de diferenciação o influxo de Ca²⁺ foi significativamente reduzido após inibição de Cav1, sendo que no 8º dia de diferenciação, o influxo de Ca²⁺ foi praticamente abolido. Essas informações sugerem um importante papel de Cav1 nas Δ[Ca²⁺]_i induzidas por despolarização. Na mesma linha, EBs após 20 dias de diferenciação e imunomarcados para expressão de Cav1, apresentaram a detecção de Cav1 na maioria das células (Figura 18C).

Confirmando os dados obtidos, a mensuração da Δ[Ca²⁺]_i em células tratadas com (S)-(-)-Bay K8644, um ativador específico de Cav1, gerou Δ[Ca²⁺]_i dose-dependentes com exceção do 8º dia, no qual Cav1 apresentou maior sensibilidade pelo ativador (Figura 18D). Esses dados sugerem que que Cav1 atue diferentemente em cada momento da diferenciação. Esses resultados tornaram indispensável o estudo da influência de Cav1 na diferenciação. Para tanto, testamos as doses de Isradipina e (S)-(-)- Bay K 8644 em um ensaio de morte celular por incorporação de DAPI e selecionamos as doses menos tóxicas para usarmos no tratamento crônico ao longo da diferenciação (Figura 19).

Esse ensaio baseia-se no fato de que células que tenham a membrana plasmática íntegra não permitem a entrada de DAPI (intercalante fluorescente de bases do DNA), portanto somente são coradas as células que estão danificadas ou em processo de morte celular. Dessa forma, selecionamos as doses ideais de 1µM para Isradipina, e de 0,1µM para (S)-(-)- Bay K 8644. Curiosamente, doses de

Isradipina maiores que 1 μ M apresentaram a formação de cristais e morte de ~100% das células (Figura 19).

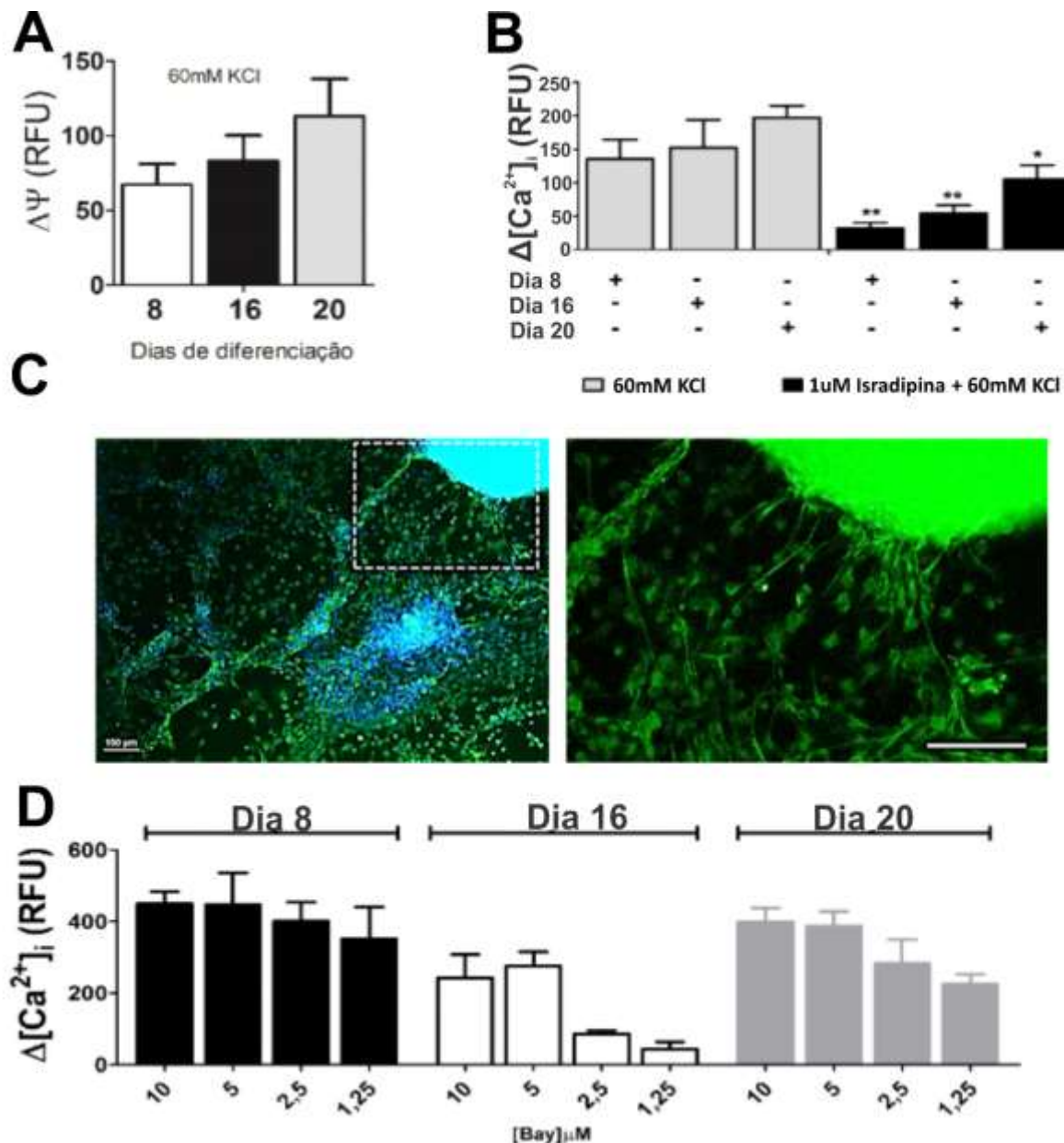


Figura 18. VGCC do tipo L (Cav1) na diferenciação neural de CTE. **A.** Mensuração da variação no potencial de membrana ($\Delta\Psi$) de células após 8, 16 e 20 dias de diferenciação após aplicação de 60mM de KCl. 3 experimentos independentes. **B.** $\Delta[Ca^{2+}]_i$ em células após 8, 16 e 20 dias de diferenciação após aplicação de KCl na presença e ausência de Isradipina, um bloqueador de Cav1. Anova * $p\leq 0,05$, 3 experimentos independentes. **C.** Imagens de células após 20 dias de diferenciação neural imunomarcadas para Cav1 (em verde) e adquiridas por microscopia. Experimento representativo de 3 experimentos independentes. Cromatina em azul (DAPI). Escala 100 μ m. **D.** $\Delta[Ca^{2+}]_i$ em células após 8, 16 e 20 dias de diferenciação após aplicação de diferentes concentrações de (S)-(-)- Bay K 8644 (Bay), um ativador de Cav1. 3 experimentos independentes.

Além dessas concentrações definidas de Isradipina e (S)-(-)- Bay K 8644, utilizamos DMSO (0,1%) como controle para tratar as células cronicamente a partir do 6º dia de diferenciação. Dados obtidos por PCR em tempo real mostraram que tanto a inibição como a ativação de Cav1 levou a uma diminuição da expressão de nestina no 8º dia (Figura 20A).

As células tratadas com Isradipina também apresentaram uma diminuição na expressão das proteínas neuronais TUJ1 no 8º dia e MAP-2 no 8º e 16º dia, enquanto que (S)-(-)- Bay K 8644 aumentou a expressão de MAP-2 em células no 8º dia (Figura 20B e D). Além desses resultados, a inibição do canal levou a um aumento na expressão de S100 β , proteína típica de astrócitos (Figura 20C). Dessa maneira, os dados evidenciam que Cav1 é importante para a diferenciação neural, tanto sua ativação que induz a diferenciação para neurônios quanto sua inibição que induz diferenciação para linhagens gliais, ou seja, Cav1 participa tanto da neurogênese quanto da gliogênese.

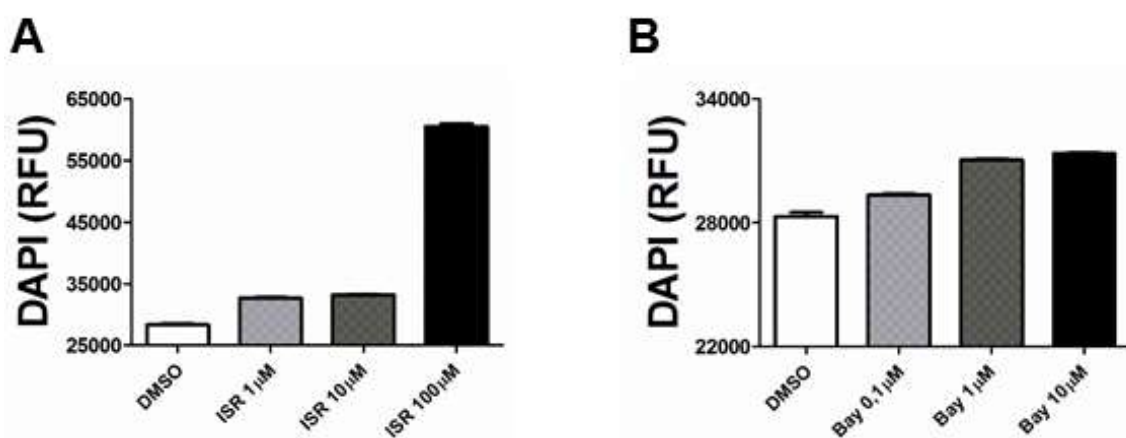


Figura 19. Toxicidade dos moduladores de Cav1. Células após 8 dias de diferenciação foram tratadas por 24hs com diferentes concentrações de **A.** Isradipina (bloqueador de Cav1) e **B.** (S)-(-)- Bay K 8644 (ativador de Cav1) e posteriormente incubados com DAPI, intercalante fluorescente de DNA não permeável à membrana plasmática intacta. 3 experimentos independentes.

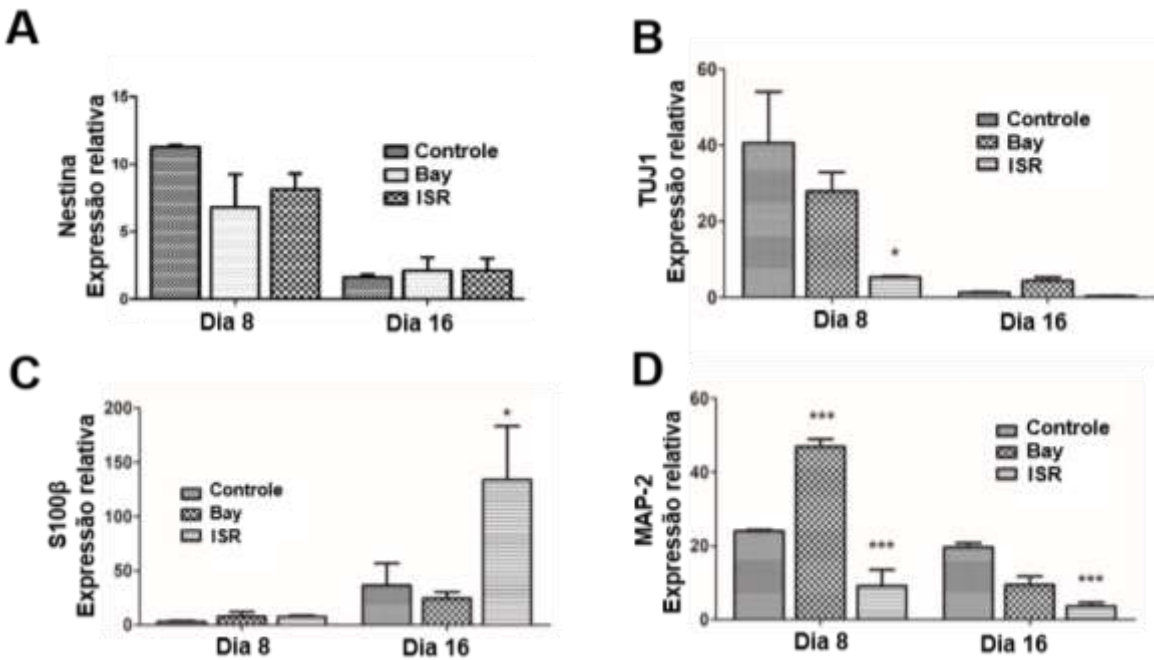


Figura 20. Participação de Cav1 na diferenciação neural de CTE. Células diferenciadas após 8 e 16 dias sob tratamento crônico de 0,1µM (S)-(--) Bay K 8644 (ativador de Cav1) e 1µM de Isradipina, desde o 6º dia de diferenciação, tiveram a expressão gênica relativa de genes específicos para: **A.** precursores neurais (Nestina), **B.** neurônio jovem (TUJ1), **C.** astrócito (S100 β), e **D.** neurônios maduros (MAP-2) avaliados por PCR em tempo real. Dados normalizados pela expressão do gene endógeno GAPDH. ANOVA de uma via *P≤0,05, **≤P0,01, ***≤P0,001 de 3 experimentos independentes.

Além de estudarmos a influência de Cav1 na escolha do destino celular na diferenciação, nós também investigamos se esses canais poderiam modular as oscilações espontâneas de cálcio, uma vez que já está bem descrito na literatura (Spitzer et al. 2000; Lautermilch & Spitzer 2000) que a sinalização intracelular mediada por Ca²⁺ induz a expressão de diferentes genes, podendo definir o destino celular. A transição de proliferação para neurogênese envolve o aumento coordenado da atividade de fatores pró-neurais bHLH (Mash1, Neurogenina1 e Neurogenina 2) e a diminuição dos fatores Hes e Id. Conforme o desenvolvimento prossegue, se houver inibição de fatores bHLH nos progenitores, ocorre a formação de astrócitos (Ross et al. 2003).

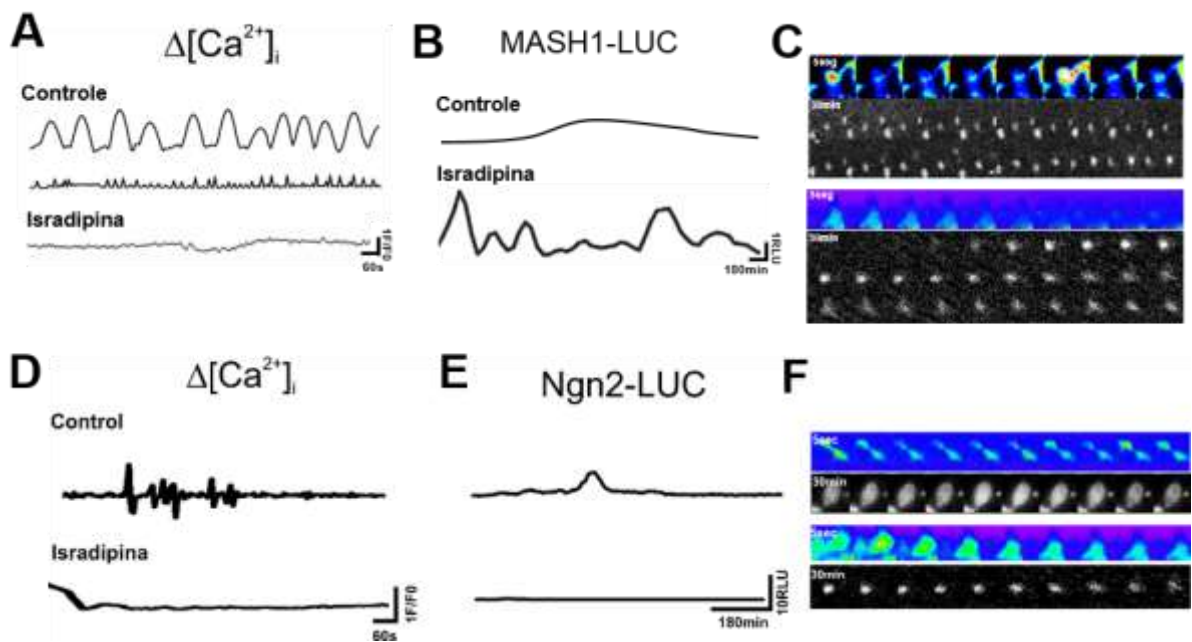


Figura 21. Perfil da $\Delta[\text{Ca}^{2+}]_i$ espontânea e expressão em tempo real de Mash1 e Ngn2 em NSC e corpos embriôides com oito dias de diferenciação e modulação por VGCC.

A. NSC foram marcadas com Fluo3-AM e sua intensidade medida como forma indireta de $[\text{Ca}^{2+}]_i$ por 20min. B. Perfil da expressão de Ngn2 em NSCs tratadas com 1 μM de isradipina. C. Montagem sequencial das imagens do vídeo para verificação de alterações $\Delta[\text{Ca}^{2+}]_i$, de Ca^{2+} e de emissão de luminescência referente a expressão de Mash1. D. Corpos embriôides de E14 TG2A foram submetidos à diferenciação induzida por ácido retinóico 5 μM e marcados com Fluo3-AM e sua intensidade medida como forma indireta de $[\text{Ca}^{2+}]_i$ por 20min. Perfil das oscilações espontâneas em EBs com 7 dias de diferenciação tratados ou não com 1 μM de isradipina (bloqueador de Cav1). E. Perfil da expressão de Ngn2 em EBs com 7 dias de diferenciação tratados com 1 μM de isradipina. F. Montagem sequencial das imagens do vídeo para verificação de alterações $\Delta[\text{Ca}^{2+}]_i$ e luminescência.

A partir dos dados obtidos, escolhemos estudar 2 genes pró-neurais que estão em equilíbrio durante a diferenciação neural, Mash1 e Neurogenina 2, e analisar a expressão de ambos em tempo real juntamente com as oscilações espontâneas de $[\text{Ca}^{2+}]_i$.

Em colaboração com o Prof. Ryoichiro Kageyama da Universidade de Kyoto, nós utilizamos células tronco neurais extraídas de telencéfalo de camundongos transgênicos que possuem a enzima luciferase como gene repórter fusionada à Mash1. Assim, com a adição de luciferina no meio de cultura, pudemos observar em

tempo real a expressão de Mash1 (Figura 21B-C) após 20 min filmando as oscilações espontâneas de Ca^{2+} em células tratadas com Isradipina (Figura 21A e C). Foi possível notar que a cultura de células tronco neurais apresentou células com oscilações predominantemente pico ou onda e que o tratamento com Isradipina aboliu as $\Delta[\text{Ca}^{2+}]_i$ espontâneas. No entanto, a expressão de Mash1 tornou-se oscilatória (Figura 3A-C), efeito característico de células precursoras neurais antes de se diferenciarem, como já descrito por Imayoshi e colaboradores (Imayoshi et al. 2013).

Para a análise de Ngn-2, nós transfetamos células E14tg2a com plasmídeos contendo as sequências para o promotor e a proteína Ngn2 fusionadas à enzima luciferase sob regulação do promotor pCMV. O plasmídeo continha o gene de resistência para Puromicina e mCherry fluorescente, facilitando a seleção das células positivas.

Após esses ensaios nós diferenciamos as células Ngn2-Luc para o estágio de precursores neurais e no 7º dia de diferenciação, nós tratamos com Isradipina e mensuramos tanto as oscilações de $[\text{Ca}^{2+}]_i$ como a expressão de Ngn2 em tempo real. Observamos que nesse modelo celular o tratamento com Isradipina aboliu tanto as oscilações de $[\text{Ca}^{2+}]_i$ como a expressão de Ngn2, indicando uma participação importante das $\Delta[\text{Ca}^{2+}]_i$ na regulação da transcrição de Ngn2 (Figura 21 D-F).

Na literatura está bem descrito que em células tronco neurais Mash1 determina a diferenciação tanto para neurônios como para oligodendrócitos (Parras et al. 2004; Parras et al. 2002) e que Mash1 e Ngn2 são expressos em populações complementares de progenitores neurais (Parras et al. 2004; Parras et al. 2002). Dessa forma, juntamente com o que descrevemos acima sobre os papéis dos fatores de transcrição no desenvolvimento, podemos inferir que a inibição de Cav1 leva a

ativação de Mash1 oscilatório que, na falta de Ngn1 e 2, induz a diferenciação para astrócito ou mantém a células indiferenciadas no estado de precursores. Além disso, a ativação Cav1 levaria ao aumento de Ngn2, que quando modulado por retinóides, culmina na ativação de Mash1 estável e a diferenciação para neurônios.

Podemos concluir que o ajuste fino da atividade desses canais é extremamente importante para a diferenciação de progenitores neurais, pois tanto o aumento quanto a diminuição na atividade são capazes de modular a expressão de fatores de transcrição relacionados à neurogênese, alterando o destino celular.

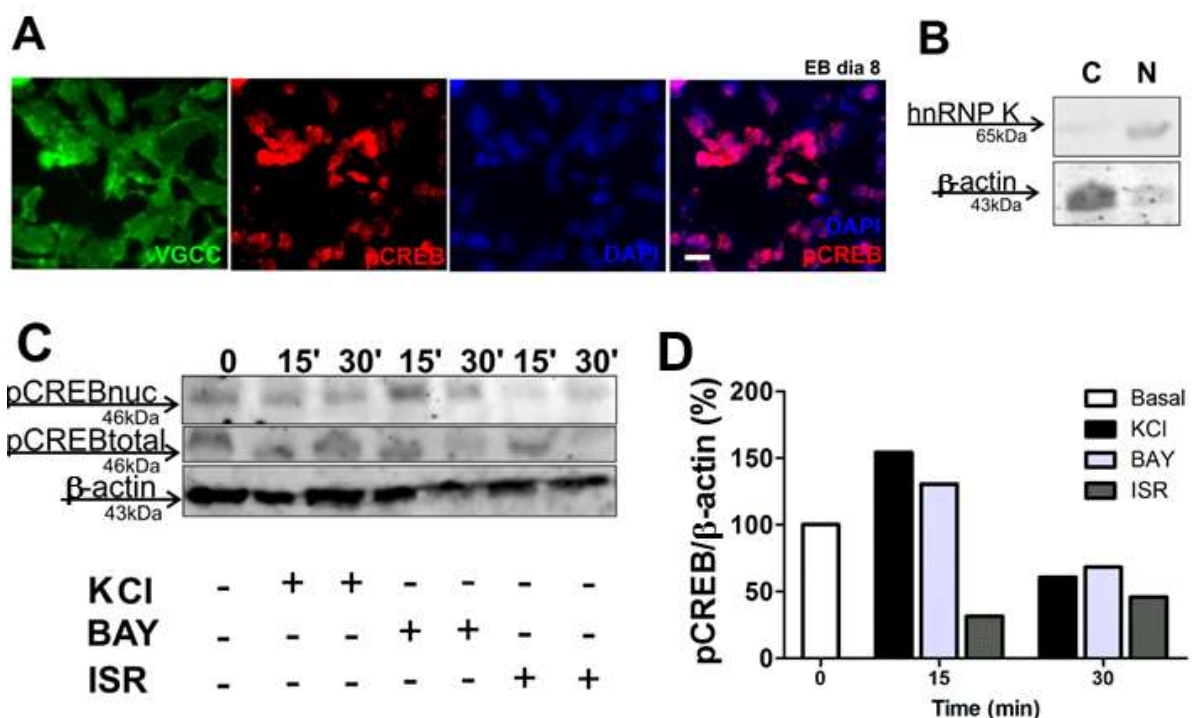


Figura 22. Participação de Cav1 na diferenciação neural induzida por ácido retinóico em células tronco embrionárias. Corpos embriônicos de células E14TG2A foram submetidos à diferenciação induzida por ácido retinóico 5µM **A.** Imunomarcação de células diferenciadas por 8 dias para expressão de Cav1 (verde), CREB fosforilada (vermelho) e marcação para cromatina (DAPI, azul). Escala 10 µm. Experimento representativo de 3 experimentos independentes. **B.** Extrato proteico de fracionamento celular separados em gel 10% SDS-PAGE e transferidos para membrana de nitrocelulose e imunomarcados para *heterogeneous nuclear ribonucleoprotein K* (hnRNP K, proteína nuclear) ou α-actina (proteína citosólica). Citosol (C), núcleo (N). **C.** Lisados de células com 8 dias de diferenciação após despolarização com KCl ou tratadas com ativador (100nM (S)-(-) - Bay K 8644) ou com um bloqueador (1uM isradipina) de Cav1 por 15 ou 30 min e imunomarcados para CREB fosforilada. **D.** Densitometria de bandas dos dados em C pelo software Image J. 1 N experimental.

A fim de elucidarmos como Cav1, que modula as $\Delta[\text{Ca}^{2+}]_i$ espontâneas e altera o destino celular de precursores neurais, pode modular a neurogênese, analisamos a expressão e localização de CREB fosforilada (pCREB) no núcleo, já que este é um fator de transcrição bem descrito na literatura como efetuador de Cav1 em células neuronais (Bito et al, 1996). Por microscopia de fluorescência, foi possível observar que células no dia 8 de diferenciação (precursores neurais) apresentaram coexpressão de Cav1 e pCREB (Figura 22A).

Além do mais, estimulamos as células no 8º dia de diferenciação com KCl, modulamos a atividade de Cav1 com 100nM de (S)-(-) - Bay K 8644 ou com 1 μ M de isradipina, e sequencialmente coletamos os lisados celulares fracionados de núcleo e citosol para uma análise quantitativa. Para garantirmos a qualidade do processo de fracionamento, nós imunomarcamos as amostras apenas citosólicas para α -actina, que é uma proteína citosólica, e nucleares para hnRNP K (heterogeneous nuclear ribonucleoprotein K) que é uma proteína nuclear. Como demonstrado na figura 22B, podemos constatar que há pouquíssima contaminação entre frações. A figura 22C traz os dados que mostram que a despolarização por KCl e a ativação com (S)-(-) - Bay K 8644 levam a um aumento na marcação para pCREB nas frações nucleares após 15min de estímulo. A Isradipina por sua vez apresenta menos pCREB nuclear em comparação com a amostra controle-basal sem estímulo. Esses dados indicam que a atividade de Cav1 induz a translocação de pCREB para o núcleo e que após 30min não há mais efeito (Figura 22C e D).

4.3.2 Conclusão sobre a participação de canais para Ca^{2+} voltagem-dependentes na indução da diferenciação neuronal

Em posse dos dados dessa tese podemos concluir que a inibição da neurogênese após bloqueio de Cav1 dá-se pela regulação no padrão de expressão de Mash1 oscilatório vs estável. A forma estável leva ao início da neurogênese enquanto que a oscilatória mantém a célula em seu estado indiferenciado. Portanto, para que a neurogênese ocorra, deve haver a ativação de Cav1 e consequentemente a indução das $\Delta[\text{Ca}^{2+}]_i$ do tipo pico que estimulam a fosforilação e a translocação de CREB para o núcleo, ativando a transcrição estável de Mash1, e culminando na diferenciação neuronal.

4.4 RECEPTORES PURINÉRGICOS

Os receptores purinérgicos, como descrito na introdução, são expressos por quase todo tipo celular e podem ser detectados em embriões no início do desenvolvimento, e podem modular a gastrulação (Burnstock & Ulrich 2011; Zimmermann 2006). Dessa maneira, torna-se imprescindível o esclarecimento dos papéis de subtipos de receptor purinérgicos na biologia de CTE e na diferenciação neural.

4.4.1 Caracterização do sistema purinérgico na diferenciação neural

Por PCR em tempo real, verificamos que a maioria dos receptores purinérgicos do tipo P2X (P2X_{2,3,4,6,7}) apresentam expressão gênica relativa decrescente no decorrer da diferenciação neural induzida por ácido retinóico, com exceção de P2X5 que se manteve estável (Figura23 A-F). Já para os receptores do tipo P2Y (Figura 23 G-M), observa-se que a expressão de apenas P2Y12 e P2Y13 decaiu, enquanto que

para P2Y1 e P2Y14 aumentou-se. A expressão de subtipos P2Y2 e P2Y6 possui um padrão oscilatório, ou seja, houve um pico no nível de expressão com 8 dias de diferenciação, sugerindo um possível papel desses receptores na obtenção ou manutenção de precursores neurais.

O receptor P2X1 está bem descrito como não expresso em células neuronais, o que nos levou a analisar sua expressão somente nas células indiferenciadas e no início da diferenciação. Todavia, não foi possível detectar por PCR em tempo real a expressão desse receptor por não encontrarmos um par de iniciadores que tivesse uma eficiência de replicação suficiente para a análise utilizando o método $\Delta\Delta Ct$. Sendo assim, analisamos por *Western Blotting* os níveis proteicos desse receptor e notamos que sua expressão se restringiu ao segundo dia do protocolo (Figura 23 N), momento no qual os corpos embriôides estão no estágio similar de gástrula com os 3 folhetos embrionários, indicando um possível papel do receptor P2X1 no início do desenvolvimento embrionário.

Para que os receptores do tipo P2 sejam ativados é necessário que haja ATP disponível no meio extracelular, que pode ser liberado pela própria célula ou por células ao entorno. Portanto, averiguamos indiretamente os níveis de ATP liberados por 5min no meio extracelular por luminescência (a reação catalisada por luciferase na presença de ATP emite luz). Vimos que os níveis de ATP se mantiveram altos até o 12º dia de diferenciação (Figura 23 O), ou seja, enquanto existem precursores neurais, corroborando um possível papel dos receptores purinérgicos do tipo P2 na biologia dessas células.

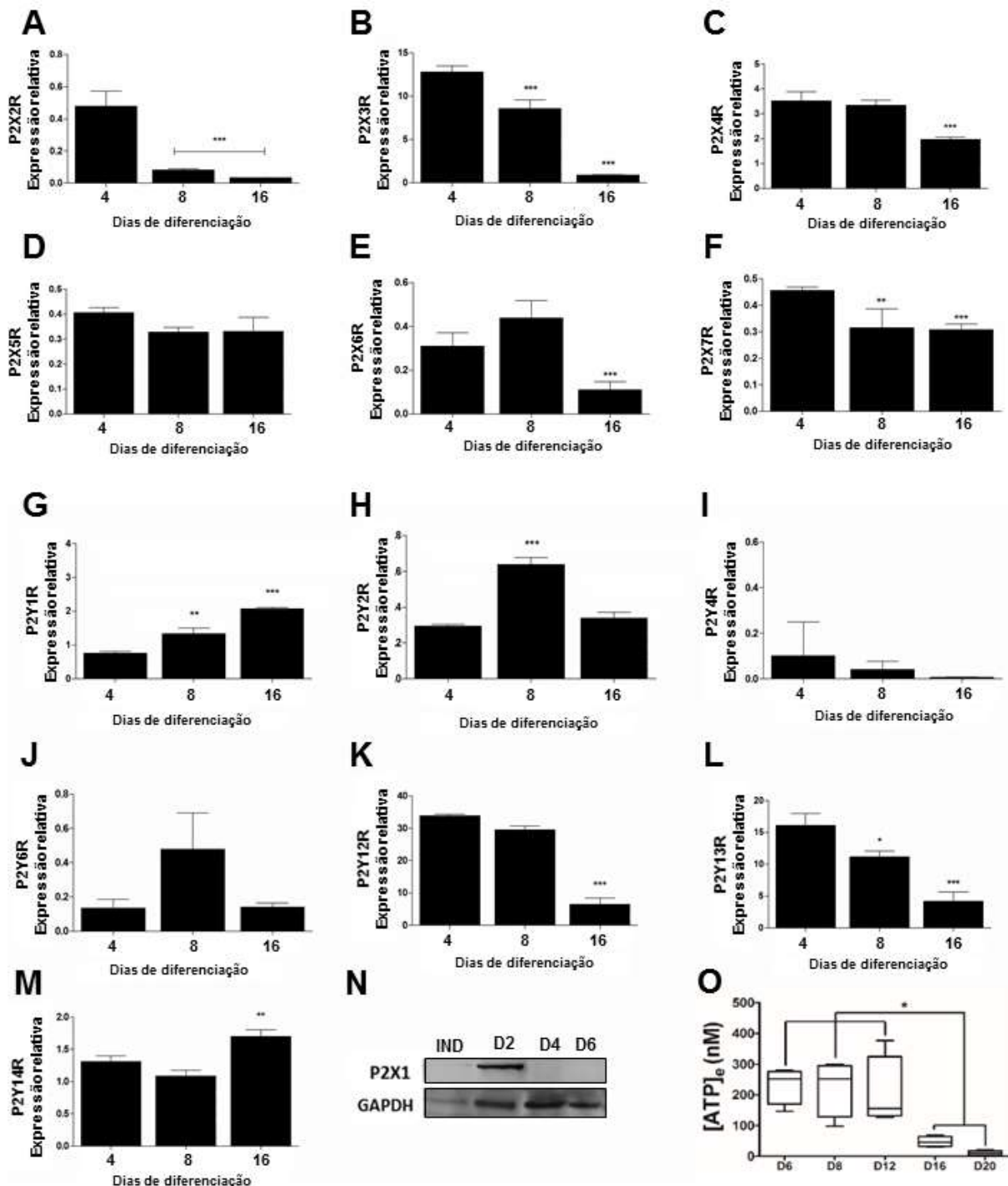


Figura 23. Padrões de expressão de receptores purinérgicos do tipo P2 e níveis de ATP extracelular na diferenciação neural de CTE. Níveis da expressão gênica relativa de corpos embrióides diferenciados por 4, 8 e 16 para os receptores purinérgicos P2X2-7 (A-F) e P2Y1,2,4,6,12,13 e 14 (G-M). Dados normalizados pela expressão do gene endógeno GAPDH. ANOVA de uma via, *P≤0,05, **P≤0,01, ***P≤0,001. N. Análise dos níveis proteicos do receptor P2X1 ao longo da diferenciação neural induzida por AR por western blotting. O. Concentrações de ATP extracelular liberados após 5minutos de incubação em células diferenciadas por 6, 8, 12, 16 e 20 dias, medidos indiretamente por bioluminescência. ANOVA de uma via *P≤0,05.

4.4.2 Papéis do receptor P2X7 em CTE

O receptor P2X7 é o mais amplamente estudado dentre todos os receptores purinérgicos, visto que normalmente complexa-se com outros P2X7 formando um homomultímero, além de possuir moduladores farmacológicos comerciais mais específicos, facilitando o seu estudo (Duan & Neary 2006).

Dessa forma, focamos primeiramente em investigar os possíveis papéis desse receptor em nosso protocolo de diferenciação de CTE (para os resultados obtidos veja também (Glaser et al. 2014)). Primeiramente, observamos por microscopia confocal que tanto as células no estado indiferenciado como no 8º dia de diferenciação apresentavam a expressão do receptor P2X7 na membrana celular (Figura 24). Contudo, a análise por *western blotting* dos níveis proteicos demonstrou que a expressão desse receptor diminui ao longo do processo de diferenciação neural, concomitantemente aos níveis de Oct4 (fator de transcrição relacionado à pluripotência), sendo que nas células indiferenciadas foram apresentadas uma banda de ~75KD e outra de ~100KDa (Figura 25A-C). Já foi descrito que a espécie de 75KDa pode ser a forma glicosilada e funcional do receptor (Young et al. 2007), mas ainda não foi descrito uma espécie do receptor com 100KDa.

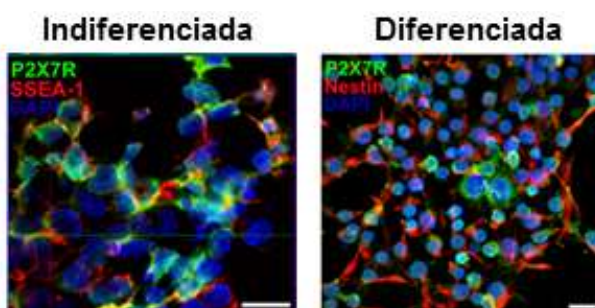


Figura 24. Expressão e localização do receptor P2X7 por microscopia confocal. CTE indiferenciadas e diferenciadas por 8 dias após estímulo com 5µM de AR foram co-imunomarcados para expressão de P2X7(verde), SSEA-1 ou Nestina (vermelho). Cromatina em azul (DAPI). Escala 50µm. Experimento representativo de 3 experimentos independentes.

Curiosamente, apenas a banda de 100KDa foi revelada quando imunomarcou-se as membranas utilizando um anticorpo que reconhece apenas a porção intracelular C-terminal do receptor, região presente apenas na isoforma canônica (Figura 25A) e ausente na truncada. A marcação é confiável, visto que as bandas de 75 e 100KDa não foram detectadas em lisados proteicos de cérebro de animais Knockout para P2X7 (P2X7^{-/-}) (Figura 25D).

Por esse motivo, sugerimos que as duas bandas podem representar formas variantes de *splicing* alternativo do gene para P2X7R. No intuito de determinar o padrão de expressão das diferentes isoformas de P2X7R, realizou-se RT-PCR utilizando iniciadores específicos e, como demonstrado na figura 25E, somente os transcritos das isoformas 1 e 2 (também chamadas de A e B) foram expressos. Vale destacar que as isoformas A e B correspondem às formas canônica e truncada de P2X7, respectivamente. Essas informações, juntamente com os dados obtidos por Western Blotting, sugerem que as duas bandas observadas equivalem às isoformas P2X7A e P2X7B.

A expressão da isoforma B decaiu conforme o andamento da diferenciação. Como essa isoforma não é capaz de formar grandes poros na membrana, ao contrário da isoforma A (Cheewatrakoolpong et al. 2005; Masin et al. 2012), nós especulamos que a expressão da isoforma B durante a fase inicial da diferenciação possa ser um mecanismo contra a morte celular causada pela formação dos poros, permitindo que mais células proliferem e diferenciem.

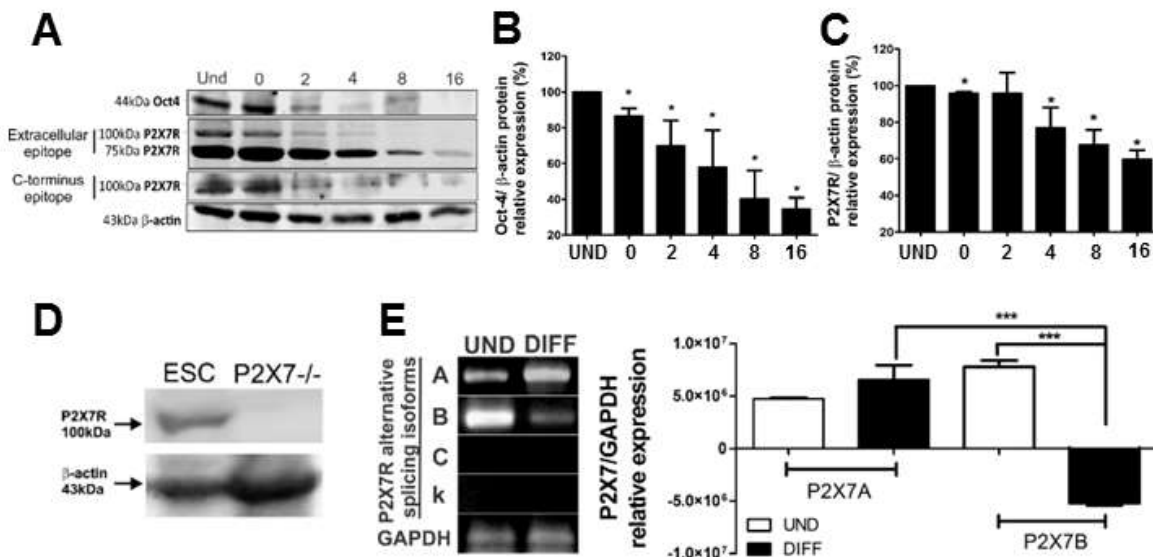


Figura 25. Níveis de expressão gênica e proteica do receptor P2X7 e de suas variantes de splicing alternativo. **A.** CTE (UND) e células após 2,4,8 e 16 dias de indução da diferenciação neural tiveram os níveis proteicos de Oct4, β-actina e P2X7, foram analisados por Western Blotting. Um anticorpo que reconhece a porção extracelular e outro que reconhece a porção C-terminal do receptor P2X7 foram utilizados. **B. e C.** Quantificação dos níveis proteicos de Oct4 e P2X7 por densitometria de bandas de 3 experimentos independentes. Barras representam media e \pm erro padrão (S.E.). Anova de uma via (*p<0,05, **p<0,01, ***p<0,001 comparado à UND). **D.** Detecção de P2X7 em amostras de CTE e de cérebros de animais knockout para P2X7 (P2X7^{-/-}). **E.** Expressão diferencial de isoformas de splicing alternativo do receptor P2X7 em células indiferenciadas (UND) e diferenciadas por 8 dias (DIFF) determinadas por RT-PCR e a respectiva análise por densitometria de bandas comparadas a expressão de GAPDH. Anova de uma via (*p<0,05, **p<0,01, ***p<0,001).

De acordo com a expressão do receptor P2X7, a análise da indução na $\Delta[\text{Ca}^{2+}]_i$ com os agonistas ATP e Bz-ATP (agonista específico para P2X7R) por verificação de alterações $\Delta[\text{Ca}^{2+}]_i$ ou por microfluorimetria indicou que o EC₅₀ em células indiferenciadas foi de $4,1 \pm 1,8\mu\text{M}$ para estimulação por ATP e $1,7 \pm 2,2\mu\text{M}$ para o Bz-ATP, enquanto que para as células diferenciadas foi de $4.1 \pm 1.4\mu\text{M}$ e $4.7 \pm 1.5\mu\text{M}$ (Figura 26 A e B). Os estímulos foram específicos, visto que o pré-tratamento por 2 min com inibidores do receptor P2X7 ($10\mu\text{M}$ de KN-62 e $1\mu\text{M}$ de A438079 Figura 26C e D) aboliu a resposta induzida por $10\mu\text{M}$ de Bz-ATP. Alguns estudos já demonstraram que a ativação de P2X7R necessita de doses altas de ATP (100-1000 μM) para desencadear morte celular (Burnstock & Williams 2000), e Francesco Di Virgilio

demonstrou que o receptor, quando ativado por doses menores, pode induzir efeitos tróficos (Di Virgilio et al. 2009).

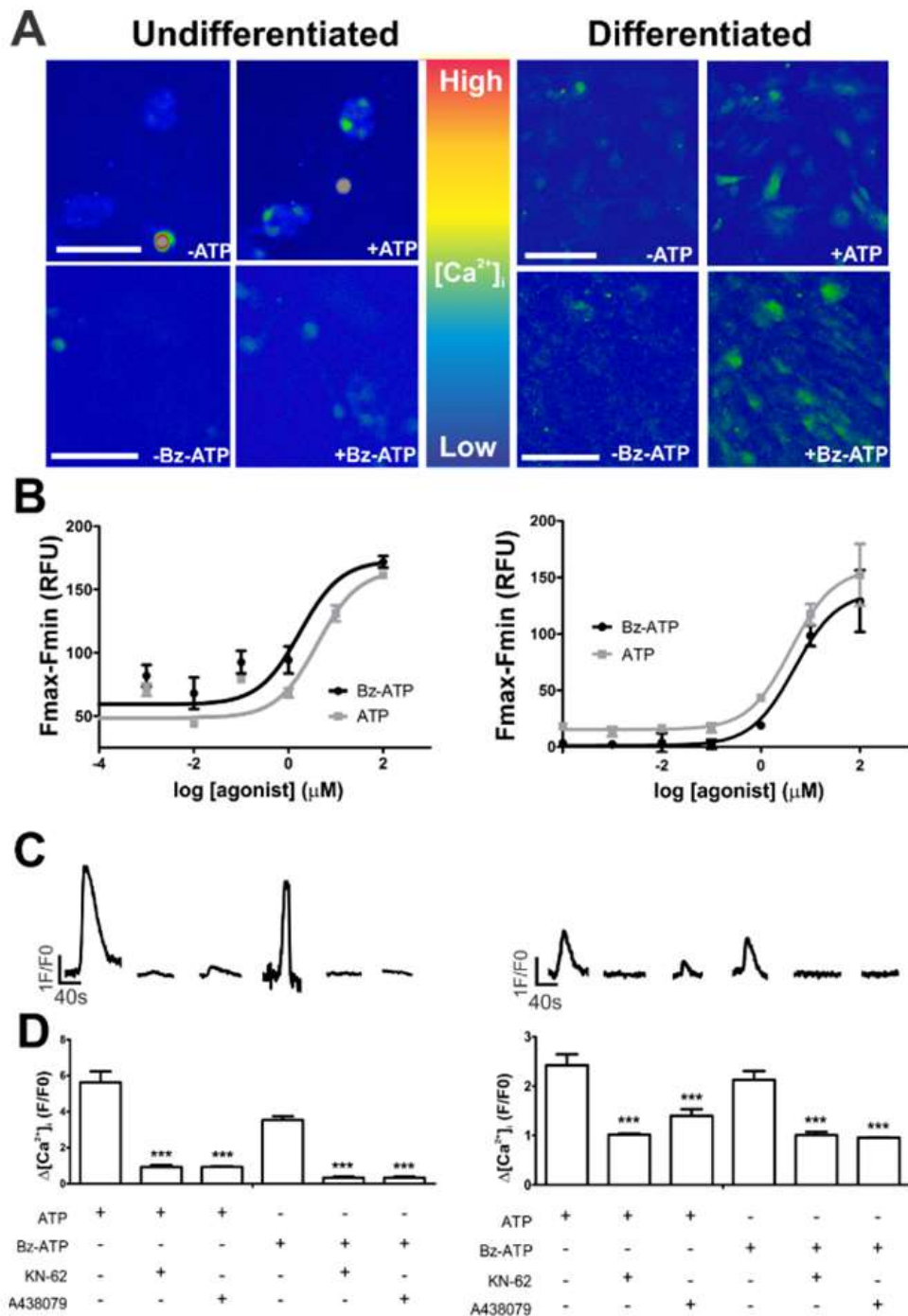


Figura 26. $\Delta[\text{Ca}^{2+}]_i$ induzidas por ATP e Bz-ATP em células indiferenciadas e diferenciadas por 8 dias. $\Delta[\text{Ca}^{2+}]_i$ evocadas por ATP e Bz-ATP foram determinadas por verificação de alterações $\Delta[\text{Ca}^{2+}]_i$ por microscopia e por microfluorimetria. **A.** Por microscopia foi aplicado 10 μM de ATP ou Bz-ATP. 1 frame/seg. **B.** Para microfluorimetria concentrações crescentes de ATP ou Bz-ATP foram adicionados. Regressão não linear para ajuste da curva para calcular EC₅₀. **C e D.** Inibidores específicos do receptor P2X7 foram pré-aplicados por 2 min e bloquearam a resposta evocada por Bz-ATP. Dados representam média ± erro padrão de 3 experimentos independentes.

A expressão do receptor P2X7 em células neurais já foi documentado anteriormente, como em embriões de ratos E15.5 que expressam o transcrito de P2X7R em células tronco neurais (Tsao et al. 2013). Na mesma linha, células Neuro-2a e SH-SY5Y quando tratadas com AR diminuem a expressão do receptor P2X7 (Wu et al. 2009; Orellano et al. 2010), o que corrobora nossa hipótese de que a expressão e ativação diferencial de P2X7R é necessário para a diferenciação de CTE em neurônios.

Diversos trabalhos já demonstram que P2X7R pode regular a proliferação celular, principalmente em tumores (Di Virgilio et al. 2009; Lemoli et al. 2004; Bianco et al. 2006; Adinolfi et al. 2012). Para a compreensão do papel do receptor P2X7 na proliferação de CTE, analisamos a distribuição do ciclo celular em células indiferenciadas cultivadas por 96hs na presença de Bz-ATP (0.1 e 1 μ M) ou KN-62 (10 μ M). Os dados demonstram um aumento de 35% para 48% na quantidade de células proliferando (na fase S) na presença do agonista Bz-ATP e uma diminuição de 48% para 31% nas células expostas a KN-62. Corroborando esses dados, a análise da curva de crescimento celular em células tratadas com inibidores do receptor P2X7 (KN-62 e A438079) demonstrou um atraso na proliferação celular, indicando que a atividade do P2X7R modula a proliferação de CTE por acelerar a entrada das células no ciclo celular (Figura 27).

Um possível mecanismo que esteja envolvido na redução de proliferação observada, pode ser através da contribuição do receptor P2X7 para $\Delta[\text{Ca}^{2+}]_i$ que são requeridas para a progressão de G1/S em CTE (Kapur et al. 2007). Normalmente, CTE pulam o ponto de checagem na fase G1 para proliferarem mais rapidamente (Savatier et al. 1994; Savatier et al. 2002), e essa fase só é estendida para o comprometimento na diferenciação (Orford & Scadden 2008; Zhu et al. 2005).

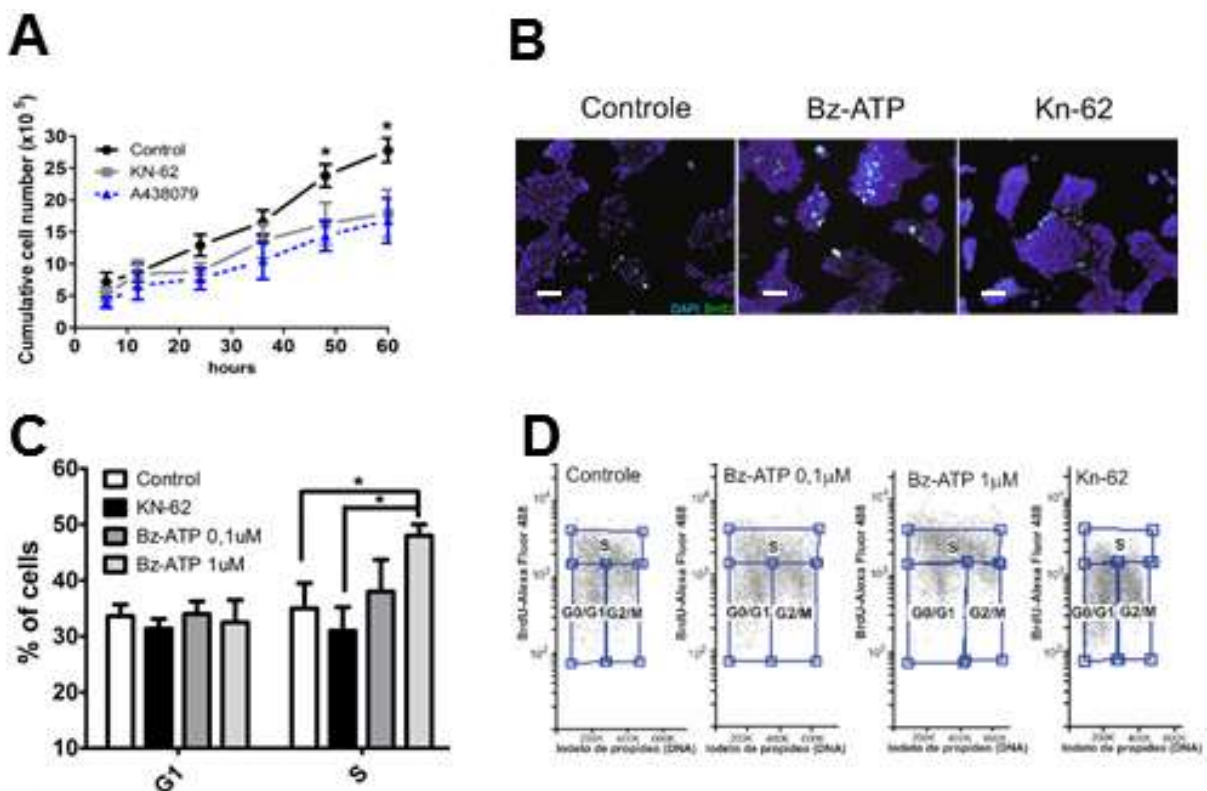


Figura 27. Inibição da proliferação de CTE na presença de inibidores para o receptor P2X7. A. 3×10^5 células/ml foram semeadas e tratadas com inibidores KN-62 ($10\mu\text{M}$) ou A438079 ($1\mu\text{M}$) diariamente e o número de células quantificados. Dados representam média \pm erro padrão de 3 experimentos independentes em triplicata (* $p<0,05$ comparado ao controle). B. Proliferação de CTE tratadas com $1\mu\text{M}$ Bz-ATP e $10\mu\text{M}$ KN-62 indicada pela incorporação de BrdU (verde) por microscopia de fluorescência. Cromatina em azul (DAPI). Escala $50\mu\text{m}$. C e D. Análise do ciclo celular de CTE tratadas com $0,1$ e $1\mu\text{M}$ Bz-ATP e $10\mu\text{M}$ KN-62 indicada pela incorporação de BrdU e marcação do DNA total com iodeto de propídeo por citometria de fluxo. Dados representam média \pm erro padrão de 3 experimentos independentes em triplicata (* $p<0,05$ comparado ao controle).

Dados previamente obtidos em nosso laboratório utilizando células P19 de carcinoma embrionário destacaram a importância do receptor P2X7 na proliferação glial. No presente estudo, utilizando CTE diferenciadas em precursores neurais na presença de Bz-ATP ($10\mu\text{M}$) ou KN-62 ($10\mu\text{M}$), realizou-se análises de expressão gênica de marcadores da diferenciação neural como: nestina, TUJ1 e SSEA-1, um trissacarídeo expresso por células tronco neurais e embrionárias (Capela & Temple 2006; Capela & Temple 2002), além de doublecortina (Dcx), que é expressa por neurônios em migração e diferenciação (Francis et al. 1999). O tratamento com KN-62 levou a um aumento na expressão de SSEA-1 ($> 8,5$ vezes), Dcx ($> 9,1$ vezes) e

TUJ1 (>4,8 vezes) (Figura 28A-D), enquanto que os níveis de nestina não foram alterados.

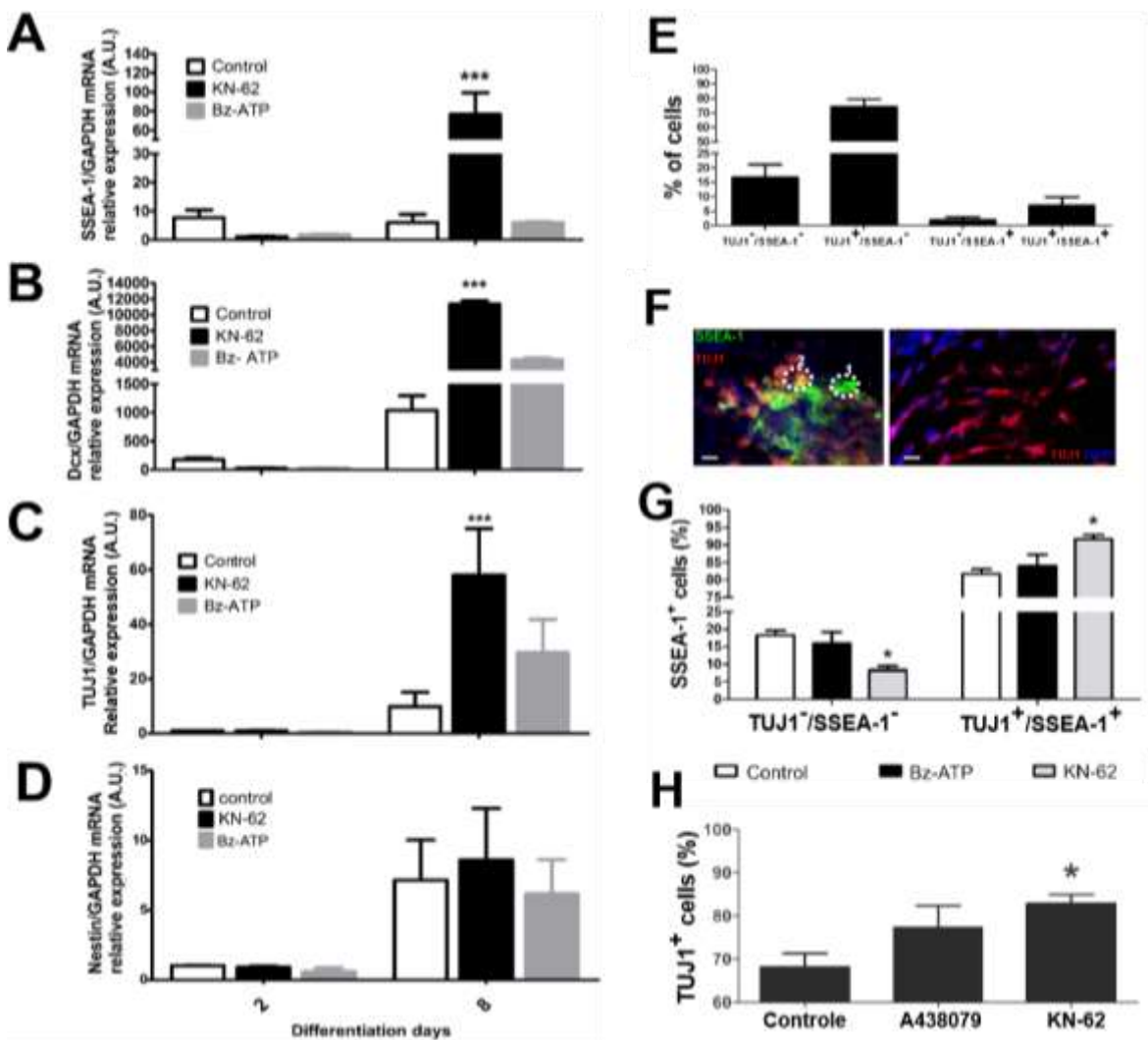


Figura 28. Efeitos da modulação do receptor P2X7 no progresso da diferenciação neural. Análise da expressão gênica relativa de A. SSEA-1, B. Dcx, C. TUJ1 e D. nestina em CTE diferenciadas por 2 e 8 dias e tratadas com 1µM Bz-ATP e 10µM KN-62. O gene GAPDH foi utilizado como normalizador da expressão. Dados representam média ± erro padrão de 3 experimentos independentes em triplicata ANOVA de 2 vias ***P≤0,01. E e F. Análise da expressão de SSEA-1 e TUJ1 por citometria de fluxo e microscopia confocal em células diferenciadas por 8 dias. Células circuladas: 1. Células expressando apenas SSEA-1, 2. Células coexpressando SSEA-1 e TUJ1. Escala 50µm G. Análise da expressão de SSEA-1 e TUJ1 por citometria de fluxo em células diferenciadas por 8 dias na presença de 1µM Bz-ATP, 1µM A438079 ou 10µM KN-62 por 6 dias. Analise estatística de Anova de uma via de 6 experimentos independentes (* p≤0,05 comparado ao controle).

Por citometria de fluxo e microscopia de fluorescência de células coimunomarcadas para SSEA-1 e TUJ1, nota-se que a população de células em diferenciação é heterogênea, pois aproximadamente 70% das células expressam

somente TUJ1 e possuem morfologia neuronal e extensões de neuritos, aproximadamente 15% das células eram duplamente negativas e 15% das células expressam tanto SSEA-1 como TUJ1. Essa população positiva para TUJ1 e SSEA-1, apesar de expressarem uma proteína marcadora de neurônio jovem, revelaram características morfológicas diferentes de neurônios por serem esferoides e parecidas com células indiferenciadas que expressam SSEA-1 (Figura 28E e F).

A inibição do receptor P2X7 promoveu a diferenciação neuronal, visto que o tratamento com KN-62 levou ao aumento no número de células TUJ1 positivas dentre as que são SSEA-1 positivas, e diminuiu o número de células negativas para TUJ1(Figura 28G e H). Provavelmente, a população de células que expressam apenas SSEA-1 não está comprometida, ao passo que as células que expressam SSEA-1 e TUJ1 estão comprometidas para o destino neuronal.

SSEA-1 é um carboidrato, serve como molécula de adesão (Kerr & Stocks 1992)e é expresso em vários tipos celulares, como em células tronco neurais no cérebro adulto (Capela & Temple 2006; Capela & Temple 2002; Uchida et al. 2000). Ademais, TUJ1 pode ser expresso em neurônios imaturos da zona proliferativa da região ventricular e subventricular do telencéfalo em desenvolvimento. No início do desenvolvimento, precursores neuroniais que estão em divisão expressam TUJ1 (Memberg & Hall 1995). Esse tipo de precursor é um neuroblasto, uma célula que divide e diferencia em neurônio após a fase migratória (Hynes et al. 1986). Essas células são normalmente originadas a partir da diferenciação de células neuroepiteliais que expressam SSEA-1 e estão comprometidas com o destino neuronal.

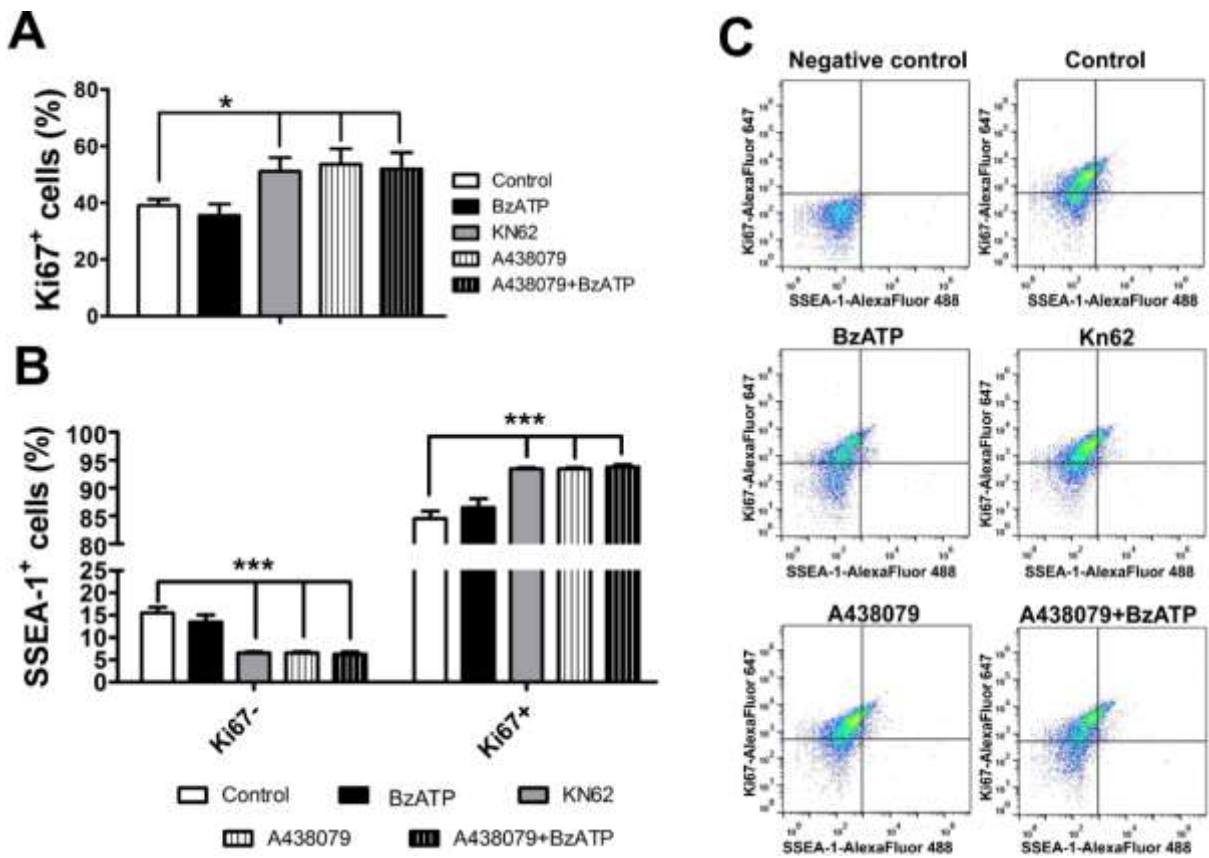


Figura 29. Expressão do antígeno Ki67 de células proliferativas na população de células positivas para SSEA-1 na presença de moduladores da atividade do receptor P2X7. A. Determinação da população positiva para Ki67 por citometria de fluxo de células diferenciadas por 8 dias e tratadas com Bz-ATP (10µM), KN-62 (10µM) ou A438079 (1µM). B. Determinação das porcentagens celulares de Ki67/SSEA-1⁺ e Ki67⁺/SSEA-1⁺ para as condições descritas em A. C. Gráficos Dot-plot de células diferenciadas por 8 dias para dupla marcação de Ki67/SSEA-1 como descrito em B. ANOVA de uma via de 5 experimentos independentes (*p<0,05, ***p<0,001 comparado ao controle).

A análise da coexpressão de SSEA-1 e Ki67 por citometria de fluxo revelou que a maioria das células expressavam ambos os marcadores, corroborando os dados anteriores de que as células que expressam TUJ1 e SSEA-1 sejam neuroblastos. Ainda mais, a inibição do receptor P2X7 levou ao aumento de células expressando Ki67 e SSEA-1.

Resumindo nossos dados, a inibição do receptor P2X7 mostrou-se essencial para que células tronco neuroepiteliais se diferenciem em neuroblastos, constatação

obtida pela observação de que, após o comprometimento, as células ainda possuem capacidade proliferativa (Figura 29). Células SSEA-1⁺/TUJ1⁻ podem ser células tronco neuroepiteliais que originam neuroblastos (SSEA-1⁺/TUJ1⁺) que por sua vez se diferenciam em neurônios (SSEA-1⁻/TUJ1⁺), processo no qual a expressão do receptor P2X7 deve decair para favorecer a diferenciação.

4.4.3 Envolvimento dos receptores purinérgicos nas $\Delta[\text{Ca}^{2+}]_i$ espontâneas e na expressão de fatores de transcrição pró-neurais

A transição do estado proliferativo para neurogênese envolve o aumento coordenado da atividade de fatores pró-neurais bHLH (Mash1, Neurogenin1 e Neurogenin2) e uma diminuição dos fatores Hes e Id. Além de estudarmos a influência de Cav1 nas $\Delta[\text{Ca}^{2+}]_i$ espontâneas, nós também acompanhamos as $\Delta[\text{Ca}^{2+}]_i$ geradas após a aplicação de ATP, Bz-ATP (agonista de receptores P2X) e 2SUTP (agonista dos subtipos P2Y2 e P2Y4) (Donnelly-Roberts et al. 2009; El-Tayeb et al. 2006) em:

- a. células precursoras neurais de animais transgênicos portadores do constructo Mash1 fusionado à Luciferase; e b. em células tronco embrionárias transgênicas para Ngn2 fusionado à Luciferase, diferenciadas previamente em precursores neurais.

Além disso, analisamos como as $\Delta[\text{Ca}^{2+}]_i$ moduladas por esses receptores purinérgicos influenciam na expressão de Mash1 e Ngn2.

Dessa forma constatamos que, em células precursoras neurais, a aplicação de Bz-ATP levou ao aumento na frequência de $\Delta[\text{Ca}^{2+}]_i$ espontâneas e aumento em Ngn2, sem influenciar a expressão de Mash1 (Figura 30 e 31). Já a aplicação de 2SUTP levou também a um aumento no número de disparos de $\Delta[\text{Ca}^{2+}]_i$ espontâneas, porém mais distribuídas em intervalos regulares, e consequentemente levou a um aumento na expressão de Mash1 sem alterar o perfil da curva (padrão não oscilatório).

EGTA (quelante de cálcio extracelular) e tapsigargina (depletor da concentração de cálcio no retículo endoplasmático) também foram empregados nos ensaios. Observamos que ambos impediram tanto as $\Delta[\text{Ca}^{2+}]_i$ quanto a expressão dos fatores pró-neurais.

Em posse desses resultados, podemos propor que a ativação de P2X7R leva ao aumento na expressão de Ngn2, e a ativação dos receptores P2Y2 e P2Y4 aumenta a expressão de Mash1 na forma estável. Como constatamos que P2X7R deve ser inibido para que as células diferenciem em neuroblastos, podemos especular que esse aumento desordenado na amplitude das oscilações leve a um sinal inibitório para a diferenciação, enquanto que disparos organizados e bem distribuídos em intervalos de tempo induzam a diferenciação.

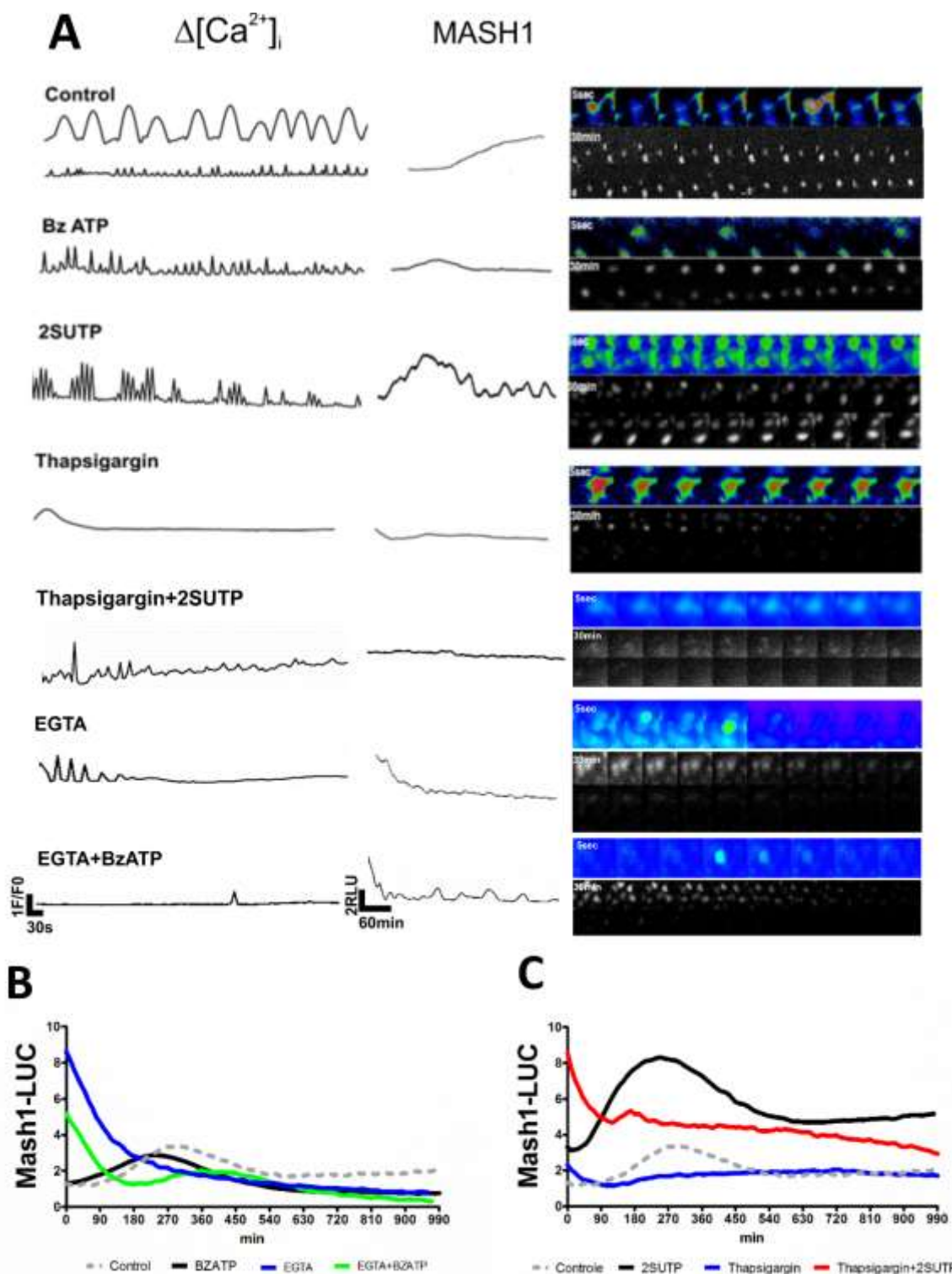


Figura 30. Perfil da $\Delta[\text{Ca}^{2+}]$ espontânea e expressão em tempo real de Mash1 em NSC e modulação por receptores purinérgicos. **A.** Análise a nível unicelular. NSC foram marcadas com Fluo3-AM e sua intensidade medida como forma indireta de $[\text{Ca}^{2+}]_i$ por 20min. No centro estão os perfis da expressão de Mash1 em NSCs tratadas com 10 μM de Bz-ATP, 1 μM de 2SUTP, 1 μM de Tapsigargin, 2mM de EGTA. À direita estão as montagens sequenciais das imagens do vídeo para verificação de alterações $\Delta[\text{Ca}^{2+}]_i$ e luminescência. **B.** Análise total da população celular. Perfil da expressão de Mash1 na população de NSC com o receptor P2X7 ativado e com depleção de Ca^{2+} extracelular. **C.** Perfil da expressão de Mash1 na população de NSC com os receptores P2Y2 e P2Y4 ativados e com depleção de Ca^{2+} do retículo endoplasmático. Dados representativos de 3 ns experimentais.

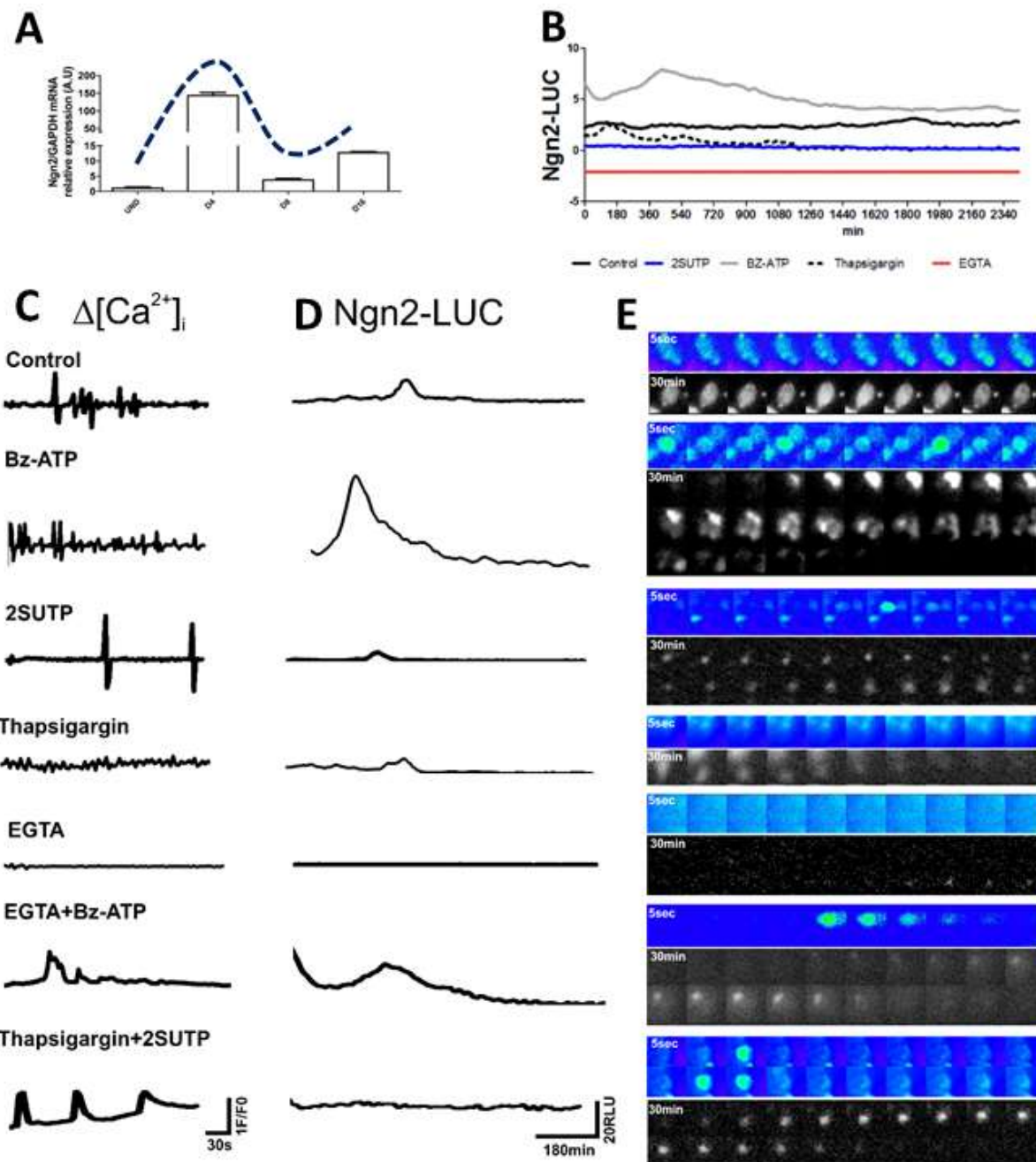


Figura 31. Perfil da $\Delta[\text{Ca}^{2+}]_i$ espontânea e expressão em tempo real de Ngn2 em corpos embriônicos com oito dias de diferenciação e modulação por receptores purinérgicos.

A. Níveis de expressão gênica relativa de Ngn2 ao longo da diferenciação neural de CTE. Valores normalizados pela expressão do gene endógeno GAPDH. B. Análise da população total de CTE previamente diferenciadas em precursores neurais e tratadas com 10 μM Bz-ATP, 1 μM de 2SUTP, 1 μM de Tapsigargina, 2mM de EGTA foram filmadas por 2 dias e foi gravada a luminescência emitida, correspondente à expressão de Ngn2. 1imagem/10min C. Análise total da população celular. CTE previamente diferenciadas em precursores neurais e tratadas com 10 μM Bz-ATP, 1 μM de 2SUTP, 1 μM de Tapsigargina, 2mM de EGTA foram marcadas com Fluo3-AM e sua intensidade medida como forma indireta de $[\text{Ca}^{2+}]_i$ por 20min 1frame/5seg. D. Análise a nível unicelular. Perfis da expressão de Ngn2 em NSCs tratadas com 10 μM de Bz-ATP, 1 μM de 2SUTP, 1 μM de Tapsigargina, 2mM de EGTA. E. Análise a nível unicelular. Montagens sequenciais das imagens do vídeo para verificação de alterações $\Delta[\text{Ca}^{2+}]_i$ e luminescência. Dados representativos de 3 ns experimentais.

4.4.4 Conclusão parcial sobre receptores purinérgicos

Nossos dados mostraram que, enquanto existiam precursores neurais, os níveis de ATP se mantiveram altos durante a diferenciação neural induzida por AR. Além disso, todos os receptores do tipo P2 estavam expressos, em diferentes intensidades.

A atividade do receptor P2X7 modula a proliferação de CTE por acelerar a entrada das células no ciclo celular, e sua expressão também deve decair ao longo da diferenciação para favorecer a diferenciação de neuroblastos.

Além do mais, a ativação de P2X7R pode levar ao aumento na expressão de Ngn2 por aumentar a frequência de disparos de $\Delta[\text{Ca}^{2+}]_i$ espontâneas do tipo pico, e a ativação dos receptores P2Y2 e P2Y4 pode aumentar a expressão de Mash1 por aumentar a frequência e amplitude de picos de maneira ritmada, induzindo a diferenciação.

4.5 $\Delta[\text{Ca}^{2+}]_i$ ESPONTÂNEAS REGULANDO O DESTINO NEURAL

4.5.1 Convergência entre os sinais gerados por receptores purinérgicos e VGCC

A fim de esclarecermos e compilarmos os dados obtidos sobre o papel dos receptores purinérgicos e de Cav1 durante a diferenciação neural juntamente com $\Delta[\text{Ca}^{2+}]_i$ espontâneas, nós quantificamos os dados de expressão máxima de Mash1 e Ngn2 descritos no item anterior e fizemos uma relação de Mash1 por Ngn2 que chamamos de índice neurogênico.

$$\text{Índice neurogênico} = \text{Mash1} / \text{Ngn2}$$

Observa-se que tanto 2SUTP como Isradipina levaram a um aumento nessa relação (Figura 32). Sabemos que o tratamento com Isradipina bloqueou a neurogênese mantendo as células em estágio de precursores pelo padrão oscilatório de Mash1. No entanto para 2SUTP ainda não tínhamos dados que mostrassesem tal relação.

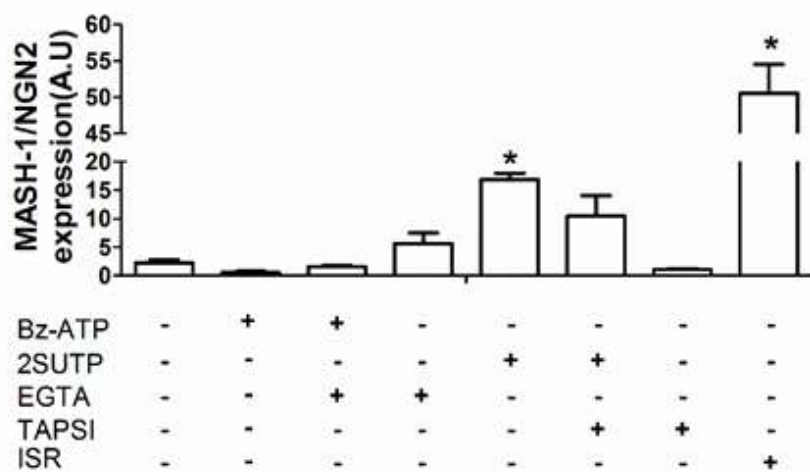


Figura 32. Índice neurogênico (Mash1/Ngn2). As mensurações obtidas na figura qq e qqq foram reunidas em uma relação e plotadas acima. As células foram tratadas com Bz-ATP (agonista de P2X7R), 2SUTP (agonista de P2Y2 e P2Y4), Thapsigargin (depletor do retículo endoplasmático), EGTA (quelante de Ca²⁺) e Isradipina (bloqueador de canais para Ca²⁺ voltagem dependentes do tipo L). * P≤0,05.2

Com essa finalidade, nós fizemos PCR em tempo real para diferentes tipos de neurônios (fenótipos neuronais) de amostras tratadas com moduladores de receptores purinérgicos e observamos que 2SUTP levou a um aumento na expressão de GAD65, um marcador de neurônios GABAérgicos (Figura 33), possivelmente por aumentar a frequência ritmada de $\Delta[\text{Ca}^{2+}]_i$ espontâneas e a expressão de Mash1estável. Esses dados corroboram os obtidos por Ciccolini no qual aumento na frequência de oscilações globais acelerou a diferenciação GABAérgica de precursores neurais (Ciccolini et al. 2003).

Portanto podemos concluir que as $\Delta[\text{Ca}^{2+}]_i$ espontâneas ao longo do processo de diferenciação podem ser moduladas tanto por VGCC como por receptores purinérgicos e que consequentemente modulam fatores de transcrição capazes de decidir o destino celular neuronal, alterando o equilíbrio entre Mash1 e Ngn2.

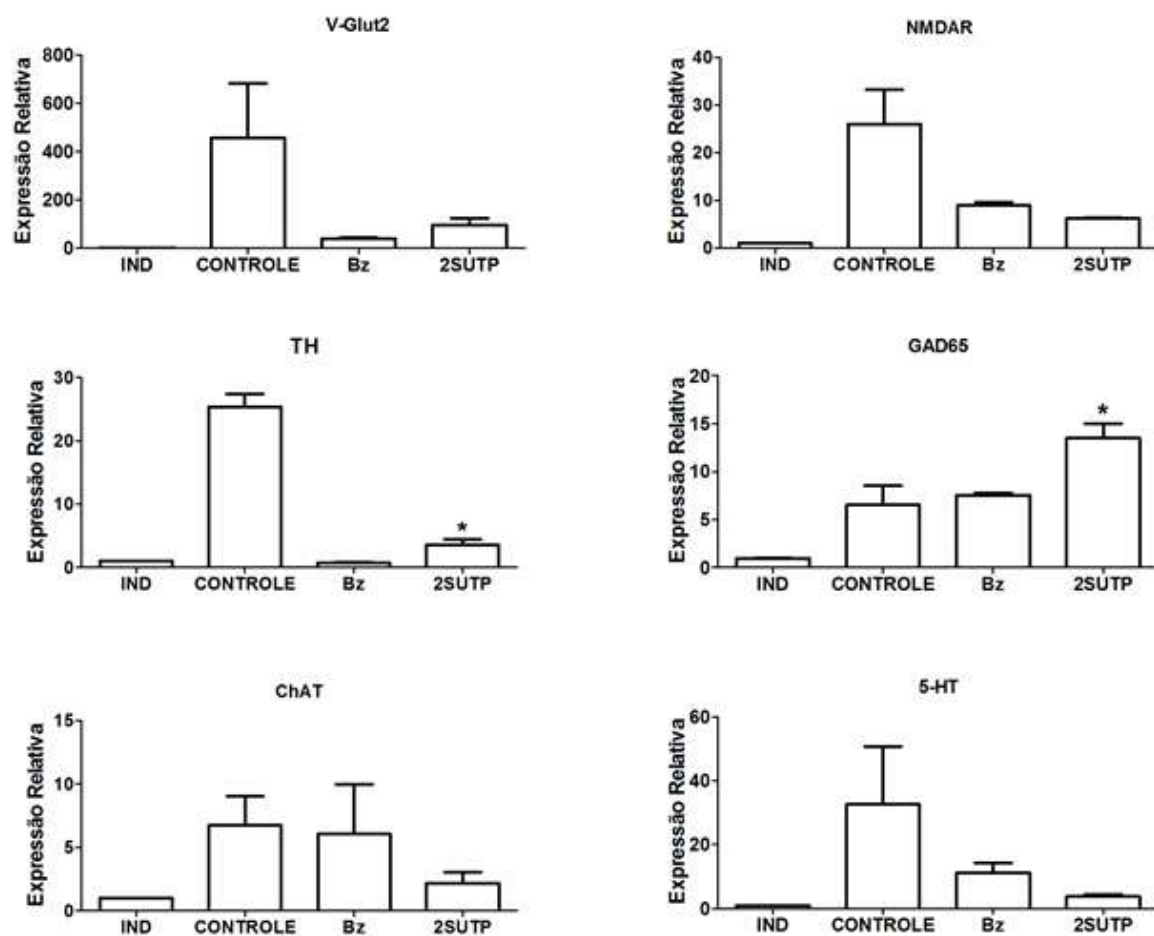


Figura 33. Modulação dos receptores P2X7, P2Y2 e P2Y4 e influência nos fenótipos neurais obtidos a partir da diferenciação neural de CTE. Análise da expressão gênica relativa de CTE diferenciadas por 16 dias e tratadas cronicamente desde o 6º dia com 1 μM Bz-ATP e 1 μM de 2SUTP para os genes V-Glut2 (glutamatérgicos), NMADR (glutamatérgicos), TH (tirosina hidroxilase, dopaminérgico), GAD65 (GABAérgico), ChAT (acetilcolinesterase, colinérgico), 5-HT (5-hidroxitriptamina, serotoninérgico). Dados foram normalizados pela expressão do gene endógeno GAPDH. Anova de uma via * $P \leq 0,05$.

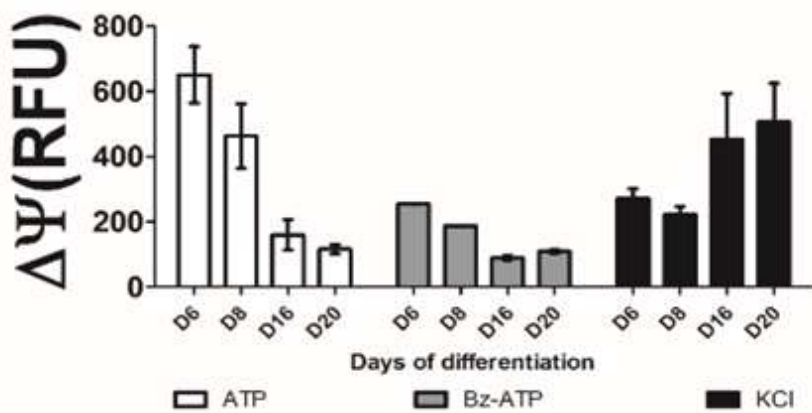


Figura 34. ATP extracelular e influência no potencial de membrana de corpos embrióides ao longo da diferenciação neural. Corpos Embrióides de E14 TG2A foram submetidos à diferenciação induzida por ácido retinóico 5uM. Variação no potencial de membrana ($\Delta\Psi$) de EBs tratados com agonista de receptor P2X7 (1 μ M Bz-ATP), 10 μ M ATP e 60mM de KCl.

Como vários artigos já descreveram a capacidade de ATP em despolarizar a membrana celular (Buisman et al. 1988) e a fim de esclarecermos se haveria alguma relação entre os receptores purinérgicos e os VGCC, nós aplicamos ATP e Bz-ATP nas células e medimos a variação no potencial de membrana celular. Demostramos que ATP e Bz-ATP são capazes de despolarizar os precursores neurais, sendo que o estímulo com ATP, que é agonista de uma gama maior de receptores purinérgicos que o Bz-ATP, apresentou uma amplitude maior (Figura 34).

4.5.2 Conclusão parcial

Esses dados indicam que a ativação de receptores purinérgicos ativados por ATP induzem uma despolarização da membrana celular de precursores neurais, podendo levar à ativação de Cav1, que precede o aumento da expressão estável de Mash1, culminando na diferenciação neuronal.

CONCLUSÕES FINAIS

5. CONCLUSÕES FINAIS

Nossos dados sugerem que:

- A indução da diferenciação neural de células tronco embrionárias assemelha-se numa forma simplificada ao encontrado no embrião em desenvolvimento, visto os fenótipos neuronais obtidos, tais como neurônios motores, sensoriais, dopaminérgicos, colinérgicos, glutamatérgicos e GABAérgicos, sendo que o corpo embrióide apresenta um gradiente de SHH produzido por ele mesmo, assim como observado no embrião. Além disso, as etapas da diferenciação são bem determinadas, sendo facilmente distinguível entre a indução da diferenciação neuroectodermal, neurogênese, a gliogênese e a maturação neuronal.
- Assim como em *Xenopus*, a diferenciação neural de células murinas também apresentam oscilações espontâneas na $[Ca^{2+}]_i$ do tipo pico e onda. Além desses padrões identificamos um novo padrão que chamamos de unique e que possui uma duração longa (~3min).
- Ondas são desencadeadas por liberação de cálcio intracelular induzido por IP3 e que picos por Ca^{2+} de origem extracelular, enquanto que unique depende das duas fontes de cálcio.
- A inibição na neurogênese após bloqueio de Cav1 dá-se pela desestabilização na expressão Mash1. Portanto, para que a neurogênese ocorra, Cav1 deve ser ativado, as $\Delta[Ca^{2+}]_i$ ocorrem e induzem a fosforilação e a translocação de CREB para o núcleo, que consequentemente ativa a transcrição estável de Mash1, que leva então à diferenciação neuronal.
- Os níveis de ATP se mantiveram altos durante a diferenciação neural induzida por AR enquanto existiam precursores neurais

➤ Todos os receptores do tipo P2 estavam expressos, variando apenas os níveis de expressão.

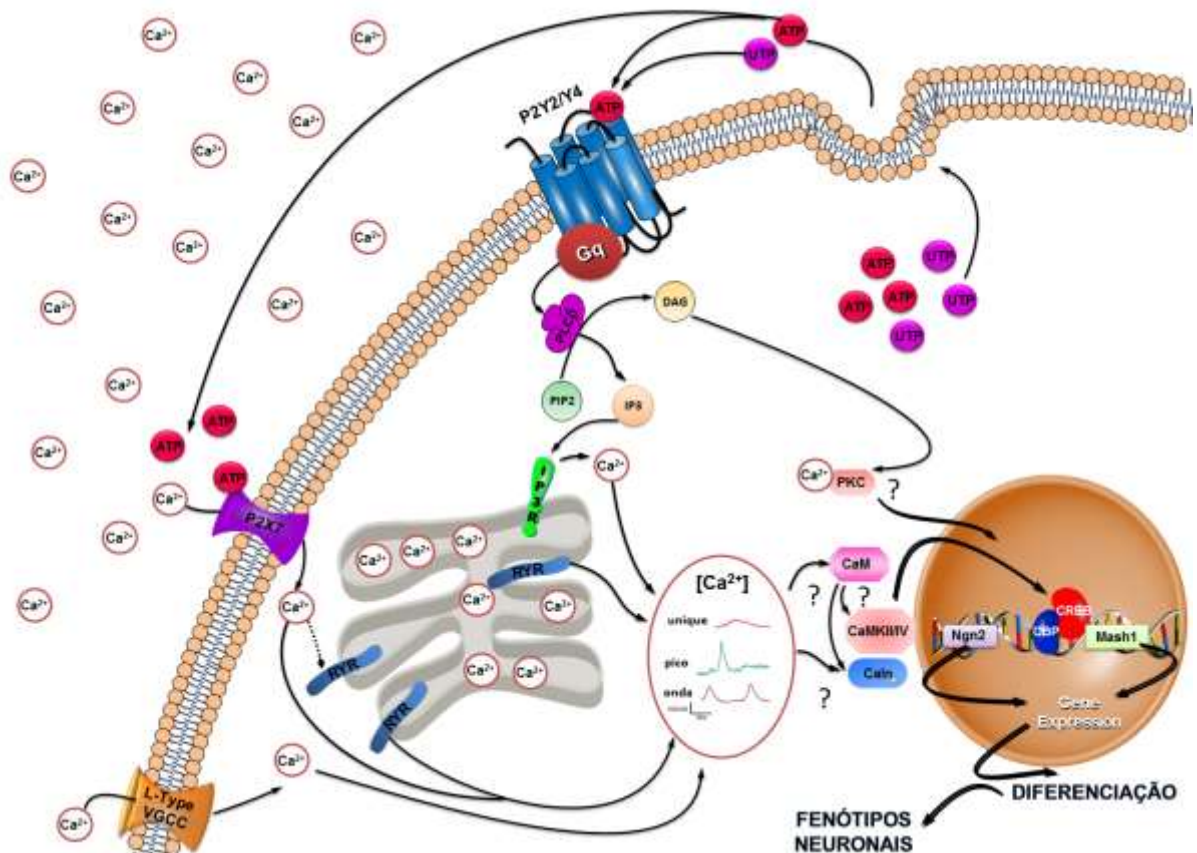


Figura 35. Conclusão dos dados obtidos e possíveis interações descritas na literatura. ATP e UTP podem ser liberados no meio extracelular ativando receptores purinérgicos do tipo P2X ou P2Y e consequentemente induzindo a entrada de cálcio extracelular (P2X7) ou extrusão e cálcio dos estoques intracelulares (P2Y2 e Y4) através de ativação de IP3R ou RYR. Canais para Ca^{2+} voltagem dependentes do tipo L podem ser ativados por um potencial de ação elétrico durante uma despolarização e permitir a entrada de cálcio extracelular. O aumento de cálcio pode levar a indução de oscilações de cálcio que ativam quinases e fosfatases dependentes da concentração de Ca^{2+} , do local e do tempo, levando a ativação ou inibição de fatores de transcrição que modulam a expressão de Ngn2 e Mash1 e definem o destino celular. CREB pode ser fosforilado e manter a expressão de Mash1 estável após ativação de Canais para Ca^{2+} voltagem dependentes do tipo L. A Ativação de P2Y2 e P2Y4 favorecem a expressão de Mash1 estável e a diferenciação para neurônio GABAérgico. Possíveis quinases e fosfatases descritas na literatura como mediadores do processo estão identificadas com o símbolo de interrogação (?) na ilustração.

- A atividade do receptor P2X7 modula a proliferação de CTE por acelerar a entrada das células no ciclo celular, e sua expressão também deve decair ao longo da diferenciação para favorecer a diferenciação de neuroblastos.
- A ativação do receptor P2X7 pode levar ao aumento na expressão de Ngn2 por aumentar a frequência de disparos de $\Delta[\text{Ca}^{2+}]_i$ espontâneas do tipo pico, e P2Y2 e P2Y4 podem aumentar a expressão de Mash1 por aumentar a frequência e amplitude de $\Delta[\text{Ca}^{2+}]_i$ do tipo picos de maneira ritmada, induzindo a diferenciação.
- A despolarização através da ativação de receptores purinérgicos seguidos da ativação de Cav1, e a ativação de P2Y2, P2Y4 e Cav1 podem levar ao aumento da expressão estável de Mash1 resultando na diferenciação neuronal.

Portanto, o trabalho demonstrou que receptores purinérgicos podem atuar como moduladores de ajuste fino do destino neural, por alterar os padrões de oscilações espontâneas na $[\text{Ca}^{2+}]_i$ do tipo pico e consequentemente a ativação de fatores de transcrição pró-neurais.

6.REFERÊNCIAS BIBLIOGRÁFICAS

- Abbracchio, M.P. et al., 2006. International Union of Pharmacology LVIII: update on the P2Y G protein-coupled nucleotide receptors: from molecular mechanisms and pathophysiology to therapy. *Pharmacol Rev*, 58(3), pp.281–341.
- Abrançhes, E. et al., 2009. Neural differentiation of embryonic stem cells in vitro: a road map to neurogenesis in the embryo. *PLoS One*, 4(7), p.e6286.
- Adinolfi, E. et al., 2012. Expression of P2X7 receptor increases in vivo tumor growth. *Cancer Res*, 72(12), pp.2957–2969.
- Ando, H. et al., 2003. IRBIT, a novel inositol 1,4,5-trisphosphate (IP3) receptor-binding protein, is released from the IP3 receptor upon IP3 binding to the receptor. *J Biol Chem*, 278(12), pp.10602–10612.
- Bain, G. et al., 1995. Embryonic stem cells express neuronal properties in vitro. *Dev Biol*, 168(2), pp.342–357.
- Bain, G. et al., 1996. Retinoic acid promotes neural and represses mesodermal gene expression in mouse embryonic stem cells in culture. *Biochem Biophys Res Commun*, 223(3), pp.691–694.
- Bazan, E. et al., 2004. In vitro and in vivo characterization of neural stem cells. *Histol Histopathol*, 19(4), pp.1261–1275.
- Ten Berge, D. et al., 2008. Wnt signaling mediates self-organization and axis formation in embryoid bodies. *Cell Stem Cell*, 3(5), pp.508–518.
- Berridge, M.J., 2012. Calcium signalling remodelling and disease. *Biochem Soc Trans*, 40(2), pp.297–309.
- Berridge, M.J., 2013. Dysregulation of neural calcium signaling in Alzheimer disease, bipolar disorder and schizophrenia. *Prion*, 7(1), pp.2–13.
- Berridge, M.J., 2009. Inositol trisphosphate and calcium signalling mechanisms. *Biochim Biophys Acta*, 1793(6), pp.933–940.

- Berridge, M.J., Bootman, M.D. & Roderick, H.L., 2003. Calcium signalling: dynamics, homeostasis and remodelling. *Nat Rev Mol Cell Biol*, 4(7), pp.517–529.
- Berridge, M.J., Lipp, P. & Bootman, M.D., 2000. The versatility and universality of calcium signalling. *Nat Rev Mol Cell Biol*, 1(1), pp.11–21.
- Bertrand, N., Castro, D.S. & Guillemot, F., 2002. Proneural genes and the specification of neural cell types. *Nat Rev Neurosci*, 3(7), pp.517–530.
- Bianco, F. et al., 2006. A role for P2X7 in microglial proliferation. *J Neurochem*, 99(3), pp.745–758.
- Bosanac, I. et al., 2002. Structure of the inositol 1,4,5-trisphosphate receptor binding core in complex with its ligand. *Nature*, 420(6916), pp.696–700.
- Brini, M. et al., 2013. The plasma membrane calcium pump in health and disease. *FEBS J*, 280(21), pp.5385–5397.
- Briscoe, J. & Ericson, J., 2001. Specification of neuronal fates in the ventral neural tube. *Curr Opin Neurobiol*, 11(1), pp.43–49.
- Buisman, H.P. et al., 1988. Extracellular ATP induces a large nonselective conductance in macrophage plasma membranes. *Proc Natl Acad Sci U S A*, 85(21), pp.7988–7992.
- Buonanno, A. & Fields, R.D., 1999. Gene regulation by patterned electrical activity during neural and skeletal muscle development. *Curr Opin Neurobiol*, 9(1), pp.110–120.
- Burnstock, G. et al., 1970. Evidence that adenosine triphosphate or a related nucleotide is the transmitter substance released by non-adrenergic inhibitory nerves in the gut. *Br J Pharmacol*, 40(4), pp.668–688.
- Burnstock, G., 2007. Purine and pyrimidine receptors. *Cell Mol Life Sci*, 64(12), pp.1471–1483.
- Burnstock, G., 2006. Purinergic signalling. *Br J Pharmacol*, 147 Suppl , pp.S172–81.
- Burnstock, G., 1997. The past, present and future of purine nucleotides as signalling molecules. *Neuropharmacology*, 36(9), pp.1127–1139.
- Burnstock, G. & Ulrich, H., 2011. Purinergic signaling in embryonic and stem cell development. *Cell Mol Life Sci*, 68(8), pp.1369–1394.

- Burnstock, G. & Williams, M., 2000. P2 purinergic receptors: modulation of cell function and therapeutic potential. *J Pharmacol Exp Ther*, 295(3), pp.862–869.
- Capela, A. & Temple, S., 2006. LeX is expressed by principle progenitor cells in the embryonic nervous system, is secreted into their environment and binds Wnt-1. *Dev Biol*, 291(2), pp.300–313.
- Capela, A. & Temple, S., 2002. LeX/ssea-1 is expressed by adult mouse CNS stem cells, identifying them as nonpendymal. *Neuron*, 35(5), pp.865–875.
- Carafoli, E. et al., 2001. Generation, control, and processing of cellular calcium signals. *Crit Rev Biochem Mol Biol*, 36(2), pp.107–260.
- Carafoli, E. & Brini, M., 2000. Calcium pumps: structural basis for and mechanism of calcium transmembrane transport. *Curr Opin Chem Biol*, 4(2), pp.152–161.
- Chafouleas, J.G. et al., 1982. Calmodulin and the cell cycle: involvement in regulation of cell-cycle progression. *Cell*, 28(1), pp.41–50.
- Cheewatrakoolpong, B. et al., 2005. Identification and characterization of splice variants of the human P2X7 ATP channel. *Biochem Biophys Res Commun*, 332(1), pp.17–27.
- Cheng, H. & Lederer, W.J., 2008. Calcium sparks. *Physiol Rev*, 88(4), pp.1491–1545.
- Ciccolini, F. et al., 2003. Local and global spontaneous calcium events regulate neurite outgrowth and onset of GABAergic phenotype during neural precursor differentiation. *J Neurosci*, 23(1), pp.103–111.
- Ciruela, F. et al., 2010. Adenosine receptors interacting proteins (ARIPs): Behind the biology of adenosine signaling. *Biochim Biophys Acta*, 1798(1), pp.9–20.
- Collins, T.J. et al., 2001. Mitochondrial Ca(2+) uptake depends on the spatial and temporal profile of cytosolic Ca(2+) signals. *J Biol Chem*, 276(28), pp.26411–26420.
- Cunha, R.A. et al., 1996. Preferential activation of excitatory adenosine receptors at rat hippocampal and neuromuscular synapses by adenosine formed from released adenine nucleotides. *Br J Pharmacol*, 119(2), pp.253–260.

- Daadi, M.M. et al., 2012. Dopaminergic neurons from midbrain-specified human embryonic stem cell-derived neural stem cells grafted in a monkey model of Parkinson's disease. *PLoS One*, 7(7), p.e41120.
- Dolmetsch, R.E. et al., 2001. Signaling to the nucleus by an L-type calcium channel-calmodulin complex through the MAP kinase pathway. *Science*, 294(5541), pp.333–339.
- Dona, F. et al., 2009. Alteration of purinergic P2X4 and P2X7 receptor expression in rats with temporal-lobe epilepsy induced by pilocarpine. *Epilepsy Res*, 83(2-3), pp.157–167.
- Donnelly-Roberts, D.L. et al., 2009. Mammalian P2X7 receptor pharmacology: comparison of recombinant mouse, rat and human P2X7 receptors. *Br J Pharmacol*, 157(7), pp.1203–1214.
- Duan, S. & Neary, J.T., 2006. P2X(7) receptors: properties and relevance to CNS function. *Glia*, 54(7), pp.738–746.
- Dubyak, G.R. & el-Moatassim, C., 1993. Signal transduction via P2-purinergic receptors for extracellular ATP and other nucleotides. *Am J Physiol*, 265(3 Pt 1), pp.C577–606.
- Elmslie, K.S., 2004. Calcium channel blockers in the treatment of disease. *J Neurosci Res*, 75(6), pp.733–741.
- EI-Tayeb, A., Qi, A. & Muller, C.E., 2006. Synthesis and structure-activity relationships of uracil nucleotide derivatives and analogues as agonists at human P2Y2, P2Y4, and P2Y6 receptors. *J Med Chem*, 49(24), pp.7076–7087.
- Evans, M.J. & Kaufman, M.H., 1981. Establishment in culture of pluripotential cells from mouse embryos. *Nature*, 292(5819), pp.154–156.
- Feske, S. et al., 2006. A mutation in Orai1 causes immune deficiency by abrogating CRAC channel function. *Nature*, 441(7090), pp.179–185.
- Fill, M. & Copello, J.A., 2002. Ryanodine receptor calcium release channels. *Physiol Rev*, 82(4), pp.893–922.
- Foskett, J.K. et al., 2007. Inositol trisphosphate receptor Ca²⁺ release channels. *Physiol Rev*, 87(2), pp.593–658.

- Fraichard, A. et al., 1995. In vitro differentiation of embryonic stem cells into glial cells and functional neurons. *J Cell Sci*, 108 (Pt 1), pp.3181–3188.
- Francis, F. et al., 1999. Doublecortin is a developmentally regulated, microtubule-associated protein expressed in migrating and differentiating neurons. *Neuron*, 23(2), pp.247–256.
- Franzini-Armstrong, C. & Protasi, F., 1997. Ryanodine receptors of striated muscles: a complex channel capable of multiple interactions. *Physiol Rev*, 77(3), pp.699–729.
- Furuichi, T. et al., 1989. Primary structure and functional expression of the inositol 1,4,5-trisphosphate-binding protein P400. *Nature*, 342(6245), pp.32–38.
- Gajovic, S. et al., 1997. Retinoic acid mediates Pax6 expression during in vitro differentiation of embryonic stem cells. *Differentiation*, 62(4), pp.187–192.
- Glaser, T. et al., 2014. Modulation of mouse embryonic stem cell proliferation and neural differentiation by the P2X7 receptor. *PLoS ONE*, 9(5).
- Glaser, T., Resende, R.R. & Ulrich, H., 2013. Implications of purinergic receptor-mediated intracellular calcium transients in neural differentiation. *Cell communication and signaling : CCS*, 11(1), p.12.
- Gomez, T.M. & Spitzer, N.C., 1999. In vivo regulation of axon extension and pathfinding by growth-cone calcium transients. *Nature*, 397(6717), pp.350–355.
- Gonzalez-Cordero, A. et al., 2013. Photoreceptor precursors derived from three-dimensional embryonic stem cell cultures integrate and mature within adult degenerate retina. *Nat Biotechnol*, 31(8), pp.741–747.
- Greer, P.L. & Greenberg, M.E., 2008. From synapse to nucleus: calcium-dependent gene transcription in the control of synapse development and function. *Neuron*, 59(6), pp.846–860.
- Guillemot, F., 2007. Cell fate specification in the mammalian telencephalon. *Prog Neurobiol*, 83(1), pp.37–52.
- Hall, V. et al., 2013. Early embryonic development, assisted reproductive technologies, and pluripotent stem cell biology in domestic mammals. *Vet J*, 197(2), pp.128–142.

- Hallett, M.B., Davies, E. V & Campbell, A.K., 1990. Oxidase activation in individual neutrophils is dependent on the onset and magnitude of the Ca²⁺ signal. *Cell Calcium*, 11(10), pp.655–663.
- Hardingham, G.E., Arnold, F.J. & Bading, H., 2001. Nuclear calcium signaling controls CREB-mediated gene expression triggered by synaptic activity. *Nat Neurosci*, 4(3), pp.261–267.
- Hogan, P.G. et al., 2003. Transcriptional regulation by calcium, calcineurin, and NFAT. *Genes Dev*, 17(18), pp.2205–2232.
- Hynes, R.O., Patel, R. & Miller, R.H., 1986. Migration of neuroblasts along preexisting axonal tracts during prenatal cerebellar development. *J Neurosci*, 6(3), pp.867–876.
- Imayoshi, I. et al., 2013. Oscillatory control of factors determining multipotency and fate in mouse neural progenitors. *Science*, 342(6163), pp.1203–1208.
- Imayoshi, I. & Kageyama, R., 2014. Oscillatory control of bHLH factors in neural progenitors. *Trends Neurosci*, 37(10), pp.531–538.
- Kapur, N., Mignery, G.A. & Banach, K., 2007. Cell cycle-dependent calcium oscillations in mouse embryonic stem cells. *Am J Physiol Cell Physiol*, 292(4), pp.C1510–8.
- Kerr, M.A. & Stocks, S.C., 1992. The role of CD15-(Le(X))-related carbohydrates in neutrophil adhesion. *Histochem J*, 24(11), pp.811–826.
- Kim, M. et al., 2009. Regulation of mouse embryonic stem cell neural differentiation by retinoic acid. *Dev Biol*, 328(2), pp.456–471.
- Kostyuk, P. & Verkhratsky, A., 1994. Calcium stores in neurons and glia. *Neuroscience*, 63(2), pp.381–404.
- Krebs, J., Agellon, L.B. & Michalak, M., 2015. Ca(2+) homeostasis and endoplasmic reticulum (ER) stress: An integrated view of calcium signaling. *Biochem Biophys Res Commun*, 460(1), pp.114–121.
- Kruger, N.J., 1994. The Bradford method for protein quantitation. *Methods Mol Biol*, 32, pp.9–15.
- Lautermilch, N.J. & Spitzer, N.C., 2000. Regulation of calcineurin by growth cone calcium waves controls neurite extension. *J Neurosci*, 20(1), pp.315–325.

- Lee, S.H. et al., 2000. Efficient generation of midbrain and hindbrain neurons from mouse embryonic stem cells. *Nat Biotechnol*, 18(6), pp.675–679.
- Lemoli, R.M. et al., 2004. Extracellular nucleotides are potent stimulators of human hematopoietic stem cells in vitro and in vivo. *Blood*, 104(6), pp.1662–1670.
- Leon, D., Hervas, C. & Miras-Portugal, M.T., 2006. P2Y1 and P2X7 receptors induce calcium/calmodulin-dependent protein kinase II phosphorylation in cerebellar granule neurons. *Eur J Neurosci*, 23(11), pp.2999–3013.
- Liang, X. et al., 2011. Isl1 is required for multiple aspects of motor neuron development. *Mol Cell Neurosci*, 47(3), pp.215–222.
- Lin, J.H. et al., 2007. Purinergic signaling regulates neural progenitor cell expansion and neurogenesis. *Dev Biol*, 302(1), pp.356–366.
- Lipp, P. et al., 1997. Nuclear calcium signalling by individual cytoplasmic calcium puffs. *EMBO J*, 16(23), pp.7166–7173.
- Ma, L. et al., 2012. Human embryonic stem cell-derived GABA neurons correct locomotion deficits in quinolinic acid-lesioned mice. *Cell Stem Cell*, 10(4), pp.455–464.
- Maeda, N., Niinobe, M. & Mikoshiba, K., 1990. A cerebellar Purkinje cell marker P400 protein is an inositol 1,4,5-trisphosphate (InsP₃) receptor protein. Purification and characterization of InsP₃ receptor complex. *EMBO J*, 9(1), pp.61–67.
- Malmersjo, S. et al., 2013. Ca²⁺ and cAMP signaling in human embryonic stem cell-derived dopamine neurons. *Stem Cells Dev*, 19(9), pp.1355–1364.
- Marenholz, I., Heizmann, C.W. & Fritz, G., 2004. S100 proteins in mouse and man: from evolution to function and pathology (including an update of the nomenclature). *Biochem Biophys Res Commun*, 322(4), pp.1111–1122.
- Martin, G.R., 1981. Isolation of a pluripotent cell line from early mouse embryos cultured in medium conditioned by teratocarcinoma stem cells. *Proc Natl Acad Sci U S A*, 78(12), pp.7634–7638.

- Martinez-Monedero, R. et al., 2008. Differentiation of inner ear stem cells to functional sensory neurons. *Dev Neurobiol*, 68(5), pp.669–684.
- Masamizu, Y. et al., 2006. Real-time imaging of the somite segmentation clock: revelation of unstable oscillators in the individual presomitic mesoderm cells. *Proc Natl Acad Sci U S A*, 103(5), pp.1313–1318.
- Masin, M. et al., 2012. Expression, assembly and function of novel C-terminal truncated variants of the mouse P2X7 receptor: re-evaluation of P2X7 knockouts. *Br J Pharmacol*, 165(4), pp.978–993.
- McGraw, C.F., Somlyo, A. V & Blaustein, M.P., 1980. Probing for calcium at presynaptic nerve terminals. *Fed Proc*, 39(10), pp.2796–2801.
- Meissner, G., 1994. Ryanodine receptor/Ca²⁺ release channels and their regulation by endogenous effectors. *Annu Rev Physiol*, 56, pp.485–508.
- Mellstrom, B. et al., 2008. Ca²⁺-operated transcriptional networks: molecular mechanisms and in vivo models. *Physiol Rev*, 88(2), pp.421–449.
- Memberg, S.P. & Hall, A.K., 1995. Dividing neuron precursors express neuron-specific tubulin. *J Neurobiol*, 27(1), pp.26–43.
- Mikoshiba, K., 2007. IP₃ receptor/Ca²⁺ channel: from discovery to new signaling concepts. *J Neurochem*, 102(5), pp.1426–1446.
- Miras-Portugal, M.T. et al., 2015. Nucleotides in neuroregeneration and neuroprotection. *Neuropharmacology*.
- Mironov, S.L., 1994. Metabotropic ATP receptor in hippocampal and thalamic neurones: pharmacology and modulation of Ca²⁺ mobilizing mechanisms. *Neuropharmacology*, 33(1), pp.1–13.
- Moscat, J., Diaz-Meco, M.T. & Rennert, P., 2003. NF-kappaB activation by protein kinase C isoforms and B-cell function. *EMBO Rep*, 4(1), pp.31–36.
- Muller, M.R. & Rao, A., 2010. NFAT, immunity and cancer: a transcription factor comes of age. *Nat Rev Immunol*, 10(9), pp.645–656.

- Nieto, M. et al., 2001. Neural bHLH genes control the neuronal versus glial fate decision in cortical progenitors. *Neuron*, 29(2), pp.401–413.
- North, R.A., 1996. P2X receptors: a third major class of ligand-gated ion channels. *Ciba Found Symp*, 198, pp.91–99.
- Ohtani, K. et al., 2013. Jmjd3 controls mesodermal and cardiovascular differentiation of embryonic stem cells. *Circ Res*, 113(7), pp.856–862.
- Okabe, S. et al., 1996. Development of neuronal precursor cells and functional postmitotic neurons from embryonic stem cells in vitro. *Mech Dev*, 59(1), pp.89–102.
- Ong, H.L. et al., 2014. Physiological functions and regulation of TRPC channels. *Handb Exp Pharmacol*, 223, pp.1005–1034.
- Orellano, E.A. et al., 2010. Inhibition of neuronal cell death after retinoic acid-induced down-regulation of P2X7 nucleotide receptor expression. *Mol Cell Biochem*, 337(1-2), pp.83–99.
- Orford, K.W. & Scadden, D.T., 2008. Deconstructing stem cell self-renewal: genetic insights into cell-cycle regulation. *Nat Rev Genet*, 9(2), pp.115–128.
- Pal, R. et al., 2013. Development of a multiplex PCR assay for characterization of embryonic stem cells. *Methods Mol Biol*, 1006, pp.147–166.
- Parekh, A.B., 2003. Store-operated Ca²⁺ entry: dynamic interplay between endoplasmic reticulum, mitochondria and plasma membrane. *J Physiol*, 547(Pt 2), pp.333–348.
- Parras, C.M. et al., 2002. Divergent functions of the proneural genes Mash1 and Ngn2 in the specification of neuronal subtype identity. *Genes Dev*, 16(3), pp.324–338.
- Parras, C.M. et al., 2004. Mash1 specifies neurons and oligodendrocytes in the postnatal brain. *EMBO J*, 23(22), pp.4495–4505.
- Peltier, J. & Schaffer, D. V, 2010. Systems biology approaches to understanding stem cell fate choice. *IET Syst Biol*, 4(1), pp.1–11.
- Pinto, M.C. et al., 2015. Calcium signaling and cell proliferation. *Cell Signal*, 27(11), pp.2139–2149.

- Renoncourt, Y. et al., 1998. Neurons derived in vitro from ES cells express homeoproteins characteristic of motoneurons and interneurons. *Mech Dev*, 79(1-2), pp.185–197.
- Resende, R.R. et al., 2009. Influence of spontaneous calcium events on cell-cycle progression in embryonal carcinoma and adult stem cells. *Biochim Biophys Acta*, 1803(2), pp.246–260.
- Resende, R.R. et al., 2010. Intracellular Ca²⁺ regulation during neuronal differentiation of murine embryonal carcinoma and mesenchymal stem cells. *Stem Cells Dev*, 19(3), pp.379–394.
- Resende, R.R. et al., 2007. P19 embryonal carcinoma cells as in vitro model for studying purinergic receptor expression and modulation of N-methyl-D-aspartate-glutamate and acetylcholine receptors during neuronal differentiation. *Neuroscience*, 146(3), pp.1169–1181.
- Resende, R.R., Britto, L.R. & Ulrich, H., 2008. Pharmacological properties of purinergic receptors and their effects on proliferation and induction of neuronal differentiation of P19 embryonal carcinoma cells. *Int J Dev Neurosci*, 26(7), pp.763–777.
- Rezania, A. et al., 2012. Maturation of human embryonic stem cell-derived pancreatic progenitors into functional islets capable of treating pre-existing diabetes in mice. *Diabetes*, 61(8), pp.2016–2029.
- Rohwedel, J., Guan, K. & Wobus, A.M., 1999. Induction of cellular differentiation by retinoic acid in vitro. *Cells Tissues Organs*, 165(3-4), pp.190–202.
- Rolletschek, A. et al., 2001. Differentiation of embryonic stem cell-derived dopaminergic neurons is enhanced by survival-promoting factors. *Mech Dev*, 105(1-2), pp.93–104.
- Ross, S.E., Greenberg, M.E. & Stiles, C.D., 2003. Basic helix-loop-helix factors in cortical development. *Neuron*, 39(1), pp.13–25.
- Sala, F. & Hernandez-Cruz, A., 1990. Calcium diffusion modeling in a spherical neuron. Relevance of buffering properties. *Biophys J*, 57(2), pp.313–324.
- Salter, M.W. & Hicks, J.L., 1995. ATP causes release of intracellular Ca²⁺ via the phospholipase C beta/IP3 pathway in astrocytes from the dorsal spinal cord. *J Neurosci*, 15(4), pp.2961–2971.
- Sauer, H. et al., 1998. Spontaneous calcium oscillations in embryonic stem cell-derived primitive endodermal cells. *Exp Cell Res*, 238(1), pp.13–22.

- Savatier, P. et al., 2002. Analysis of the cell cycle in mouse embryonic stem cells. *Methods Mol Biol*, 185, pp.27–33.
- Savatier, P. et al., 1994. Contrasting patterns of retinoblastoma protein expression in mouse embryonic stem cells and embryonic fibroblasts. *Oncogene*, 9(3), pp.809–818.
- Schwindt, T.T. et al., 2010. Directed differentiation of neural progenitors into neurons is accompanied by altered expression of P2X purinergic receptors. *J Mol Neurosci*, 44(3), pp.141–146.
- Sharma, V. & O'Halloran, D.M., 2014. Recent structural and functional insights into the family of sodium calcium exchangers. *Genesis*, 52(2), pp.93–109.
- Sharp, A.H. et al., 1993. Differential immunohistochemical localization of inositol 1,4,5-trisphosphate- and ryanodine-sensitive Ca²⁺ release channels in rat brain. *J Neurosci*, 13(7), pp.3051–3063.
- Shukla, V. et al., 2005. Functional expression of the ecto-ATPase NTPDase2 and of nucleotide receptors by neuronal progenitor cells in the adult murine hippocampus. *J Neurosci Res*, 80(5), pp.600–610.
- Da Silva, R.L., Resende, R.R. & Ulrich, H., 2007. Alternative splicing of P2X6 receptors in developing mouse brain and during in vitro neuronal differentiation. *Exp Physiol*, 92(1), pp.139–145.
- Smedler, E. & Uhlen, P., 2014. Frequency decoding of calcium oscillations. *Biochim Biophys Acta*, 1840(3), pp.964–969.
- Smith, A.G. et al., 1988. Inhibition of pluripotential embryonic stem cell differentiation by purified polypeptides. *Nature*, 336(6200), pp.688–690.
- Sobeih, M.M. & Corfas, G., 2002. Extracellular factors that regulate neuronal migration in the central nervous system. *Int J Dev Neurosci*, 20(3-5), pp.349–357.
- Spitzer, N.C., 2002. Activity-dependent neuronal differentiation prior to synapse formation: the functions of calcium transients. *J Physiol Paris*, 96(1-2), pp.73–80.
- Spitzer, N.C. et al., 2000. Coding of neuronal differentiation by calcium transients. *Bioessays*, 22(9), pp.811–817.
- Spitzer, N.C., Root, C.M. & Borodinsky, L.N., 2004. Orchestrating neuronal differentiation: patterns of Ca²⁺ spikes specify transmitter choice. *Trends Neurosci*, 27(7), pp.415–421.

- Stavridis, M.P. & Smith, A.G., 2003. Neural differentiation of mouse embryonic stem cells. *Biochem Soc Trans*, 31(Pt 1), pp.45–49.
- Streb, H. et al., 1983. Release of Ca²⁺ from a nonmitochondrial intracellular store in pancreatic acinar cells by inositol-1,4,5-trisphosphate. *Nature*, 306(5938), pp.67–69.
- Strubing, C. et al., 1995. Differentiation of pluripotent embryonic stem cells into the neuronal lineage in vitro gives rise to mature inhibitory and excitatory neurons. *Mech Dev*, 53(2), pp.275–287.
- Stutzmann, G.E. & Mattson, M.P., 2011. Endoplasmic reticulum Ca(2+) handling in excitable cells in health and disease. *Pharmacol Rev*, 63(3), pp.700–727.
- Takasato, M. et al., 2013. Directing human embryonic stem cell differentiation towards a renal lineage generates a self-organizing kidney. *Nat Cell Biol*, 16(1), pp.118–126.
- Theatre, E., Bours, V. & Oury, C., 2009. A P2X ion channel-triggered NF-kappaB pathway enhances TNF-alpha-induced IL-8 expression in airway epithelial cells. *Am J Respir Cell Mol Biol*, 41(6), pp.705–713.
- Tonelli, F.M. et al., 2012. Stem cells and calcium signaling. *Adv Exp Med Biol*, 740, pp.891–916.
- Trujillo, C.A. et al., 2009. Novel perspectives of neural stem cell differentiation: from neurotransmitters to therapeutics. *Cytometry A*, 75(1), pp.38–53.
- Tsao, H.K., Chiu, P.H. & Sun, S.H., 2013. PKC-dependent ERK phosphorylation is essential for P2X7 receptor-mediated neuronal differentiation of neural progenitor cells. *Cell Death Dis*, 4, p.e751.
- Uchida, N. et al., 2000. Direct isolation of human central nervous system stem cells. *Proc Natl Acad Sci U S A*, 97(26), pp.14720–14725.
- Ulrich, H., Abbracchio, M.P. & Burnstock, G., 2012. Extrinsic purinergic regulation of neural stem/progenitor cells: implications for CNS development and repair. *Stem Cell Rev*, 8(3), pp.755–767.
- Ulrich, H. & Majumder, P., 2006. Neurotransmitter receptor expression and activity during neuronal differentiation of embryonal carcinoma and stem cells: from basic research towards clinical applications. *Cell Prolif*, 39(4), pp.281–300.

- Vanderheyden, V. et al., 2009. Regulation of inositol 1,4,5-trisphosphate-induced Ca²⁺ release by reversible phosphorylation and dephosphorylation. *Biochim Biophys Acta*, 1793(6), pp.959–970.
- Verkhratsky, A., Krishtal, O.A. & Burnstock, G., 2009. Purinoceptors on neuroglia. *Mol Neurobiol*, 39(3), pp.190–208.
- Di Virgilio, F., 2012. Purines, purinergic receptors, and cancer. *Cancer Res*, 72(21), pp.5441–5447.
- Di Virgilio, F., Ferrari, D. & Adinolfi, E., 2009. P2X(7): a growth-promoting receptor-implications for cancer. *Purinergic Signal*, 5(2), pp.251–256.
- Walton, P.D. et al., 1991. Ryanodine and inositol trisphosphate receptors coexist in avian cerebellar Purkinje neurons. *J Cell Biol*, 113(5), pp.1145–1157.
- Wang, R. & Lewin, G.R., 2011. The Cav3.2 T-type calcium channel regulates temporal coding in mouse mechanoreceptors. *J Physiol*, 589(Pt 9), pp.2229–2243.
- Westrum, L.E. & Gray, E.G., 1986. New observations on the substructure of the active zone of brain synapses and motor endplates. *Proc R Soc Lond B Biol Sci*, 229(1254), pp.29–38.
- Wheeler, D.G. et al., 2008. CaMKII locally encodes L-type channel activity to signal to nuclear CREB in excitation-transcription coupling. *J Cell Biol*, 183(5), pp.849–863.
- Wilson, L. & Maden, M., 2005. The mechanisms of dorsoventral patterning in the vertebrate neural tube. *Dev Biol*, 282(1), pp.1–13.
- Wobus, A.M. et al., 1994. Cardiomyocyte-like cells differentiated in vitro from embryonic carcinoma cells P19 are characterized by functional expression of adrenoceptors and Ca²⁺ channels. *In Vitro Cell Dev Biol Anim*, 30A(7), pp.425–434.
- Wu, C.Y. et al., 2012. Efficient differentiation of mouse embryonic stem cells into motor neurons. *J Vis Exp*, (64), p.e3813.
- Wu, P.Y. et al., 2009. Functional decreases in P2X7 receptors are associated with retinoic acid-induced neuronal differentiation of Neuro-2a neuroblastoma cells. *Cell Signal*, 21(6), pp.881–891.
- Xia, X.M. et al., 1998. Mechanism of calcium gating in small-conductance calcium-activated potassium channels. *Nature*, 395(6701), pp.503–507.

- Yamasaki, A. et al., 2015. Identification of the role of bone morphogenetic protein (BMP) and transforming growth factor-beta (TGF-beta) signaling in the trajectory of serotonergic differentiation in a rapid assay in mouse embryonic stem cells in vitro. *J Neurochem*, 132(4), pp.418–428.
- Yan, Y. et al., 2015. Differential effects of acellular embryonic matrices on pluripotent stem cell expansion and neural differentiation. *Biomaterials*, 73, pp.231–242.
- Young, M.T., Pelegrin, P. & Surprenant, A., 2007. Amino acid residues in the P2X7 receptor that mediate differential sensitivity to ATP and BzATP. *Mol Pharmacol*, 71(1), pp.92–100.
- Zhu, D. et al., 2005. Icariin-mediated modulation of cell cycle and p53 during cardiomyocyte differentiation in embryonic stem cells. *Eur J Pharmacol*, 514(2-3), pp.99–110.
- Zimmermann, H., 2006. Nucleotide signaling in nervous system development. *Pflugers Arch*, 452(5), pp.573–588.

7. ANEXOS

Súmula Curricular

TALITA GLASER

Endereço: Departamento de Bioquímica, Instituto de Química, Universidade de São Paulo Av. Prof. Lineu Prestes, 748 – 05508-000- São Paulo- Brasil
 Email: talita.glaser@usp.br / tali.gla@gmail.com

1. FORMAÇÃO

- 2005-2009: Graduação em Ciência Biológicas (Bacharel) pela Universidade de São Paulo.
- 2009-2011: Graduação em Ciência Biológicas (Licenciatura) pela Universidade de São Paulo.
- Desde 2010: Doutorado-direto em Ciência Biológicas, modalidade Bioquímica pela Universidade de São Paulo. Instituto de Química.
- 2014: Estágio de pesquisa na Universidade de Quioto, Japão. Doutorado sanduiche.

2. HISTÓRICO PROFISSIONAL, SERVIÇOS E DISTINÇÕES ACADÊMICAS E PRÊMIOS.

- 2006-2010: Iniciação Científica no InCor/HCFMUSP.
- 2007-2010: Bolsa acadêmica iniciação científica FAPESP para desenvolvimento do projeto: ESTUDO DAS DIFERENTES ISOENZIMAS DA PKC NA DIFERENCIACAO DE CELULAS TRONCO EMBRIONARIAS EM CARDIOMIOCITOS.
- 2009: Professora no curso Embryonic Stem Cells as a Model System for Mammalian Development/ 2nd Symposium for the Latin American Stem Cell Network
- 2010: Bolsa acadêmica doutorado direto FAPESP para desenvolvimento do projeto: MODULACAO DA DIFERENCIACAO NEURONAL DE CELULAS TRONCO EMBRIONARIAS TRANSIENTES DE CALCIO INTRACELULARES E ATIVACAO DE RECEPTORES PURINERGICOS.
- 2011: Assistente de docência na disciplina Bioquímica Metabólica QBQ3400 para alunos da graduação Química Ambiental.
- 2011: Professora convidada para o curso VI Curso de verão – Bioquímica e biologia molecular, IQ-USP.
- 2012: Assistente de docência na disciplina Bioquímica: Estrutura de Biomoléculas e Metabolismo QBQ0230 para alunos da graduação Ciências Biológicas.
- 2012: Professora convidada para o curso sobre células tronco no V Encontro de Ciências da vida na UNESP Ilha Solteira, São Paulo.

- 2012: Professora convidada para o curso "Experimental models for stem cell research" na UFRO Temuco-Chile.
- 2012: Menção honrosa por melhor poster e apresentação oral no congresso: 1st Brazilian meeting for Calcium Signaling
- 2013: Assistente de docência na disciplina Bioquímica: Estrutura de Biomoléculas e Metabolismo QBQ0230 para alunos da graduação Ciências Biológicas.
- 2015: Prêmio João José Freitas Sarkis por melhor pôster no congresso Fifth Meeting Brazilian Purine Club/ II International Congress of Purinergic Signaling in South America

3. LISTA DE PUBLICAÇÕES

Artigos publicados em revistas científicas:

- 1) Kinin-B1 and B2 receptor activity in proliferation and neural phenotype determination of mouse embryonic stem cells. Nascimento IC, Glaser T, Nery AA, Pillat MM, Pesquero JB, Ulrich H. *Cytometry A*. 2015 Aug 4. doi: 10.1002/cyto.a.22726. [Epub ahead of print] PMID: 26243460
- 2) Neuronal adhesion, proliferation and differentiation of embryonic stem cells on hybrid scaffolds made of xanthan and magnetite nanoparticles. Glaser T, Bueno VB, Cornejo DR, Petri DF, Ulrich H. *Biomed Mater*. 2015 Jul 8;10(4):045002. doi: 10.1088/1748-6041/10/4/045002. PMID: 26154495
- 3) A Cyclic GMP-Dependent K⁺ Channel in the Blastocladiomycete Fungus *Blastocladiella emersonii*. Avelar GM, Glaser T, Leonard G, Richards TA, Ulrich H, Gomes SL. *Eukaryot Cell*. 2015 Sep;14(9):958-63. doi: 10.1128/EC.00087-15. Epub 2015 Jul 6. PMID: 26150416
- 4) Intracellular Calcium Measurements for Functional Characterization of Neuronal Phenotypes. Glaser T, Castillo AR, Oliveira Á, Ulrich H. *Methods Mol Biol*. 2015 Jul 1. PMID: 26126448
- 5) Modulation of Mouse Embryonic Stem Cell Proliferation and Neural Differentiation by the P2X7 Receptor. Talita Glaser, Sophia La Banca de Oliveira, Arquimedes Cheffer, Renata Beco, Patrícia Martins, Maynara Fornazari, Claudiana Lameu, Helio Miranda Costa Junior, Robson Coutinho-Silva, Henning Ulrich. *PLoS ONE* 2014 May 9(5): e96281. doi:10.1371/journal.pone.0096281.
- 6) Cytometry in the brain: studying differentiation to diagnostic applications in brain disease and regeneration therapy H Ulrich, J Bocsi, T Glaser, A Tárnok Cell proliferation 47 (1), 12-19.2014
- 7) Implications of purinergic receptor-mediated intracellular calcium transients in neural differentiation. Glaser T, Resende RR, Ulrich H. *Cell Commun Signal*. 2013 Feb 17;11(1):12. doi: 10.1186/1478-811X-11-12.
- 8) Characterization of ectonucleotidases in human medulloblastoma cell lines: ecto-5'NT/CD73 in metastasis as potential prognostic factor. Cappellari AR, Rockenbach L, Dietrich F, Clarimundo V, Glaser T, Braganhol E, Abujamra AL, Roesler R, Ulrich H,

- Battastini AM. PLoS One. 2012;7(10):e47468. doi: 10.1371/journal.pone.0047468. Epub 2012 Oct 18.
- 9) Human mesenchymal stem cells: from immunophenotyping by flow cytometry to clinical applications. Nery AA, Nascimento IC, Glaser T, Bassaneze V, Krieger JE, Ulrich H. Cytometry A. 2013 Jan;83(1):48-61. doi: 10.1002/cyto.a.22205. Epub 2012 Oct 1. Review.
 - 10) Regulation of neurogenesis and gliogenesis of retinoic acid-induced P19 embryonal carcinoma cells by P2X2 and P2X7 receptors studied by RNA interference. Yuahasi KK, Demasi MA, Tamajusuku AS, Lenz G, Sogayar MC, Fornazari M, Lameu C, Nascimento IC, Glaser T, Schwindt TT, Negraes PD, Ulrich H. Int J Dev Neurosci. 2012 Apr;30(2):91-7. doi: 10.1016/j.ijdevneu.2011.12.010. Epub 2012 Jan 13.
 - 11) Perspectives of purinergic signaling in stem cell differentiation and tissue regeneration. Glaser T, Cappellari AR, Pillat MM, Iser IC, Wink MR, Battastini AM, Ulrich H. Purinergic Signal. 2012 Sep;8(3):523-37. doi: 10.1007/s11302-011-9282-3. Epub 2011 Dec 6. Review.
 - 12) Phosphoproteomics profiling suggests a role for nuclear β IPKC in transcription processes of undifferentiated murine embryonic stem cells. Costa-Junior HM, Garavello NM, Duarte ML, Berti DA, Glaser T, de Andrade A, Labate CA, Ferreira AT, Perales JE, Xavier-Neto J, Krieger JE, Schechtman D. J Proteome Res. 2010 Dec 3;9(12):6191-206. doi: 10.1021/pr100355k. Epub 2010 Nov 1.

Capítulos de livros:

- 1) MICELI MAINARDI PILLAT, TALITA GLASER, TELMA TIEMI SCHWINDT, HENNING ULRICH. An Introduction to Proliferation and Migration of Stem and Cancer Cells. Trends in stem cell proliferation and cancer research. RR Resende, H Ulrich – 2013 editora Springer.
- 2) GLASER, T.; OLIVEIRA, Á.; SARDA-ARROYO, L.; ULRICH, A. H.. Growth and Neurotrophic Factor Receptors in Neural Differentiation. In: Jan Pruszak. (Org.). Neural Surface Antigens: From Basic Biology Towards Biomedical Applications. 1ed.: Academic Press, 2015, v. 1, p. 77-90.

4. PARTICIPAÇÃO EM EVENTOS, CONGRESSOS, EXPOSIÇÕES E FEIRAS

- 1) 4th Brazilian Purine Club Meeting - Perspectives of Purinergic Signaling: From Structures to Functions and Translational Research. P2X RECEPTORS IN PROLIFERATION AND NEURAL PHENOTYPE DETERMINATION OF EMBRYONIC STEM CELLS. 2013. (Congresso).
- 2) 3º Encontro do Clube Brasileiro de Purinas. ROLES OF PURINERGIC SYSTEM IN EMBRYONIC STEM CELL BIOLOGY. 2012. (Congresso).
- 3) disciplina QBQ 0215 Bioquímica, Estrutura de Biomoléculas e Metabolismo no Instituto de Química-USP.CÉLULAS TRONCO. 2012. (Seminário).
- 4) 1º Simpósio Brasileiro de sinalização de cálcio-UFMG. OSCILAÇÕES ESPONTÂNEAS NA $[Ca^{2+}]_i$ DURANTE A DIFERENCIACÃO NEURAL DE CÉLULAS TRONCO EMBRIONÁRIAS. 2012. (Simpósio).

- 5) V Encontro de Ciências da Vida na UNESP de ilha Solteira.Células Tronco. 2012. (Oficina).
- 6) Experimental models for stem cell research.Embryonic stem cells. 2012. (Outra).
- 7) IV Joint German- Italian Purine Club Meeting. UPREGULATION OF P2X RECEPTOR EXPRESSION AND ACTIVITY DURING MAINTENANCE OF PLURIPOTENT STATE OF EMBRYONIC STEM CELLS. 2011. (Congresso).
- 8) VI Curso de Verão- Bioquímica e Biologia Molecular.O MARAVILHOSO MUNDO DAS CÉLULAS TRONCO. 2011. (Seminário).
- 9) VI Curso de Verão- Bioquímica e Biologia Molecular IQ-USP.SINALIZAÇÃO INTRACELULAR MEDIADA POR CÁLCIO EM NEURÔNIOS DIFERENCIADOS DE CÉLULAS TRONCO. 2011. (Oficina).
- 10) V Congresso Brasileiro de células tronco e terapia celular. Direction of embryonic stem cell differentiation into diverse neural phenotypes. 2010. (Congresso).
- 11) I Meeting on Stem Cell Research PERSPECTIVES OF STEM CELLS. 2010. (Simpósio).
- 12) 49th Annual Meeting of the American Society for Cell Biology. PKC isoenzymes in murine embryonic stem cell differentiation to cardiomyocytes. 2009. (Congresso).
- 13) XIV Congresso da Sociedade Brasileira de Biologia Celular. THE ROLE OF PKCs IN THE DIFFERENTIATION OF MURINE EMBRYONIC STEM CELLS IN CARDIOMYOCYTES. 2008. (Congresso).
- 14) XXII Reunião anual da FeSBE. O PAPEL DA PKC ϵ NA DIFERENCIACÃO DE CÉLULAS TRONCO EMBRIONÁRIAS MURINAS PARA CARDIOMIÓCITOS 1Glaser, T.*; 2Cesario E*; 4Krieger JE; 1, 2, 4Laboratório de Genética e Cardiologia Molecular, InCor-HCFMUSP; 2007. (Congresso).

Perspectives of purinergic signaling in stem cell differentiation and tissue regeneration

Talita Glaser · Angélica Regina Cappellari · Micheli Mainardi Pillat ·
Isabele Cristiana Iser · Márcia Rosângela Wink · Ana Maria Oliveira Battastini ·
Henning Ulrich

Received: 13 September 2011 / Accepted: 9 November 2011 / Published online: 6 December 2011
© Springer Science+Business Media B.V. 2011

Abstract Replacement of lost or dysfunctional tissues by stem cells has recently raised many investigations on therapeutic applications. Purinergic signaling has been shown to regulate proliferation, differentiation, cell death, and successful engraftment of stem cells originated from diverse origins. Adenosine triphosphate release occurs in a controlled way by exocytosis, transporters, and lysosomes or in large amounts from damaged cells, which is then subsequently degraded into adenosine. Paracrine and autocrine mechanisms induced by immune responses present critical factors for the success of stem cell therapy. While P1 receptors generally exert beneficial effects including anti-inflammatory activity, P2 receptor-mediated actions depend on the subtype of stimulated receptors and localization of tissue repair. Pro-inflammatory actions and excitatory tissue damages mainly result from P2X7 receptor activation, while other purinergic receptor subtypes participate in proliferation and differentiation, thereby providing adequate niches for stem cell engraftment and novel mechanisms for cell therapy and endogenous tissue repair. Therapeutic applications based on regulation of purinergic

signaling are foreseen for kidney and heart muscle regeneration, Clara-like cell replacement for pulmonary and bronchial epithelial cells as well as for induction of neurogenesis in case of neurodegenerative diseases.

Keywords ATP · Adenosine nucleotides · Purinergic signaling · Tissue injury · Differentiation · Immune system

An overview of purinergic signaling

Receptors for purines and pyrimidines are classified based on their agonist specificity. P1 receptors subtypes are selective for adenosine and are classical 7-transmembrane metabotropic receptors coupled to several families of Gi, Go, and Gs proteins. There are four types of adenosine receptors (A_1 , A_{2A} , A_{2B} , and A_3) differing in their pharmacological and functional properties [1]. P2 receptors are divided into P2X and P2Y subtypes based on their structural characteristics. P2X receptors are ATP-activated, ligand-gated cationic ($\text{Na}^+/\text{K}^+/\text{Ca}^{2+}$) channels [2, 3], assembled in trimeric form from P2X1 to P2X7 subunits [1, 3]. Metabotropic P2Y purinoreceptors expressed by mammals are divided into P2Y_{1,2,4,6,11,12,13,14} subtypes based on phylogenetic similarity and are stimulated by ATP, ADP, UTP, UDP, or UDP glucose [1]. Purinergic receptors are expressed by almost every cell type and are one of the first expressed neurotransmitter receptors in development [4–6]. The extracellular nucleotide/nucleoside availability is controlled by a highly efficient enzymatic cascade, which includes the members of the ectonucleoside triphosphate diphosphohydrolase (E-NTPDases, NTPDase1–8), ectonucleotide pyrophosphatase/phosphodiesterase (E-NPPs), ecto-alkaline phosphatases, and ecto-5'-nucleotidase/CD73. These enzymes catalyze the complete nucleotide

T. Glaser · M. M. Pillat · H. Ulrich (✉)
Departamento de Bioquímica , Instituto de Química,
Universidade São Paulo,
Av. Prof. Lineu Prestes, 748-Bloco 8S/Room 0858,
CEP: 05508-900 São Paulo, SP, Brazil
e-mail: henning@iq.usp.br

A. R. Cappellari · A. M. O. Battastini
Departamento de Bioquímica, ICBS,
Universidade Federal do Rio Grande do Sul,
Porto Alegre, RS, Brazil

I. C. Iser · M. R. Wink
Departamento de Ciências Básicas da Saúde,
Universidade Federal de Ciências da Saúde de Porto Alegre,
Porto Alegre, RS, Brazil

hydrolysis (e.g., ATP) to nucleosides (e.g., adenosine) and represent a powerful tool for controlling the effects mediated by extracellular purines [7–9].

Stem cells and purinergic signaling

Replacement of lost or dysfunctional tissues has recently raised many investigations on possible therapeutic application of stem cells. An impressive number of clinical trials and animal studies have already been performed to determine the therapeutic potential of various stem cells models [10, 11]. The first isolation of embryonic stem (ES) cells from mouse goes back to 1981 followed by human ES cell isolation and culture in 1998 [12, 13]. Organ-specific stem cells were isolated from embryonic and adult tissues including brain, bone marrow, umbilical cord, skeletal and cardiac muscles, and adipose tissue [14]. Pluripotent ES cells are capable to originate any somatic cell type, while tissue-specific stem cells are mostly multipotent and subsequently originate cell types found in these specific tissues. Both, ES and tissue-specific stem cells can proliferate symmetrically replicating themselves for self-renewal or asymmetrically giving rise to a stem cell and another more differentiated cell type. The most promising and recently discovered stem cell model for basic research and even therapy is the induced pluripotent stem cell (iPS cell), reprogrammed in 2006 from differentiated mouse cells and in 2007 from human cells [15, 16]. The recent described capacity of genetically reprogrammed somatic cells towards pluripotent ones could bypass obstacles, such as the lack of histocompatibility and ethical concerns, by allowing the generation of autologous cells from the patient. This new pluripotent cell source initially obtained by overexpression of the genes Klf-4, Oct4, Sox2, and c-Myc responsible for pluripotency [reviewed by 17] has opened expectations for treatment of many diseases. Importantly, iPS cells derived from different species demonstrated the potential to differentiate into tissues derived from the three germ layers, such as known from ES cells. However, care must be taken on using these cells as well as ES cells for transplantation purposes due to their possible tumorigenic potential.

Therapeutic application of stem cells in patients is particularly promising for treatment of heart disease, where new cardiomyocytes could restore contractile function after myocardial infarction. Cell regeneration therapy could be also relevant for repair of pancreatic function in diabetes with the replacement of β insulin-secreting cells [18]. Further possible applications are foreseen for the treatment of the damaged neuronal system and neurodegenerative diseases. For instance, efforts are being made to replace dopaminergic neurons in Parkinson's disease [19] or to use the stem cell therapy to restore motorneuron function in

patients suffering from spinal cord injuries [16]. However, the little obtained progress in many cases did not satisfy the high expectations made. Moreover, observed functional improvements observed in the treated tissues did not often result from the integration of stem cells into existing tissue architectures. It is evident that transplanted cells contribute to endogenous tissue repair through paracrine mechanisms more than by differentiating themselves. For instance, the success of neural progenitor cell (NPC) engrafting into the spinal cord of Sprague–Dawley rats, subjected to contusion at T8–T9 levels, was limited by allodynia due to the death of transplanted cells [7]. However, injection of conditioned media recovered from cultured stem cells promoted arterogenesis and functional improvement when injected into the damaged heart [20]. Therefore, it has been postulated that trophic factors represent the principle mechanism responsible for tissue repair.

Usual strategies for cell replacement therapy are based on the isolation of a stem cell source from a donor or the patient, followed by induction to proliferate and/or differentiate into tissue types which shall be repaired. Cell death and rejection of transplanted cells are mostly due to immune responses and the absence of adequate stem cell niches at the localization of transplantation. Although mechanisms by which the local milieu influences stem cell differentiation and tissue engraftment need yet to be elucidated, it seems that the fate of bone marrow stem cells is determined by the environment in which they engraft rather than by an intrinsically programmed fate. As support for such hypothesis, positive inotropic (pharmacologic augmentation of contractility) or chronotropic stimuli (heart rate increase by exercise) promoted and intensified the differentiation of bone marrow-derived stem cells into cardiomyocyte phenotypes [21]. Furthermore, stem cells secret trophic and immunomodulatory factors controlling local and systematic inflammatory responses. Such factors, liberated by, i.e., bone marrow stem cells are therapeutically important, since they stimulate local tissue regeneration and/or recruitment of endogenous stem or progenitor cells. Moreover, some studies have demonstrated that mesenchymal stem cells (MSC) can diminish the apoptosis degree and infarct size of the damaged areas by secreting a wide range of cytoprotective molecules like vascular endothelial growth factor, basic fibroblast growth factor, insulin-like growth factor 1, stromal cell-derived factor-1, platelet-derived growth factor, interleukin-1 beta, or hepatocyte growth factor [22].

Other factors with such therapeutic potential are UTP, UDP, ADP, and adenosine acting through purinergic receptors. Nucleotides, released after tissue injury and cell death and hydrolyzed by ectonucleotidases, also regulate immune cell function induced by damage-associated molecular pattern molecules [23]. Moreover, ATP released from immune cells participates in autocrine as well as in paracrine feedback loops with regulatory functions during T-cell

activation in the immune synapse (junction between T cell and antigen-presenting cell) [24]. During the inflammatory process following cell transplantation and hindering repair, purines exert trophic functions and keep several immune functions under control, including the release of prostanoids, activation of matrix metalloproteinase-9, cytokines and chemokines, proliferation, differentiation/maturation and stimulation of immune cells, endothelial adhesion, free radical production, degranulation, phagocytosis, fusion, and cell death [25]. Depending on the involved purinergic receptor subtype, ATP often exerts proinflammatory effects while adenosine induces mainly anti-inflammatory effects [25]. Several studies demonstrated that the absence or inhibition of the P2X7 receptor (a mediator of the pro-inflammatory effects of ATP) results in less severe outcomes in chronic inflammatory diseases and enhanced functional recovery [23, 26, 27].

Besides importance of purinergic receptor agonists in differentiated immune cells, these compounds also modulate hematopoietic stem cell (HSC) self-renewal, expansion, and differentiation with implications not only in hematopoiesis, but also in tissue repair and regenerative medicine [28, 29]. For instance, ATP induces the proliferation of human HSC and contributed through P2X receptor activation during inflammation process [29, 30]. UTP also induces proliferation and migration of HSCs [30, 31] while adenosine potentiates the stimulatory effect of growth factors and cytokines on HSC proliferation and differentiation [8]. Moreover, human MSCs at early stages of culture (P0–P5) spontaneously release ATP reducing cell proliferation. Increased human MSC proliferation is induced by the unselective P2 receptor antagonist pyridoxalphosphate-6-azophenyl-2',4'-disulfonate (PPADS) and by the selective P2Y1 receptor antagonist 2'-deoxy-N6-methyladenosine-3',5'-bisphosphate (MRS 2179). In summary, ATP modulates HSC and MSC proliferation and likely acts as one of the early factors determining their cell fate [32]. Furthermore, nucleotides also contribute to inflammatory responses and cell fate decisions occurring in the brain. P2X7 receptors expressed by NPCs are responsible for cell death, being in agreement with observations that high levels of extracellular ATP in inflammatory central nervous system (CNS) lesions hinder successful NPC engraftment [33].

The extracellular nucleotide/nucleoside availability is controlled by a highly efficient enzymatic cascade, which includes the members of the E-NTPDases (NTPDase1–8), E-NPPs, ecto-alkaline phosphatases, and ecto-5'-nucleotidase/CD73. These enzymes are responsible for nucleotide hydrolysis (e.g. ATP) into nucleosides (e.g., adenosine) and represent a powerful mechanism for controlling the effects mediated by extracellular purines [9, 34]. Although purinergic signaling has been extensively studied, only few studies are found in the literature demonstrating the involvement of extracellular nucleotide metabolizing

enzymes in stem cell biology. Expression and activities of members of ectonucleotidase families as well as purinergic receptor subtypes have been detected in different types of stem and progenitor cells. Recent works have identified the presence of NTPDase2 in adult mouse hippocampal progenitors [35] and in type B cells of the subventricular zone (SVZ) [36], two neurogenic regions of the adult mammalian brain. In accordance, neurospheres cultured from the adult mouse SVZ express NTPDase2, the tissue nonspecific isoform of alkaline phosphatase (TNAP) and functional P2 receptors in synergism with growth factors for enhancing cell proliferation [37]. In addition, deletion of TNAP expression or inhibition of its enzymatic activity in neural progenitors reduces cell proliferation and differentiation into neurons or oligodendrocytes [38]. These published data corroborate the importance of NTPDase2 and TNAP, two potential ATP scavengers, as novel markers for progenitor cells both in the adult and developing brain [39]. Reinforcing these results, spontaneous ATP release was observed in murine NPCs and, interestingly, purinergic receptors antagonists were able to suppress progenitor cell proliferation [40]. Moreover, neuronal differentiation was accompanied by a decrease in ATP release and a loss of functional P2Y receptors, suggesting that purine nucleotides act as proliferation-inducing factors for NPCs and downregulators of neuronal differentiation, once again pointing at the importance of purinergic signaling and involved enzymes for neurogenesis in the adult brain [40]. These data are in agreement with results of our laboratory [41], showing down-regulation of P2Y1 receptor expression and activity in differentiating P19 mouse embryonal carcinoma cells. This observation is in line with functions of the P2Y1 subtype in promoting proliferation of undifferentiated cells, but not induction of neuronal differentiation. Finally, the studies presented here demonstrate the potential participation of ectonucleotidases in the biology of stem or progenitor cells from different tissues. Initial results on roles of these ecto-enzymes will encourage more studies for better understanding of their importance in stem cell biology, differentiation, and tissue repair. In the following, we will discuss new trends of stem cell research related to purinergic signaling and the perspectives of using these discoveries as tools for future tissue repair in clinical trials as this new approach develops (see Fig. 1 for a scheme of the possible therapeutic use of purines in combination with stem cells).

Purinergic signaling and perspectives in tissue regeneration

Implications of the purinergic system in stem cell biology and tissue regeneration will be discussed with emphasis on

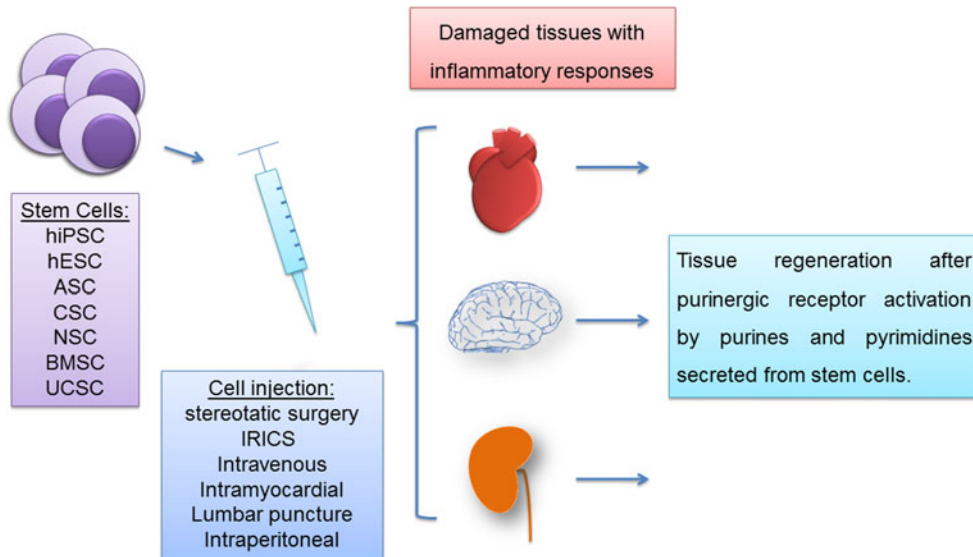


Fig. 1 Therapeutic potential of stem cells and supposed effects of purinergic signaling. Stem cells of diverse origins, such as from adipose, cardiac, and neural tissues can restore and regenerate damaged tissues by secreting paracrine factors including purines and pyrimidines. ATP and adenosine interfere with tissue reactions following transplantation of stem cells of various origins in different ways. (1) Nucleotides modulate the immune response and thereby reduce inflammation processes and the risk of transplant rejection and cell death. (2) Purines and pyrimidines promote proliferation and differentiation of transplanted and endogenous stem cells by providing

adequate stem cell niches. (3) Purines and pyrimidines induce migration of endogenous stem cells to the site of injury and increase engraftment rates. Stem cell types with therapeutic applications are human induced-pluripotent stem cells (hiPSC), human embryonic stem cells (hESC), adipose stem cells (ASC), cardiac stem cells (CSC), neural stem cells (NSC), bone marrow stem cells (BMSC), and umbilical cord stem cells (UCSC) which are transplanted by using stereotaxic surgery (SS), intracoronary retrograde infusion through coronary sinus (IRICS) or intravenous, intramyocardial, or intraperitoneal injection or lumbar puncture

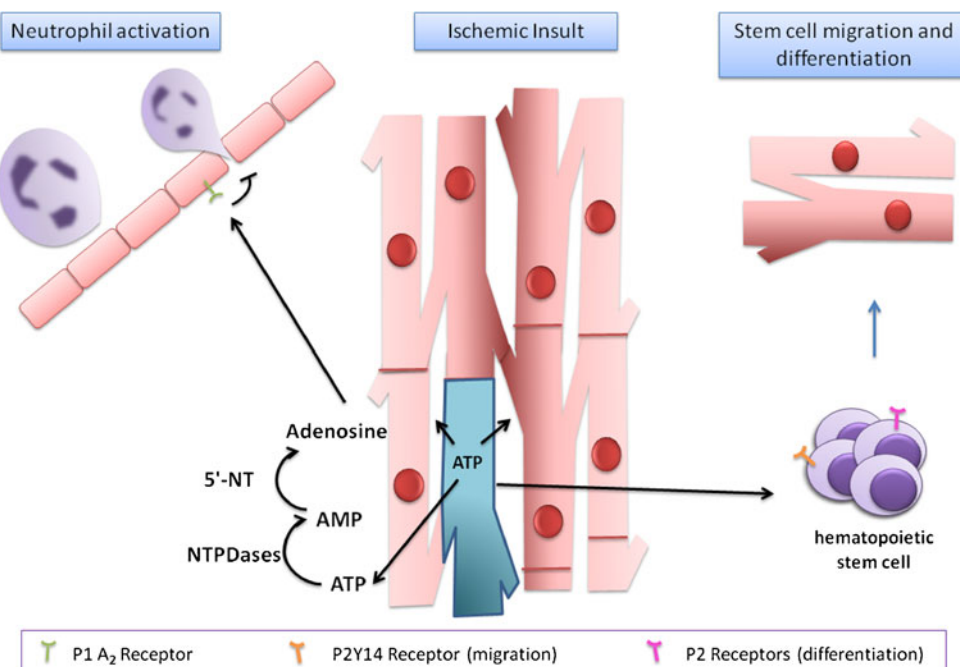
the recent hypothesis that paracrine effects present the most important mechanisms in this process. Since this idea is very recent, few data are available directly relating the purinergic system with stem cell differentiation and tissue regeneration; however, the authors of this review are confident that the present article will encourage research in order to better understand the participation of purinergic signaling in this context.

Heart injury

The heart is an organ composed basically of fibroblasts and cardiomyocytes, terminal-differentiated cells which give the heart the pumping ability. During ischemia and other injuries, the most affected cells are the cardiomyocytes because they die and a scar is formed due to the inability of renewing these cells. The scar stiffens the heart, decreasing its capability and efficiency in pumping the blood. Therefore, intense efforts are being made for the restoration of lost cells by cell therapy and maintenance of cardiac function in patients with heart injury. Many stem cells types have been studied in order to select the best model for cardiac cell therapy. ES cells, iPS cells as well as adult stem cells (bone marrow, adipose tissue-derived, and cardiac stem cells) are already tested in animal models and humans with often promising results [42, 43].

The most promising model is provided by cardiac stem cells (CSCs) that reside in small populations in the adult mammalian myocardium and have the potential to differentiate into cardiomyocytes and other cell types, such as endothelial and vascular smooth muscle cells [44–47]. However, differentiation of these cells is rare under physiological conditions [48]. For therapeutic purposes, CSCs can be generated by expanding autologous cells ex vivo or stimulating the regeneration capacity of these cells in vivo. Nevertheless, one of the biggest problems hindering the therapeutic use of stem cells lies still in the difficulty of keeping stem cells alive following transplantation. Cell death occurs before cells can engraft in their environment due to inflammation-signaling responses, or cells do not even identify the injured tissue site for engraftment. Therefore, signaling factors necessary for cell establishment at the location of transplantation are being investigated. Such paracrine factors include ATP and adenosine and their respective receptor subtypes. P2Y14 receptors expressed by bone marrow HSCs induce migration of these cells to the localization of injury followed by induction of differentiation at the site mediated by activation of other purinergic receptors [49] (Fig. 2). Adenosine plays many roles in the heart including regulation of growth, differentiation, angiogenesis, coronary blood flow, cardiac conduction and heart rate, substrate

Fig. 2 ATP-and adenosine-induced actions following cardiac ischemic insult. After myocardial injury following an ischemic insult, dead cells release ATP into the extracellular space. The released ATP stimulates P2Y14 receptors expressed by hematopoietic stem cells and possibly purinergic receptors on cardiac stem cells. NTPDases (ecto-nucleoside triphosphate diphosphohydrolases) dephosphorylate ATP via ADP to AMP, and 5'-nucleotidase (5'-NT) catalyzes the hydrolysis of AMP to adenosine inducing anti-inflammatory responses by activation of A_{2A} and A_{2B} receptors, blocking neutrophil activation and migration



metabolism, and sensitivity to adrenergic stimulation [50], and also functions as an endogenous determinant of ischemic tolerance [50]. The two A₂ receptor subtypes (A_{2A} and A_{2BA}) possess important anti-inflammatory and immunomodulatory functions, and probably control the impact of inflammatory processes during ischemic and post-ischemic damage. Vinten-Johansen and colleagues confirm protective functions of A_{2A} receptors in cardiac tissue by inhibition of neutrophil activation and neutrophil–vascular interactions as seen in Fig. 2 [51, 52].

Extracellular pyridoxal-5'-phosphate (PLP), a synthesis precursor of PPADS, is considered a P2 receptor antagonist. When this compound is used in the micromolar concentration range, it prevents ATP-induced calcium influx in isolated rat cardiomyocytes, inhibiting the positive inotropic effects of ATP on isolated perfused hearts and blocking ATP binding to the cardiac sarcolemma. Recent research suggests that at least part of the protective effect observed during reperfusion by PLP may be mediated through its inhibitory action on purinergic receptors. The possible receptors expressed in cardiomyocytes and subject to inhibition by PLP are P2Y1, P2Y2, P2Y4, P2Y6, and P2Y11 subtypes [53]. Taking together, the strategy of cell therapy following a heart attack could base on activation of P2Y14 purinergic receptors expressed by bone marrow stem cells which then would induce migration to the site of injury and thus could restore heart tissue before the formation of a scar. Furthermore, concomitant activation of A₂ receptors would decrease the damage caused by ischemia due to the anti-inflammatory activity of these receptors in preventing the activation of neutrophils which may cause further damage tissue. However, reservations

remain regarding stimulation of P2Y receptors in cardiomyocytes due to their involvement in apoptosis induction. Taken together, fundamental roles exist for the purinergic system in cardiac protection and preconditioning suggesting possible applications together with stem cell therapy.

Bladder dysfunction and glomerular injury

Much effort has been spent for establishing a stem cell therapy for the regeneration of tissues, including nephron and bladder. The urinary system is composed basically by kidneys, ureters, bladder, and urethra, and disorders in any of these structures can cause much pain and suffering for the patient. Hemodialysis and implementation of tubes are usually used for the treatment of patients with urogenital diseases; however, unfortunately, there is no cure for many diseases. Different stem cell types have been tested for therapeutic applications with varying success. For therapy of bladder dysfunction, Nishijima et al. transplanted bone marrow stem cells by intrabladder injection resulting in restored bladder contraction in rats [54]. Huang et al. transplanted adipose-derived stem cells by intrabladder or intravenous injection resulting in improved tissue parameters and urodynamics in a rat model of overactive bladder [55]. Interestingly, De Coppi et al. showed that intrabladder transplantation of amniotic fluid or bone marrow stem cells promoted post-injury bladder remodeling by a paracrine mechanism [56]. According to Hallman et al., the repair of injured renal epithelium is thought to be mediated by surviving renal proximal tubular cells that must dedifferentiate to allow for proliferation and migration necessary for epithelial regeneration. ATP and its intracellular signaling

have also crucial functions in this regeneration process. Kartha et al. showed that adenine nucleotides stimulate migration of kidney epithelial cells in an *in vitro* culture resembling wounded kidney. In these experiments, cells were treated with 10 μM of different adenine nucleotides, and the number of cells that migrated into the lesioned area of 1 mm² in size was counted 24 h later [57]. Increases in migration were induced by cAMP, adenosine, AMP, and ATP suggesting purinergic receptors activation; however, P1 receptors may promote contrary functions in this context, as adenosine can induce apoptosis in glomerular mesangial cells causing glomerular injury [58]. Babelova et al. showed that the secretion of the pro-inflammatory master cytokine interleukin (IL)-1β during inflammatory renal injury interacts with purinergic P2X4/P2X7 receptors [59]. Moreover, P2X7 receptor expression in glomeruli was augmented tenfold in diabetic and hypertensive rat models when compared to that of healthy rat glomeruli [60]. Purinergic signaling has also been related to renal protection via A_{2a} adenosine receptor activation in conditions of reperfusion injury [61]. In summary, for treatment of renal epithelium injury, transplantation of bone marrow or adipose tissue stem cells are promising. Migration to the injured sites can be induced by injecting cAMP, adenosine, AMP, and ATP suggesting purinergic receptor activation. On the other site, P1 receptor inhibition is indicated due to the contribution of these receptors to apoptosis under these conditions.

Parkinson's disease

Probably most effort has been put into the study of the applicability of cellular therapy in the nervous system due to its enormous impact on patient's life and a lack of therapeutic strategies to cure neurodegenerative diseases and spinal cord injuries. We describe here some recent discoveries related to purinergic signaling with impact on tissue repair in the neuronal system.

Parkinson's disease (PD) is a neurodegenerative illness caused by death of dopaminergic neurons in the substantia nigra pars, but the underlying mechanisms of neuronal death remain largely unknown. Dopaminergic neurons are responsible for dopamine neurotransmitter secretion and control body movements. The absence of this molecule in patients with PD generates tremor rigidity, postural instability, and loss of motor coordination affecting writing capability among other disturbances. Increased survival is achieved by surgical therapies and medications, principally based on administration of L-DOPA, but its prolonged use may generate uncontrollable movements known as dyskinesia [63, 64]. Purinergic signaling has implications in PD, since treatment with ATP enhances the

release of dopamine from dopaminergic neurons of the *substantia nigra*. However, at the same time, ATP release may activate P2X7 receptors expressed by neighboring cells thereby promoting cell death and contributing to an increase of the necrotic volume [62–65]. Furthermore, Feuvre et al. [66] provided evidence that P2X7 receptor activation following ATP release induces expression of proteins involved in the inflammatory response followed by liberation of cytokines. In addition, ATP together with glutamate released in neurodegenerative disorders may change intracellular Ca²⁺ homeostasis, mainly in neurons, with major importance for the disease progress [67].

Primary cultures of rat dopaminergic neurons express P2X1-7 and P2Y1 receptors together with D1 and D2 dopamine receptors [68]. P2Y receptor antagonists are potent neuroprotecting agents in the brain cortex, hippocampus, and cerebellum by modulating excessive neurotransmitter release in brain disorders [69, 70]; however, these effects would be undesirable in PD, since even PPADS blocking P2 receptors was shown to decrease dopamine secretion [71, 72]. A wide range of different strategies is under investigation for PD treatment, with a major focus research on stem cell therapy applications. Exogenous molecules are known to guide neural differentiation and are responsible for the high grade of phenotype specification, including induction of axonal growth and establishment of synaptic contact [73]. Milosevic et al. [74] detected P2Y4, P2Y6, and P2X4 receptor expression in cultured human NPCs from human fetal midbrain. UTP and UDP are known as agonists of the P2Y2/P2Y4 and P2Y6 receptors, respectively [75]. The treatment of hNPCs with UTP, in the presence of EGF and FGF2, increases cell proliferation. Moreover, UTP and UDP in the presence of specific culture medium enhance dopaminergic cell differentiation, and these effects are reduced by antagonists of P2 receptors.

Adenosine A_{2A} receptors are selectively located on striatopallidal neurons and are capable of forming functional heteromeric complexes with dopamine D2 and metabotropic glutamate mGlu5 receptors. A_{2A} receptor antagonists have emerged as an attractive nondopaminergic target to improve the motor deficits that characterize PD, based on the regional and unique cellular distribution of this receptor, being in agreement with data showing that A_{2A} receptor antagonists improve motor symptoms in animal models of Parkinson's disease and in initial clinical trials. Some experimental data also indicate that A_{2A} receptor antagonists do not induce neuroplasticity phenomena which complicate long-term dopaminergic treatments [76].

These data suggest the involvement of purinergic signaling in dopaminergic cell differentiation and possible applications for purinergic receptors in *in vitro* differenti-

ation cultures for posterior PD cell therapy [74]. However, more studies are needed to clarify whether extracellular nucleotides may contribute to favorable endogenous niches for stem cell transplantation or even recruit endogenous NPCs for dopaminergic differentiation.

Alzheimer's disease

The pathogenicity of Alzheimer's disease (AD) involves amyloids plaques and neurofibrillary tangle formation in the neuron extracellular medium. AD patients present an elevated production and secretion of the amyloid β peptide (A β) by neurons into the extracellular medium with progressive deposit of fibrils with high-grade toxicity, generating neuronal dysfunction and cell death [77–79]. This initial deposit triggers an inflammatory process with microglia and astrocyte recruitment to the injury site. Then, elevating cytokine secretion promotes A β internalization by neurons elevating neuronal damage [80–82]. ATP is released in high concentrations as result of cell death and enhances the local inflammatory effects besides increasing vulnerability of neurons by A β [61, 81]. Microglial cells recruited to the injury site showed elevated increased P2X7 receptor expression, as observed in animal models and human patients [83, 84]. P2X7 receptor activation by elevated ATP concentration promotes the secretion of the cytokines by microglial cells and activated oxygen species, increasing inflammation and stimulating A β -plaque formation, which also stimulates ATP liberation [82, 85, 86]. Furthermore, the P2Y1 subtype is expressed in AD typical structures such as A β plaques and neurofibrillary tangles, and receptor immunostaining was notably high in AD brain suggesting that P2Y1 receptors may participate in signaling events triggering neurodegenerative processes [61, 81, 82]. A₁ and A_{2A} adenosine receptor subtypes are expressed in the cortex, hippocampus, and microglia in the brain of patients suffering from AD. The A_{2A} receptor was suggested to contribute to memory deficits. The administration of caffeine, an antagonist of A₁ and A_{2A} receptors, promoted the protection against A β -induced neurotoxicity. Moreover, in vivo studies with A_{2A} antagonists resulted in reduced A β production and still protected against A β toxicity [87].

Hippocampus and the subventricular zone are the brain structures most affected in AD and are also the main sites of NPC localization. Increased NPC proliferation was observed in different illness stages; however, subsequent differentiation of these cells was not detected [88, 89]. NPCs implanted into the brain of a rat model of migrated to the disease site. Moreover, the presence of NPCs decreased microgliosis and the expression and secretion of pro-inflammatory cytokines, both characteristic conditions for AD. Elevated

neuroprotection was also observed together with augmented expression of MAP-2, a marker protein for mature neurons. However, NPCs were nestin-positive and negative for expression of neuronal marker proteins in immunostaining assays, indicating that neuronal differentiation did not occur [90]. Secreted A β 1–42, a more toxic form of the amyloid peptide causing cell death, evoked a reduction of NPC proliferation [91]. Nowadays, acetylcholinesterase inhibitors are being used to enhance cholinergic function and induce a temporary cognition improvement. Implants of NPCs derived from the cholinergic regions of the forebrain, appear to be a valid approach for cell therapy. ATP, a natural cotransmitter of acetylcholine, may gain importance in this context for helping to reestablish defective cholinergic transmission.

Several cell lines and animal models are used to assess mechanisms of neural differentiation and the interrelationship of action of various metabotropic and ionotropic receptors in this process. Trujillo et al. [62] suggested the intrinsic regulation between purinergic, cholinergic, and kallikrein–kinin systems for phenotype determination during neural differentiation. Using P19 embryonal carcinoma cells as in vitro model for neuronal differentiation, our group observed that functional purinergic receptors are essential for cell differentiation into neurons with functional cholinergic receptors [41].

According to Delarasse et al. [92], activation of P2X7 receptors stimulates soluble amyloid precursor protein α release from mouse neuroblastoma cells. In view of that, a possible treatment for AD could include inhibition of P2 receptors to decrease inflammatory responses, together with NPC injection secreting factors for reduction of inflammatory responses. Further studies will also reveal whether stimulation with ATP will help restoring cholinergic functions.

Epilepsy

Epilepsy is a brain disturbance manifested by frequent seizures with constant neural activation. It may be accompanied by massive glial cell proliferation, initiating following neurodegenerative processes. Several anti-epileptic agents inhibit the ability of astrocytes in transmitting intracellular Ca²⁺ waves. In view of that, purinergic receptor antagonists should offer a novel treatment for blocking Ca²⁺ wave propagation stimulated by ATP [93]. As further proof for such mechanism, injection of high doses of ATP into rat cortex promoted an increase in seizure occurrence, which could be antagonized by suramin [94]. Hippocampi from chronic epileptic rats demonstrated elevated P2X7 receptor expression and abnormal responses to ATP, suggesting a possible participation of this system in the pathophysiology of epilepsy [95]. Potent drugs are administrated in high doses in rats and mice to promote sequential seizures and behavioral and electrographic

changes [62]. In a rat epilepsy model, kainate application elevated microglial purinergic receptor expression, mainly P2X7 and P2Y12 receptor subtypes. Both receptors are associated with the active state of microglia, inducing inflammatory responses and microglia migration, respectively [95]. In a temporal lobe epilepsy model induced by pilocarpine injection, P2X4 receptor expression was significantly reduced in pyramidal neurons reflecting a neuronal loss in a chronic status, while elevated P2X7 receptor expression was observed in glial cells suggesting again its participation in the inflammatory response [95]. Oses [96] observed a decrease in P2X receptor expression in rat hippocampus following convulsive periods which may be associated with progressing neurodegeneration and seizure worsening during epilepsy. However, adenosine acting through A1 receptors in an epilepsy model induced by pilocarpine promoted significant protection against seizures [95, 97]. As a possible mechanism, adenosine participates in cell proliferation regulation and apoptosis eliminating useless and damaged cells during repair, without the necessity of neurotoxic mediators or immunomodulators. Furthermore, adenosine can control astrocyte proliferation triggered by other purine nucleotides [98].

Cell transplantation strategies have been employed for the treatment of epileptic disorders, but the effect of exogenous neural stem cells is unknown. Chua et al. evaluated possible anti-epileptogenic effect of NSCs in adult rats with status epilepticus and showed that NSCs differentiate into inhibitory interneurons and decrease neuronal excitability, preventing spontaneous recurrent seizure formation in adult rats with pilocarpine-induced temporal lobe epilepsy [99]. Therefore, a novel cellular source for the local therapeutic delivery of adenosine, a stem cell-based delivery system for adenosine, was generated by disruption of both alleles of adenosine kinase (AK) in mouse ES cells. These Ak^{-/-} ES cells were differentiated into glial precursor cells and released significant amounts of adenosine. Rats with adenosine releasing Ak^{-/-} ES cell-derived implants displayed transient protection against convulsive seizures and a profound reduction of after-discharge activity in EEG recordings, providing a proof-of-principle evidence that Ak^{-/-} ES cell-derived brain implants suppress seizure activity by a paracrine mode of action [100]. In summary, stem cell therapy may be successful for epilepsy if transplanted NSCs feature a paracrine effect by releasing adenosine, which decreases the number of seizures, besides their ability to differentiate into inhibitory interneurons.

Trauma, ischemia, and hypoxia in the CNS

During several injury conditions such as trauma, ischemia, and hypoxia, ATP secretion is an important signaling

molecule involved in repair of damaged tissue. After spinal cord injury, a large peritraumatic region sustains pathological processes to keep high ATP concentrations in the extracellular medium [61] involving P2X7 receptor activation and cell death as already discussed in this review. For instance, P2X7 receptors are expressed in neurons, astrocytes, and microglia of brain tissue suffering from ischemic conditions [82, 101]. Accordingly, administration of P2 receptor antagonists improved cell function and reduced cell death in the peritraumatic zone [81]. Moreover, after lesions in the peripheral nervous system, P2X3 receptor expression in intact neurons, suggesting a role for this receptor in post-traumatic repair [102]. Following trauma, astrocytes increased expression of P2X4 receptors thereby inducing thrombospondin-1 secretion, which constitutes an extracellular molecule for synapse formation contributing to CNS remodeling [81, 103]. However, as already said, ATP also promotes neuronal apoptosis, necrosis and astrocytic death after traumatic events. P2 receptors promote the recruitment of microglial cells from distal areas to the traumatic core [104]. In vivo studies showed that P2X4 and P2Y12 receptors stimulated migration of microglial cells to the injury area after trauma, followed by expression of P2Y6 receptors favoring the secondary damage moment, the debris phagocytosis [82]. Experimental evidence indicates liberation of adenosine into the extracellular medium after tissue damage together with down-regulation of AK expression, leading to adenosine accumulation and neuroprotection following injury [105]. ATP in the extracellular medium may attract astrocytes and microglia to the site of injury in order to assist tissue repair [106]. In the normal adult brain, ATP secreted by astrocytes stimulates NPC proliferation and migration, while P2Y receptor antagonists reversed this effect by inhibiting proliferation. During the neurogenesis process, NPCs revealed NTPDase activity for controlling ATP concentration and subsequently directing neuronal and glial differentiation [40]. In summary, treatment of spinal cord injury and other traumatic and ischemic disorders of the CNS would benefit from P2 receptor inhibition in order to reduce cell death, followed by activation of P2X3 and P2X4 receptors for induction of synapse formation. Thereby, extracellular adenosine accumulation leads to neuroprotection during injury while ATP may attract astrocytes and microglia to the site of injury to assist tissue repair. In vitro NPC differentiation is directed by P2Y receptors; such mechanism should be further validated in animal models.

Skin injury

Skin is a stratified epithelium, where the epidermis is the outermost part of this tissue and dermis is innermost. Epidermis is mainly constituted by keratinocytes (90–95%)

and these cells are arranged in continuous layers from the inside towards outer layers: the basal layer, the stratum spinosum, the granular layer and stratum corneum. The epidermis is capable of self-renewal by presenting adult stem cells, which proliferate and can originate a new epidermis to cover all body surfaces. These stem cells are located in a portion of the follicle hair known as bulge migrating upwards to the proliferative basal layer. Keratinocytes migrate from the basal layer to the skin surface with concomitant differentiation [107–109]. In physiological and in pathological conditions, many kind of cells related to nervous and immune systems, can generate ATP extravasation and accumulation in the extracellular medium of keratinocytes. Two important functions are attributed to this nucleotide such as modulation of keratinocyte proliferation and differentiation [110]. Many studies have shown that these effects are mediated by ATP action through P2X and P2Y receptor subtypes, and it is known that the epidermis expresses P2X5, P2X7, P2Y1, and P2Y2 subtypes with diverse functions [111–113].

P2Y1 and P2Y2 receptors expressed in basal layers of the fetal and adult epidermis [111, 113] were immune colocalized with the cell proliferation markers Ki67 and PCNA (proliferation cell nuclear antigen) [111]. The P2Y1 receptor agonist 2-methylthio-ADP (P2Y1 agonist) and UTP activating P2Y2 receptors induced proliferation in cell cultures of basal keratinocytes [113]. P2Y1 and P2Y2 subtypes are coupled to Phospholipase C via G_{q/11} proteins with generation of Inositol 3-phosphate and, in sequence, induce intracellular calcium mobilization [113] leading to Cl[−] conductance and starting keratinocyte differentiation [112]. In an in vivo wound-healing model, the P2Y1 receptor is expressed in epidermal basal layers and the wound edge, while the P2Y2 subtype is expressed in basal and suprabasal layers, but is not expressed in the wound edge. Alterations of distribution patterns of purinergic receptors occur during phenotype changes as keratinocytes become migratory cells in the wound-healing process [110]. P2X5 receptors are expressed in undifferentiated basal and intermediate layers of fetal epidermis with high immunoreactivity for cytokeratin-10, an initial differentiation marker [111]. In wounded epidermis, keratinocytes of the wound edge increase P2X5 receptor expression [111]. P2X7 receptor expression was detected together with labeling for caspase-3 and TUNEL, markers for terminal differentiation and apoptosis, respectively, suggesting that this receptor eliminates not any more needed cells during final epidermis development [111]. Furthermore, the P2X7 subtype is also expressed in corneum stratum in adult epidermis suggesting its participation in apoptotic control [111, 113]. During wound healing processes, P2X7 receptor expression was not detected [111]. ATP is released by keratinocytes into the extracellular space by mechanical stress and external damage and achieves elevated extracellular, cytotoxic levels. Elevated ATP concentrations

(300 μM) were applied together with UV radiation as external damage model in cultured human epidermal keratinocytes. Both situations augmented significantly P2X7 receptor and reduced P2Y2 receptor expression while P2X5 and P2Y1 subtype expression levels were not altered. These events associated with elevated extracellular ATP concentration result in skin inflammation, demonstrating the role of purinergic signaling in skin physiology and disease induction [112]. Purinergic signaling could promote skin injury therapy by selective activation of P2Y1 and P2Y2 receptors favoring the phenotype of migratory cells without induction of inflammatory responses.

Pulmonary epithelium injury

The airway epithelium is exposed to environmental pollutants, allergens and pathogens that might lead to tissue damage or the development of a variety of infectious and inflammatory diseases such as chronic bronchitis, chronic obstructive pulmonary disease, asthma, and fibrosis. In this context, stem and progenitor cells are involved in lung regeneration. They are located within the basal layer of the upper airways, within or near pulmonary neuroendocrine cell rests, at the bronchoalveolar junction, and within the epithelial surface [114–116]. The airway epithelium represents the first barrier to inhaled particles and pathogens and because of this, it suffers constant damages. Thus, the mechanism of the repair of damaged epithelium has been widely studied. Epithelial progenitors termed Clara cells (transit-amplifying cells) are broadly distributed and after injury differentiate into ciliated cells [117, 118]. In addition to Clara cells, bronchiolar airways have also rare stem cells that contribute to repair of the tissue [119]. Both Clara and stem cells present the CD45^{neg} CD31^{neg} CD34^{neg} Scal^{low} phenotype. However, it is possible to distinguish between the two cell types based on high (AF^{high}) and low autofluorescence (AF^{low}), respectively [120]. Clara-like cells are another cell type that exhibits many features of pluripotent stem cells and apparently contributes to epithelial regeneration [120–122]. They can be discriminated from Clara cells by their resistance to naphthalene and their close association with pulmonary neuroepithelial bodies (NEBs) [123, 124]. ATP released from secretory vesicles of rodent NEBs [125] in response to depolarization in lung slices promotes paracrine effects on surrounding Clara-like cells by activation of P2Y2 receptors. Considering the stem cell-like characteristics of Clara-like cells, this purinergic signaling might be of great importance for airway epithelial repair after injury [123].

Furthermore, ATP regulates diverse processes involved in host defense such as anion transport, ciliary function and mucin expression and is also suggested to function in wound repair [126–128]. ATP-mediated P2 purinergic receptor

activation promotes bronchial epithelial migration and epithelial repair. This is suggested to occur after activation of dual oxidase 1 mediated by release of ATP during injury [123]. In addition, adenosine also stimulates cell migration, proliferation, and angiogenesis [129, 130]. Experimental evidence suggests that adenosine evokes wound closure via A_{2A} receptor activation, since A_{2A} agonists promote early wound closure while A_{2A} antagonists impede the healing process [131]. The continuous denudation and repair of airway epithelium occurs especially in inflammatory airways diseases such as asthma [132]. Asthma is a chronic inflammatory airway disease orchestrated by eosinophils, mast cells, Th2 lymphocytes, and dendritic cells (DCs) [133]. ATP is reported to be important for the genesis and maintenance of this disease. For instance, ATP triggers and maintains asthmatic inflammation by activating DCs and enhancing its Th2-priming capacity [134, 135]. Another study demonstrated that this allergic inflammation in humans and mice is associated with the functional up-regulation of P2X7 receptor expression on immune cells (macrophages and eosinophils) and that P2X7 receptor signaling (e.g., via modulating of DC function) is involved in ATP-mediated pro-asthmatic effects [136]. P2X7 receptor $-/-$ knock-out animals or animals treated with a selective P2X7 receptor antagonist showed a strong reduction in all cardinal features of acute allergic airway inflammation including airway eosinophilia, goblet cell hyperplasia, and bronchial hyperresponsiveness to methacholine [137]. Thus, P2X7 receptor antagonists might be a new therapeutic option for the

treatment of severe asthma. Moreover, adenosine is also important in asthmatic inflammation. Inhaled adenosine induced bronchoconstriction in patients suffering from chronic asthma or obstructive pulmonary disorder (COPD), and adenosine receptor blockade prevented this bronchoconstriction [138]. Adenosine-mediated effects through A_{2B} and A₃ receptor activation play key roles in mast cells producing pro-inflammatory mediators (histamine, IL-8, and degranulation) [139, 140]. Therefore, CVT-6883, an A_{2B} receptor antagonist, is being evaluated in phase I clinical studies for the management of asthma and COPD in human patients. Mobilization of hematopoietic progenitor cells from the bone marrow comprises also a feature of asthmatic inflammation [141–143]. However, in the airway, these progenitor cells have the potential to generate *in situ* mature inflammatory cells, principally eosinophils [142, 144]. Moreover, it has been suggested that purinergic signaling in HSCs is important for genesis of asthma. Some studies indicate that this allergy is transferable and curable with allogeneic hematopoietic cell transplantation, but more studies are still necessary [144, 145]. In summary, for pulmonary epithelium repair, promotion of P2 purinergic receptor-mediated effects inducing bronchial epithelial migration and epithelial repair would be a valid strategy, while adenosine stimulates migration, proliferation and angiogenesis. Hematopoietic progenitor cells from the bone marrow have the potential to generate *in situ* mature inflammatory cells; therefore, it would be necessary to inhibit this effect while the epithelium is regenerating.

Table 1 Functions of purinergic receptor in stem cells and tissue repair

Tissue/cell	Purinergic receptors	Action
Kidney epithelial cells	↑P2R	Induction of cell migration in wounded kidney
Kidney	↑P1 A2aR	Protection during reperfusion (ischemia)
Heart	↑P1 A2A and A2BR	Anti-inflammatory function (ischemia)
Heart	↓P2Y1, P2Y2, P2Y4, P2Y6, P2Y11R	Protection during reperfusion (ischemia)
Substantia nigra	↑P2X7R	Induction of cell death (Parkinson's Disease)
Brain cortex, hippocampus and cerebellum	↑P2YR	Modulation of neurotransmitter release (healthy tissue)
Human neural progenitor cell	↑P2Y4, P2Y6R	Induction of proliferation/dopaminergic differentiation of NPCs
Brain	↑P2X7R	Cytokine secretion by microglial (increasing inflammation)
Brain	↓A1, A2AR	Protection against A β plaque-mediated neurotoxicity (Alzheimer's disease)
Skin	↑P2Y1, P2Y2R	Induction of proliferation / migration of basal keratinocytes (wounded tissue)
Epidermis	↑P2X5R	Induction of differentiation to keratinocytes (wounded tissue)
Epithelial pulmonary cells	↑P2Y2R	Activation of Clara-like cells for tissue repair (tissue damage)
Bronchial epithelial cells	↑P1 A2AR	Activation of cell migration and wound repair

↑ upregulation and ↓ downregulation of purinergic receptor expression

Conclusions

Stem cell transplantation and engraftment depends on the secretion of anti-inflammatory molecules, in addition to extrinsic and endogenous factors promoting differentiation into distinct cell types depending on the injury site. While adenosine receptors often, but not every time, exert beneficial effects in providing adequate stem cell niches, functions of P2Y and P2X receptors depend very much on the tissue and the expression pattern of these receptors (see Table 1). Therapeutic applications based on activation of purinergic signaling are foreseen for kidney and heart muscle regeneration, while other disease conditions will yet need further investigation. While nucleotides have been shown to promote differentiation of dopaminergic neurons destroyed in Parkinson's disease, other neuronal diseases involve excitatory cell damage mostly due to P2X7 receptor action. Therapeutic inhibition of such receptor activity would be required for improving disease conditions. Finally, the need of P2Y2 and A_{2A} receptor activation during Clara-like cell differentiation into pulmonary and bronchial epithelial cells just corroborates the fact that purinergic signaling is well involved in tissue repair, specially mediated by stem cells. More work need to be done for elucidation of crucial concepts which could revolutionize cell therapy.

Acknowledgments HU acknowledges grant support from Fundação de Amparo à Pesquisa do Estado de São Paulo (FAPESP) and CNPq (Conselho Nacional de Desenvolvimento Científico e Tecnológico), Brazil, project no. 2006/61285-9. TG, PDN, and CL are supported by fellowships from FAPESP. ARC, MMP, and IC are grateful for fellowships from CNPq. Grant support by FAPERGS/CNPq - PRONEX, Brazil, is also acknowledged.

References

- Verkhratsky A, Krishnal OA, Burnstock G (2009) Purinoceptors on neuroglia. *Mol Neurobiol* 39(3):190–208. doi:10.1007/s12035-009-8063-2
- Burnstock G (1997) The past, present and future of purine nucleotides as signalling molecules. *Neuropharmacology* 36(9):1127–1139
- North RA (1996) P2X receptors: a third major class of ligand-gated ion channels. *Ciba Found Symp* 198:91–105, discussion 105–109
- Burnstock G, Campbell G, Satchell D, Smythe A (1997) Evidence that adenosine triphosphate or a related nucleotide is the transmitter substance released by non-adrenergic inhibitory nerves in the gut. 1970. *Br J Pharmacol* 120(4 Suppl):337–357, discussion 334–336
- Burnstock G (1986) The changing face of autonomic neuro-transmission. *Acta Physiol Scand* 126(1):67–91
- Burnstock G, Ulrich H (2011) Purinergic signaling in embryonic and stem cell development. *Cell Mol Life Sci* 68(8):1369–1394. doi:10.1007/s00018-010-0614-1
- Hofstetter CP, Holmstrom NA, Lilja JA, Schweinhardt P, Hao J, Spenger C, Wiesenfeld-Hallin Z, Kurpad SN, Frisen J, Olson L (2005) Allodynia limits the usefulness of intraspinal neural stem cell grafts; directed differentiation improves outcome. *Nat Neurosci* 8(3):346–353. doi:10.1038/nn1405
- Hofer M, Vacek A, Pospisil M, Weiterova L, Hola J, Streitova D, Znojil V (2006) Adenosine potentiates stimulatory effects on granulocyte-macrophage hematopoietic progenitor cells in vitro of IL-3 and SCF, but not those of G-CSF, GM-CSF and IL-11. *Physiol Res* 55(5):591–596
- Zimmermann H (2001) Ectonucleotidases: some recent developments and a note on nomenclature. *Drug Dev Res* 52(1–2):44–56. doi:10.1002/ddr.1097
- Trounson A, Thakar RG, Lomax G, Gibbons D (2011) Clinical trials for stem cell therapies. *BMC Med* 10:9–52. doi:10.1186/1741-7015-9-52
- Lodi D, Iannitti T, Palmieri B (2011) Stem cells in clinical practice: applications and warnings. *J Exp Clin Cancer Res* 30(9). doi:10.1186/1756-9966-30-9
- Evans MJ, Kaufman MH (1981) Establishment in culture of pluripotential cells from mouse embryos. *Nature* 292(5819):154–156
- Thomson JA, Itskovitz-Eldor J, Shapiro SS, Waknitz MA, Swiergiel JJ, Marshall VS, Jones JM (1998) Embryonic stem cell lines derived from human blastocysts. *Science* 282(5391):1145–1147
- Pelacho B, Mazo M, Gavira JJ, Prosper F (2011) Adult stem cells: from new cell sources to changes in methodology. *J Cardiovasc Transl Res* 4(2):154–160. doi:10.1007/s12265-010-9245-z
- Takahashi K, Yamanaka S (2006) Induction of pluripotent stem cells from mouse embryonic and adult fibroblast cultures by defined factors. *Cell* 126(4):663–676. doi:10.1016/j.cell.2006.07.024
- Takahashi K, Tanabe K, Ohnuki M, Narita M, Ichisaka T, Tomoda K, Yamanaka S (2007) Induction of pluripotent stem cells from adult human fibroblasts by defined factors. *Cell* 131(5):861–872. doi:10.1016/j.cell.2007.11.019
- Yamanaka S, Blau HM (2010) Nuclear reprogramming to a pluripotent state by three approaches. *Nature* 465(7299):704–712. doi:10.1038/nature09229
- Passier R, van Laake LW, Mummery CL (2008) Stem-cell-based therapy and lessons from the heart. *Nature* 453(7193):322–329. doi:10.1038/nature07040
- Dambrot C, Passier R, Atsma D, Mummery CL (2011) Cardiomyocyte differentiation of pluripotent stem cells and their use as cardiac disease models. *Biochem J* 434(1):25–35. doi:10.1042/BJ20101707
- Gnechi M, He H, Noiseux N, Liang OD, Zhang L, Morello F (2006) Evidence supporting paracrine hypothesis for Akt-modified mesenchymal stem cell-mediated cardiac protection and functional improvement. *FASEB J* 20(6):661–669
- Laflamme MA, Myerson D, Saffitz JE (2002) Evidence for cardiomyocyte repopulation by extracardiac progenitors in transplanted human hearts. *Circ Res* 90:634–640
- Uemura R, Xu M, Ahmad N, Ashraf M (2006) Bone marrow stem cells prevent left ventricular remodeling of ischemic heart through paracrine signaling. *Circ Res* 98(11):1414–1421
- Khakh BS, North RA (2006) P2X receptors as cell-surface ATP sensors in health and disease. *Nature* 442(7102):527–532. doi:10.1038/nature04886
- Junger WG (2011) Immune cell regulation by autocrine purinergic signalling. *Nat Rev Immunol* 11(3):201–212. doi:10.1038/nri2938
- Di Virgilio F, Falzoni S, Mutini C, Sanz JM, Chiozzi P (1998) Purinergic P2X7 receptor: a pivotal role in inflammation and immunomodulation. *Drug Dev Res* 45(3–4):doi:10.1002/(SICI)1098-2299(199811/12)45:3/4<207::AID-DDR18>3.0.CO;2-N
- Surprenant A, North RA (2009) Signaling at purinergic P2X receptors. *Annu Rev Physiol* 71:333–359. doi:10.1146/annurev.physiol.70.113006.100630

27. Carroll WA, Donnelly-Roberts D, Jarvis MF (2009) Selective P2X(7) receptor antagonists for chronic inflammation and pain. *Purinergic Signal* 5(1):63–73. doi:[10.1007/s11302-008-9110-6](https://doi.org/10.1007/s11302-008-9110-6)
28. Sak K, Boeynaems JM, Everaus H (2003) Involvement of P2Y receptors in the differentiation of haematopoietic cells. *J Leukoc Biol* 73(4):442–447
29. Casati A, Frascoli M, Traggiai E, Proietti M, Schenck U, Grassi F (2011) Cell-autonomous regulation of hematopoietic stem cell cycling activity by ATP. *Cell Death Differ* 18(3):396–404. doi:[10.1038/cdd.2010.107](https://doi.org/10.1038/cdd.2010.107)
30. Lemoli RM, Ferrari D, Fogli M, Rossi L, Pizzirani C, Forchap S, Chiozzi P, Vaselli D, Bertolini F, Foutz T, Aluigi M, Baccarani M, Di Virgilio F (2004) Extracellular nucleotides are potent stimulators of human hematopoietic stem cells in vitro and in vivo. *Blood* 104 (6):1662–1670. doi:[10.1182/blood-2004-03-08342004-03-0834](https://doi.org/10.1182/blood-2004-03-08342004-03-0834)
31. Rossi L, Manfredini R, Bertolini F, Ferrari D, Fogli M, Zini R, Salati S, Salvestri V, Gulinelli S, Adinolfi E, Ferrari S, Di Virgilio F, Baccarani M, Lemoli RM (2007) The extracellular nucleotide UTP is a potent inducer of hematopoietic stem cell migration. *Blood* 109 (2):533–542. doi:[10.1182/blood-2006-01-035634](https://doi.org/10.1182/blood-2006-01-035634)
32. Coppi E, Pugliese AM, Urbani S, Melani A, Cerbai E, Mazzanti B, Bosi A, Saccardi R, Pedata F (2007) ATP modulates cell proliferation and elicits two different electrophysiological responses in human mesenchymal stem cells. *Stem Cells* 25 (7):1840–1849
33. Delaras C, Gonnord P, Galante M, Auger R, Daniel H, Motta I, Kanellopoulos JM (2009) Neural progenitor cell death is induced by extracellular ATP via ligation of P2X7 receptor. *J Neurochem* 109(3):846–857
34. Robson SC, Sevigny J, Zimmermann H (2006) The E-NTPDase family of ectonucleotidases: structure function relationships and pathophysiological significance. *Purinergic Signal* 2(2):409–430. doi:[10.1007/s11302-006-9003-5](https://doi.org/10.1007/s11302-006-9003-5)
35. Shukla V, Zimmermann H, Wang L, Kettenmann H, Raab S, Hammer K, Sevigny J, Robson SC, Braun N (2005) Functional expression of the ecto-ATPase NTPDase2 and of nucleotide receptors by neuronal progenitor cells in the adult murine hippocampus. *J Neurosci Res* 80(5):600–610. doi:[10.1002/jnr.20508](https://doi.org/10.1002/jnr.20508)
36. Braun N, Sevigny J, Mishra SK, Robson SC, Barth SW, Gerstberger R, Hammer K, Zimmermann H (2003) Expression of the ecto-ATPase NTPDase2 in the germinal zones of the developing and adult rat brain. *Eur J Neurosci* 17(7):1355–1364
37. Mishra SK, Braun N, Shukla V, Fullgrabe M, Schomerus C, Korf HW, Gachet C, Ikebara Y, Sevigny J, Robson SC, Zimmermann H (2006) Extracellular nucleotide signaling in adult neural stem cells: synergism with growth factor-mediated cellular proliferation. *Development* 133(4):675–684. doi:[10.1242/dev.02233](https://doi.org/10.1242/dev.02233)
38. Kermer V, Ritter M, Albuquerque B, Leib C, Stanke M, Zimmermann H (2010) Knockdown of tissue nonspecific alkaline phosphatase impairs neural stem cell proliferation and differentiation. *Neurosci Lett* 485(3):208–211. doi:[10.1016/j.neulet.2010.09.013](https://doi.org/10.1016/j.neulet.2010.09.013)
39. Langer D, Ikebara Y, Takebayashi H, Hawkes R, Zimmermann H (2007) The ectonucleotidases alkaline phosphatase and nucleoside triphosphate diphosphohydrolase 2 are associated with subsets of progenitor cell populations in the mouse embryonic, postnatal and adult neurogenic zones. *Neuroscience* 150(4):863–879. doi:[10.1016/j.neuroscience.2007.07.064](https://doi.org/10.1016/j.neuroscience.2007.07.064)
40. Lin JH, Takano T, Arcuino G, Wang X, Hu F, Darzynkiewicz Z, Nunes M, Goldman SA, Nedergaard M (2007) Purinergic signaling regulates neural progenitor cell expansion and neurogenesis. *Dev Biol* 302(1):356–366. doi:[10.1016/j.ydbio.2006.09.017](https://doi.org/10.1016/j.ydbio.2006.09.017)
41. Resende RR, Britto LR, Ulrich H (2008) Pharmacological properties of purinergic receptors and their effects on proliferation and induction of neuronal differentiation of P19 embryonal carcinoma cells. *Int J Dev Neurosci* 26(7):763–777. doi:[10.1016/j.ijdevneu.2008.07.008](https://doi.org/10.1016/j.ijdevneu.2008.07.008)
42. Xie X, Sun A, Huang Z, Zhu W, Wang S, Zou Y, Ge J (2011) Another possible cell source for cardiac regenerative medicine: reprogramming adult fibroblasts to cardiomyocytes and endothelial progenitor cells. *Med Hypotheses* 76(3):365–367. doi:[10.1016/j.mehy.2010.10.041](https://doi.org/10.1016/j.mehy.2010.10.041)
43. Martinez EC, Kofidis T (2011) Adult stem cells for cardiac tissue engineering. *J Mol Cell Cardiol* 50(2):312–319. doi:[10.1016/j.yjmcc.2010.08.009](https://doi.org/10.1016/j.yjmcc.2010.08.009)
44. Beltrami AP, Barlucchi L, Torella D, Baker M, Limana F, Chimenti S, Kasahara H, Rota M, Musso E, Urbanek K, Leri A, Kajstura J, Nadal-Ginard B, Anversa P (2003) Adult cardiac stem cells are multipotent and support myocardial regeneration. *Cell* 114(6):763–776
45. Laugwitz KL, Moretti A, Lam J, Gruber P, Chen Y, Woodard S, Lin LZ, Cai CL, Lu MM, Reth M, Platoshyn O, Yuan JX, Evans S, Chien KR (2005) Postnatal islet1+ cardioblasts enter fully differentiated cardiomyocyte lineages. *Nature* 433(7026):647–653. doi:[10.1038/nature03215](https://doi.org/10.1038/nature03215)
46. Martin CM, Meeson AP, Robertson SM, Hawke TJ, Richardson JA, Bates S, Goetsch SC, Gallardo TD, Garry DJ (2004) Persistent expression of the ATP-binding cassette transporter, Abcg2, identifies cardiac SP cells in the developing and adult heart. *Dev Biol* 265(1):262–275
47. Oh H, Bradfute SB, Gallardo TD, Nakamura T, Gaussion V, Mishina Y, Pocius J, Michael LH, Behringer RR, Garry DJ, Entman ML, Schneider MD (2003) Cardiac progenitor cells from adult myocardium: homing, differentiation, and fusion after infarction. *Proc Natl Acad Sci USA* 100(21):12313–12318. doi:[10.1073/pnas.2132126100](https://doi.org/10.1073/pnas.2132126100)
48. Hsieh PC, Segers VF, Davis ME, MacGillivray C, Gannon J, Molkentin JD, Robbins J, Lee RT (2007) Evidence from a genetic fate-mapping study that stem cells refresh adult mammalian cardiomyocytes after injury. *Nat Med* 13(8):970–974. doi:[10.1038/nm1618](https://doi.org/10.1038/nm1618)
49. Lee BC, Cheng T, Adams GB, Attar EC, Miura N, Lee SB, Saito Y, Olszak I, Dombrowski D, Olson DP, Hancock J, Choi PS, Haber DA, Luster AD, Scadden DT (2003) P2Y-like receptor, GPR105 (P2Y14), identifies and mediates chemotaxis of bone-marrow hematopoietic stem cells. *Genes Dev* 17(13):1592–1604. doi:[10.1101/gad.107150317/13/1592](https://doi.org/10.1101/gad.107150317/13/1592)
50. Headrick JP, Hack B, Ashton KJ (2003) Acute adenosinergic cardioprotection in ischemic-reperfused hearts. *Am J Physiol Heart Circ Physiol* 285(5):H1797–H1818. doi:[10.1152/ajpheart.00407.2003285/5/H1797](https://doi.org/10.1152/ajpheart.00407.2003285/5/H1797)
51. Jordan JE, Zhao ZQ, Sato H, Taft S, Vinten-Johansen J (1997) Adenosine A2 receptor activation attenuates reperfusion injury by inhibiting neutrophil accumulation, superoxide generation and coronary endothelial adherence. *J Pharmacol Exp Ther* 280 (1):301–309
52. Zhao ZQ, Todd JC, Sato H, Ma XL, Vinten-Johansen J (1997) Adenosine inhibition of neutrophil damage during reperfusion does not involve K(ATP)-channel activation. *Am J Physiol* 273(4 Pt 2):H1677–H1687
53. Millart H, Alouane L, Oszust F, Chevallier S, Robinet A (2009) Involvement of P2Y receptors in pyridoxal-5'-phosphate-induced cardiac preconditioning. *Fundam Clin Pharmacol* 23(3):279–292. doi:[10.1111/j.1472-8206.2009.00677.x](https://doi.org/10.1111/j.1472-8206.2009.00677.x)
54. Nishijima S, Sugaya K, Miyazato M, Kadekawa K, Oshiro Y, Uchida A, Hokama S, Ogawa Y (2007) Restoration of bladder contraction by bone marrow transplantation in rats with underactive bladder. *Biomed Res* 28(5):275–280
55. Huang YC, Shindel AW, Ning H, Lin G, Harraz AM, Wang G, Garcia M, Lue TF, Lin CS (2010) Adipose derived stem cells ameliorate hyperlipidemia associated detrusor overactivity in a rat model. *J Urol* 183(3):1232–1240. doi:[10.1016/j.juro.2009.11.012](https://doi.org/10.1016/j.juro.2009.11.012)

56. De Coppi P, Callegari A, Chiavegato A, Gasparotto L, Piccoli M, Taiani J, Pozzobon M, Boldrin L, Okabe M, Cozzi E, Atala A, Gamba P, Sartore S (2007) Amniotic fluid and bone marrow derived mesenchymal stem cells can be converted to smooth muscle cells in the cryo-injured rat bladder and prevent compensatory hypertrophy of surviving smooth muscle cells. *J Urol* 177(1):369–376. doi:[10.1016/j.juro.2006.09.103](https://doi.org/10.1016/j.juro.2006.09.103)
57. Kartha S, Toback FG (1992) Adenine nucleotides stimulate migration in wounded cultures of kidney epithelial cells. *J Clin Invest* 90(1):288–292. doi:[10.1172/JCI115851](https://doi.org/10.1172/JCI115851)
58. Zhao Z, Kapoian T, Shepard M, Lianos EA (2002) Adenosine-induced apoptosis in glomerular mesangial cells. *Kidney Int* 61(4):1276–1285. doi:[10.1046/j.1523-1755.2002.00256.x](https://doi.org/10.1046/j.1523-1755.2002.00256.x)
59. Babelova A, Moreth K, Tsalastra-Greul W, Zeng-Brouwers J, Eickelberg O, Young MF, Bruckner P, Pfeilschifter J, Schaefer RM, Grone HJ, Schaefer L (2009) Biglycan, a danger signal that activates the NLRP3 inflammasome via toll-like and P2X receptors. *J Biol Chem* 284(36):24035–24048. doi:[10.1074/jbc.M109.014266](https://doi.org/10.1074/jbc.M109.014266)
60. Vonend O, Turner CM, Chan CM, Loesch A, Dell'Anna GC, Sri KS, Burnstock G, Unwin RJ (2004) Glomerular expression of the ATP-sensitive P2X receptor in diabetic and hypertensive rat models. *Kidney Int* 66(1):157–166. doi:[10.1111/j.1523-1755.2004.00717.x](https://doi.org/10.1111/j.1523-1755.2004.00717.x)
61. Lee HT, Emala CW (2001) Systemic adenosine given after ischemia protects renal function via A(2a) adenosine receptor activation. *Am J Kidney Dis* 38(3):610–618. doi:[10.1053/ajkd.2001.26888](https://doi.org/10.1053/ajkd.2001.26888)
62. Burnstock G (2008) Purinergic signalling and disorders of the central nervous system. *Nat Rev Drug Discov* 7(7):575–590. doi:[10.1038/nrd2605](https://doi.org/10.1038/nrd2605)
63. Trujillo CA, Schwindt TT, Martins AH, Alves JM, Mello LE, Ulrich H (2009) Novel perspectives of neural stem cell differentiation: from neurotransmitters to therapeutics. *Cytometry A* 75(1):38–53. doi:[10.1002/cyto.a.20666](https://doi.org/10.1002/cyto.a.20666)
64. Morley JF, Hurtig HI (2010) Current understanding and management of Parkinson disease: five new things. *Neurology* 75(18 Suppl 1):S9–S15. doi:[10.1212/WNL.0b013e3181fb3628](https://doi.org/10.1212/WNL.0b013e3181fb3628)
65. Jun D, Kim K (2004) ATP-mediated necrotic volume increase (NVI) in substantia nigra pars compacta dopaminergic neuron. Abstract Viewer/Itinerary Planner; Program no. 222.18. Society for Neuroscience, Washington, DC
66. Le Feuvre R, Brough D, Rothwell N (2002) Extracellular ATP and P2X7 receptors in neurodegeneration. *Eur J Pharmacol* 447(2–3):261–269
67. Heine C, Wegner A, Grosche J, Allgaier C, Illes P, Franke H (2007) P2 receptor expression in the dopaminergic system of the rat brain during development. *Neuroscience* 149(1):165–181. doi:[10.1016/j.neuroscience.2007.07.015](https://doi.org/10.1016/j.neuroscience.2007.07.015)
68. Scheibler P, Pesic M, Franke H, Reinhardt R, Wirkner K, Illes P, Norenberg W (2004) P2X2 and P2Y1 immunofluorescence in rat neostriatal medium-spiny projection neurones and cholinergic interneurones is not linked to respective purinergic receptor function. *Br J Pharmacol* 143(1):119–131. doi:[10.1038/sj.bjp.0705916](https://doi.org/10.1038/sj.bjp.0705916)
69. Zona C, Marchetti C, Volonte C, Mercuri NB, Bernardi G (2000) Effect of P2 purinoceptor antagonists on kainate-induced currents in rat cultured neurons. *Brain Res* 882(1–2):26–35
70. Burnstock G (2006) Pathophysiology and therapeutic potential of purinergic signaling. *Pharmacol Rev* 58(1):58–86. doi:[10.1124/pr.58.1.5](https://doi.org/10.1124/pr.58.1.5)
71. Krugel U, Kittner H, Illes P (1999) Adenosine 5'-triphosphate-induced dopamine release in the rat nucleus accumbens in vivo. *Neurosci Lett* 265(1):49–52
72. Krugel U, Kittner H, Franke H, Illes P (2001) Accelerated functional recovery after neuronal injury by P2 receptor blockade. *Eur J Pharmacol* 420(2–3):R3–R4
73. Gaspard N, Vanderhaeghen P (2011) From stem cells to neural networks: recent advances and perspectives for neurodevelopmental disorders. *Develop Med Child Neurol* 53(1):13–17. doi:[10.1111/j.1469-8749.2010.03827.x](https://doi.org/10.1111/j.1469-8749.2010.03827.x)
74. Milosevic J, Brandt A, Roemuss U, Arnold A, Wegner F, Schwarz SC, Storch A, Zimmermann H, Schwarz J (2006) Uracil nucleotides stimulate human neural precursor cell proliferation and dopaminergic differentiation: involvement of MEK/ERK signalling. *J Neurochem* 99(3):913–923. doi:[10.1111/j.1471-4159.2006.04132.x](https://doi.org/10.1111/j.1471-4159.2006.04132.x)
75. Ralevic V, Burnstock G (1998) Receptors for purines and pyrimidines. *Pharmacol Rev* 50(3):413–492
76. Morellia M, Di Paolob T, Wardasc J, Calonb F, Xiaod D, Schwarzschild MA (2007) Role of adenosine A2A receptors in parkinsonian motor impairment and L-DOPA-induced motor complications. *Prog Neurobiol* 83(5):293–309
77. Haughey NJ, Mattson MP (2003) Alzheimer's amyloid beta-peptide enhances ATP/gap junction-mediated calcium-wave propagation in astrocytes. *Neuromolecular Med* 3(3):173–180. doi:[10.1385/NMM:3:3:173](https://doi.org/10.1385/NMM:3:3:173)
78. Thathiah A, De Strooper B (2011) The role of G protein-coupled receptors in the pathology of Alzheimer's disease. *Nat Rev Neurosci* 12(2):73–87. doi:[10.1038/nrn2977](https://doi.org/10.1038/nrn2977)
79. Ballard C, Gauthier S, Corbett A, Brayne C, Aarsland D, Jones E (2011) Alzheimer's disease. *Lancet* 377(9770):1019–1031. doi:[10.1016/S0140-6736\(10\)61349-9](https://doi.org/10.1016/S0140-6736(10)61349-9)
80. Zhang YX, Yamashita H, Ohshita T, Sawamoto N, Nakamura S (1995) ATP increases extracellular dopamine level through stimulation of P2Y purinoceptors in the rat striatum. *Brain Res* 691(1–2):205–212
81. Franke H, Illes P (2006) Involvement of P2 receptors in the growth and survival of neurons in the CNS. *Pharmacol Ther* 109(3):297–324. doi:[10.1016/j.pharmthera.2005.06.002](https://doi.org/10.1016/j.pharmthera.2005.06.002)
82. Sanz JM, Chiozzi P, Ferrari D, Colaianna M, Idzko M, Falzoni S, Fellin R, Trabace L, Di Virgilio F (2009) Activation of microglia by amyloid beta requires P2X7 receptor expression. *J Immunol* 182(7):4378–4385. doi:[10.4049/jimmunol.0803612](https://doi.org/10.4049/jimmunol.0803612)
83. McLarnon JG, Ryu JK, Walker DG, Choi HB (2006) Upregulated expression of purinergic P2X(7) receptor in Alzheimer disease and amyloid-beta peptide-treated microglia and in peptide-injected rat hippocampus. *J Neuropathol Exp Neurol* 65(11):1090–1097. doi:[10.1097/01.jnen.0000240470.97295.d300005072-200611000-00008](https://doi.org/10.1097/01.jnen.0000240470.97295.d300005072-200611000-00008)
84. Rampe D, Wang L, Ringheim GE (2004) P2X7 receptor modulation of beta-amyloid- and LPS-induced cytokine secretion from human macrophages and microglia. *J Neuroimmunol* 147(1–2):56–61
85. Majumder P, Trujillo CA, Lopes CG, Resende RR, Gomes KN, Yuahasi KK, Britto LR, Ulrich H (2007) New insights into purinergic receptor signaling in neuronal differentiation, neuroprotection, and brain disorders. *Purinergic Signal* 3(4):317–331. doi:[10.1007/s11302-007-9074-y](https://doi.org/10.1007/s11302-007-9074-y)
86. Haughey NJ, Nath A, Chan SL, Borchard AC, Rao MS, Mattson MP (2002) Disruption of neurogenesis by amyloid beta-peptide, and perturbed neural progenitor cell homeostasis, in models of Alzheimer's disease. *J Neurochem* 83(6):1509–1524
87. Ballard C, Gauthier S, Corbett A, Brayne C, Jones AD, Jones E (2011) Alzheimer's disease. *Lancet* 377(9770):1019–1031
88. Resende RR, Majumder P, Gomes KN, Britto LR, Ulrich H (2007) P19 embryonal carcinoma cells as in vitro model for studying purinergic receptor expression and modulation of N-methyl-D-aspartate-glutamate and acetylcholine receptors during neuronal differentiation. *Neuroscience* 146(3):1169–1181. doi:[10.1016/j.neuroscience.2007.02.041](https://doi.org/10.1016/j.neuroscience.2007.02.041)
89. Lindvall O, Kokka Z (2010) Stem cells in human neurodegenerative disorders—time for clinical translation? *J Clin Invest* 120(1):29–40. doi:[10.1172/JCI40543](https://doi.org/10.1172/JCI40543)

90. Ryu JK, Cho T, Wang YT, McLarnon JG (2009) Neural progenitor cells attenuate inflammatory reactivity and neuronal loss in an animal model of inflamed AD brain. *J Neuroinflammation* 6:39. doi:[10.1186/1742-2094-6-39](https://doi.org/10.1186/1742-2094-6-39)
91. Chuang TT (2010) Neurogenesis in mouse models of Alzheimer's disease. *Biochim Biophys Acta* 1802(10):872–880. doi:[10.1016/j.bbadi.2009.12.008](https://doi.org/10.1016/j.bbadi.2009.12.008)
92. Delarasse C, Auger R, Gonnord P, Fontaine B, Kanelopoulos JM (2011) The purinergic receptor P2X7 triggers α -secretase-dependent processing of the amyloid precursor protein. *J Bio Chem* 286:2596–2606. doi:[10.1074/jbc.M110.200618](https://doi.org/10.1074/jbc.M110.200618)
93. Knutson LJ, Murray TF (1997) Adenosine and ATP epilepsy. In: Jacobson KA, Jarvis MF (eds) Purinergic approaches in experimental therapeutics. Wiley, New York, pp 423–447
94. Avignone E, Ulmann L, Levavasseur F, Rassendren F, Audinat E (2008) Status epilepticus induces a particular microglial activation state characterized by enhanced purinergic signaling. *J Neurosci* 28 (37):9133–9144. doi:[10.1523/JNEUROSCI.1820-08.2008](https://doi.org/10.1523/JNEUROSCI.1820-08.2008)
95. Dona F, Ulrich H, Persike DS, Conceicao IM, Blini JP, Cavalheiro EA, Fernandes MJ (2009) Alteration of purinergic P2X4 and P2X7 receptor expression in rats with temporal-lobe epilepsy induced by pilocarpine. *Epilepsy Res* 83(2–3):157–167. doi:[10.1016/j.epilepsyres.2008.10.008](https://doi.org/10.1016/j.epilepsyres.2008.10.008)
96. Oses JP (2006) Modification by kainate-induced convulsions of the density of presynaptic P2X receptors in the rat hippocampus. *Purinergic Signalling* 2:252–253
97. Burnstock G (2007) Physiology and pathophysiology of purinergic neurotransmission. *Physiol Rev* 87(2):659–797. doi:[10.1152/physrev.00043.2006](https://doi.org/10.1152/physrev.00043.2006)
98. Ciccarelli R, Ballerini P, Sabatino G, Rathbone MP, D'Onofrio M, Caciagli F, Di Iorio P (2001) Involvement of astrocytes in purine-mediated reparative processes in the brain. *Int J Dev Neurosci* 19(4):395–414
99. Chua K, Kima M, Junga K, Jeond D, Leea S, Kima J, Jeongf S, Kimg SU, Leea SK, Shind H, Roha J (2004) Human neural stem cell transplantation reduces spontaneous recurrent seizures following pilocarpine-induced status epilepticus in adult rats. *Brain Res* 1023(2):213–221. doi:[10.1016/j.brainres.2004.07.045](https://doi.org/10.1016/j.brainres.2004.07.045)
100. Guttinger M, Fedele D, Koch P, Padrun V, Pralong WF, Brustle O, Boison D (2005) Suppression of kindled seizures by paracrine adenosine release from stem cell-derived brain implants. *Epilepsia* 46(8):1162–1169
101. Franke H, Gunther A, Grosche J, Schmidt R, Rossner S, Reinhardt R, Faber-Zuschratter H, Schneider D, Illes P (2004) P2X7 receptor expression after ischemia in the cerebral cortex of rats. *J Neuropathol Exp Neurol* 63(7):686–699
102. Tsuzuki K, Kondo E, Fukuoka T, Yi D, Tsujino H, Sakagami M, Noguchi K (2001) Differential regulation of P2X(3) mRNA expression by peripheral nerve injury in intact and injured neurons in the rat sensory ganglia. *Pain* 91(3):351–360
103. Bianco F, Ceruti S, Colombo A, Fumagalli M, Ferrari D, Pizzirani C, Matteoli M, Di Virgilio F, Abbracchio MP, Verderio C (2006) A role for P2X7 in microglial proliferation. *J Neurochem* 99(3):745–758. doi:[10.1111/j.1471-4159.2006.04101.x](https://doi.org/10.1111/j.1471-4159.2006.04101.x)
104. Ceruti S, Villa G, Genovese T, Mazzon E, Longhi R, Rosa P, Bramanti P, Cuzzocrea S, Abbracchio MP (2009) The P2Y-like receptor GPR17 as a sensor of damage and a new potential target in spinal cord injury. *Brain* 132(Pt 8):2206–2218. doi:[10.1093/brain/awp147](https://doi.org/10.1093/brain/awp147)
105. Cunha RA (2005) Neuroprotection by adenosine in the brain: from A(1) receptor activation to A (2A) receptor blockade. *Purinergic Signal* 1(2):111–134. doi:[10.1007/s11302-005-0649-1](https://doi.org/10.1007/s11302-005-0649-1)
106. Nedeljkovic N, Bjelobaba I, Subasic S, Lavrnja I, Pekovic S, Stojkov D, Vjestica A, Rakic L, Stojiljkovic M (2006) Up-regulation of ectonucleotidase activity after cortical stab injury in rats. *Cell Biol Int* 30(6):541–546. doi:[10.1016/j.cellbi.2006.03.001](https://doi.org/10.1016/j.cellbi.2006.03.001)
107. Fuchs E, Raghavan S (2002) Getting under the skin of epidermal morphogenesis. *Nat Rev Genet* 3(3):199–209. doi:[10.1038/nrg758nrg758](https://doi.org/10.1038/nrg758nrg758)
108. Kanitakis J (2002) Anatomy, histology and immunohistochemistry of normal human skin. *Eur J Dermatol* 12(4):390–399, quiz 400–391
109. Fujishita K, Koizumi S, Inoue K (2006) Upregulation of P2Y2 receptors by retinoids in normal human epidermal keratinocytes. *Purinergic Signal* 2(3):491–498. doi:[10.1007/s11302-005-7331-5](https://doi.org/10.1007/s11302-005-7331-5)
110. Holzer AM, Granstein RD (2004) Role of extracellular adenosine triphosphate in human skin. *J Cutan Med Surg* 8(2):90–96. doi:[10.1007/s10227-004-0125-5](https://doi.org/10.1007/s10227-004-0125-5)
111. Greig AV, James SE, McGrouther DA, Terenghi G, Burnstock G (2003) Purinergic receptor expression in the regeneration epidermis in a rat model of normal and delayed wound healing. *Exp Dermatol* 12(6):860–871
112. Greig AV, Linge C, Cambrey A, Burnstock G (2003) Purinergic receptors are part of a signaling system for keratinocyte proliferation, differentiation, and apoptosis in human fetal epidermis. *J Invest Dermatol* 121(5):1145–1149. doi:[10.1046/j.1523-1747.2003.12567.x](https://doi.org/10.1046/j.1523-1747.2003.12567.x)
113. Inoue K, Denda M, Tozaki H, Fujishita K, Koizumi S (2005) Characterization of multiple P2X receptors in cultured normal human epidermal keratinocytes. *J Invest Dermatol* 124(4):756–763. doi:[10.1111/j.0022-202X.2005.23683.x](https://doi.org/10.1111/j.0022-202X.2005.23683.x)
114. Burnstock G, Verkhratsky A (2010) Long-term (trophic) purinergic signalling: purinoceptors control cell proliferation, differentiation and death. *Cell Death Dis* 1:e9. doi:[10.1038/cddis.2009.11](https://doi.org/10.1038/cddis.2009.11)
115. Volonte C, Amadio S, D'Ambrosi N, Colpi M, Burnstock G (2006) P2 receptor web: complexity and fine-tuning. *Pharmacol Ther* 112(1):264–280. doi:[10.1016/j.pharmthera.2005.04.012](https://doi.org/10.1016/j.pharmthera.2005.04.012)
116. Snyder JC, Teisanu RM, Stripp BR (2009) Endogenous lung stem cells and contribution to disease. *J Pathol* 217(2):254–264. doi:[10.1002/path.2473](https://doi.org/10.1002/path.2473)
117. Chistiakov DA (2010) Endogenous and exogenous stem cells: a role in lung repair and use in airway tissue engineering and transplantation. *J Biomed Sci* 17:92. doi:[10.1186/1423-0127-17-92](https://doi.org/10.1186/1423-0127-17-92)
118. Sueblinvong V, Weiss DJ (2010) Stem cells and cell therapy approaches in lung biology and diseases. *Transl Res* 156(3):188–205
119. Evans MJ, Cabral-Anderson LJ, Freeman G (1978) Role of the Clara cell in renewal of the bronchiolar epithelium. *Lab Invest* 38 (6):648–653
120. Stripp BR (2008) Hierarchical organization of lung progenitor cells: is there an adult lung tissue stem cell? *Proc Am Thorac Soc* 5(6):695–698. doi:[10.1513/pats.200801-011AW](https://doi.org/10.1513/pats.200801-011AW)
121. Teisanu RM, Lagasse E, Whitesides JF, Stripp BR (2009) Prospective isolation of bronchiolar stem cells based upon immunophenotypic and autofluorescence characteristics. *Stem Cells* 27(3):612–622. doi:[10.1634/stemcells.2008-0838](https://doi.org/10.1634/stemcells.2008-0838)
122. Borthwick DW, Shahbazian M, Krantz QT, Dorin JR, Randell SH (2001) Evidence for stem-cell niches in the tracheal epithelium. *Am J Respir Cell Mol Biol* 24(6):662–670
123. Reynolds SD, Giangreco A, Power JH, Stripp BR (2000) Neuroepithelial bodies of pulmonary airways serve as a reservoir of progenitor cells capable of epithelial regeneration. *Am J Pathol* 156(1):269–278. doi:[10.1016/S0002-9440\(10\)64727-X](https://doi.org/10.1016/S0002-9440(10)64727-X)
124. De Proost I, Pintelon I, Wilkinson WJ, Goethals S, Brouns I, Van Nassauw L, Riccardi D, Timmermans JP, Kemp PJ, Adriaensen D (2009) Purinergic signaling in the pulmonary neuroepithelial body microenvironment unraveled by live cell imaging. *FASEB J* 23(4):1153–1160. doi:[10.1096/fj.08-109579](https://doi.org/10.1096/fj.08-109579)
125. Reynolds SD, Hong KU, Giangreco A, Mango GW, Guron C, Morimoto Y, Stripp BR (2000) Conditional clara cell ablation reveals a self-renewing progenitor function of pulmonary neuroendocrine cells. *Am J Physiol Lung Cell Mol Physiol* 278 (6):L1256–L1263

126. Brouns I, Oztay F, Pintelon I, De Proost I, Lembrechts R, Timmermans JP, Adriaensen D (2009) Neurochemical pattern of the complex innervation of neuroepithelial bodies in mouse lungs. *Histochem Cell Biol* 131(1):55–74. doi:[10.1007/s00418-008-0495-7](https://doi.org/10.1007/s00418-008-0495-7)
127. Conway JD, Bartolotta T, Abdullah LH, Davis CW (2003) Regulation of mucin secretion from human bronchial epithelial cells grown in murine hosted xenografts. *Am J Physiol Lung Cell Mol Physiol* 284(6):L945–L954. doi:[10.1152/ajplung.00410.200200410.2002](https://doi.org/10.1152/ajplung.00410.200200410.2002)
128. Schwiebert EM, Zsembery A (2003) Extracellular ATP as a signalling molecule for epithelial cells. *Biochim Biophys Acta* 1615(1–2):7–32
129. Wesley UV, Bove PF, Hristova M, McCarthy S, van der Vliet A (2007) Airway epithelial cell migration and wound repair by ATP-mediated activation of dual oxidase 1. *J Biol Chem* 282(5):3213–3220. doi:[10.1074/jbc.M606533200](https://doi.org/10.1074/jbc.M606533200)
130. Ethier MF, Chander V, Dobson JG Jr (1993) Adenosine stimulates proliferation of human endothelial cells in culture. *Am J Physiol* 265(1 Pt 2):H131–H138
131. Montesinos MC, Desai A, Chen JF, Yee H, Schwarzschild MA, Fink JS, Cronstein BN (2002) Adenosine promotes wound healing and mediates angiogenesis in response to tissue injury via occupancy of A_(2A) receptors. *Am J Pathol* 160(6):2009–2018. doi:[10.1016/S0002-9440\(10\)61151-0](https://doi.org/10.1016/S0002-9440(10)61151-0)
132. Allen-Gipson DS, Wong J, Spurzem JR, Sisson JH, Wyatt TA (2006) Adenosine A_{2A} receptors promote adenosine-stimulated wound healing in bronchial epithelial cells. *Am J Physiol Lung Cell Mol Physiol* 290(5):L849–L855. doi:[10.1152/ajplung.00373.2005](https://doi.org/10.1152/ajplung.00373.2005)
133. Erjefalt JS, Persson CG (1997) Airway epithelial repair: breathtakingly quick and multipotentially pathogenic. *Thorax* 52(11):1010–1012
134. Wills-Karp M (1999) Immunologic basis of antigen-induced airway hyperresponsiveness. *Annu Rev Immunol* 17:255–281. doi:[10.1146/annurev.immunol.17.1.255](https://doi.org/10.1146/annurev.immunol.17.1.255)
135. Idzko M, Hammad H, van Nimwegen M, Kool M, Willart MA, Muskens F, Hoogsteden HC, Luttmann W, Ferrari D, Di Virgilio F, Virchow JC Jr, Lambrecht BN (2007) Extracellular ATP triggers and maintains asthmatic airway inflammation by activating dendritic cells. *Nat Med* 13(8):913–919. doi:[10.1038/nm1617](https://doi.org/10.1038/nm1617)
136. la Sala A, Sebastiani S, Ferrari D, Di Virgilio F, Idzko M, Norgauer J, Girolomoni G (2002) Dendritic cells exposed to extracellular adenosine triphosphate acquire the migratory properties of mature cells and show a reduced capacity to attract type 1 T lymphocytes. *Blood* 99(5):1715–1722
137. Muller T, Vieira RP, Grimm M, Durk T, Cicco S, Zeiser R, Jakob T, Martin SF, Blumenthal B, Sorichter S, Ferrari D, Di Virgilio F, Idzko M (2011) A potential role for P2X7R in allergic airway inflammation in mice and humans. *Am J Respir Cell Mol Biol* 44(4):456–464. doi:[10.1165/rcmb.2010-0129OC](https://doi.org/10.1165/rcmb.2010-0129OC)
138. Polosa R, Holgate ST (2006) Adenosine receptors as promising therapeutic targets for drug development in chronic airway inflammation. *Curr Drug Targets* 7(6):699–706
139. Zhong H, Shlykov SG, Molina JG, Sanborn BM, Jacobson MA, Tilley SL, Blackburn MR (2003) Activation of murine lung mast cells by the adenosine A₃ receptor. *J Immunol* 171(1):338–345
140. Ryzhov S, Zaynagetdinov R, Goldstein AE, Novitskiy SV, Dikov MM, Blackburn MR, Biaggioni I, Feoktistov I (2008) Effect of A_{2B} adenosine receptor gene ablation on proinflammatory adenosine signaling in mast cells. *J Immunol* 180(11):7212–7220
141. Gibson PG, Manning PJ, O’Byrne PM, Girgis-Gabardo A, Dolovich J, Denburg JA, Hargreave FE (1991) Allergen-induced asthmatic responses. Relationship between increases in airway responsiveness and increases in circulating eosinophils, basophils, and their progenitors. *Am Rev Respir Dis* 143(2):331–335
142. Dorman SC, Efthimiadis A, Babirad I, Watson RM, Denburg JA, Hargreave FE, O’Byrne PM, Sehmi R (2004) Sputum CD34+IL-5Ralpha⁺ cells increase after allergen: evidence for in situ eosinophilopoiesis. *Am J Respir Crit Care Med* 169(5):573–577. doi:[10.1164/rccm.200307-1004OC](https://doi.org/10.1164/rccm.200307-1004OC)
143. Catalli AE, Thomson JV, Babirad IM, Duong M, Doyle TM, Howie KJ, Newbold P, Craggs RI, Foster M, Gauvreau GM, O’Byrne PM, Sehmi R (2008) Modulation of beta1-integrins on hemopoietic progenitor cells after allergen challenge in asthmatic subjects. *J Allergy Clin Immunol* 122(4):803–810. doi:[10.1016/j.jaci.2008.07.021](https://doi.org/10.1016/j.jaci.2008.07.021)
144. Southam DS, Widmer N, Ellis R, Hirota JA, Inman MD, Sehmi R (2005) Increased eosinophil-lineage committed progenitors in the lung of allergen-challenged mice. *J Allergy Clin Immunol* 115(1):95–102. doi:[10.1016/j.jaci.2004.09.022](https://doi.org/10.1016/j.jaci.2004.09.022)
145. Daikeler T, Tyndall A (2007) Autoimmunity following hematopoietic stem-cell transplantation. *Best Pract Res Clin Haematol* 20(2):349–360. doi:[10.1016/j.beha.2006.09.008](https://doi.org/10.1016/j.beha.2006.09.008)

REVIEW

Open Access

Implications of purinergic receptor-mediated intracellular calcium transients in neural differentiation

Talita Glaser¹, Rodrigo R Resende² and Henning Ulrich^{1*}

Abstract

Purinergic receptors participate, in almost every cell type, in controlling metabolic activities and many physiological functions including signal transmission, proliferation and differentiation. While most of P2Y receptors induce transient elevations of intracellular calcium concentration by activation of intracellular calcium pools and forward these signals as waves which can also be transmitted into neighboring cells, P2X receptors produce calcium spikes which also include activation of voltage-operating calcium channels. P2Y and P2X receptors induce calcium transients that activate transcription factors responsible for the progress of differentiation through mediators including calmodulin and calcineurin. Expression of P2X2 as well as of P2X7 receptors increases in differentiating neurons and glial cells, respectively. Gene expression silencing assays indicate that these receptors are important for the progress of differentiation and neuronal or glial fate determination. Metabotropic receptors, mostly P2Y1 and P2Y2 subtypes, act on embryonic cells or cells at the neural progenitor stage by inducing proliferation as well as by regulation of neural differentiation through NFAT translocation. The scope of this review is to discuss the roles of purinergic receptor-induced calcium spike and wave activity and its codification in neurodevelopmental and neurodifferentiation processes.

Keywords: Purinergic receptors, Intracellular calcium transients, Neural differentiation, Neural fate specification

The importance of establishing cellular replacement therapies is increasing nowadays. These therapies are based on stem cells due to their capability of originating other cell types by differentiation, or even releasing factors that can reduce inflammatory responses and promote homing of adult stem cells of the proper patient to the site of injury. However, the molecular mechanisms of development, cell differentiation, successful cell engraftment and recruitment of endogenous stem cells in case of injury need yet to be resolved. Thus, major efforts are being undertaken in order to understand the process of neural differentiation, mediated by intracellular signaling triggered by external and internal stimuli, resulting in differential gene transcription pattern and neural phenotype determination.

Intracellular calcium signaling and purinergic receptors

Among different pathways coordinating intracellular signaling, the most prominent is intracellular calcium signaling (ICS), controlling various cellular processes including proliferation, motility, apoptosis and differentiation [1]. ICS is impressively diverse and consists of mechanisms that differ in frequency, amplitude and spatio-temporal patterning depending on an extensive molecular repertoire of signaling components. The free intracellular calcium concentration ($[Ca^{2+}]_i$) of a resting cell is in the range of 10–100 nM. Following physiological stimulation, $[Ca^{2+}]_i$ levels can rise up to 1–2 μ M concentrations. ICS is codified by the peak amplitude and frequency of $[Ca^{2+}]_i$ transients, promoted by the entry of external Ca^{2+} through Ca^{2+} channels or the release of Ca^{2+} from internal stores. These internal stores are deposited within internal membrane structures such as the endoplasmic reticulum (ER). Following activation of G-protein-coupled receptors, phospholipase C- β

* Correspondence: henning@iq.usp.br

¹Departamento de Bioquímica, Instituto de Química, Universidade de São Paulo, Avenida Professor Lineu Prestes, 748, São Paulo CEP 05508-900, Brazil
Full list of author information is available at the end of the article

(PLC- β) cleaves phosphatidylinositol 4,5-bisphosphate, releasing diacylglycerol and inositol-1,4,5-trisphosphate (IP3) which diffuses into the cell for activation of IP3 receptors (IP3R) and releasing Ca^{2+} from the ER. Moreover, Ca^{2+} enters the cytosol and activates ryanodine receptor (RYR) channels following activation of voltage-operated channels (VOCs), or receptor-operated channels (ROCs); this process is called Ca^{2+} -induced Ca^{2+} release [2-4].

There are mainly two types of spontaneous intracellular Ca^{2+} transients: waves and spikes. The first one is mediated by IP3R and/or RYR activation and involves sensitivity to $[\text{Ca}^{2+}]_i$ levels. This Ca^{2+} entry pathway is active at resting potential and is amplified by Ca^{2+} release from intracellular stores, and increases $[\text{Ca}^{2+}]_i$ to a lower level than that attained by spikes. In the presence of gap junctions connecting cells, these intracellular waves can spread to neighboring cells, thereby coordinating neural activity and physiological processes of many cells [5,6]. Compared to Ca^{2+} spikes, waves reveal a lower frequency with a mean duration of more than 30s, as observed in growth cones; their generation does not depend on action potentials. Waves occur locally and decay with distance from the site of initiation.

Calcium spikes depend on Ca^{2+} influx through VOCs or ROCs and Ca^{2+} release from intracellular stores (Ca^{2+} induced Ca^{2+} release via RYR), and achieve mean $[\text{Ca}^{2+}]_i$ levels of 500 nM. They are characterized by their frequency (mean duration approximately 10s), and occur throughout an excitable cell, since they involve Ca^{2+} -dependent action potentials.

Spontaneous Ca^{2+} spike frequency in cultured neurons initially varies from 1-10/h and then declines. Similar patterns of spike activity were observed in neural tube stages *in vivo* [2,7] and during neuronal differentiation of embryonal carcinoma (CSC, a model for pluripotent embryonic stem cells) and adult bone marrow mesenchymal (hMSC) stem cells [8,9]. Notably, these low frequencies of calcium transients regulate gene transcription and are suggested to be essential for the progress of neural differentiation and phenotype specification [2,10-12].

Chemical and electrical signals, mediated by metabotropic and ionotropic receptors and VOCs promote intracellular calcium signaling and subsequent induction of differentiation. Adenosine 5'-triphosphate (ATP)-activated metabotropic and ionotropic receptors, also denominated as purinergic receptors, have drawn a lot of attention, due to their wide expression in almost every cell including stem cells. These receptors belong to the first neurotransmitter receptors expressed during development [13,14]. ATP is the mainly purinergic messenger molecule and is released from cells in physiological conditions by exocytosis, transporters or even lysosomes.

When the release occurs by damaged cells in an uncontrolled manner, ATP contributes to cell death and disease states. Once released into the extracellular space, ATP is degraded by ectonucleotidases producing the signaling molecules adenosine diphosphate (ADP), adenosine monophosphate [15] and adenosine [14]. Based on pharmacological and structural properties, purinergic receptors are divided into metabotropic P1 and P2Y receptors as well as P2X ionotropic receptors.

P1 receptors subtypes are selective for adenosine and are classical seven-transmembrane metabotropic receptors coupled to several families of Gi, Go and Gs proteins. There are four types of adenosine receptors (A1, A2A, A2B and A3) differing by pharmacological and functional properties [15]. A1 and A3 receptors exert inhibitory effects on adenylyl cyclase activity (mediated through Gi/o proteins) and also regulate PLC- β activity and thus IP3 synthesis [14]. P2 receptor subtypes are activated by ATP, ADP, uridine-5'-triphosphate (UTP), uridine-5'-diphosphate (UDP) or UDP-glucose. P2 receptors are further divided into P2X and P2Y subtypes based on their structural characteristics [13].

P2X receptors as ATP-gated cationic ($\text{Na}^+/\text{K}^+/\text{Ca}^{2+}$) channels [13,16], are assembled in trimeric form as homomeric or heteromeric receptors from seven subunits (P2X1-P2X7). Recombinant P2X1, P2X2, P2X3, P2X4, P2X2/3, P2X2/6, P2X4/6, P2X1/5 as well as P2X7 receptors, when activated in a silent environment of cells not expressing any endogenous purinergic receptor, were all shown to be permeable for Ca^{2+} [17]. P2X receptors are mostly expressed by excitable cells, and Ca^{2+} entry through P2X receptor channels provides an important regulation mechanism of physiological responses *in vivo*, while aberrant Ca^{2+} entry, mostly mediated by P2X7 receptors, is suggested to be involved in pathophysiological conditions such as cell death, neuroinflammation and excitotoxic brain damage during epilepsy [18-22].

Metabotropic P2Y purinergic receptors activated by ATP, ADP, UTP, UDP or UDP glucose are composed by P2Y1,2,4,6,11,12,13,14 subtypes based on phylogenetic similarity [14]. P2Y1,2,4,6,11 subtypes are coupled to Gq/G11 proteins activating PLC- β , thus inducing IP3-mediated Ca^{2+} release from the ER [13,14,23]. P2Y12,13,14 receptors inhibit adenylyl cyclase activity via Gi/o proteins. These latter-mentioned receptors also participate in regulating $[\text{Ca}^{2+}]_i$ levels. For instance, P2Y receptor subtypes acting via Gi/o proteins can regulate N-type Ca^{2+} channel activity [24-26]. P2Y receptors are expressed in the central and autonomic nervous systems as well as by most non-excitable cells where they exert long-term effects by regulating crucial cellular functions including proliferation and differentiation [14].

Recent studies have focused on changes of expression patterns and functions of this receptor family during

differentiation from embryonic into neuronal cells [8,27]. The developmental fate of differentiating stem cells depends on the 'niche' in which the cells exist, and several associated signaling systems have been pinpointed [28,29]. In this review, we discuss the importance of ICS for the differentiation process of stem cells into neural cells with special emphasis on purinergic receptor function during Ca^{2+} signaling.

Purinergic receptors triggering ICS in the nervous system and neural differentiation

Many of the signal transduction pathways that control cell metabolism, survival and differentiation are activated by elevation of $[\text{Ca}^{2+}]_i$ levels following activation of purinergic receptors. Moreover, numerous experimental data point at essential functions of purinergic signaling in neural differentiation and brain development. It has been well established that purinergic receptor activation triggers $[\text{Ca}^{2+}]_i$ transients that are involved in developmental processes of the embryo [30,31]. Pioneering studies of Nicholas Spitzer that the progress of neurogenesis and phenotype determination, such as neurotransmitter specification, is encoded by naturally occurring patterns

of $[\text{Ca}^{2+}]_i$ transients, are in agreement with essential functions of purinergic receptor signaling for cortex development. As detailed above, P2X receptors by inducing Ca^{2+} influx generate repetitive $[\text{Ca}^{2+}]_i$ transients in spike form with activation of RYR while P2Y receptors act through IP3-induced intracellular Ca^{2+} release which then is propagated in wave form (Figure 1).

Ionotropic purinergic receptors also participate in regulation of neural proliferation and neurogenesis by inducing calcium spikes. In agreement, P2X2 and P2X6 receptor subunit expression was enhanced together with the enrichment of neurons during differentiation of rat embryonic telencephalon [32]. For instance, P2X receptor activity is suggested to be involved in hippocampal neurogenesis by inducing proliferation of hippocampal progenitor cells [33]. The P2X7 receptor usually participates in pore formation, but its abundant presence in synaptic structure suggests a role in synaptic plasticity establishment [26]. Some experimental data indicate that P2X7 receptors, rather than connexin-hemichannels, mediate ATP release and amplification of astrocytic intercellular Ca^{2+} signaling [34]. In view of that, it will be worth to study the participation of P2X7 receptors in

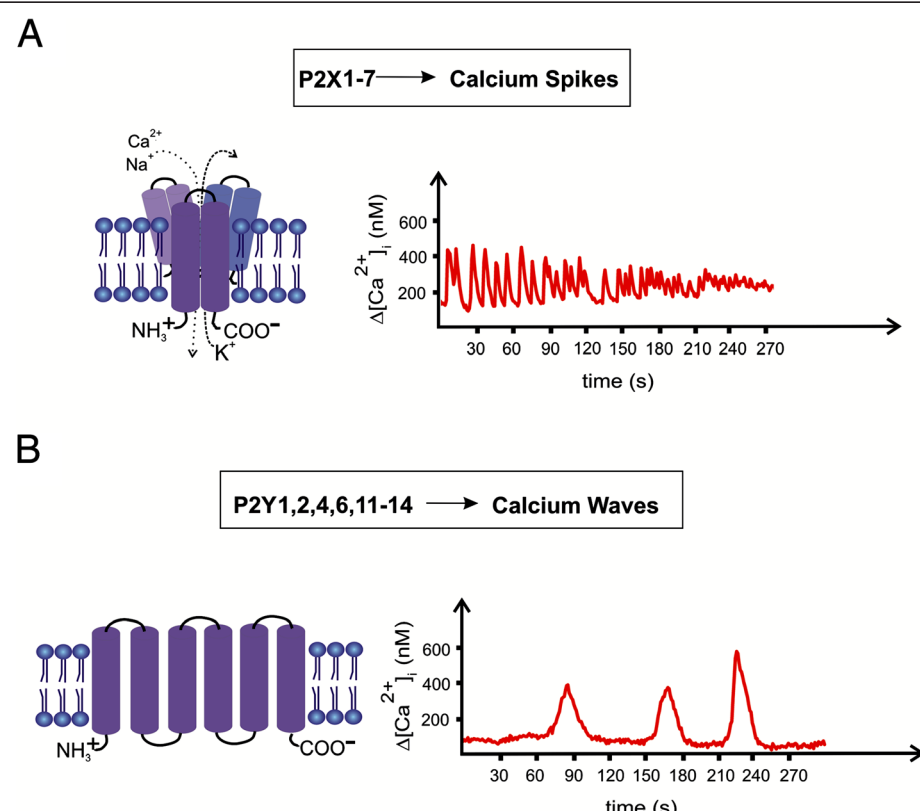


Figure 1 Oscillations of $[\text{Ca}^{2+}]_i$ levels and purinergic receptors. Ionotropic P2X receptors trigger calcium spikes characterized by amplitudes and frequency (A), while metabotropic P2Y receptors induce calcium waves with lower amplitudes and frequencies (B). P2X receptors are composed of three subunits, with two transmembrane loops each. G protein-coupled metabotropic P2Y receptors are composed of 7 transmembrane loops.

directing of migration and neurogenesis, such as shown for P2Y1 receptors in radial glial cells during cortex development [6].

Ionotropic purinergic receptors were also involved in the progress of pluripotent P19 CSC differentiation and neural phenotype determination. Functions of P2X2 and P2X7 receptor subtypes in conditions of down-regulation of receptor gene expression were studied by stable RNA interference. Knock-down of P2X2 receptor expression along neural differentiation resulted in diminished expression of β -3-tubulin expression indicating interference with the progress of neurogenesis. On the other hand, P2X7 receptor expression and activity was related to induction of proliferation and gliogenesis, since permanent P2X7 receptor RNA interference resulted in reduced 5'-bromo-2'-deoxyuridine (BrdU) incorporation and glial fibrillary acidic (GFAP) protein expression [35] (see Figure 2 for a comprehensive scheme of metabotropic and ionotropic purinergic receptor implication in proliferation and differentiation induction of P19 CSC).

Our laboratory has shown that a full-length and an alternatively spliced form of the mouse P2X6 receptor gene are expressed in mouse P19 CSC, an *in vitro* model for early neuroectodermal differentiation. The truncated alternatively spliced form was present at the undifferentiated stage of P19 CSC, and was predominant compared to the full-length form during the whole course of neuronal differentiation of these cells [37] suggesting that splicing could provide a mechanism for regulation of P2X6 subunit expression and formation of functional P2X receptors with P2X6 subunit contribution.

The involvement of these receptors in ATP-induced $[Ca^{2+}]_i$ transients was probed in pharmacological studies. Moreover, embryonic P19 CSC expressed various other functional subtypes including P2Y1, P2Y2 and P2X4 receptors or P2X-heteromultimeric receptors. In neuronal-differentiated cells, P2Y2, P2Y6, P2X2 and possibly P2X2/P2X6 heteromeric receptors were the major mediators of purinergic receptor-mediated $[Ca^{2+}]_i$ elevations.

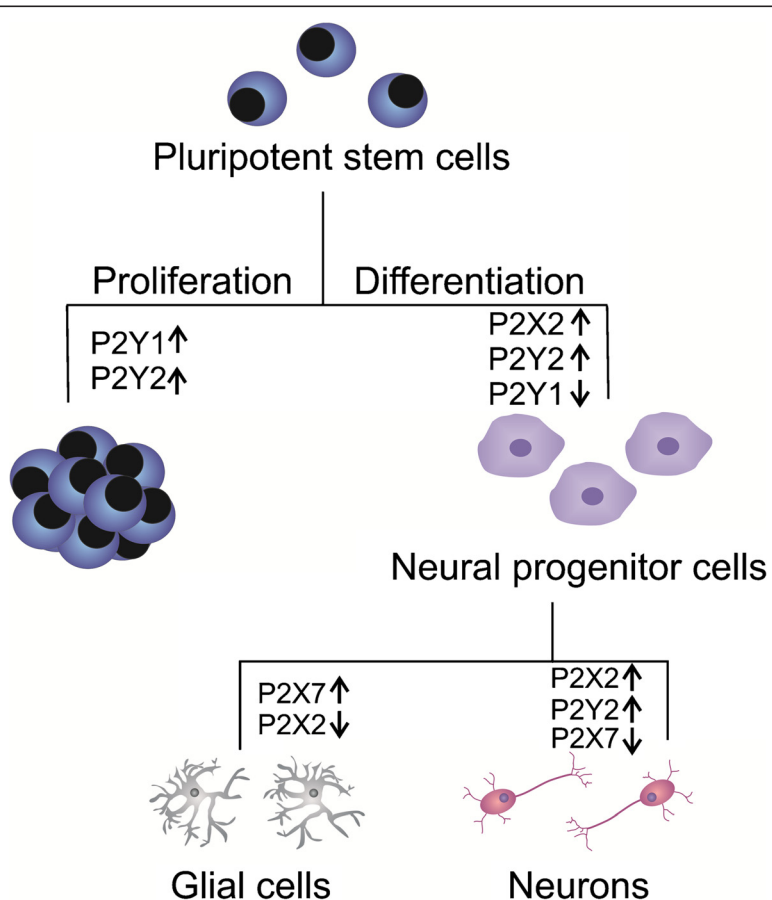


Figure 2 Functions of P2X and P2Y receptor subtypes in stem cell biology. P2Y1 and P2Y2 receptors regulate proliferation of pluripotent stem cells such as studied using P19 embryonal carcinoma cells as *in vitro* model. P2Y2 and P2Y1 receptors promote proliferation and neural differentiation of pluripotent and neural progenitor cells. P2Y2, P2X2 and P2X7 receptors participate in later differentiation and neural phenotype determination. P2X2 and P2X7 receptor expression/activity levels provide a further switch for neuronal or glial fate of P19 cell differentiation. Arrows indicate increases or decreases in receptor expression and activity levels in respective stages of differentiation [36].

P2Y1 receptor activation produces $[Ca^{2+}]_i$ transients which are then propagated in wave form through neighbouring cells by gap junctions and connexin 43-hemichannels resulting in cell cycle synchronization of migrating neural progenitors and radial glia cells in the subventricular zone for cortex development [6]. ATP has also been shown to induce proliferation of human neural stem cells (NSC) cultured from telencephalon tissues from a 15-week gestational age embryo [38]. P2Y1 receptor-mediated $[Ca^{2+}]_i$ transients resulted in Ca^{2+} /calmodulin (CaM)-dependent protein kinase II (CaMKII) activation in cell soma and neurites of cerebellar granule neurons, followed by cAMP/ Ca^{2+} response element binding protein (CREB) phosphorylation and modulation of gene transcription [39]. Neurotrophic effects, such as observed in Neuro2A cells, were induced by P2Y1 receptor signaling [40]. Here, low-frequency global and local Ca^{2+} transients induced by purinergic receptor activation during early stages of differentiation of neural progenitor cells promoted neurite outgrowth and the onset of GABAergic neurotransmitter phenotype specification. Surprisingly, spontaneous Ca^{2+} signals in individual precursors were not synchronized with Ca^{2+} transients in surrounding cells, indicating the existence of a different pathway, not depending on connexin 43-hemichannel-mediated intercellular Ca^{2+} signaling [41].

Calcium ions also play an important role in proliferation and differentiation of hMSCs. Spontaneous $[Ca^{2+}]_i$ oscillations occur without agonist stimulation in hMSCs. These $[Ca^{2+}]_i$ transient are mediated by IP3-induced Ca^{2+} release and controlled by an autocrine/paracrine signaling pathway in which ATP is secreted via a hemi-gap junction channel and then stimulates the P2Y₁ receptor, resulting in the activation of PLC- β for IP3 production. Furthermore, $[Ca^{2+}]_i$ oscillations are associated with nuclear factor of activated T-cell (NFAT) translocation into the nucleus of undifferentiated hMSCs, providing a new role for $[Ca^{2+}]_i$ oscillations in such stem cells [42].

The P2Y2 receptor subtype, another purinergic receptor involved in neural differentiation, which activates of PLC- β , intracellular Ca^{2+} release and intercellular Ca^{2+} waves, important for embryonic development [43]. However in neural stem cells, Lin and coworkers [44] described that neural progenitor proliferation is modulated by an autocrine loop. These cells release ATP and thus activate P2Y receptors for proliferation maintenance. Blockade of proliferation and induction to neural differentiation occurred only when purinergic receptor activity had been antagonized and $[Ca^{2+}]_i$ transients had diminished.

In undifferentiated P19 CSC, ATP provoked acceleration of proliferation via P2Y1 and P2Y2 receptor activation. P19 CSC that progressed to the progenitor stage revealed down-regulated P2Y1 receptor expression,

while activation of IP3-sensitive intracellular Ca^{2+} stores was mediated by P2Y2 receptors. The progress of neuronal differentiation and phenotype transition was determined by analysis of nestin and neuron-specific enolase gene and protein expression levels [27,45].

Activation of transcription factors by ICS

It is important to highlight that during differentiation many immediate early genes are activated in order to regulate cell's genomic responses to environmental stimuli. Underlying intracellular mechanisms are not clear yet; however, Sheng and coworkers showed that c-fos expression, an immediate early gene, depends on calcium influx. This increase activates the calcium response element (CaRE) and thus results in phosphorylation/activation of the CaRE binding protein and consequently c-fos transcription [46].

The transcription factor CREB is activated in neurons in response to trans-synaptic signaling and regulates the expression of genes important for adaptive neuronal responses, such as behavioral adaptation to changes in the environment [47], as well as for more complex neural functions, such as learning and memory formation [48]. Target genes include immediate early genes, such as c-fos [46], and molecules essential for synaptic function, including brain derived neurotrophic factor (BDNF) [49,50] and neuronal nitric oxide synthase (nNOS) [51]. In addition to its functions in mature neurons, CREB regulates cell proliferation, differentiation, and survival responses in a range of cell types in developing vertebrates [52-54]. CREB is inactive as a transcription factor until a cell is exposed to any one of a range of extracellular stimuli that trigger CREB phosphorylation at a specific site. Ser133 within its kinase-inducible domain promotes association of CREB with a co-adaptor protein, the CREB binding protein (CBP). The recruitment of CBP by CREB to the promoter of a CREB target gene then induces the assembly of an active polymerase II transcription complex, thus leading to target gene activation [55]. The kinetics of CREB Ser142 and Ser143 phosphorylation suggest that, when both of these phosphorylation events occur together with Ser133 phosphorylation, they promote CREB activation [56]. Moreover, experimental evidence indicates that Ca^{2+}/CaM dependent kinase IV (CaMKIV) and CREB play a critical role in mediating calcium-induced dendritic growth in cortical neurons. A constitutively active form of CaMKIV induces dendritic growth in the absence of extracellular stimulation and activates the transcription factor CREB [57].

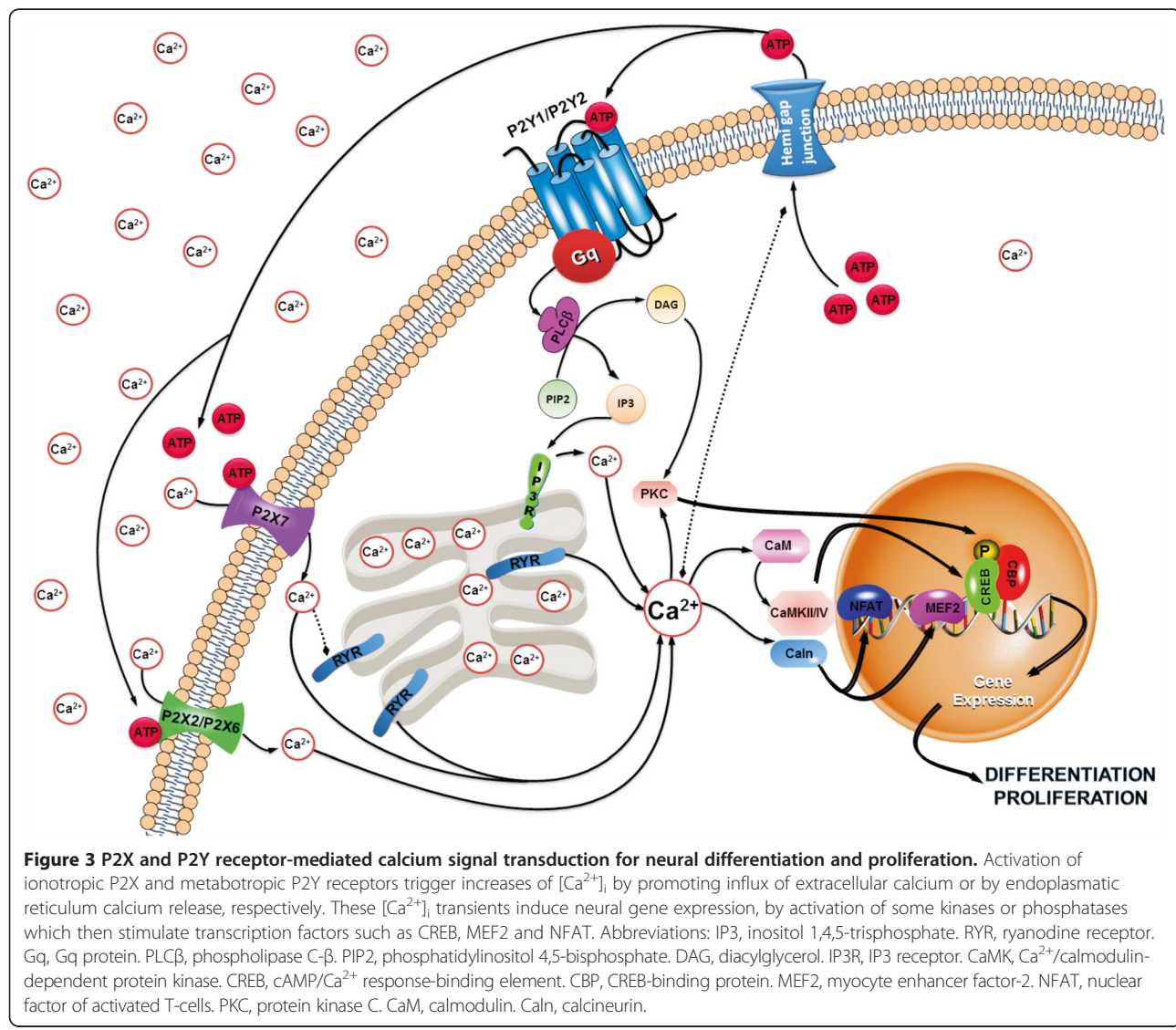
In hippocampal neurons, signaling to CREB activation can be triggered by elevations in nuclear calcium concentration alone and does not require import of cytoplasmic proteins into the nucleus. The nucleus is particularly

suites to integrate neuronal firing patterns, and specifies the transcriptional outputs through a burst frequency and nuclear calcium amplitude conversion. Calcium release from intracellular stores promotes calcium wave propagation into the nucleus, which is critical for CREB-mediated transcription by synaptic receptors. Pharmacological modulation of nuclear calcium or modulation of gene expression levels of proteins involved in this process may directly affect stem cell differentiation during development [58].

Another important regulatory molecule that is sensible to changes in $[Ca^{2+}]_i$ is the transcription factor myocyte enhancer factor-2 (MEF2), which is highly expressed in neurons and during embryogenesis. Experimental evidence indicates roles for MEF2 as a calcium-dependent regulator of neuronal differentiation and function. The calcium-binding protein CaM is activated by signals that trigger rises in $[Ca^{2+}]_i$ resulting in Ca^{2+} -bound CaM

association with calcineurin (Cn), and thus releases Cn from its repressive effects. Cn dephosphorylates NFAT and MEF2, allowing them to translocate into the nucleus and consequently switch on gene transcription [59]. When Ca^{2+} entry is prevented or Cn activity is inhibited, NFAT is rephosphorylated by NFAT kinases and rapidly leaves the nucleus ($t_{1/2} \sim 15$ min), and NFAT-dependent gene expression is terminated [60-63]. As a result of this absolute dependence on Ca^{2+} /Cn signaling, NFAT has a remarkable ability to sense dynamic changes in intracellular Ca^{2+} levels and frequencies of Ca^{2+} oscillations in cells [64] (Figure 3). Furthermore, activation of CaMKII, through high-amplitude calcium spikes [65], induces neural gene expression through transcription factors of the MEF2 family [59].

Gene expression induced by $[Ca^{2+}]_i$ transients, triggered by activation of VOCs and [66] and purinergic P2X or P2Y receptors, could comprise general regulation



mechanisms of neural differentiation. Such hypothesis is in agreement with the observation that purinergic signaling is present and critical in switching on genes for development of the nervous system and the eye of the *Xenopus* around the time of gastrulation [67–69]. Ca^{2+} waves occur during early development, between stages 9 and 12 in the dorsal ectoderm of *Xenopus* [70]. From stage 10 onwards, $[\text{Ca}^{2+}]_i$ transients are limited to regions of forebrain, midbrain and eyes overlapping with the approximate location and time of ATP release [69,71]. The relationship between P2 receptor and transcription factor activation by ICS is well illustrated in Figure 3.

Conclusions

ICS is an important issue to study because of its versatility, which controls different cell processes essential for cellular function, including stem cell differentiation. Much evidence points at an important physiological role of extracellular ATP during neuronal development by stimulating proliferation and/or differentiation of NSC and progenitor cells depending on the repertoire of P2 receptor subtype expression. Agonists and antagonists might provide novel and powerful tools for modulating these cell functions for therapy of developmental diseases and regeneration therapy in neurodegenerative diseases. P2X and P2Y purinergic receptors promote proliferation by a mechanism in which ATP induces increases in $[\text{Ca}^{2+}]_i$ in form of waves or spikes, leading to activation of various effectors, followed by an alteration in transcription factor expression and activity patterns such as CREB, NFAT and MEF2, which are involved in stimulation of neural gene transcription. Better understanding of these processes will establish the importance of purinergic signaling in stem cell biology.

Abbreviations

$[\text{Ca}^{2+}]_i$: Cytosolic free Ca^{2+} concentration; ADP: Adenosine 5'-diphosphate; AMP: Adenosine monophosphate; ATP: Adenosine 5'-triphosphate; BDNF: Brain derived neurotrophic factor; CAM: Calmodulin; CaMK: Ca^{2+} /Calmodulin dependent kinase; CaRE: Calcium response element; CBP: CREB binding protein; Cn: Calcineurin; CREB: Camp/ Ca^{2+} response element binding protein; CSC: Embryonal carcinoma cells; ER: Endoplasmic reticulum; hMSC: Adult bone marrow mesenchymal; ICS: Intracellular calcium signaling; IP3: Inositol-1,4,5-Trisphosphate; MEF2: Myocyte enhancer factor-2; NFAT: Nuclear factor of activated T-Cells; nNOS: neuronal nitric oxide synthase; PLC- β : PhospholipaseC- β ; ROCs: Receptor-operated channels; RYR: Ryanodine receptor; UDP: Uridine-5'-diphosphate; UTP: Uridine-5'-triphosphate; VOCs: Voltage-operated channels.

Competing interests

The authors declare to have no competing interests.

Authors' contribution

All authors contributed to the writing of the manuscript. Figures 1–3 were designed by T.G. All authors read and approved the final manuscript.

Acknowledgments

H.U. acknowledges grant support from Fundação de Amparo à Pesquisa do Estado de São Paulo (FAPESP), Project No. 2006/61285-9 and 2012/50880-4, Conselho Nacional de Desenvolvimento Científico e Tecnológico (CNPq),

and the Provost's Office for Research of the University of São Paulo (Programa de Incentivo à Pesquisa, Project No. 2011.1.9333.1.3, NAPNA-USP), Brazil. R.R.R. is grateful for grant support by CNPq-MCT and Instituto Nacional de Ciência e Tecnologia de Nanomateriais de Carbono, CNPq and Fundação de Amparo à Pesquisa do Estado de Minas Gerais (FAPEMIG), Brazil. T.G.'s doctoral thesis is supported by a fellowship from FAPESP.

Author details

¹Departamento de Bioquímica, Instituto de Química, Universidade de São Paulo, Avenida Professor Lineu Prestes, 748, São Paulo CEP 05508-900, Brazil.

²Departamento de Bioquímica e Imunologia, Instituto de Ciências Biológicas, Universidade Federal de Minas Gerais, Belo Horizonte, Brazil.

Received: 3 September 2012 Accepted: 4 February 2013

Published: 17 February 2013

References

- Berridge MJ: Elementary and global aspects of calcium signalling. *J Exp Biol* 1997, **200**:315–319.
- Berridge MJ, Lipp P, Bootman MD: The versatility and universality of calcium signalling. *Nat Rev Mol Cell Biol* 2000, **1**:11–21.
- Berridge MJ: Inositol trisphosphate and calcium signalling. *Nature* 1993, **361**:315–325.
- Clapham DE: Calcium signaling. *Cell* 1995, **80**:259–268.
- Spitzer NC, Lautermilch NJ, Smith RD, Gomez TM: Coding of neuronal differentiation by calcium transients. *Bioessays* 2000, **22**:811–817.
- Ulrich H, Abbracchio MP, Burnstock G: Extrinsic Purinergic Regulation of Neural Stem/Progenitor Cells: Implications for CNS Development and Repair. *Stem Cell Reviews and Reports* 2012, **8**(3):755–67.
- Spitzer NC, Root CM, Borodinsky LN: Orchestrating neuronal differentiation: patterns of Ca^{2+} spikes specify transmitter choice. *Trends Neurosci* 2004, **27**:415–421.
- Resende RR, da Costa JL, Kihara AH, Adhikari A, Lorencon E: Intracellular Ca^{2+} regulation during neuronal differentiation of murine embryonal carcinoma and mesenchymal stem cells. *Stem Cells Dev* 2010, **19**:379–394.
- Resende RR, Adhikari A, da Costa JL, Lorencon E, Ladeira MS, Guatimosim S, Kihara AH, Ladeira LO: Influence of spontaneous calcium events on cell-cycle progression in embryonal carcinoma and adult stem cells. *Biochim Biophys Acta* 2010, **1803**:246–260.
- Lipp P, Thomas D, Berridge MJ, Bootman MD: Nuclear calcium signalling by individual cytoplasmic calcium puffs. *EMBO J* 1997, **16**:7166–7173.
- Spitzer NC: Activity-dependent neuronal differentiation prior to synapse formation: the functions of calcium transients. *J Physiol Paris* 2002, **96**:73–80.
- Tonelli FM, Santos AK, Gomes DA, da Silva SL, Gomes KN, Ladeira LO, Resende RR: Stem cells and calcium signaling. *Adv Exp Med Biol* 2012, **740**:891–916.
- Burnstock G: The past, present and future of purine nucleotides as signalling molecules. *Neuropharmacology* 1997, **36**:1127–1139.
- Verkhratsky A, Krishtal OA, Burnstock G: Purinoceptors on neuroglia. *Mol Neurobiol* 2009, **39**:190–208.
- Burnstock G, Campbell G, Satchell D, Smythe A: Evidence that adenosine triphosphate or a related nucleotide is the transmitter substance released by non-adrenergic inhibitory nerves in the gut. *Br J Pharmacol* 1970, **40**:668–688.
- North RA: P2X receptors: a third major class of ligand-gated ion channels. *CIBA Found Symp* 1996, **198**:91–105. discussion 105–109.
- Egan TM, Khakh BS: Contribution of calcium ions to P2X channel responses. *J Neurosci* 2004, **24**:3413–3420.
- Burnstock G: Purinergic signalling. *Br J Pharmacol* 2006, **147**(Suppl 1):S172–S181.
- Burnstock G: Pathophysiology and therapeutic potential of purinergic signalling. *Pharmacol Rev* 2006, **58**:58–86.
- Dona F, Ulrich H, Persike DS, Conceicao IM, Blini JP, Cavalheiro EA, Fernandes MJ: Alteration of purinergic P2X4 and P2X7 receptor expression in rats with temporal-lobe epilepsy induced by pilocarpine. *Epilepsy Res* 2009, **83**:157–167.
- Glaser T, Cappellari AR, Pillat MM, Iser IC, Wink MR, Battastini AM, Ulrich H: Perspectives of purinergic signaling in stem cell differentiation and tissue regeneration. *Purinergic Signal* 2012, **8**(3):523–37.
- Majumder P, Trujillo CA, Lopes CG, Resende RR, Gomes KN, Yuahasi KK, Britto LR, Ulrich H: New insights into purinergic receptor signaling in

- neuronal differentiation, neuroprotection, and brain disorders. *Purinergic Signal* 2007, **3**:317–331.
- 23. Dubyak GR, El-Moatassim C: Signal transduction via P2-purinergic receptors for extracellular ATP and other nucleotides. *Am J Physiol* 1993, **265**:C577–606.
 - 24. Abbracchio MP, Burnstock G, Boeynaems JM, Barnard EA, Boyer JL, Kennedy C, Knight GE, Fumagalli M, Gachet C, Jacobson KA, Weisman GA: International Union of Pharmacology LVIII: update on the P2Y G protein-coupled nucleotide receptors: from molecular mechanisms and pathophysiology to therapy. *Pharmacol Rev* 2006, **58**:281–341.
 - 25. Burnstock G: Physiology and pathophysiology of purinergic neurotransmission. *Physiol Rev* 2007, **87**:659–797.
 - 26. Burnstock G: Purine and pyrimidine receptors. *Cell Mol Life Sci* 2007, **64**:1471–1483.
 - 27. Resende RR, Majumder P, Gomes KN, Britto LR, Ulrich H: P19 embryonal carcinoma cells as *in vitro* model for studying purinergic receptor expression and modulation of N-methyl-D-aspartate-glutamate and acetylcholine receptors during neuronal differentiation. *Neuroscience* 2007, **146**:1169–1181.
 - 28. Czyz J, Wobus A: Embryonic stem cell differentiation: the role of extracellular factors. *Differentiation* 2001, **68**:167–174.
 - 29. Watt FM, Hogan BL: Out of Eden: stem cells and their niches. *Science* 2000, **287**:1427–1430.
 - 30. Mironov SL: Metabotropic ATP receptor in hippocampal and thalamic neurones: pharmacology and modulation of Ca²⁺ mobilizing mechanisms. *Neuropharmacology* 1994, **33**:1–13.
 - 31. Salter MW, Hicks JL: ATP causes release of intracellular Ca²⁺ via the phospholipase C beta/IP3 pathway in astrocytes from the dorsal spinal cord. *J Neurosci* 1995, **15**:2961–2971.
 - 32. Schwindt TT, Trujillo CA, Negraes PD, Lameu C, Ulrich H: Directed differentiation of neural progenitors into neurons is accompanied by altered expression of P2X purinergic receptors. *J Mol Neurosci* 2011, **44**:141–146.
 - 33. Shukla V, Zimmermann H, Wang L, Kettenmann H, Raab S, Hammer K, Sevigny J, Robson SC, Braun N: Functional expression of the ecto-ATPase NTPDase2 and of nucleotide receptors by neuronal progenitor cells in the adult murine hippocampus. *J Neurosci Res* 2005, **80**:600–610.
 - 34. Suadicani SO, Brosnan CF, Scemes E: P2X7 receptors mediate ATP release and amplification of astrocytic intercellular Ca²⁺ signaling. *J Neurosci* 2006, **26**:1378–1385.
 - 35. Yuahasi KK, Demasi MA, Tamajusuku AS, Lenz G, Sogayar MC, Fornazari M, Lameu C, Nascimento IC, Glaser T, Schwindt TT, et al: Regulation of neurogenesis and gliogenesis of retinoic acid-induced P19 embryonal carcinoma cells by P2X2 and P2X7 receptors studied by RNA interference. *Int J Dev Neurosci* 2012, **30**:91–97.
 - 36. Ulrich H: Purinergic receptors in stem cell biology. In (*Org.*) *Stem Cells and Cancer Stem Cells*, vol. 8. 1st edition. Edited by Hayat MA. Dordrecht: Springer; 2012:267–274.
 - 37. da Silva RL, Resende RR, Ulrich H: Alternative splicing of P2X6 receptors in developing mouse brain and during *in vitro* neuronal differentiation. *Exp Physiol* 2007, **92**:139–145.
 - 38. Ryu JK, Choi HB, Hatori K, Heisel RL, Pelech SL, McLarnon JG, Kim SU: Adenosine triphosphate induces proliferation of human neural stem cells: Role of calcium and p70 ribosomal protein S6 kinase. *J Neurosci Res* 2003, **72**:352–362.
 - 39. Leon D, Hervas C, Miras-Portugal MT: P2Y1 and P2X7 receptors induce calcium/calmodulin-dependent protein kinase II phosphorylation in cerebellar granule neurons. *Eur J Neurosci* 2006, **23**:2999–3013.
 - 40. Lakshmi S, Joshi PG: Activation of Src/kinase/phospholipase C/mitogen-activated protein kinase and induction of neurite expression by ATP, independent of nerve growth factor. *Neuroscience* 2006, **141**:179–189.
 - 41. Ciccolini F, Collins TJ, Sudhoelter J, Lipp P, Berridge MJ, Bootman MD: Local and global spontaneous calcium events regulate neurite outgrowth and onset of GABAergic phenotype during neural precursor differentiation. *J Neurosci* 2003, **23**:103–111.
 - 42. Kawano S, Otsu K, Kuruma A, Shoji S, Yanagida E, Muto Y, Yoshikawa F, Hirayama Y, Mikoshiba K, Furuichi T: ATP autocrine/paracrine signaling induces calcium oscillations and NFAT activation in human mesenchymal stem cells. *Cell Calcium* 2006, **39**:313–324.
 - 43. Webb SE, Miller AL: Calcium signalling during embryonic development. *Nat Rev Mol Cell Biol* 2003, **4**:539–551.
 - 44. Lin JH, Takano T, Arcuino G, Wang X, Hu F, Darzynkiewicz Z, Nunes M, Goldman SA, Nedergaard M: Purinergic signaling regulates neural progenitor cell expansion and neurogenesis. *Dev Biol* 2007, **302**:356–366.
 - 45. Resende RR, Britto LR, Ulrich H: Pharmacological properties of purinergic receptors and their effects on proliferation and induction of neuronal differentiation of P19 embryonal carcinoma cells. *Int J Dev Neurosci* 2008, **26**:763–777.
 - 46. Sheng M, McFadden G, Greenberg ME: Membrane depolarization and calcium induce c-fos transcription via phosphorylation of transcription factor CREB. *Neuron* 1990, **4**:571–582.
 - 47. Ginty DD, Kornhauser JM, Thompson MA, Bading H, Mayo KE, Takahashi JS, Greenberg ME: Regulation of CREB phosphorylation in the suprachiasmatic nucleus by light and a circadian clock. *Science* 1993, **260**:238–241.
 - 48. Frank DA, Greenberg ME: CREB: a mediator of long-term memory from mollusks to mammals. *Cell* 1994, **79**:5–8.
 - 49. Shieh PB, Hu SC, Bobb K, Timmusk T, Ghosh A: Identification of a signaling pathway involved in calcium regulation of BDNF expression. *Neuron* 1998, **20**:727–740.
 - 50. Tao X, Finkbeiner S, Arnold DB, Shaywitz AJ, Greenberg ME: Ca²⁺ influx regulates BDNF transcription by a CREB family transcription factor-dependent mechanism. *Neuron* 1998, **20**:709–726.
 - 51. Sasaki M, Gonzalez-Zulueta M, Huang H, Herring WJ, Ahn S, Ginty DD, Dawson VL, Dawson TM: Dynamic regulation of neuronal NO synthase transcription by calcium influx through a CREB family transcription factor-dependent mechanism. *Proc Natl Acad Sci U S A* 2000, **97**:8617–8622.
 - 52. Bonni A, Brunet A, West AE, Datta SR, Takasu MA, Greenberg ME: Cell survival promoted by the Ras-MAPK signaling pathway by transcription-dependent and -independent mechanisms. *Science* 1999, **286**:1358–1362.
 - 53. Riccio A, Ahn S, Davenport CM, Blendy JA, Ginty DD: Mediation by a CREB family transcription factor of NGF-dependent survival of sympathetic neurons. *Science* 1999, **286**:2358–2361.
 - 54. Walton M, Woodgate AM, Muravlev A, Xu R, During MJ, Dragunow M: CREB phosphorylation promotes nerve cell survival. *J Neurochem* 1999, **73**:1836–1842.
 - 55. Kwok RP, Lundblad JR, Chrivia JC, Richards JP, Bachinger HP, Brennan RG, Roberts SG, Green MR, Goodman RH: Nuclear protein CBP is a coactivator for the transcription factor CREB. *Nature* 1994, **370**:223–226.
 - 56. Kornhauser JM, Cowan CW, Shaywitz AJ, Dolmetsch RE, Griffith EC, Hu LS, Haddad C, Xia Z, Greenberg ME: CREB transcriptional activity in neurons is regulated by multiple, calcium-specific phosphorylation events. *Neuron* 2002, **34**:221–233.
 - 57. Redmond L, Kashani AH, Ghosh A: Calcium regulation of dendritic growth via CaM kinase IV and CREB-mediated transcription. *Neuron* 2002, **34**:999–1010.
 - 58. Hardingham GE, Arnold FJ, Bading H: Nuclear calcium signaling controls CREB-mediated gene expression triggered by synaptic activity. *Nat Neurosci* 2001, **4**:261–267.
 - 59. McKinsey TA, Zhang CL, Olson EN: MEF2: a calcium-dependent regulator of cell division, differentiation and death. *Trends Biochem Sci* 2002, **27**:40–47.
 - 60. Garrity PA, Chen D, Rothenberg EV, Wold BJ: Interleukin-2 transcription is regulated *in vivo* at the level of coordinated binding of both constitutive and regulated factors. *Mol Cell Biol* 1994, **14**:2159–2169.
 - 61. Loh C, Carew JA, Kim J, Hogan PG, Rao A: T-cell receptor stimulation elicits an early phase of activation and a later phase of deactivation of the transcription factor NFAT1. *Mol Cell Biol* 1996, **16**:3945–3954.
 - 62. Loh C, Shaw KT, Carew J, Viola JP, Luo C, Perrino BA, Rao A: Calcineurin binds the transcription factor NFAT1 and reversibly regulates its activity. *J Biol Chem* 1996, **271**:10884–10891.
 - 63. Timmerman LA, Clipstone NA, Ho SN, Northrop JP, Crabtree GR: Rapid shuttling of NF-AT in discrimination of Ca²⁺ signals and immunosuppression. *Nature* 1996, **383**:837–840.
 - 64. Hogan PG, Chen L, Nardone J, Rao A: Transcriptional regulation by calcium, calcineurin, and NFAT. *Genes Dev* 2003, **17**:2205–2232.
 - 65. Lautermilch NJ, Spitzer NC: Regulation of calcineurin by growth cone calcium waves controls neurite extension. *J Neurosci* 2000, **20**:315–325.
 - 66. Canellada A, Cano E, Sanchez-Ruiloba L, Zafra F, Redondo JM: Calcium-dependent expression of TNF-alpha in neural cells is mediated by the calcineurin/NFAT pathway. *Mol Cell Neurosci* 2006, **31**:692–701.
 - 67. Bogdanov YD, Dale L, King BF, Whittick N, Burnstock G: Early expression of a novel nucleotide receptor in the neural plate of Xenopus embryos. *J Biol Chem* 1997, **272**:12583–12590.

68. Cheung KK, Ryten M, Burnstock G: Abundant and dynamic expression of G protein-coupled P2Y receptors in mammalian development. *Dev Dyn* 2003, **228**:254–266.
69. Masse K, Bhamra S, Eason R, Dale N, Jones EA: Purine-mediated signalling triggers eye development. *Nature* 2007, **449**:1058–1062.
70. Leclerc C, Neant I, Webb SE, Miller AL, Moreau M: Calcium transients and calcium signalling during early neurogenesis in the amphibian embryo *Xenopus laevis*. *Biochim Biophys Acta* 2006, **1763**:1184–1191.
71. Dale N: Dynamic ATP signalling and neural development. *J Physiol* 2008, **586**:2429–2436.

doi:10.1186/1478-811X-11-12

Cite this article as: Glaser et al.: Implications of purinergic receptor-mediated intracellular calcium transients in neural differentiation. *Cell Communication and Signaling* 2013 11:12.

**Submit your next manuscript to BioMed Central
and take full advantage of:**

- Convenient online submission
- Thorough peer review
- No space constraints or color figure charges
- Immediate publication on acceptance
- Inclusion in PubMed, CAS, Scopus and Google Scholar
- Research which is freely available for redistribution

Submit your manuscript at
www.biomedcentral.com/submit





Modulation of Mouse Embryonic Stem Cell Proliferation and Neural Differentiation by the P2X7 Receptor

Talita Glaser¹, Sophia La Banca de Oliveira¹, Arquimedes Cheffer¹, Renata Beco¹, Patrícia Martins¹, Maynara Fornazari¹, Claudiana Lameu¹, Helio Miranda Costa Junior², Robson Coutinho-Silva², Henning Ulrich^{1*}

1 Departamento de Bioquímica; Instituto de Química, Universidade de São Paulo, São Paulo, Brasil, **2** Instituto de Biofísica Carlos Chagas Filho, Universidade Federal do Rio de Janeiro - UFRJ, Rio de Janeiro, RJ, Brazil

Abstract

Background: Novel developmental functions have been attributed to the P2X7 receptor (P2X7R) including proliferation stimulation and neural differentiation. Mouse embryonic stem cells (ESC), induced with retinoic acid to neural differentiation, closely assemble processes occurring during neuroectodermal development of the early embryo.

Principal Findings: P2X7R expression together with the pluripotency marker Oct-4 was highest in undifferentiated ESC. In undifferentiated cells, the P2X7R agonist Bz-ATP accelerated cell cycle entry, which was blocked by the specific P2X7R inhibitor KN-62. ESC induced to neural differentiation with retinoic acid, reduced Oct-4 and P2X7R expression. P2X7R receptor-promoted intracellular calcium fluxes were obtained at lower Bz-ATP ligand concentrations in undifferentiated and in neural-differentiated cells compared to other studies. The presence of KN-62 led to increased number of cells expressing SSEA-1, Dcx and β 3-tubulin, as well as the number of SSEA-1 and β 3-tubulin-double-positive cells confirming that onset of neuroectodermal differentiation and neuronal fate determination depends on suppression of P2X7R activity. Moreover, an increase in the number of Ki-67 positive cells in conditions of P2X7R inhibition indicates rescue of progenitors into the cell cycle, augmenting the number of neuroblasts and consequently neurogenesis.

Conclusions: In embryonic cells, P2X7R expression and activity is upregulated, maintaining proliferation, while upon induction to neural differentiation P2X7 receptor expression and activity needs to be suppressed.

Citation: Glaser T, de Oliveira SLB, Cheffer A, Beco R, Martins P, et al. (2014) Modulation of Mouse Embryonic Stem Cell Proliferation and Neural Differentiation by the P2X7 Receptor. PLoS ONE 9(5): e96281. doi:10.1371/journal.pone.0096281

Editor: Jan Pruszak, University of Freiburg, Germany

Received November 4, 2013; **Accepted** April 4, 2014; **Published** May 5, 2014

Copyright: © 2014 Glaser et al. This is an open-access article distributed under the terms of the Creative Commons Attribution License, which permits unrestricted use, distribution, and reproduction in any medium, provided the original author and source are credited.

Funding: This work was supported by the Brazilian funding agencies: CNPq and FAPESP. TG was recipient of Fundação de Amparo à Pesquisa do Estado de São Paulo (Fapesp) fellowship. The funders had no role in study design, data collection and analysis, decision to publish, or preparation of the manuscript.

Competing Interests: Henning Ulrich is a PLoS ONE Editorial Board member. This does not alter the authors' adherence to all the PLoS ONE policies on sharing data and materials.

* E-mail: henning@iq.usp.br

Introduction

Purinergic receptors are classified as P1 adenosine and P2 ATP receptors based on their selectivity for adenosine and nucleotide agonists. While P1 and P2Y subtypes are G-protein-coupled metabotropic receptors, P2X receptors are resembled as homo- or hetero-trimeric ligand-gated ion channels from seven possible subunits. The ion channels formed by P2X1-P2X7 subunits are permeable to Na^+ , K^+ and Ca^{2+} ions, while at high agonist concentrations P2X7 receptor (P2X7R) subtypes assemble cation ion channels that are capable of pore forming, allowing the unselective flow of compounds with molecular masses of 700Da besides the uncontrolled entry of ions, including Ca^{2+} , into the cell which may induce intrinsic cell death programs [1,2,3]. Moreover, the P2X7R has an intracellular domain that couples receptor activation to intracellular signaling events and is classically involved with apoptosis [4,5]. However, P2X7 receptors have also been involved in cell survival and increased proliferation of cancer cells [4,6,7,8] at low extracellular ATP concentration [9]. These divergent roles can be explained by the fact that now is

possible to dissociate the channel from pore function, and therefore these might be two separate molecular entities [10,11].

Being expressed in almost every cell and attributed to multiple cellular functions, purinergic receptors have been detected in early embryonic development [12]. P2 receptor antagonists injected into the early gastrula (first invagination) stage of the *Xenopus* embryo, impaired development with embryos having no head, trunk, somite and notochord and sometimes no tail; in midway gastrula, the embryos had no heads, but with trunks and tails [13].

Maiken Nedergaard's group showed that neuronal differentiation is accompanied by a marked down-regulation of purinergic signaling and the neural progenitor cells themselves were the source of local ATP secretion [14]. Furthermore in the brain of newborn rats a 6 kb RNA was detected corresponding to the P2X7R transcript, which was not detectable in adult brains [15], suggesting possible developmental functions of the P2X7R.

Complex developmental mechanisms are often studied in simplified environment by using stem cell models. Embryonic stem cells (ESC) are isolated from blastocysts inner cell mass maintaining *in vitro* their capability of self-renewal, proliferating in

Table 1. Primer sequences for PCR experiments.

Gene	Forward (5'-3')	Reverse (5'-3')
GAPDH	TGCACCACCAACTGCTAG	GGATGCAGGGATGATGTTC
SSEA-1	CGGACCGACTCGGATGTCT	TTGGATCGCTCTGGAATAGA
Dcx	GAGTGGGGCTTCGAGTGAT	AAAGAAAGCCGTGCGCTTG
β3-tubulin	AGA CCT ACT GCA TCG ACA ATG AAG	GCT CAT GGT AGC AGA CAC AAG G
Nestin	GAG AGT CGC TTA GAG GTG CA	CCA CTT CCA GAC TCC GGG AC
Oct-4	ATG CCG TGA AGT TGG AGA AG	TGT ACC CCA AGG TGA TCC TC
P2X7R	GCACGAATTATGGCACCGTC	CCCCACCCCTGTGACATTCT
IsoA	TGAGACAAACAAAGTCACCCG	TCAGTAGGGATACTTGAAGCC
IsoB	TGCTCTCTGACCGGCGTTG	TCAGGTGCGCATACATACATG
IsoC	TGCTCTCTGACCGGCGTTG	GAAACAAGTATCTAGGTTGG
IsoK	GCCC GTGAGCCACTTATGC	TCAGTAGGGATACTTGAAG

doi:10.1371/journal.pone.0096281.t001

an undifferentiated state, being pluripotent (capable to differentiate into all cell types of an adult organism) and having a stable karyotype [5,16]. Besides their contribution to elucidation of developmental mechanisms, ESC have been extensively studied during last decades as a promise to cure diverse diseases and injuries. In this study we used E14TG2a cell line, because beyond maintaining ESC characteristics, these cells can grow in feeder free cultures, avoiding contamination by fibroblasts during differentiation process [17,18].

Extracellular ATP induces proliferation and regulates proliferation in pluripotent stem cell models expressing various purinergic receptor subtypes [5,19,20,21,22,23]. Here, we provide evidence for so far unknown roles of the P2X7R in embryonic stem cell biology including maintenance of proliferation and induction to neuroectodermal differentiation.

Methods

P2X7R (−/−) knock-out mice

P2X7 (−/−) knock-out mice, developed by the method of Dr James Mobley (PGRD, Pfizer Inc, Groton, CT, USA) were housed in controlled temperature of 22±2°C and 60–70% humidity and unlimited access to food and water *ad libitum* under 12 h light-dark cycle. Animal maintenance and sacrificing for isolation of whole-brain tissue was in agreement with the regulations of the Local Animal Ethics Committee of the Federal University of Rio de Janeiro, Brazil.

Culture and differentiation of E14Tg2A mouse embryonic stem cell

The feeder cell independent E14Tg2A embryonic stem (ES) cell line was kindly provided by Dr. Deborah Schechtman, Instituto de Química, University of São Paulo. Cells were first isolated by Hooper et al, 1987 [18] and further characterized by Magin et al. 1992 [18]. Cells were cultured as described by Fornazari and coworkers [24]. Basically, cells were grown in DMEM containing 15% Fetal Bovine Serum (FBS), 2 mM sodium pyruvate, 1% non-essential amino acids, 10³ U/mL Leukemia Inhibitory Factor (LIF), 0.1 mM β-mercaptoethanol and 10 mM HEPES, pH 7.4, at 37°C in a water-saturated atmosphere containing 5% CO₂. For neural differentiation, 5×10⁶ cells were cultured in 90×15 mm non-adherent plates in DMEM supplemented with 20% FBS, 1% non-essential amino acids and 0.1 mM β-mercaptoethanol for

48 h to induce embryoid body formation. Following substitution of the culture medium, cells were cultured as a suspension for 4 further days in the presence of 5 μM retinoic acid. Embryoid bodies were seeded in 125 mm adherent cell culture flasks and grown for further 4 or 12 days.

ESC growth curve assay

Cells were plated at a 30×10⁴ density in p35 mm previous gelatinized plates. Cells were removed from duplicate plates by use of trypsin and resuspended in 1 ml of Hanks' balanced salt solution containing 0.5% formalin to fix them after 8, 12, 24, 36, 48 and 60 h. Cell numbers were determined with a Neubauer chamber (0.100 mm depth, 0.0025 mm² area) on an inverted microscope Axiovert 200 (Zeiss).

Protein extraction and western blotting assays

For preparation of cell lysates, E14Tg2A undifferentiated and differentiated cells were trypsinized, centrifuged for 10 min at 400 g, washed with PBS and centrifuged again. The pellet was then dissolved in lysis buffer (20 mM Tris-HCl, 1 mM EDTA, 0.5% NP40, 20% Glycerol pH = 7.5) plus a protease inhibitor cocktail (Thermo Life Sciences) and phosphatase inhibitors (2 mM orthovanadate and 5 mM sodium fluoride, Thermo Life Sciences), incubated for 15 min on ice, and then centrifuged for 25 min at 2000×g and 4°C. The same procedure was performed with total brain lysates of P2X7R (−/−) animals.

Protein quantification was measured by the Coomassie Blue method [33] with bovine serum albumin as the standard. Thirty micrograms of protein in sample buffer were separated by SDS-PAGE on a 10% polyacrylamide gel at a constant voltage of 140 V. Then proteins were transferred onto a nitrocellulose membrane (Thermo-scientific) in a wet system for 1 hour at constant amperage of 400 mA. For blocking of nonspecific binding, 5% BSA in TBS-T was added for 30 min under agitation at room temperature. The membranes were then incubated with primary antibodies for Oct-4 (polyclonal rabbit 1:1000 Millipore), P2X7 receptor extracellular epitope (monoclonal rabbit 1:2000 AbCam), P2X7 receptor C-terminus epitope (polyclonal rabbit 1:1000 Alomone) and α-actin (1:1000 Sigma-Aldrich) overnight at 4°C. Membranes were then washed and probed with the respective secondary antibodies, Alexa Fluor 488 or 647 (Invitrogen, Life Technologies), for 1 h under agitation at room temperature. Primary and secondary antibodies were diluted in

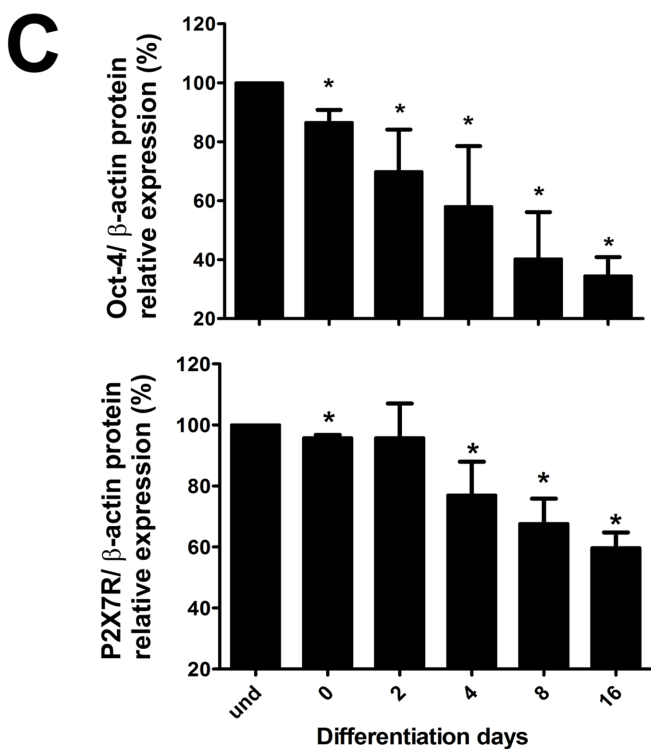
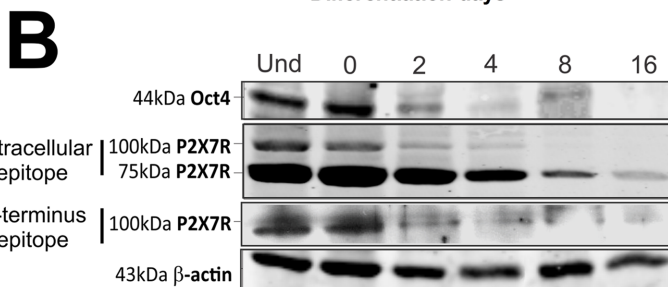
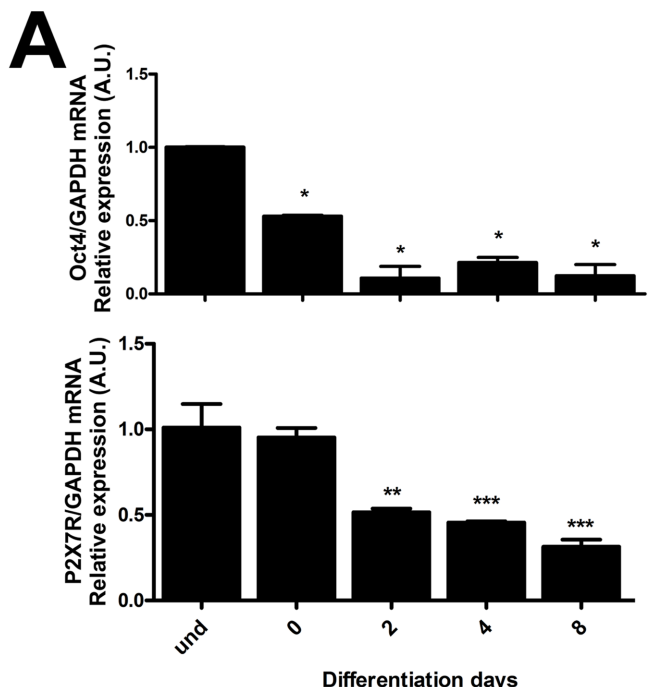


Figure 1. P2X7 receptor and Oct-4 expression in undifferentiated mouse ESC and cells induced to neural differentiation. P2X7 receptor and Oct-4 expression levels in undifferentiated (UND) and cells induced to differentiation (days 0–8) were determined by (A) real-time PCR and (B,C) Western blotting assays as described in Materials and Methods. For real-time PCR, quantitative analysis of the relative expression of P2X7R and Oct-4 in E14Tg2A cell line was performed using GAPDH mRNA transcription rates as endogenous control for normalization of expression levels. For Western blotting, P2X7R and Oct-4 expression levels were obtained and analyzed by densitometric analysis of protein bands and were compared to β -actin expression levels. The P2X7R was identified by two antibodies, which recognize the extracellular or C-terminus domain. Bars represent mean \pm standard errors (S.E.) of three independent experiments performed in triplicate. Data were analyzed for statistical relevance with the One-Way ANOVA test followed by the Bonferroni post hoc test (* $p<0.05$, ** $p<0.01$, *** $p<0.001$ compared to control data).

doi:10.1371/journal.pone.0096281.g001

1% BSA and TBS-T. Membranes were washed in TBS-T and scanned with Typhoon– GE Healthcare. The resulting bands were subjected to densitometric analysis with the ImageJ software. Oct-4 and P2X7R levels were normalized by comparison to β -actin expression.

Calcium-imaging in E14Tg2A embryonic stem single cells

Undifferentiated and differentiated E14Tg2A ESC were loaded with 5 μ M of Fluo3-AM for 45 min at 37°C in DMEM High glucose in 0.5% Me2SO and 0.06% of the nonionic surfactant pluronic acid F-127 (Sigma Aldrich). After loading with Fluo-3AM, the cells were incubated with extracellular buffer (140 mM NaCl, 3 mM KCl, 1 mM MgCl₂, 2 mM CaCl₂, 10 mM HEPES, 10 mM glucose at pH 7.4) [25]. Ca²⁺ imaging was performed by using the Inverted Research Microscope ECLIPSE-TiS (Nikon, Melville, NY) equipped with a 14 bit high-resolution CCD camera Cool-SNAP HQ2 (Photometrics, Tucson, AZ) and analyzed with NIS-Element software (Nikon) using image acquisition rates of two frames per second. Fluo-3 fluorescence was excited with a xenon lamp at 488 nm, and the emitted light was detected using a band-pass filter at 515–530 nm. Intracellular calcium influx was monitored in cells stimulated with 10 μ M ATP and 10 μ M Bz-ATP. Forty cells were analyzed for each data point and the calcium influx was determined as mean variation between Fluo-3AM fluorescence intensities obtained during the stimulus (F) and the rest state (F₀), normalized by its basal fluorescence (F_b). (F-F₀)/F_b.

Calcium measurements by microfluorimetry

Changes in [Ca²⁺]_i were determined by microfluorimetry using the FlexStation III (Molecular Devices Corp., Sunny Valley, CA), following the instructions of the manufacturer [26]. Briefly, for undifferentiated cells, they were seeded a night before starting the experiment at a density of 5–3 \times 10⁴ cells/well and for 8 days differentiated cells, 2 EBs/well were seeded in 96-well black

microplate with clear bottom, with 100 μ l of cell culture medium per well. Cells were incubated for 60 min at 37°C with the FlexStation Calcium Assay Kit (Molecular Devices Corp.) containing 2.5 mM probenecid in a final volume of 200 μ l per well. Fluorescence of samples was excited at 485 nm, and fluorescence emission was detected at 525 nm.

Samples were read at 1.52 s intervals for 120 s with a total of 79 read-outs per well. Following 20 s of monitoring basal fluorescence intensity for [Ca²⁺]_i levels of nonstimulated cells, agonists (ATP and Bz-ATP) were applied onto the cells, and induced-[Ca²⁺]_i transients were monitored for up to 200 s. Responses to agonist addition were determined as peak fluorescence minus the basal fluorescence intensity using the SoftMax2Pro software (Molecular Devices Corp.). Data were expressed as mean values \pm standard errors (S.E.).

Immunofluorescence staining assay

For immunofluorescence detection of specific marker proteins for respective differentiation stages, E14Tg2A cells were grown and induced to differentiate on rounded coverslips (1 cm diameter). Cells were fixed with 4% paraformaldehyde in phosphate-buffered saline (PBS) for 15 min, washed three times with PBS and then incubated for 30 min in a blocking solution containing 0.05% Triton-X 100 and 2% FBS. Cells were incubated overnight at 4°C with primary antibodies raised against mouse monoclonal anti stage-specific embryonic antigen-1 (SSEA-1) (1:200, Chemicon, Bioscience Research Reagents, Temecula, CA), rabbit polyclonal anti- β III tubulin (1:200, Millipore, Billerica, MA), Oct-4 rabbit polyclonal (1:1000 Millipore), rabbit monoclonal P2X7R (1:2000 AbCam, Cambridge, MA) and nestin (1:1000 Millipore) antibodies. The slides were washed three times with PBS, followed by one hour incubation with Alexa Fluor 488 or 555 goat anti-mouse (1:800, Sigma). In control experiments, the primary antibody was omitted, and immunostaining was never observed. Counterstaining of cell nuclei was achieved with 0.1% of

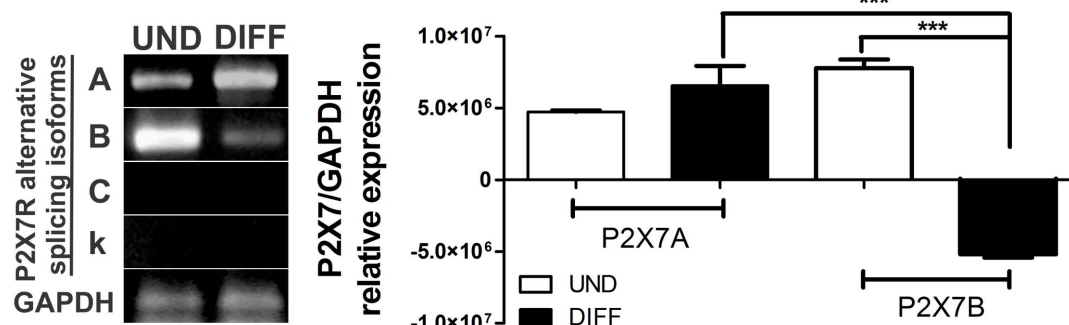


Figure 2. Differential expression of P2X7R alternative splicing isoforms in undifferentiated and neural-differentiated ESC. (A) P2X7 receptor isoform A, B, C and k expression in undifferentiated (UND) and cells following 8 days of neural differentiation (DIFF) was determined by RT-PCR. (B) P2X7R isoforms expression levels were obtained and analyzed by densitometric analysis of DNA bands and were compared to GAPDH expression levels. Data were analyzed for statistical relevance with the One-Way ANOVA test followed by the Bonferroni post hoc test (* $p<0.05$, ** $p<0.01$, *** $p<0.001$ compared to control data).

doi:10.1371/journal.pone.0096281.g002

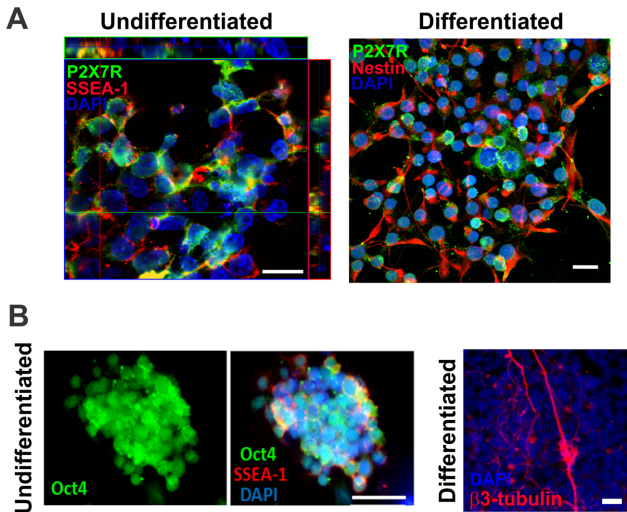


Figure 3. Immunofluorescence studies of P2X7 receptor and differentiation-stage specific proteins in undifferentiated and differentiated ESC. P2X7R expression and co-localization with differentiation-stage specific proteins was determined by confocal microscopy and immunofluorescence assays as described in Materials and Methods. **(A)**, Left panel: Co-localization between SSEA-1 (stage-specific embryonic antigen-1) and P2X7R immunofluorescence in undifferentiated ES cells. Co-localization of the protein is shown by Z-stack analysis. Right panel: Double-immunostaining for nestin (neural stem and precursor marker) and P2X7R expression in cells induced to differentiation for 8 days. **(B)**, Left panel: Immunostaining for Oct-4 (pluripotency marker) in undifferentiated cells. Middle panel: Immunostaining for Oct-4 and SSEA-1 in undifferentiated cells. Right panel: Staining pattern for the neuron-specific marker β -tubulin in neural-differentiated cells. Cell nuclei were visualized by DAPI staining. Scale bar, 50 μ m.

doi:10.1371/journal.pone.0096281.g003

4',6-diamidino-2-phenylindole (DAPI). After washing with PBS, the slides were mounted with Vectashield (Vector Laboratories, Burlingame, CA) and examined on an Axiovert 200 epifluorescence microscope (Zeiss, Aalen, Germany), equipped with a Nikon DMX1200F camera and Metamorph image analysis program or on a confocal microscope (Zeiss LSM 780-NLO Multiphoton) and analyzed with the LSMib software (Zeiss).

Real time polymerase chain reaction

Total RNA was extracted from undifferentiated and ESC subjected to 8 days of neural differentiation using the TRIzol Reagent (Invitrogen) following manufacturer's instruction. All samples were further treated with amplification grade DNase I (Sigma-Aldrich). Reverse transcription for cDNA synthesis was carried out on a thermal cycler using the RevertAid Reverse Transcriptase (Thermo Scientific Fermentas) first strand synthesis system according to the manufacturer's protocol (Invitrogen) in the presence of specific primers listed in (Table 1). The transcription rates of selected mRNAs were measured by real time PCR using the ABI Step One Plus instrument (Life Technologies). Real time PCR was performed in 15 μ l of buffer reaction containing of 1 ug cDNA, SYBR Green Master Mix (Life Technologies), and 5 pmol of each sequence-specific primers (Table 1). Thermal cycling conditions consisted of a denaturation for 10 min at 95°C followed by 40 cycles for denaturation for 15 s at 95°C, and annealing/extension for 1 min at 60°C, followed by melting curve analysis. The comparative $2^{-\Delta\Delta CT}$ method was employed for relative quantification of gene expression as described previously [27].

using glyceraldehyde-3-phosphate dehydrogenase (GAPDH) gene expression as an internal standard for normalization.

Polymerase chain reaction

Total RNA was extracted from undifferentiated and 8 days differentiated ESC using TRIzol Reagent (Invitrogen) following manufacturer's instruction. All samples were further treated with amplification grade DNase I (Sigma-Aldrich). Reverse transcription for cDNA synthesis was carried out on a thermal cycler using the RevertAid Reverse Transcriptase (Thermo Scientific Fermentas) to first strand synthesis system according to the manufacturer's protocol (Invitrogen). The transcription rates of selected mRNAs were measured by PCR using a thermal cycler. PCR was performed in 20 μ l of buffer reaction containing of 2 μ g cDNA, Maxima Hot Start Taq DNA Polymerase (Thermo Scientific Fermentas), and 5 pmol of each sequence-specific primers (Table 1). Thermal cycling conditions consisted of a denaturation for 10 min at 95°C followed by 40 cycles for denaturation for 15 s at 95°C, and annealing for 30 s at 60°C and extension for 1 min at 70°C, followed by final extension 10 min at 72°C. Ten microliters of the PCR reaction were analyzed on a 1.0% agarose gel containing ethidium bromide and visualized under ultraviolet light. The resulting bands were subjected to densitometric analysis with the Image J software. P2X7R isoform splicing variant expression levels were normalized by comparison to GAPDH gene expression.

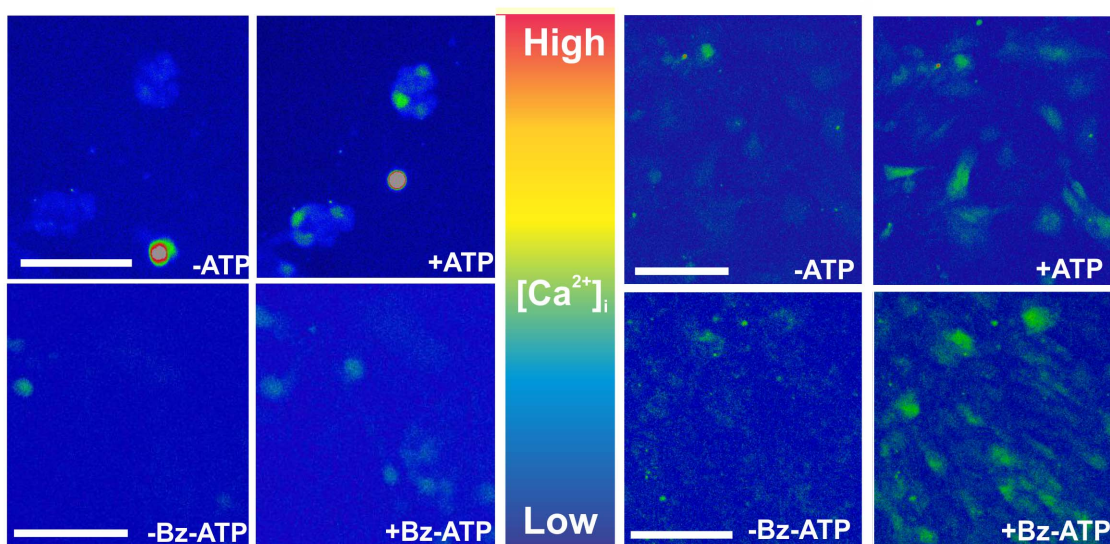
BrdU incorporation assay

Cell proliferation was measured following incubation with 20 μ M 5-bromo-2-deoxyuridine (BrdU; Sigma-Aldrich) for 1 hour. The cells were fixed with ice-cold 75% ethanol for 10 minutes, washed with PBS, incubated for 30 min in 2.0 M HCl and neutralized with 0.1 M sodium tetraborate. The cells were blocked with a 2% fetal bovine serum, 0.1% Triton-X solution in PBS for 30 minutes. After washing with PBS, they were incubated for 1 h with rat anti-BrdU antibodies (Abcam; 1:200 dilution). Alexa Fluor 488 secondary antibodies (Life Technologies) were used at 1:1000 dilution. After another washing step, propidium iodide solution (Life Technologies) at 50 μ g/ml was used as a DNA stain [28]. Cells, which had undergone through the whole process, but were not marked with the primary antibody and propidium iodide, were used as negative controls. The percentages of BrdU-positive cells and DNA contents were measured with the Attune flow cytometer (Life Technologies). Both fluorophores were excited by a 488 nm blue laser; Alexa Fluor 488 emission was captured by through a 530/30 nm filter and propidium iodide emission was captured through a 574/26 nm filter.

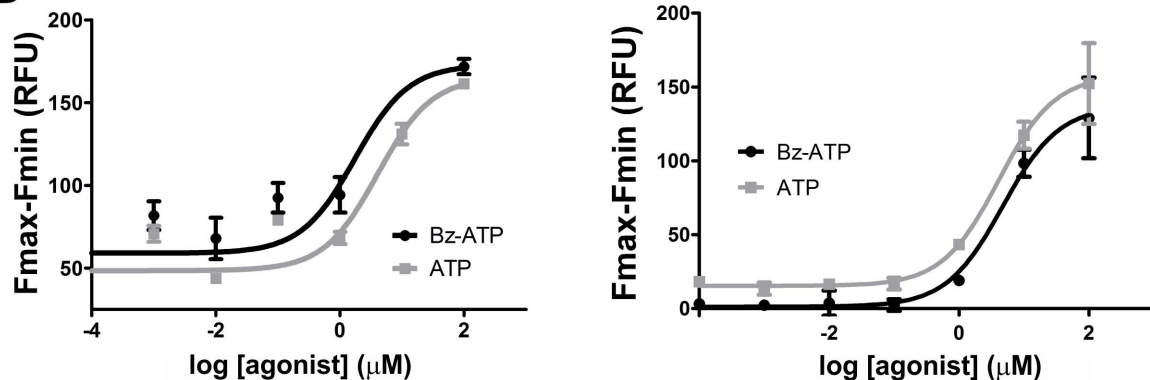
Flow cytometry analysis

The cells were fixed with a 4% paraformaldehyde solution for 30 minutes, washed in PBS and blocked with a 2% fetal bovine serum, 0.1% triton-x solution in PBS for 30 minutes. The cells were then incubated in mouse anti-SSEA1 antibodies (Millipore, 1:500 dilution) and either rabbit anti-Ki67 (Millipore, 1:500 dilution) or rabbit anti- β 3 tubulin antibodies (Sigma, 1:700 dilution) for 1 hour. The cells were incubated for 45 min. with the Alexa Fluor 488 anti-rabbit and Alexa Fluor 647 anti-mouse secondary antibodies (Life Technologies, 1:1000 dilution). Cells which had undergone through the whole process, but were not marked with the primary antibodies, were used as negative control. The percentage of marked cells was measured in the Attune flow cytometer (Life Technologies, CA). Alexa Fluor 488 was excited by a 488 nm blue laser and its emission was captured

A Undifferentiated Differentiated



B



C



D

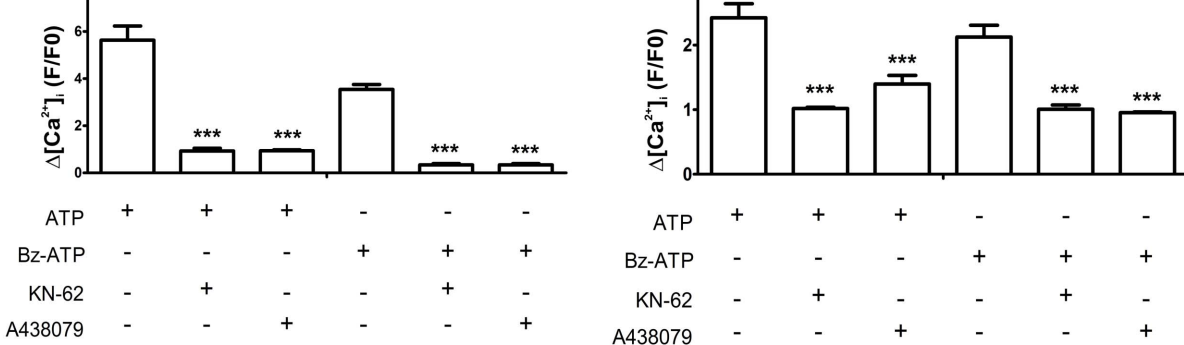


Figure 4. ATP- and Bz-ATP-induced intracellular calcium fluxes in undifferentiated and neural-differentiated ESC. ATP- and Bz-ATP-evoked P2X7R responses were determined by single-cell calcium imaging and microfluorimetry assays as described in Materials and Methods. **(A)** For calcium imaging, 10 μ M of purinergic receptor agonists, ATP or Bz-ATP, were used to stimulate receptor-mediated intracellular calcium fluxes in undifferentiated and neural-differentiated cells (day 8). **(B)** For microfluorimetry-based calcium measurements, increasing concentrations of ATP or Bz-ATP were added and time kinetics of changes in fluorescence emission was recorded. Peak values of measured $[Ca^{2+}]_i$ transients are reported. Nonlinear Regression was used for curve-fitting and calculating the EC₅₀ values. **(C and D)** P2X7R inhibitors were studied regarding their effects in blocking ATP- and Bz-ATP-induced $[Ca^{2+}]_i$ transients, as studied by calcium imaging. For these experiments, cells were pre-treated for 2 min with 10 μ M KN-62 or 1 μ M A438079 and then stimulated with 10 μ M ATP or Bz-ATP. Data represent mean values \pm S.E. of three independent experiments performed in triplicate.

doi:10.1371/journal.pone.0096281.g004

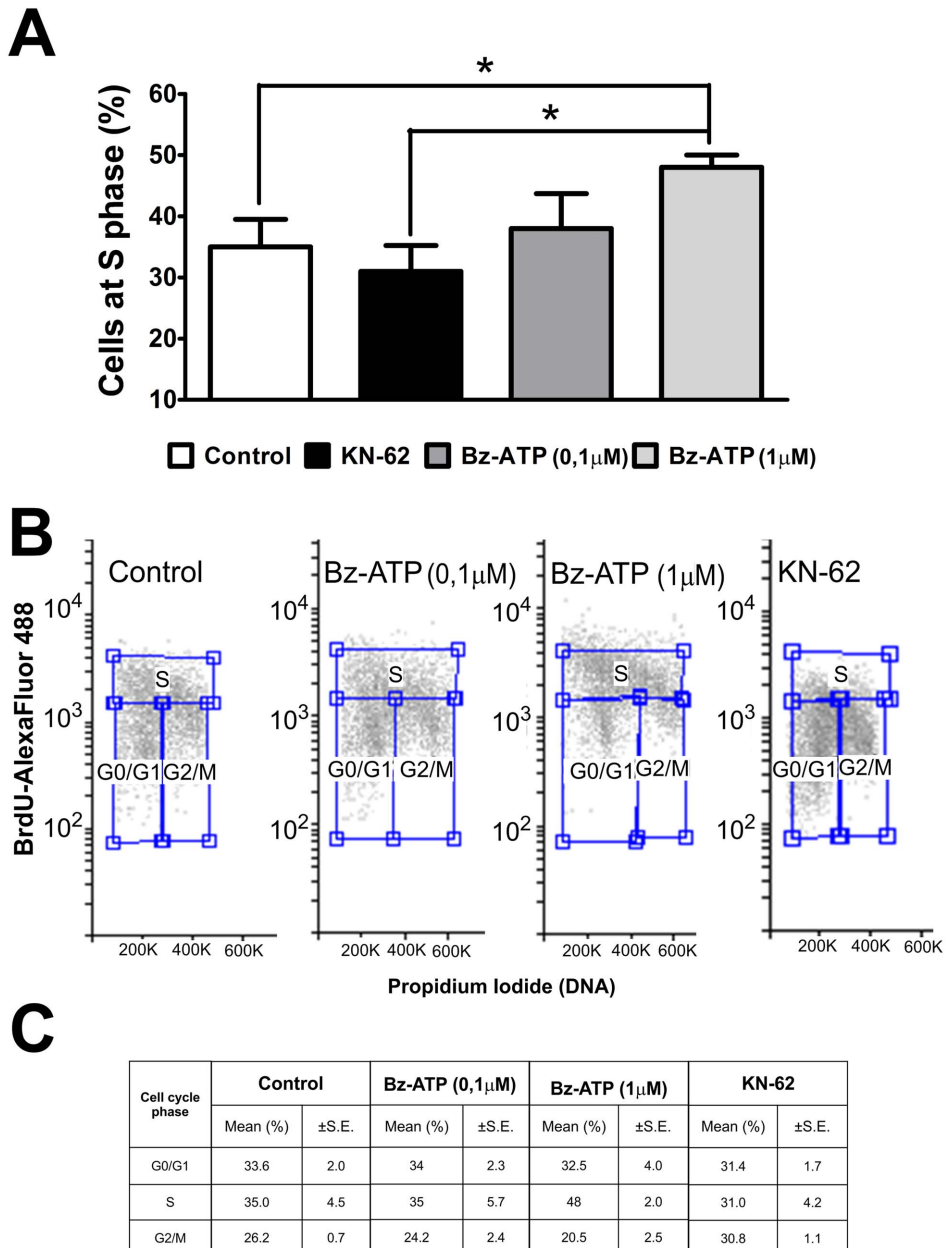


Figure 5. Proliferation of ESC in conditions of P2X7R modulation. Cell cycle analysis based on flow cytometric analysis of BrdU incorporation and propidium iodide DNA-staining were performed as described in Materials and Methods. **(A)** Cell distributions at different S-phases of ESC treated with P2X7R agonist or inhibitor, 0.1 μ M and 1 μ M Bz-ATP and 10 μ M KN-62 for 96 h, respectively. Shown data are representative for mean values \pm S.E. of five independent experiments. Data were statistical analyzed by the One-Way ANOVA test followed by the Bonferroni post hoc test with (* $p < 0.05$ compared to control data). **(B)** Representative BrdU/PI cell cycle analysis of ESC treated with Bz-ATP or KN-62 compared to untreated control cultures. **(C)** Cell cycle distributions of ESC treated for 96 h with the P2X7R agonist (0.1 μ M or 1 μ M Bz-ATP) or the P2X7R inhibitor KN-62 (10 μ M), respectively. Shown data are representative for mean values \pm S.E. of five independent experiments.

doi:10.1371/journal.pone.0096281.g005

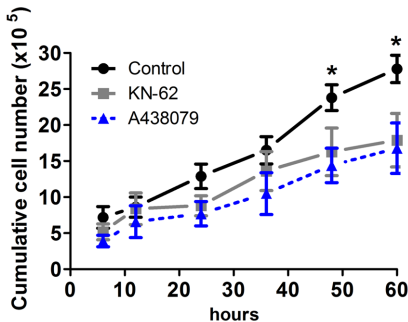


Figure 6. Inhibition of embryonic stem cell growth in the presence of P2X7R inhibitors. Cells were plated at 3×10^5 cell/ml density and P2X7R was inhibited daily with $10 \mu\text{M}$ KN-62 or $1 \mu\text{M}$ A438079 and then the number of cells were counted. Data represent mean values \pm S.E. of three independent experiments performed in triplicate (* $p<0.05$ compared to control).

doi:10.1371/journal.pone.0096281.g006

through a 530/30 filter. Alexa Fluor 647 was excited by a 638 nm red laser and its emission was captured through a 660/20 filter.

Statistical Analysis

Comparisons between experimental data were made by one- or two-way analysis of variance following the Bonferroni post-test using GraphPad Prism 5.0 software (GraphPad Software Inc., San Diego, CA). Criteria for statistical significance were set at $p<0.05$ (*), $p<0.01$ (**), or $p<0.001$ (***)�.

Results and Discussion

Functional expression and subcellular localization of P2X7 receptors in undifferentiated and neural-differentiated mouse embryonic stem cells

ESC induced for 8–16 days with *all-trans* retinoic acid to neural differentiation [29] reveal neuron-specific morphology and expression patterns, such as β 3-tubulin, and responsiveness to neurotransmitters and KCl, indicating expression of functional neurotransmitter receptors and voltage-operated ion channels [24]. In view of reports of purinergic signaling during early development [13], we correlate here Oct-4 and P2X7R gene and protein expression levels in pluripotent ESC and along neural differentiation of these cells (Figure 1A–C). P2X7R expression decayed during differentiation, such as it was observed for Oct-4. Down-regulation of Oct-4 has been reported when pluripotent cells undergo differentiation [30,31].

In undifferentiated ESC, P2X7R expression pattern showed one band with a molecular weight of 75 KDa and another one with 100 KDa. During the progress of differentiation the expression of both isoforms decayed, but remained expressed (Figure 1B). On one hand, a molecular complex of approximately 100 KDa has been described as a result of a complex formed by P2X7 and P2X4 subunits [32], but this is not applicable, because we performed SDS-PAGE of total cell extracts. On the other hand, previously published experimental evidence suggests that the 75 KDa form could present the glycosylated and functional form of the P2X7 receptor [33]. In order to resolve this question, immunostaining with another polyclonal antibody that recognizes just the intracellular C-terminus domain, that is present only in the canonical isoform, revealed the 100 KDa species in ESC undergoing neural differentiation (Figure 1B). The immunostaining is reliable given that no 100 and 75 KDa band staining was detectable in brains of P2X7R ($-/-$) knockout mouse brains

(Figure S1). Therefore, we suggested that detection of two different isoforms resulted from the expression of alternative splicing variants.

In order to determine the expression pattern for the different P2X7 splice variants along the neuronal differentiation of E14Tg2a cells, RT-PCR with specific sets of primers (Table 1) for each variant was performed. As shown in Figure 2A, only the transcripts encoding the isoforms A and B were expressed both by undifferentiated and differentiated cells. It is noteworthy that the isoforms A and B correspond to the canonical full-length P2X7A variant and the truncated P2X7B variant, respectively. This truncated variant is identical with the P2X7A variant between residues 1–430, but it has a much shorter C-terminus (its C-terminus is just 87 amino acid residues long, in comparison to the P2X7A C-terminus with circa 240 amino acid residues). Although there is no statistical difference in the relative expression of the isoform A between undifferentiated and differentiated cells, the isoform A is more abundantly expressed than the isoform B in differentiated cells. On the other hand, the relative expression of the transcript encoding the isoform B decreased significantly when the cells differentiated (Figure 2B). Summing up, our results suggest that in undifferentiated cells both the P2X7 splice variants are equally expressed. But upon onset of differentiation, the relative expression of the variant A remains constant, while the relative expression of the variant B decayed significantly. These results are in agreement with the previous ones obtained in Western-blot experiments (Figure 1B). The two observed bands are likely to correspond to the P2X7A and P2X7B variants. This is reinforced by the fact that, by using an antibody against a C-terminus epitope, just the circa 100 KDa band is observed. This antibody is not capable of identifying the P2X7B variant, since this lacks the epitope. However, two bands are observed, when an antibody against the extracellular domain is used in Western-blot experiments (Figure 1B–C). It has been already demonstrated that the isoform B, different from the P2X7A variant, is not able to form a large pore, as indicated by bromide ethidium uptake analysis [34,35]. We speculate therefore, that P2X7B isoform expression during the initial phase of differentiation may be a mechanism against cellular death allowing that more cells proliferate and differentiate, since pore formation leads eventually to apoptosis. In fact, it is possible that the P2X7B splice variant co-assembles with P2X7A receptors and suppresses cell permeabilization induced by the full-length P2X7A receptor. This mechanism has been already observed at least for the P2X7C variant [35].

Undifferentiated ESC express P2X7R altogether with SSEA-1, which is a membrane carbohydrate typically found in stem cells [36], as shown in Figure 3. The overlay of immunofluorescence images revealed co-expression as yellow regions, suggesting that the P2X7R is functionally expressed at the plasma membrane. In neural-differentiated cells (day 8) with diverse morphologies, neurons (β 3-tubulin positive cells) and neural precursors (nestin-positive cells) expressed the P2X7R throughout the cell (Figure 3).

In agreement with functional expression of purinergic receptors, we analyzed the induction of intracellular calcium transients ($[Ca^{2+}]_i$) in undifferentiated and neural-differentiated cells by the purinergic agonists ATP and Bz-ATP, which is a selective P2X7R agonist [37,38,39], by calcium imaging and microfluorimetry (Figure 4). Dose-response curves revealed EC₅₀ values of $4.1 \pm 1.8 \mu\text{M}$ and $1.7 \pm 2.2 \mu\text{M}$ in undifferentiated cells and $4.1 \pm 1.4 \mu\text{M}$ and $4.7 \pm 1.5 \mu\text{M}$ in neural-differentiated cells for stimulation by ATP and Bz-ATP, respectively (Figure 4A–B). ATP ($10 \mu\text{M}$) and Bz-ATP ($10 \mu\text{M}$) activated P2X7R function in both undifferentiated and neural-differentiated cells, as agonist-stimulated transients were abolished following pretreatment for 2 min

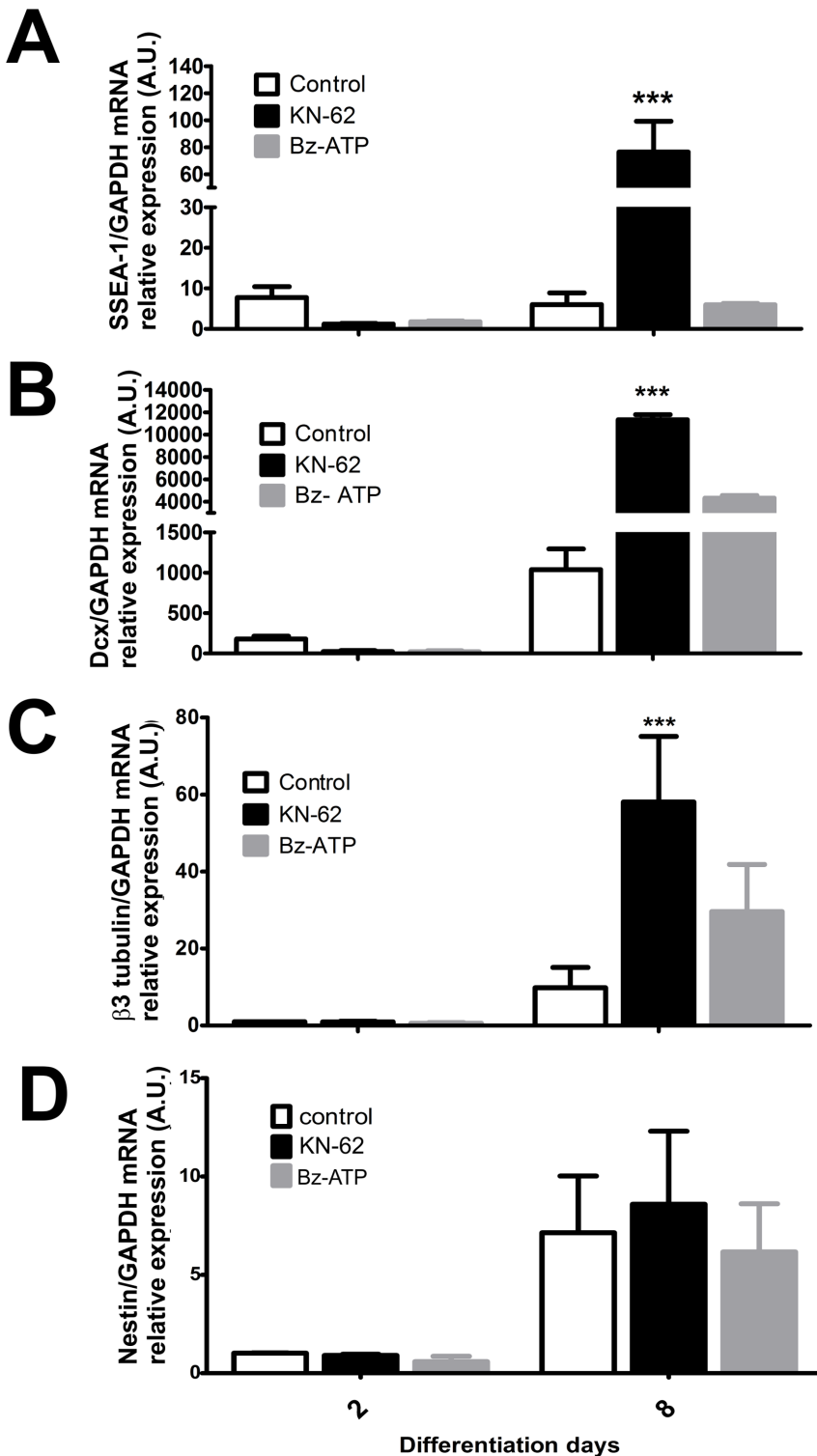


Figure 7. Effects of P2X7R agonists and antagonists on the progress of neural differentiation, studied on the gene expression level.
 Total RNA was isolated from cell cultures, and real-time PCR reactions were performed as described in Materials and Methods. Quantitative analysis of the relative expression of (A) SSEA-1, (B) Dcx, (C) β 3-tubulin and (D) nestin in E14Tg2A cell line were performed by real time-PCR where GAPDH expression was used as internal control for normalization of expression levels. ESC were treated with P2X7R agonists or inhibitors (10 μ M Bz-ATP or 10 μ M KN-62) respectively. Data were analyzed by the Two-Way ANOVA test followed by the Bonferroni post-hoc test. The experiments were performed three times in triplicate with (***) $p<0.001$ compared to control.

doi:10.1371/journal.pone.0096281.g007

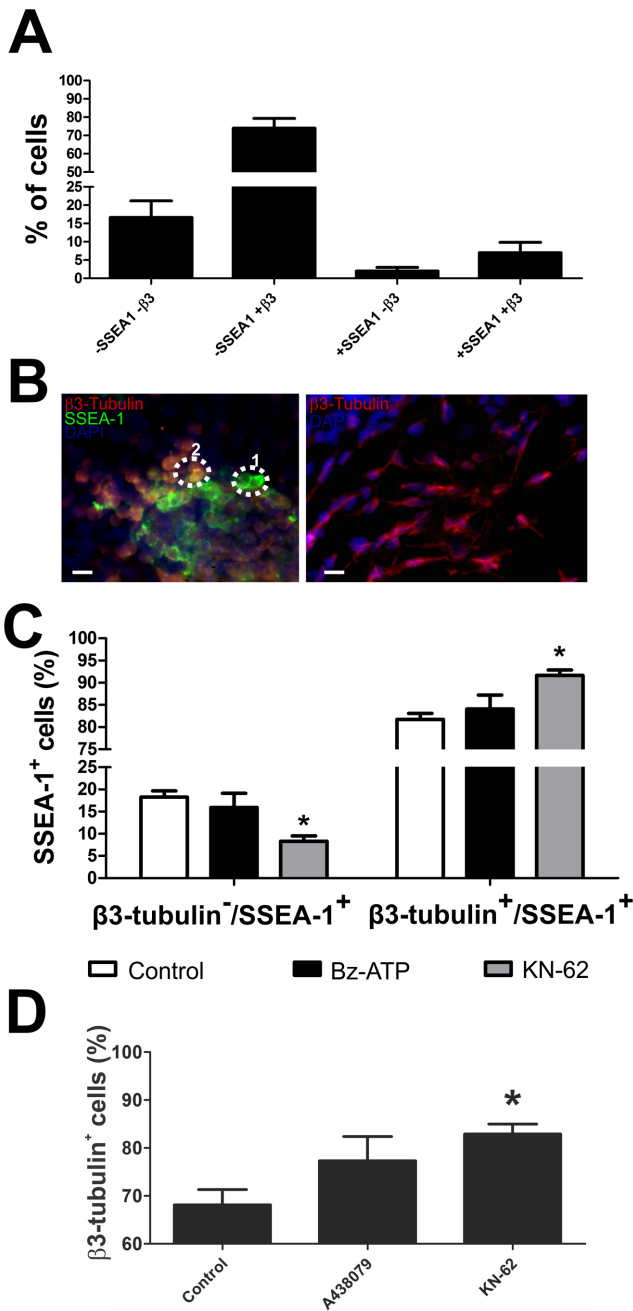


Figure 8. Modulation of neuroectodermal differentiation of mouse ESC by P2X7R activity. (A) Flow cytometry analysis of SSEA-1 and β3-tubulin protein expression in neural-differentiated ES cells. Cells were cultured and induced to differentiation as described in Materials and Methods. (B) Immunofluorescence assay of SSEA-1 and β3-tubulin expression of cells following 8 days of differentiation. Circled areas: 1. cells expressing only SSEA-1, 2. cells co-expressing SSEA-1 and β3-tubulin. Scale bar, 50 μm. (C) Flow cytometry analysis of SSEA-1-positive cells co-expressing or not β3-tubulin on day 8 of differentiation cultured in the presence of 10 μM Bz-ATP or 10 μM KN-62, respectively. (D) Percentage of β3-tubulin-positive cells differentiated in the absence or presence of 1 μM A438079 or 10 μM KN-62, as determined by flow cytometry. Statistical relevance was analyzed by the One-Way ANOVA test followed by the Bonferroni post-hoc test. Six independent experiments were performed (* p<0.05 compared to control data).

doi:10.1371/journal.pone.0096281.g008

with the P2X7R inhibitors KN-62 (10 μM) [39,40,41] and A438079 (1 μM) [42] (Figure 4C–D).

Neural-differentiated cells revealed EC₅₀ values for ATP and Bz-ATP that are not statistically different from those observed in undifferentiated cells (Figure 4B). However, agonist concentrations needed for activating this receptor were higher and response amplitudes decreased in neural-differentiated cells, suggesting that differentiated cells express P2X7R forms that are slightly less sensible to agonists than those in undifferentiated ESC. Differences in calcium responses in undifferentiated and differentiated cells may be related to expression levels of 100 and 75 KDa forms of the receptor (isoforms A and B) with the 100 KDa isoform A possibly being more sensible to activation by Bz-ATP than the 75 KDa isoform B.

Many studies have shown that activation of P2X7R needs higher concentration of agonists (100–1000 μM of ATP) [43], usually resulting in cell death; however, Francesco Di Virgilio showed recently that this receptor can be activated by lower concentrations, like we found, and induces trophic effects, mainly in tumor cells [44]. Therefore, in agreement with the here shown dose-response curves, low P2X7R agonist concentration would maintain undifferentiated stem cell functions, including pluripotency and proliferation, while higher agonist concentration, necessary for P2X7R activation in differentiated cells, would lead to different, possibly undesired effects. Such hypothesis is in agreement with the here observed P2X7R expression down-regulation following induction of ESC to neural differentiation.

Expression of P2X7R in neural-committed cells has been documented previously. For instance, embryonic rats (E15.5) express P2X7R mRNA together with the neural stem and progenitor cell marker nestin [45]. Thus, P2X7R expression levels also depend on the differentiation stage in other cellular models. Neuro-2a cells, derived from spontaneous mouse neuroblastoma, respond to retinoic acid-induction with the onset of neural differentiation together with a decrease in the expression and activity of P2X7 receptors [46]. In line with these results, RA-treated SH-SY5Y cells exhibited a neuron-like phenotype with neurites extending more than twice the length of the cell body and cell growth arrest simultaneously with down-regulation of P2X7R expression. The here cited example corroborate our hypothesis that differential expression and activity patterns of P2X7R are necessary for guiding ESC differentiation into neural phenotypes [47].

Promotion of cell cycle entry by P2X7 receptor activity

ES cells are derived without the intervention of any immortalizing agent, do not undergo senescence, they proliferate without apparent limit and are not subject to contact inhibition or anchorage dependence. In fact, no means of inducing cell-cycle arrest and quiescence in ES cells are known [48].

As already cited above, Di Virgilio and co-workers found that P2X7R promoted proliferation in tumor and microglial cells when stimulated by agonist [44]. Lemoli et al. showed that ATP modulates human hematopoietic stem cell proliferation by acting as potent early growth factor *in vitro* [49]. Thus microglial cell proliferation is blocked when P2X7R is inhibited [50]. In agreement, tumors are induced to proliferation upon P2X7R activation [51].

In order to understand modulation of ESC proliferation by P2X7R, we analyzed cell cycle distributions and cell cycle entry rates of undifferentiated cells cultured for 96 h in the absence or presence of Bz-ATP (0.1 and 1 μM) or the selective P2X7R inhibitor KN-62 (10 μM) [41]. Here, we provide evidence for an increase in the percentage of cells in S-phase (from 35% to 48%) in conditions of 1 μM Bz-ATP treatment. Accordingly, cells exposed

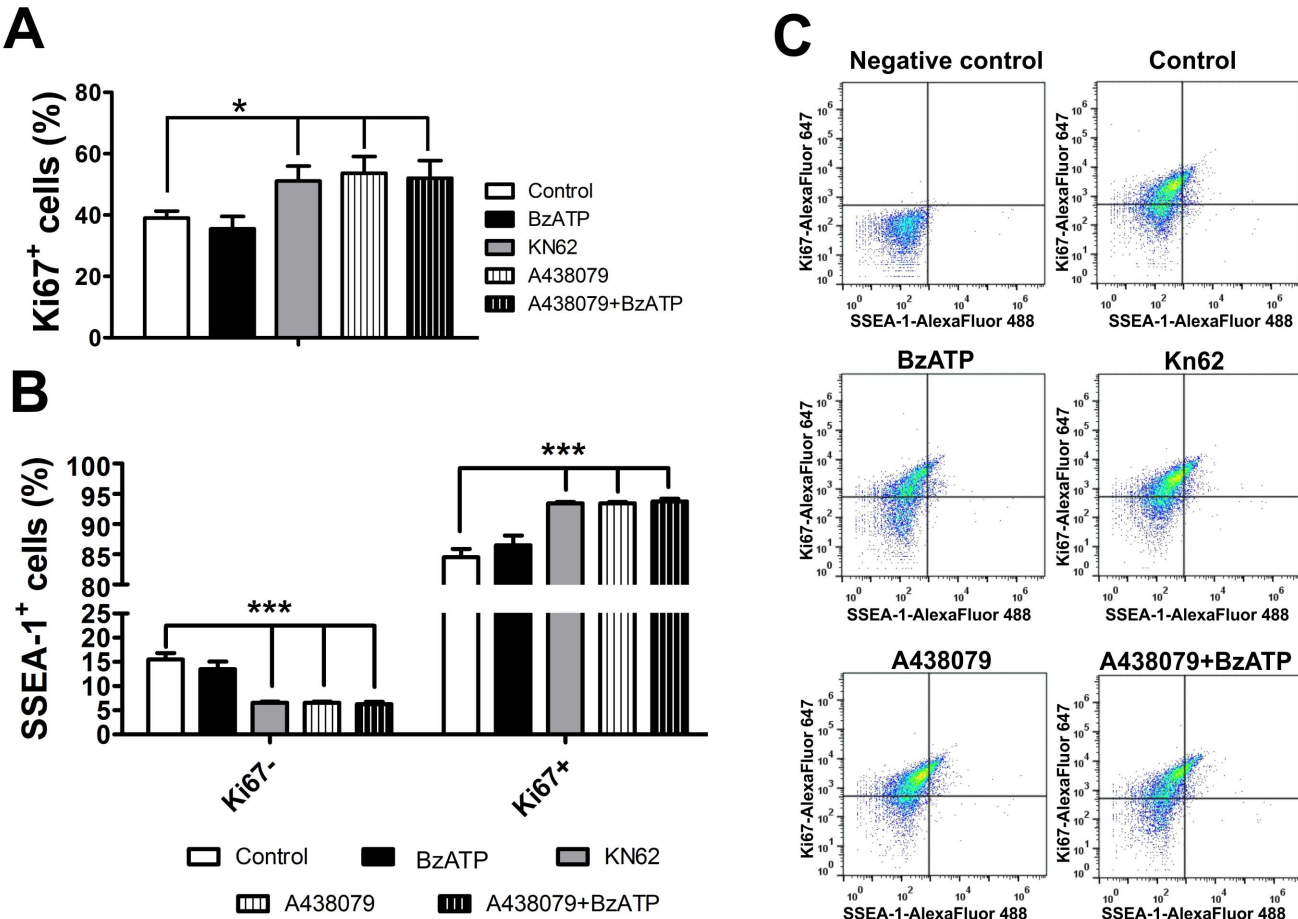


Figure 9. Expression of the proliferation antigen Ki-67 in SSEA-1 positive cells differentiated in the absence or presence of P2X7R agonists and antagonists. (A) Flow cytometry determination of Ki67⁺ cells following neural differentiation for 8 days in the absence or presence of the agonist Bz-ATP (10 μ M), the antagonists KN-62 (10 μ M) or A438079 (1 μ M), or Bz-ATP and A438079. (B) Determination of percentages of Ki67⁻/SSEA-1⁺ and Ki67⁺/SSEA-1⁺ cells for experimental conditions explained in A. (C) Representative dot-plot images for Ki67/SSEA-1 double staining for conditions described in B. Statistical relevance was analyzed by the One-Way ANOVA test followed by the Bonferroni post hoc test. Bars represent mean \pm SE of 5 independent experiments (*p<0.05, ***p<0.001 compared to control data).

doi:10.1371/journal.pone.0096281.g009

to KN-62 revealed a decrease in the percentage of cells in S phase (from 48% to 31%) (Figures 5A–C). Corroborating these data, cell growth curve assays showed a delay in proliferation of ESC treated with the P2X7R inhibitors KN-62 and A438079 (Figure 6). These results indicate that P2X7R activity results in ESC proliferation by accelerating entry into the cell cycle.

A possible underlying mechanism could be that the P2X7R contributes to cell cycle-dependent $[Ca^{2+}]_i$ transients, which are required for G1/S progression of mouse embryonic stem cells [52]. ESC usually overpass the G1 checkpoint to proliferate faster having a short G1 phase of 1.5 h [53,54]. G1 phase duration is extended in order to induce ESC differentiation commitment [55,56]. In view of that, in our work P2X7R modulation did not change the percentage of cells in G1 phase (Figure 5B–C), possibly indicating that the P2X7R is involved in proliferation, without affecting pluripotency, since P2X7R activity modulation did not affect Oct-4 marker expression (Figure S2).

P2X7 receptor modulates mouse neural precursor differentiation

The importance of P2X7R on ESC survival at the undifferentiated state has been reported previously [5]. Moreover, previous

results obtained by our laboratory using P19 embryonal carcinoma cells stably expressing shRNA for degradation of P2X7R coding mRNA established the importance of the P2X7R for glial cell proliferation and differentiation and the ratio of glial over neural cells following induction with retinoic acid [57]. Here, using ESC pre-differentiated to neural precursor cells, we show the importance of P2X7R activity modulation for the onset of ESC neuroectodermal differentiation and neuroblast maturation beyond the results obtained with P19 EC cells.

For this purpose, cells were induced to neural differentiation in the absence or presence of Bz-ATP (10 μ M) or KN-62 (10 μ M) along differentiation followed by gene expression analysis of the following differentiation stage markers: SSEA-1, expressed by stem cells undergoing neuroectodermal differentiation [58,59]; nestin, doublecortin (Dcx), expressed by migrating and differentiating neurons [60]; and β 3-tubulin, characterizing young neurons. The presence of KN-62 led to an increase of SSEA-1 (>8.5 fold), Dcx (>9.1 fold) and β 3-tubulin (>4.8 fold) gene expression (Figure 7A–C), while nestin (Figure 7D) and GFAP (glial marker, data not shown) expression levels were not affected. These results suggest that P2X7 receptor blockade promotes neurogenesis, but not gliogenesis, being in agreement with our previous study [57].

We observed by flow cytometry and by immunofluorescence assays that the population of differentiating cells is heterogeneous with around 70% of cells expressing only β 3-tubulin and revealing neuronal morphology and neurite extensions (Figure 8A and B). A population of 15% was negative for expression of SSEA-1 and β 3-tubulin, and around 15% of cells were SSEA-1 positive within 80% of them co-expressing β 3-tubulin. These β 3-tubulin-/SSEA-1-positive cells revealed morphological characteristics different from neurons; they are sphere shaped similarly to supposedly undifferentiated cells expressing SSEA-1, but not β 3-tubulin (Figure 8 A and B).

P2X7R inhibition promoted neuronal differentiation, as the presence of KN-62 led to an increase of the number of β 3-tubulin-positive cells within the SSEA-1 positive cells and decreased the β 3-tubulin negative cells (Figure 8C). Probably, the SSEA-1 $^+$ / β 3-tubulin $^-$ cells are less differentiated than SSEA-1 $^+$ / β 3-tubulin $^+$, and the inhibition of P2X7R led the neuronal commitment of SSEA-1 $^+$ / β 3-tubulin $^-$ cells.

SSEA-1 is a carbohydrate adhesion molecule [61] expressed in various types of stem cells, including the adult brain where neural stem cells reside in specific niches [58,59,62]. SSEA-1 is strongly expressed by neuroepithelial cells, being downregulated upon further differentiation, which suggests that delamination from the rosette-like structures parallels surface expression changes of these glycolipid markers [63,64]. This is consistent with the observation that SSEA-1 is present on neural stem cells *in vivo*, residing in stem cell niches of the adult brain [58]. Moreover, β 3-tubulin can be expressed in immature neurons in the proliferative ventricular and subventricular zones of the developing telencephalon distinguishing two neuronal populations: those that remain for an indefinite period of time in the proliferative zones, and those that leave the proliferative zones soon after being generated and migrate independently from radial glial fibers [65]. In early development, dividing neuronal-committed precursors express β 3-tubulin [66]. Such kind of precursor present in developing brain is the neuroblast, a cell that divides and can differentiate into a neuron after a migration phase [67]. These cells also express β 3-tubulin and are originated by neural stem cell differentiation, mainly from neuroepithelial cells expressing SSEA-1, and are committed to the neuronal fate.

Co-expression analysis of SSEA-1 and Ki-67, a marker of proliferating cells, by flow cytometry revealed that a few cells were SSEA-1 $^+$ /Ki67 $^-$, while the larger percentage of the population represents proliferating neuroblasts in agreement with their characteristics as dividing cells [68] (Figure 9A). Within the population of SSEA-1 positive cells, blockade of P2X7R activity by KN-62 or A438079 led to an increase in the number of Ki67 $^+$ cells (Figure 9B and C), recruiting progenitors into the cell cycle and differentiation. Taken together, SSEA-1 $^+$ / β 3-tubulin $^-$ cells may be stem cells (neuroepithelial) giving rise to neuroblasts (SSEA-1 $^+$ / β 3-tubulin $^+$) that finally differentiate into neurons (SSEA-1 $^-$ / β 3-

tubulin $^+$). P2X7R should then be less expressed to favor neuroblast differentiation.

Conclusions

We have provided experimental evidence for novel functions of the P2X7R in ESC biology: P2X7R expression and activity is upregulated in embryonic cells, maintaining ESC proliferation, while upon induction to neural differentiation P2X7 receptor expression and activity needs to be suppressed. Pharmacological inhibition of P2X7R activity results in a higher percentage of ESC undergoing neuroectodermal differentiation, in the rescue of quiescent progenitors into cell cycle and in the promotion of differentiation into neurons. Our data suggest that extracellular nucleotides may provide a novel and powerful tool for modulating ESC functions.

Supporting Information

Figure S1 Western blot with anti- P2X7R antibody in brain extracts of P2X7R (−/−) knock-out animals. P2X7 receptor expression was determined by Western blotting assay as described in Materials and Methods. For Western blotting, lysates of P2X7 $^{−/−}$ knockout animal brain and undifferentiated ESC were used to measure expression of P2X7R with the antibody that recognizes the extracellular domain of the receptor. (TIF)

Figure S2 Oct-4 expression during neural differentiation of ESC in conditions of P2X7R inhibition. Oct-4 expression was determined by real-time PCR assay as described in Materials and Methods. Prior to real-time PCR, cells were induced to differentiation in the absence or presence of 1 μ M Bz-ATP or 1 μ M KN-62. Relative expression levels of Oct-4 in E14Tg2A cell line were calculated using GAPDH mRNA transcription rates as endogenous control for normalization of expression levels. Bars represent mean \pm standard errors (S.E.) of three independent experiments. (TIF)

Acknowledgments

We thank Denise Yamamoto and Zilda Mendonça Izzo for technical assistance, Dr. Isis C. Nascimento for helping with cell culture, and Prof. Deborah Schechtman, Department of Biochemistry, Institute of Chemistry, University of São Paulo, for giving us the E14Tg2A cell line.

Author Contributions

Conceived and designed the experiments: TG HMCJ RCS HU. Performed the experiments: TG SLBO AC RB PM MF CL HMCJ. Analyzed the data: TG SLBO AC CL. Contributed reagents/materials/analysis tools: HMCJ RCS HU. Wrote the paper: TG RCS HU.

References

1. North RA (2002) Molecular physiology of P2X receptors. *Physiol Rev* 82: 1013–1067.
2. North RA, Surprenant A (2000) Pharmacology of cloned P2X receptors. *Annu Rev Pharmacol Toxicol* 40: 563–580.
3. Zanovello P, Bronte V, Rosato A, Pizzo P, Di Virgilio F (1990) Responses of mouse lymphocytes to extracellular ATP. II. Extracellular ATP causes cell type-dependent lysis and DNA fragmentation. *J Immunol* 145: 1545–1550.
4. Adinolfi E, Callegari MG, Ferrari D, Bolognesi C, Minelli M, et al. (2005) Basal activation of the P2X7 ATP receptor elevates mitochondrial calcium and potential, increases cellular ATP levels, and promotes serum-independent growth. *Mol Biol Cell* 16: 3260–3272.
5. Thompson BA, Storm MP, Hewinson J, Hogg S, Welham MJ, et al. (2012) A novel role for P2X7 receptor signalling in the survival of mouse embryonic stem cells. *Cell Signal* 24: 770–778.
6. Adinolfi E, Callegari MG, Cirillo M, Pinton P, Giorgi C, et al. (2009) Expression of the P2X7 receptor increases the Ca²⁺ content of the endoplasmic reticulum, activates NFATc1, and protects from apoptosis. *J Biol Chem* 284: 10120–10128.
7. Adinolfi E, Cirillo M, Woltersdorf R, Falzoni S, Chiozzi P, et al. (2010) Trophic activity of a naturally occurring truncated isoform of the P2X7 receptor. *FASEB J* 24: 3393–3404.
8. Adinolfi E, Melchiorri L, Falzoni S, Chiozzi P, Morelli A, et al. (2002) P2X7 receptor expression in evolutive and indolent forms of chronic B lymphocytic leukemia. *Blood* 99: 706–708.
9. Baricordi OR, Melchiorri L, Adinolfi E, Falzoni S, Chiozzi P, et al. (1999) Increased proliferation rate of lymphoid cells transfected with the P2X(7) ATP receptor. *J Biol Chem* 274: 33206–33208.

10. Coutinho-Silva R, Persechini PM (1997) P2Z purinoceptor-associated pores induced by extracellular ATP in macrophages and J774 cells. *Am J Physiol* 273: C1793–1800.
11. Virginio C, MacKenzie A, North RA, Surprenant A (1999) Kinetics of cell lysis, dye uptake and permeability changes in cells expressing the rat P2X7 receptor. *J Physiol* 519 Pt 2: 335–346.
12. Zimmermann H (2006) Nucleotide signaling in nervous system development. *Plugers Arch* 452: 573–588.
13. Burnstock G, Ulrich H (2011) Purinergic signaling in embryonic and stem cell development. *Cell Mol Life Sci* 68: 1369–1394.
14. Lin JH, Takano T, Arcuino G, Wang X, Hu F, et al. (2007) Purinergic signaling regulates neural progenitor cell expansion and neurogenesis. *Dev Biol* 302: 356–366.
15. Collo G, Neidhart S, Kawashima E, Kosco-Vilbois M, North RA, et al. (1997) Tissue distribution of the P2X7 receptor. *Neuropharmacology* 36: 1277–1283.
16. Eckfeldt CE, Mendenhall EM, Verfaillie CM (2005) The molecular repertoire of the ‘almighty’ stem cell. *Nat Rev Mol Cell Biol* 6: 726–737.
17. Hooper M, Hardy K, Handyside A, Hunter S, Monk M (1987) HPRT-deficient (Lesch-Nyhan) mouse embryos derived from germline colonization by cultured cells. *Nature* 326: 292–295.
18. Magin TM, McWhir J, Melton DW (1992) A new mouse embryonic stem cell line with good germ line contribution and gene targeting frequency. *Nucleic Acids Res* 20: 3795–3796.
19. da Silva RL, Resende RR, Ulrich H (2007) Alternative splicing of P2X6 receptors in developing mouse brain and during in vitro neuronal differentiation. *Exp Physiol* 92: 139–145.
20. Glaser T, Cappellari AR, Pillat MM, Iser IC, Wink MR, et al. (2012) Perspectives of purinergic signaling in stem cell differentiation and tissue regeneration. *Purinergic Signal* 8: 523–537.
21. Glaser T, Resende RR, Ulrich H (2013) Implications of purinergic receptor-mediated intracellular calcium transients in neural differentiation. *Cell Commun Signal* 11: 12.
22. Heo JS, Han HJ (2006) ATP stimulates mouse embryonic stem cell proliferation via protein kinase C, phosphatidylinositol 3-kinase/Akt, and mitogen-activated protein kinase signaling pathways. *Stem Cells* 24: 2637–2648.
23. Resende RR, Gomes KN, Adhikari A, Britto LR, Ulrich H (2008) Mechanism of acetylcholine-induced calcium signaling during neuronal differentiation of P19 embryonal carcinoma cells in vitro. *Cell Calcium* 43: 107–121.
24. Fornazari M, Nascimento IC, Nery AA, da Silva CC, Kowaltowski AJ, et al. (2011) Neuronal differentiation involves a shift from glucose oxidation to fermentation. *J Biomed Biomembr* 43: 531–539.
25. Negraes PD, Lameu C, Hayashi MA, Melo RL, Camargo AC, et al. (2011) The snake venom peptide Bj-PRO-7a is a M1 muscarinic acetylcholine receptor agonist. *Cytometry A* 79: 77–83.
26. Sykes DA, Dowling MR, Charlton SJ (2009) Exploring the mechanism of agonist efficacy: a relationship between efficacy and agonist dissociation rate at the muscarinic M3 receptor. *Mol Pharmacol* 76: 543–551.
27. Pal R, Mamidi MK, Das AK, Rao M, Bhonde R (2013) Development of a multiplex PCR assay for characterization of embryonic stem cells. *Methods Mol Biol* 1006: 147–166.
28. Oliveira SL, Pillat MM, Cheffer A, Lameu C, Schwindt TT, et al. (2013) Functions of neurotrophins and growth factors in neurogenesis and brain repair. *Cytometry A* 83: 76–89.
29. Guo X, Ying W, Wan J, Hu Z, Qian X, et al. (2001) Proteomic characterization of early-stage differentiation of mouse embryonic stem cells into neural cells induced by all-trans retinoic acid in vitro. *Electrophoresis* 22: 3067–3075.
30. Faherty S, Fitzgerald A, Keohan M, Quinlan LR (2007) Self-renewal and differentiation of mouse embryonic stem cells as measured by Oct4 expression: the role of the cAMP/PKA pathway. *In Vitro Cell Dev Biol Anim* 43: 37–47.
31. Radziszewska A, Chia Gle B, dos Santos RL, Theunissen TW, Castro LF, et al. (2013) A defined Oct4 level governs cell state transitions of pluripotency entry and differentiation into all embryonic lineages. *Nat Cell Biol* 15: 579–590.
32. Nicke A (2008) Homotrimeric complexes are the dominant assembly state of native P2X7 subunits. *Biochem Biophys Res Commun* 377: 803–808.
33. Young MT, Pelegri P, Surprenant A (2007) Amino acid residues in the P2X7 receptor that mediate differential sensitivity to ATP and BzATP. *Mol Pharmacol* 71: 92–100.
34. Cheewatrakoolpong B, Gilcrest H, Anthes JC, Greenfeder S (2005) Identification and characterization of splice variants of the human P2X7 ATP channel. *Biochem Biophys Res Commun* 332: 17–27.
35. Masin M, Young C, Lim K, Barnes SJ, Xu XJ, et al. (2012) Expression, assembly and function of novel C-terminal truncated variants of the mouse P2X7 receptor: re-evaluation of P2X7 knockouts. *Br J Pharmacol* 165: 978–993.
36. Gooi HC, Feizi T, Kapadia A, Knowles BB, Solter D, et al. (1981) Stage-specific embryonic antigen involves alpha 1 goes to 3 fucosylated type 2 blood group chains. *Nature* 292: 156–158.
37. Bianchi BR, Lynch KJ, Touma E, Niforatos W, Burgard EC, et al. (1999) Pharmacological characterization of recombinant human and rat P2X receptor subtypes. *Eur J Pharmacol* 376: 127–138.
38. Evans RJ, Lewis C, Buell G, Valera S, North RA, et al. (1995) Pharmacological characterization of heterologously expressed ATP-gated cation channels (P2x purinoreceptors). *Mol Pharmacol* 48: 178–183.
39. Hibell AD, Kidd EJ, Chessell IP, Humphrey PP, Michel AD (2000) Apparent species differences in the kinetic properties of P2X(7) receptors. *Br J Pharmacol* 130: 167–173.
40. Chessell IP, Michel AD, Humphrey PP (1998) Effects of antagonists at the human recombinant P2X7 receptor. *Br J Pharmacol* 124: 1314–1320.
41. Hibell AD, Thompson KM, Xing M, Humphrey PP, Michel AD (2001) Complexities of measuring antagonist potency at P2X(7) receptor orthologs. *J Pharmacol Exp Ther* 296: 947–957.
42. Donnelly-Roberts DL, Jarvis MF (2007) Discovery of P2X7 receptor-selective antagonists offers new insights into P2X7 receptor function and indicates a role in chronic pain states. *Br J Pharmacol* 151: 571–579.
43. Burnstock G, Williams M (2000) P2 purinergic receptors: modulation of cell function and therapeutic potential. *J Pharmacol Exp Ther* 295: 862–869.
44. Di Virgilio F, Ferrari D, Adinolfi E (2009) P2X7: a growth-promoting receptor-implications for cancer. *Purinergic Signal* 5: 251–256.
45. Tsao HK, Chiu PH, Sun SH (2013) PKC-dependent ERK phosphorylation is essential for P2X7 receptor-mediated neuronal differentiation of neural progenitor cells. *Cell Death Dis* 4: e751.
46. Wu PY, Lin YC, Chang CL, Lu HT, Chin CH, et al. (2009) Functional decreases in P2X7 receptors are associated with retinoic acid-induced neuronal differentiation of Neuro-2a neuroblastoma cells. *Cell Signal* 21: 881–891.
47. Orellano EA, Rivera OJ, Chevres M, Chorna NE, Gonzalez FA (2010) Inhibition of neuronal cell death after retinoic acid-induced down-regulation of P2X7 nucleotide receptor expression. *Mol Cell Biochem* 337: 83–99.
48. Burdon T, Smith A, Savatier P (2002) Signalling, cell cycle and pluripotency in embryonic stem cells. *Trends Cell Biol* 12: 432–438.
49. Lemoli RM, Ferrari D, Fogli M, Rossi L, Pizzirani C, et al. (2004) Extracellular nucleotides are potent stimulators of human hematopoietic stem cells in vitro and in vivo. *Blood* 104: 1662–1670.
50. Bianco F, Ceruti S, Colombo A, Fumagalli M, Ferrari D, et al. (2006) A role for P2X7 in microglial proliferation. *J Neurochem* 99: 745–758.
51. Adinolfi E, Raffaghello L, Giuliani AL, Cavazzini L, Capece M, et al. (2012) Expression of P2X7 receptor increases in vivo tumor growth. *Cancer Res* 72: 2957–2969.
52. Kapur N, Mignery GA, Banach K (2007) Cell cycle-dependent calcium oscillations in mouse embryonic stem cells. *Am J Physiol Cell Physiol* 292: C1510–1518.
53. Savatier P, Huang S, Szekely L, Wiman KG, Samarut J (1994) Contrasting patterns of retinoblastoma protein expression in mouse embryonic stem cells and embryonic fibroblasts. *Oncogene* 9: 809–818.
54. Savatier P, Lapillonne H, Jirmanova L, Vitelli L, Samarut J (2002) Analysis of the cell cycle in mouse embryonic stem cells. *Methods Mol Biol* 185: 27–33.
55. Orford KW, Scadden DT (2008) Deconstructing stem cell self-renewal: genetic insights into cell-cycle regulation. *Nat Rev Genet* 9: 115–128.
56. Zhu D, Qu L, Zhang X, Lou Y (2005) Icarin-mediated modulation of cell cycle and p53 during cardiomyocyte differentiation in embryonic stem cells. *Eur J Pharmacol* 514: 99–110.
57. Yuahasi KK, Demasi MA, Tamajusku AS, Lenz G, Sogayar MC, et al. (2012) Regulation of neurogenesis and gliogenesis of retinoic acid-induced P19 embryonal carcinoma cells by P2X2 and P2X7 receptors studied by RNA interference. *Int J Dev Neurosci* 30: 91–97.
58. Capela A, Temple S (2002) LeX/ssea-1 is expressed by adult mouse CNS stem cells, identifying them as nonpendymal. *Neuron* 35: 865–875.
59. Capela A, Temple S (2006) LeX is expressed by principle progenitor cells in the embryonic nervous system, is secreted into their environment and binds Wnt-1. *Dev Biol* 291: 300–313.
60. Francis F, Koulaokoff A, Boucher D, Chafey P, Schaar B, et al. (1999) Doublecortin is a developmentally regulated, microtubule-associated protein expressed in migrating and differentiating neurons. *Neuron* 23: 247–256.
61. Kerr MA, Stocks SC (1992) The role of CD15-(Le(X))-related carbohydrates in neutrophil adhesion. *Histochem J* 24: 811–826.
62. Uchida N, Buck DW, He D, Reitsma MJ, Masesk M, et al. (2000) Direct isolation of human central nervous system stem cells. *Proc Natl Acad Sci U S A* 97: 14720–14725.
63. Allendoerfer KL, Durairaj A, Matthews GA, Patterson PH (1999) Morphological domains of Lewis-X/FORSE-1 immunolabeling in the embryonic neural tube are due to developmental regulation of cell surface carbohydrate expression. *Dev Biol* 211: 208–219.
64. Pruszak J, Ludwig W, Blak A, Alavian K, Isacson O (2009) CD15, CD24, and CD29 define a surface biomarker code for neural lineage differentiation of stem cells. *Stem Cells* 27: 2928–2940.
65. Menezes JR, Luskin MB (1994) Expression of neuron-specific tubulin defines a novel population in the proliferative layers of the developing telencephalon. *J Neurosci* 14: 5399–5416.
66. Memberg SP, Hall AK (1995) Dividing neuron precursors express neuron-specific tubulin. *J Neurobiol* 27: 26–43.
67. Hynes RO, Patel R, Miller RH (1986) Migration of neuroblasts along preexisting axonal tracts during prenatal cerebellar development. *J Neurosci* 6: 867–876.
68. Doe CQ (2008) Neural stem cells: balancing self-renewal with differentiation. *Development* 135: 1575–1587.

Neuronal adhesion, proliferation and differentiation of embryonic stem cells on hybrid scaffolds made of xanthan and magnetite nanoparticles

This content has been downloaded from IOPscience. Please scroll down to see the full text.

2015 Biomed. Mater. 10 045002

(<http://iopscience.iop.org/1748-605X/10/4/045002>)

[View the table of contents for this issue](#), or go to the [journal homepage](#) for more

Download details:

IP Address: 143.107.52.210

This content was downloaded on 13/10/2015 at 15:51

Please note that [terms and conditions apply](#).

Biomedical Materials



PAPER

RECEIVED
1 December 2014

REVISED
13 April 2015

ACCEPTED FOR PUBLICATION
19 May 2015

PUBLISHED
8 July 2015

Neuronal adhesion, proliferation and differentiation of embryonic stem cells on hybrid scaffolds made of xanthan and magnetite nanoparticles

Talita Glaser¹, Vânia B Bueno², Daniel R Cornejo³, Denise F S Petri² and Henning Ulrich¹

¹ Departamento de Bioquímica, Instituto de Química, Universidade de São Paulo, Av. Prof. Lineu Prestes 748, 05508-000, São Paulo, SP, Brazil

² Departamento de Química Fundamental, Instituto de Química, Universidade de São Paulo, Av. Prof. Lineu Prestes 748, 05508-000, São Paulo, SP, Brazil

³ Instituto de Física, Universidade de São Paulo, São Paulo, Brazil

E-mail: dfsp@iq.usp.br, dfsp@usp.br and henning@iq.usp.br

Keywords: stem cells, scaffolds, magnetic nanostructures

Supplementary material for this article is available [online](#)

Abstract

Hybrid scaffolds made of xanthan and magnetite nanoparticles (XCA/mag) were prepared by dipping xanthan membranes (XCA) into dispersions of magnetic nanoparticles for different periods of time. The resulting hybrid scaffolds presented magnetization values ranging from 0.25 emu g^{-1} to 1.80 emu g^{-1} at 70 kOe and corresponding iron contents ranging from 0.25% to 2.3%, respectively. They were applied as matrices for *in vitro* embryoid body adhesion and neuronal differentiation of embryonic stem cells; for comparison, neat XCA and commercial plastic plates were also used. Adhesion rates were more pronounced when cells were seeded on XCA/mag than on neat XCA or plastic dishes; however, proliferation levels were independent from those of the scaffold type. Embryonic stem cells showed similar differentiation rates on XCA/mag scaffolds with magnetization of 0.25 and 0.60 emu g^{-1} , but did not survive on scaffolds with 1.80 emu g^{-1} . Differentiation rates, expressed as the number of neurons obtained on the chosen scaffolds, were the largest on neat XCA, which has a high density of negative charge, and were smallest on the commercial plastic dishes. The local magnetic field inherent of magnetite particles present on the surface of XCA/mag facilitates synapse formation, because synaptophysin expression and electrical transmission were increased when compared to the other scaffolds used. We conclude that XCA/mag and XCA hydrogels are scaffolds with distinguishable performance for adhesion and differentiation of ESCs into neurons.

1. Introduction

Neurodegenerative diseases affect at least 1% of people worldwide and cause general disabilities and high costs to the health system [1]. Stem cell therapies for recovery of neuronal loss is a promising strategy due to these cells having the capabilities of self-renew and differentiation into specialized tissue types. Clinical studies using stem cells and fetal mesencephalic tissue in Parkinson's disease are currently in progress [2–6]. The results of some of these studies showed that stem cells can graft into the brain, become functionally integrated, and promote regeneration. In this regard, mouse embryonic stem cells (ESC) revealed the best results for re-innervation and restoration of dopamine release. Nevertheless, dysfunctional grafts

led to dyskinesia after transplantation. For a hypoxia-ischemia model [7], which is a common cause of neurological disability in adults and children, even the most capable cells needed intrinsic organization and a scaffold to guide restructuring. In view of that, successful cell replacement therapy must fulfill some requirements, such as that neuronal-differentiated cells must reveal similar phenotypes, including molecular, morphological, and electrophysiological characteristics, and axonal growth must be specified from grafts to correct sites in the brain or spinal cord.

Artificial scaffolds produced by combining materials chemistry, elasticity, and topology might stimulate cell proliferation and differentiation for regenerative applications [8]. Polymeric scaffolds are potential candidates for meeting these requirements. The first

report on scaffolds for stem cells during spinal cord repair described the use of a blend composed of poly(lactic-co-glycolic acid) (PLGA) and a block copolymer of poly(lactic-co-glycolic acid)-polylysine; the advantage of PLGA is its fast (up to 60 d) degradation [9]. Neural stem cells plated on poly(glycolic acid) scaffolds were implanted around the brain infarction cavity with the result being that grafted cells were attached, impregnated, and migrated throughout this polymer, partially recovering the brain from injury [7]. Electrospun fibrous polyurethane scaffolds were successfully applied for the *in vitro* differentiation of human ESC [10]. The presence of magnetic nanoparticles in polymeric matrices particularly stimulates cell proliferation [11]. For instance, polycaprolactone scaffolds containing magnetic nanoparticles induced more active osteogenic differentiation and improved cellular mineralization in comparison to pure caprolactone [12]. Bone repair and regeneration were achieved with scaffolds composed of hydroxyapatite, collagen, and magnetic nanoparticles [13]. Myoblast cells labeled with magnetic nanoparticles, used as the basis for artificial tissue construction, formed multi-layered cell sheets in the presence of an external magnetic field [14].

In the present work, xanthan gum based scaffolds were prepared to be applied as supports for *in vitro* adhesion and neuronal differentiation of ESC. Xanthan gum was chosen because it is a biodegradable and biocompatible polysaccharide approved by the FDA (Fed. Reg. 345376) [15]. Xanthan chains can form chemical networks by reacting with citric acid, an efficient nontoxic crosslinker for polysaccharides [16–18]. Hybrid scaffolds of xanthan and nanohydroxyapatite or its equivalent strontium substituted were suitable for osteoblast growth and induced high alkaline phosphatase activity [19]. Dipping the xanthan networks for 10 seconds in an aqueous dispersion of magnetite (Fe_3O_4) nanoparticles led to hybrid scaffolds with magnetization of 0.02 emu g^{-1} at 1000 Oe and iron content of $0.4 \pm 0.1 \text{ wt\%}$, which served as outstanding scaffolds for fibroblasts proliferation [20]. In the present study hybrid scaffolds made of xanthan and magnetite nanoparticles (XCA/mag) were prepared with different magnetization values by dipping the xanthan membranes for different periods of time into the aqueous ferrofluid. XCA/mag scaffolds, neat xanthan scaffolds (XCA), and commercial plastic dishes were used for *in vitro* neuronal differentiation of ESC. ESC that previously differentiated into neural precursor cells underwent neuronal differentiation such as those observed under standard *in vitro* conditions. Only XCA/mag scaffolds with iron content lower than 1 wt% were used because scaffolds with higher amounts of iron were toxic. Cells attached better to XCA/mag than to neat XCA. Moreover, cells differentiated on XCA/mag showed increased membrane potential amplitudes on depolarization with KCl, indicating successful synapse formation.

2. Materials and methods

2.1. Scaffolds preparation and characterization

The synthesis of magnetite is described in detail elsewhere [20]. $\text{FeCl}_3 \cdot 6\text{H}_2\text{O}$ and $\text{FeCl}_2 \cdot 4\text{H}_2\text{O}$ (both from Labsynth, Diadema, Brazil) at 0.1 mol l^{-1} and 0.05 mol l^{-1} , respectively, were vigorously mixed in an IKA Vortex mixer Genius 3 (IKA Werke GmbH & Co., Staufen, Germany). NH_4OH (25 % V/V) was added to the system under stirring until the solution achieved pH 9. Nitrogen gas was bubbled directly into the media prior to reaction for removal of oxygen. Then, the system was placed in a water bath at $(24 \pm 1)^\circ\text{C}$, in which the sonotrode MS7 with acoustic power density of 130 W cm^{-2} coupled to the ultrasonic processor Hielscher UP100H (Hielscher Ultrasonics GmbH, Teltow, Germany) was immersed. The sonotrode was kept outside of the reaction flask to avoid contamination by Ti particles stemming from the device. The sonotrode operated for 10 min. The temperature inside and outside of the reaction flask remained at $24 \pm 1^\circ\text{C}$. Prior to use, the dispersion containing the magnetite (Fe_3O_4) particles was neutralized. Magnetic particles were separated by centrifugation at 1200g during 10 min. They were re-dispersed in MilliQ water and again separated. This rinsing process was repeated three times to remove the excess of reactants. One should note that no stabilizer was added to the magnetic nanoparticles dispersions. The concentration of magnetite in the dispersion was determined by gravimetric analyses as $48 \pm 2 \text{ g l}^{-1}$. The magnetic nanoparticles presented an isoelectric point of 6.5 ± 0.1 and the nearly superparamagnetic behavior at room temperature, with coercivities less than 20 Oe in all samples [20].

Xanthan gum ($M_v \sim 10^6 \text{ gmol}^{-1}$, degree of pyruvyl = 0.38, degree of acetyl = 0.41; CP Kelco, Atlanta, GA) was dissolved in water at 6 g l^{-1} in the presence of citric acid at 0.3 g l^{-1} . The solutions were homogenized with an Ika Turrax® (IKA Werke GmbH & Co., Staufen, Germany) stirrer at 18 000 rpm for 3 min and submitted to centrifugation for 5 min at 1014g to remove air bubbles prior to casting. The solution of xanthan and citric acid was cast into plastic molds and allowed to dry in an oven at 45°C overnight to form films. Crosslinking was achieved by heating the dried films at 165°C for 7 min. The resulting xanthan networks were swollen in water at 70°C for 24 h to remove sol fraction and dried at 45°C for 24 h. More details about the crosslinking reactions can be found elsewhere [17]. The resulting cross-linked xanthan films were $80 \pm 5 \mu\text{m}$ thick, stable in the pH range of 2 to 9, and after swelling in water (under equilibrium conditions) their mass increased up to 27 times compared to its original dried mass [17]. The xanthan films were immersed in the magnetic nanoparticle dispersions at pH 6 and $24 \pm 1^\circ\text{C}$ during 10 s, 1 min, 5 min, 1 h, or 24 h. At this pH, the magnetic particles are positively charged [20]. After that, the films were removed and rinsed in MilliQ water for 20 s.

This process was repeated three times more to remove particles weakly attached to polymeric matrix. Details about hybrid scaffold preparation can be seen in the movie at www.youtube.com/watch?v=PhTn2M_NRF8&index=2&list=UUqVKEBUzLfsAoMIzF8r9VTA. The xanthan films impregnated with magnetic nanoparticles were gently dried with paper tissues, freeze-dried for inductively coupled plasma atomic emission spectroscopy (ICP-AES) analyses, or dried in the oven overnight at $50 \pm 1^\circ\text{C}$ for analyses with superconducting quantum interference device (SQUID) magnetometer (model MPMS; Quantum Design, USA; details are in online supplementary information SI1; stacks.iop.org/BMM/10/045002/mmedia). ICP-AES analyses performed with Spectro Smart Analyzer Vision equipment (SPECTRO Analytical Instruments GmbH, Germany) yielded the amount of iron in the magnetite-impregnated XCA films. Freeze-dried XCA networks were analyzed (after gold coating by sputtering) by scanning electron microscopy (SEM) in a Jeol microscope FEG7401F equipped with a field-emission gun. The hybrid XCA/mag scaffolds were analyzed by FEI Inspect F50 high resolution SEM. Samples were prepared by tearing small pieces of composite films already used in the magnetization measurements. The samples moved toward the electromagnetic lens during the analyses; for this reason, the small slivers must be sandwiched within oyster TEM grids to avoid sample movement. Scanning electron images were then acquired without any coating in transmission (STEM) at the edges of the film's lower surface. More details about the experimental procedure can be found elsewhere [20].

Controls incorporating non-magnetic nanoparticles in the XCA scaffolds were included to evaluate the effects mediated by the magnetic nanoparticles. The controls, coded as XCA/HA, were XCA scaffolds with hydroxyapatite particles at 10 wt%. The preparation and characterization of this type of scaffolds are described elsewhere [19].

2.2. Cell culture and differentiation of E14Tg2A mouse embryonic stem cell

The feeder cell-independent E14Tg2A embryonic stem [21] was kindly provided by Dr Deborah Schechtman, Institute of Chemistry, University of São Paulo, Brazil. Undifferentiated cells were cultured as described by Fornazari and coworkers [22]. For neuronal differentiation, 5×10^6 cells were cultured in $90 \text{ mm} \times 15 \text{ mm}$ non-adherent plates in DMEM supplemented with 20% FBS, 1% non-essential amino acids, and 0.1 mM β -mercaptoethanol for 48 h to induce embryoid body formation. Following substitution of the culture medium, cells were maintained in suspension for another 4 d in the presence of $5 \mu\text{M}$ retinoic acid. Embryoid bodies were seeded in 125 mm adherent cell culture flasks with tissue advanced treatment (Greiner Bio One, Frickenhausen, Germany) and grown for another 4 or 12 d in DMEM/F12 medium supplemented with 1% Bottenstein's N-2 formulation

(Life Technologies, USA) and b-FGF 100 ng ml⁻¹ (Sigma-Aldrich, USA). The procedure is schematically depicted in online supplementary information SI2 (stacks.iop.org/BMM/10/045002/mmedia).

2.3. Embryoid body adhesion assay

To evaluate the effects of the different scaffolds on the cell adhesion, 50 embryoid bodies (EBs) on the day of differentiation were seeded on the scaffolds in 35 mm dishes for each experiment performed in duplicate. Following 24 h of seeding, EBs were collected in the presence of PBS containing 5 mM EDTA and then resuspended in 1 ml of Dulbecco's phosphate buffered saline (DPBS) solution. EB quantities were determined with a Neubauer chamber (0.100 mm depth, 0.0025 mm² area) on an inverted microscope (Axiovert 200; Zeiss, Aalen, Germany). Images were produced with a Nikon DMX1200F camera, equipped to the microscope, and further processed with the Image J image analysis program. To evaluate the effect of the external magnetic field (EMF) on cell adhesion and proliferation, neodymium magnet (0.4 T) arrays were placed under the culture plates containing the scaffolds (see online supplementary information SI3; stacks.iop.org/BMM/10/045002/mmedia).

2.4. Cell viability assay

To evaluate the effects of the different types of scaffolds on the cell viability, 50 EBs were seeded on the scaffolds in 35 mm dishes for each experiment performed in duplicate. Following 24 h of seeding, EBs were collected in the presence of PBS containing 5 mM EDTA and then resuspended in 1 ml of DPBS solution. An aliquot of 10 μl was mixed with 0.08% Trypan Blue dye solution and cell quantities were determined with a Neubauer chamber (0.100 mm depth, 0.0025 mm² area) on an inverted microscope (Axiovert 200; Zeiss, Aalen, Germany). Stained and unstained cells represent dead and healthy cells, respectively; cell viability should be at least 95% for healthy log-phase cultures [23].

2.5. Determination of the progress of differentiation by flow cytometry analysis

Efficiencies of the differentiation progress were measured by flow cytometry population analysis of immunostaining against neuronal markers TUJ1 and MAP2, labeling young and mature neurons, respectively. For this purpose, cells were fixed for 30 min with a 4% paraformaldehyde solution, washed in PBS, and blocked in PBS supplemented with 2% fetal bovine serum and 0.1% Triton-X100. The cells were then exposed for 1 h to mouse anti-TUJ1 (Sigma-Aldrich, St. Louis, MO; 1 : 700 dilution) or rabbit anti-MAP2 (cell signaling, Danvers, MA; 1 : 500 dilution). The cells were incubated for 45 min with Alexa Fluor 488 anti-rabbit or Alexa Fluor 647 anti-mouse secondary antibodies (Life Technologies, Grand Island, NY; 1 : 1000 dilution, respectively). Cells that were not marked with the

primary antibodies were used as negative control and were used to set gates at FlowJo software (Flowjo LLC, USA). The percentage of marked cells was measured by using a flow cytometer (Attune, Life Technologies). Alexa Fluor 488 was excited by a 488 nm blue laser and its emission was captured through a 530/30 band pass filter. Alexa Fluor 555 was excited by a 488 nm blue laser and its emission was captured through a 574/26 band pass filter. Alexa Fluor 647 was excited by a 638 nm red laser and its emission was captured through a 660/20 band pass filter.

2.6. Microfluorimetric measurements of alterations in the membrane potential

Changes in membrane potential were determined by microfluorimetry using the FlexStation III (Molecular Devices Corp., Sunny Valley, CA), following the instructions of the manufacturer. Briefly, EBs collected on day 6 of differentiation were seeded in 96-well black microplates with clear bottoms at a concentration of 2 EBs/well in 100 µl of cell culture medium. Cells were incubated for 60 min and 37 °C with the FlexStation membrane potential Assay Kit (Molecular Devices Corp.) containing 2.5mM probenecid in a final volume of 200 µl per well. Fluorescence of samples was excited at 488 nm, and fluorescence emission was detected by the 540–590 nm Band Pass Emission FLIPR Filter. Samples were read at 1 s intervals for a period of 120 s. Following 30 s of monitoring basal fluorescence intensities were used as a measure of the membrane potential levels of resting cells. A depolarizing agent (KCl at 10–100mM concentrations) was added to the cells. Responses to agent addition were determined as peak fluorescence minus the basal intensity. Fluorescence intensity was analyzed using the SoftMax2Pro software (Molecular Devices Corp.). Data were expressed as mean values ± standard errors (S.E.).

2.7. Cell proliferation evaluation by flow cytometry analysis

Cell proliferation was measured following fixation with ice-cold 75% ethanol for 10 min, washing with PBS, and blocking with 2% fetal bovine serum 0.1% Triton-X solution in PBS for 30 min. After washing with PBS, cells were incubated for 1 h with rabbit anti-Ki67 antibody (Billerica, MA; 1:500 dilution), which is a marker for proliferating cells. Alexa Fluor 488 secondary antibody (Life Technologies) was used at 1:1000 dilution. Alexa Fluor 488 was excited by a 488 nm blue laser and emission was captured through a 530/30 nm filter.

2.8. Immunofluorescence staining assay

To analyze neuron morphology during the differentiation progress, we immunolabeled the cells with neuronal markers as TUJ1 (young neurons) and performed fluorescence microscopy. For this purpose, the cells were grown and induced to differentiate on rounded coverslips (1 cm diameter) and were fixed with

a 4% paraformaldehyde solution for 30 min, washed in PBS, and blocked with 5% fetal bovine serum 0.1% Triton-X solution in PBS for 30 min. The cells were then incubated in mouse anti-TUJ1 (Sigma Aldrich, USA; 1:1000 dilution) or mouse anti-Synaptophysin (Axill, Bethesda, MD; 1:50 dilution), or rabbit anti-ISL1 (GeneTex, Irvine, CA; 1:200 dilution) or rabbit anti-Pax6 (GeneTex; 1:200 dilution) antibodies for 18 h. The cells were incubated for 45 min with the Alexa Fluor 488 anti-mouse secondary antibody (Life Technologies; 1:1000 dilution). Cells that were not marked with the primary antibodies were used as negative control. Cell nuclei were stained with 0.1% of 4',6-diamidino-2-phenylindole (DAPI), and then the slides were mounted with Vectashield (Vector Laboratories, Burlingame, CA) and examined on an Axiovert 200 epifluorescence microscope (Zeiss) equipped with a Nikon DMX1200F camera and Metamorph image analysis program. Alexa Fluor 488 was excited by a 488 nm blue light and its emission was captured through a 530/30 band pass filter.

2.9. Statistical analysis

Comparisons between experimental data were performed using one-way analysis of variance following the Bonferroni *post hoc* test using GraphPad Prism 5.0 software (GraphPad Software, La Jolla, CA). Criteria for statistical significance were set at $p < 0.05$ (*), $p < 0.01$ (**), or $p < 0.001$ (***)�.

3. Results and discussion

XCA/mag scaffolds were prepared by immersing XCA films into an aqueous dispersion of magnetic nanoparticles for 10 s, 1 min, 5 min, 1 h, or 24 h. The magnetization (σ) and the content of iron in the resulting materials increased exponentially with the immersion time, as presented in figures 1(A) and (B), respectively. XCA/mag with magnetizations of 0.25 emu g^{-1} (10 s), 0.6 emu g^{-1} (1 h = 3600 s), and 1.8 emu g^{-1} (24 h = 86 400 s), coded as XCA/mag10S, XCA/mag1H, and XCA/mag24H, respectively, were chosen as scaffolds to evaluate the effects of magnetization on the progress of proliferation and neuronal differentiation. As control experiments, neat XCA (0 emu g^{-1}) and commercial plastic dishes were also tested. At room temperature (300 K) the coercivity determined for all samples was on the order of 16 Oe (inset figure 1(A)); such a low value is characteristic of superparamagnetic particles. The iron content increased with immersion time of XCA into magnetite nanoparticle dispersions (figure 1(B)) and the films became browner, corroborating with the magnetization increased observed in figure 1(A). XCA networks presented micrometric pores, and the mean diameter of magnetic particles ranged from 6 nm to 17 nm (online supplementary information SI4; [stacks.iop.org/BMM/10/045002/mmedia](http://iop.org/BMM/10/045002/mmedia)). Most particles were observed on the network uppermost layers. Although the pores are large enough for the diffusion of

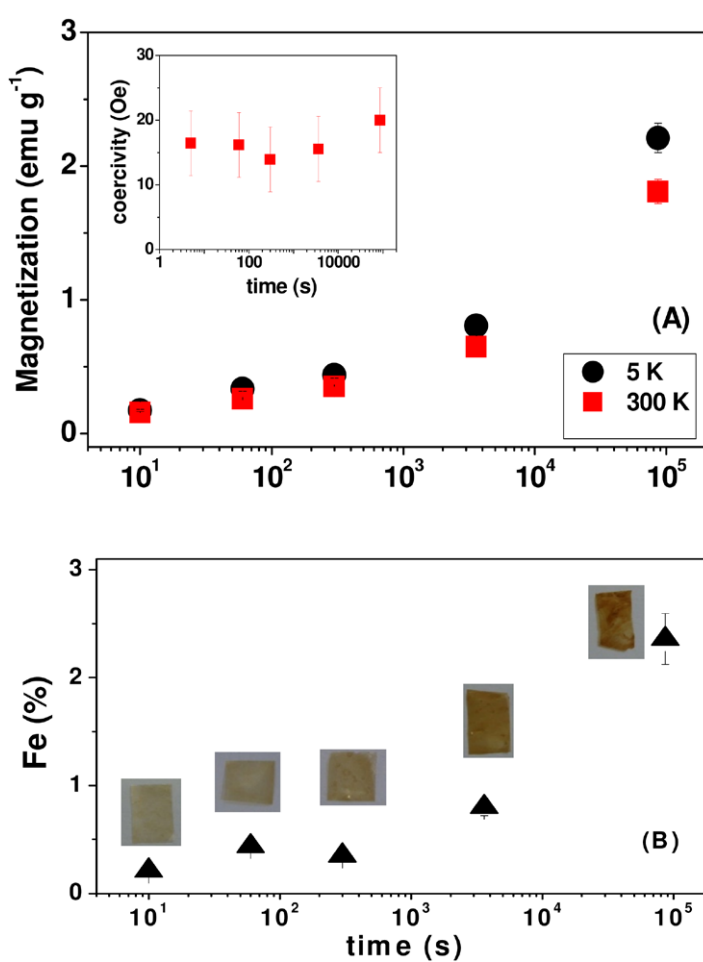


Figure 1. (A) Magnetization recorded at 5 K (black circles) and 300 K (red squares) with maximum magnetic field of 70 kOe and coercivity measured at 300 K (inset, black triangles) and (B) iron content determined by ICP-AES analyses and photographs taken for XCA/mag samples prepared by immersing XCA films into magnetite dispersion for different periods of time.

nanoparticles to the network interior, the electrostatic attraction between xanthan chain carboxylate groups and positively charged patches on magnetic particles might have driven the particles adsorption just after the first contact with the network surface (online supplementary information SI4; stacks.iop.org/BMM/10/045002/mmedia). Moreover, the chance to diffuse to the deeper layers was small because of the short period of contact.

Scaffolds for cell therapy must show good adherence to cells. In view of this, first the cell adhesion onto bare XCA and XCA/mag films was evaluated. For cell adhesion experiments embryonic stem cells (ESC) were pre-differentiated into neural precursor cells by embryoid body suspension culture, as described elsewhere [24], and then seeded for comparison of adhesion rates onto XCA, XCA/mag scaffolds, and commercial plastic dishes. XCA/mag24H scaffolds with 2.3 wt% Fe and magnetization of 1.8 emu g^{-1} were not suitable for neural cell culture because most cells died after 2 d. The cytotoxicity of superparamagnetic particles depends not only on the concentration but also on particle size, shape, and type of coating, and on the administrative route in the case of *in vivo* tests [25]. However, significant amounts of EBs adhered onto XCA/mag10S and

XCA/mag1H films with magnetizations of 0.25 emu g^{-1} and 0.6 emu g^{-1} at rates of 20-fold and 15-fold, respectively, which is larger than that observed for neat XCA or plastic dish controls, as presented in figures 2(A) and (B). Furthermore, using the XCA/mag scaffolds, more cells migrated from the EB (figures 2(A-III) and (A-IV)) to finally differentiate into neurons when compared to the further experimental conditions. For quantification of adhered cells 1 d after seeding, scaffolds were gently rinsed for removal of cells in suspension, followed by gentle detachment and counting of EBs (figure 2(B)). EBs showed significantly higher rates of attachment onto XCA/mag scaffolds (0.25 and 0.6 emu g^{-1}) than onto neat XCA or control plastic dishes. Similar effects were observed for the proliferation of fibroblasts [20]; fibroblast proliferation was larger on XCA/mag10S (0.25 emu g^{-1}) than on neat XCA.

In a previous work [20], an external static magnetic field (ESMF) of 0.4 T positioned beneath the culture plates increased the proliferation of fibroblasts plated on neat XCA or XCA/mag10S. Similarly, myogenic cell differentiation was stimulated by the presence of magnetic nanoparticles and external magnetic field [14]. To extend this effect to neurogenesis, EBs pre-differentiated for 6 d were seeded onto XCA/mag1H

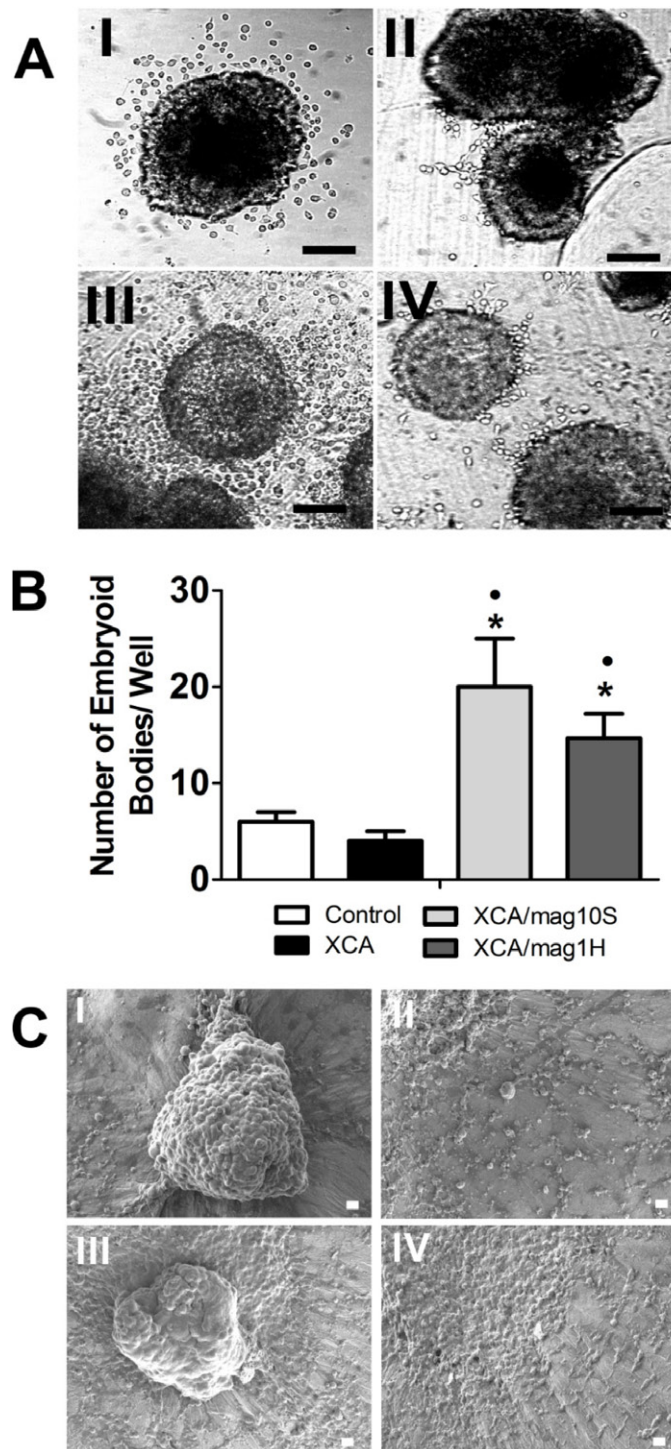


Figure 2. Cell adhesion and migration on xanthan based scaffolds during neural differentiation of ESC. (A) ESCs were induced to neural differentiation by embryoid body formation and all trans-retinoic acid application and then seeded onto commercial plastic dishes (I), neat XCA (II), XCA/mag10S (III), and XCA/mag1H (IV) scaffolds. (B) Counting of EBs attached to plastic dishes (control), neat XCA, XCA/mag10S, and XCA/mag1H. ANOVA following Bonferroni *post hoc* test * $p \leq 0.05$ compared to control. ● $p \leq 0.05$ compared to XCA. (C) Scanning electron microscopy for EBs differentiated for 14 d and seeded onto XCA/mag1H scaffolds. Cells cultured with ESMF of 0.4 T (I and II) and without ESMF (III and IV) onto XCA/mag1H. EB (I and III) and migrating cells (II and IV). Scale bar = 10 μ m.

scaffolds and cultured in the absence and in the presence of ESMF (0.4 T). SEM images obtained for cells cultivated onto XCA/mag1H scaffolds with (figures 2(C-I) and (C-II)) and without (figures 2(C-III) and (C-IV)) ESMF provided evidence for EB attachment onto XCA/mag1H and neural progenitor cell migration with a radial pattern. Thus, morphological dif-

ferences did not result from ESMF, and cell adhesion rates were also not affected by ESMF. Although various cell types, including fibroblasts [20], myoblasts [14], and osteoblasts [26], were affected by ESMF in their proliferation rates, neural cells were indifferent to ESMF stimulation. A possible explanation for this effect could be that the local electromagnetic field

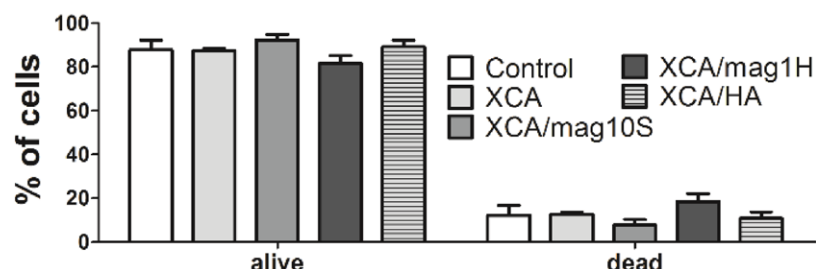


Figure 3. Cell viability of ESCs differentiated on tissue culture dishes (control), neat xanthan (XCA), XCA/mag10S, XCA/mag1H, and XCA/HA. XCA/HA refers to XCA scaffolds with hydroxyapatite particles at 10 wt%. Dissociated cells were stained with trypan blue dye for quantification of viability rates. Stained cells were dead and unstained were alive.

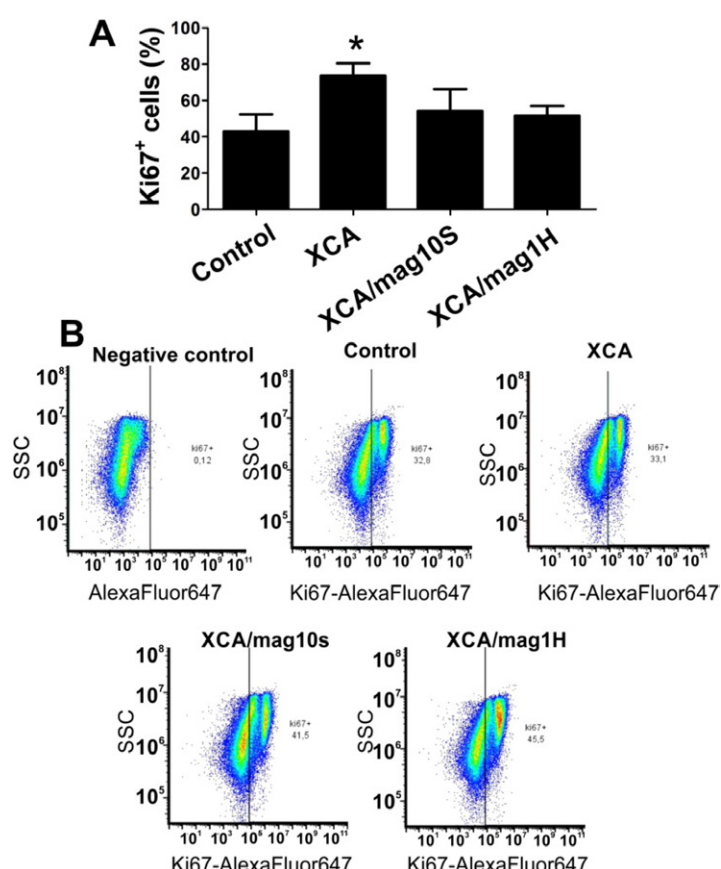


Figure 4. Cell proliferation during ESC neuronal differentiation on xanthan based scaffolds. EBs pre-differentiated for 14 d were seeded onto commercial plastic dishes. Following 14 d of culture, XCA scaffolds were immunostained for Ki67 expression and analyzed by flow cytometry as described in the methods section. Control (commercial plastic dish), neat XCA, XCA/mag10S, and XCA/mag1H. (A) Percentage of Ki67-positive immunostained cells. (B) Density plots showing gates and population distribution. Side-scattered light (SSC) and fluorescence intensity of Alexafluor 647 were analyzed. Small inserted graphs show the negative control used for setting gates.

inherent to the presence of magnetite nanoparticles was already enough to stimulate neural cell migration and differentiation.

Cell viability tests were performed for the different scaffolds. The data are presented in figure 3. They showed that none of the scaffolds tested was toxic for the cells. XCA/mag1H presented the highest cell death of approximately 19%. Elevations in cell death levels are expected as the dose of magnetic nanoparticles increases, mainly due to the release of iron ions, which can work as oxidative free radicals [27].

During the regeneration process, cells must be able to proliferate to recover the nervous system. The highest percentage of Ki67-positive cells, expressed during cell cycle progression, was observed for cells on neat XCA (figure 4). No statistically significant alterations were noted in percentages of Ki67-positive cells seeded onto control (commercial plastic dish), XCA/mag10S, and XCA/mag1H supports (figure 4), indicating that cells were still able to proliferate.

Neurogenesis of ESC might be detected by the occurrence of cells expressing neuronal marker

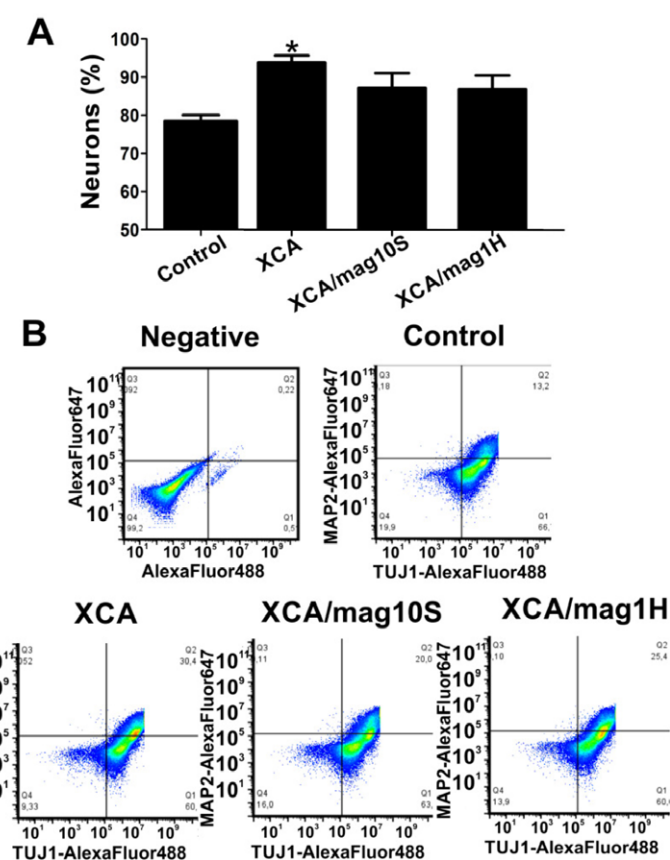


Figure 5. Neuronal differentiation efficiency. EBs differentiated for 14 d and seeded onto XCA scaffolds were immunostained for TUJ1 and MAP2, which are proteins expressed by young neurons and mature neurons, respectively, and further analyzed by flow cytometry as described in the methods section. (A) Percentage of all TUJ1- and MAP2-positive immunostained cells were summed and plotted. (B) Density plots showing gates and population distribution. Fluorescence intensities of Alexafluor 647 and Alexafluor 488 emissions were quantified. Experiments were performed as three independent experiments (* $p < 0.05$, versus control).

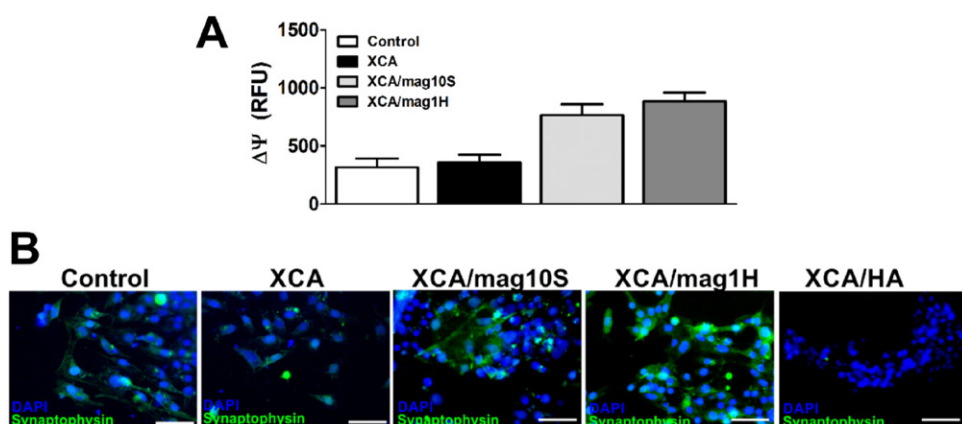


Figure 6. Neuronal differentiation of embryonic stem cells and macrostructure formation onto scaffolds. (A) For measurement of changes in membrane potential, EBs were seeded on black 96 well plates with clear bottoms with or without XCA scaffolds. Changes in the membrane potential were measured by microfluorimetry upon treatment with the depolarizing KCl. Control (commercial plastic dish), neat XCA, XCA/mag10S, and XCA/mag1H are described. (B) Fluorescence microscopy images of previously differentiated ESC onto tissue culture dish (control), neat xanthan (XCA), XCA/mag10S, XCA/mag1H, and XCA/HA immunostained for expression of synaptophysin, a synapse protein marker. Nuclei: DAPI (blue) and synaptophysin (green). Scale bar = 100 μ m.

proteins, including TUJ1 and MAP2. Figures 5(A) and (B) show that cells differentiated on neat XCA revealed a statistically significant increase in the percentage of neurons in comparison to XCA/mag10S

or XCA/mag1H or plastic dishes control, as judged by TUJ1 expression and MAP2 expression by flow cytometry, indicating that neat XCA scaffolds promote neuronal differentiation. Moreover, under KCl

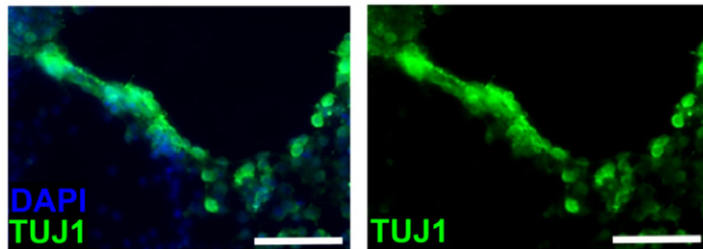


Figure 7. Neuronal differentiation of embryonic stem cells and macrostructure formation onto XCA/mag1H. Fluorescence microscopy images of previously differentiated ESC onto XCA/mag1H and immunostained for expression of TUJ1, marking neurons. There are some small neuron arrays similar to neural bundles. Nuclei: DAPI (blue) and TUJ1 (green). Scale bar = 100 μ m.

depolarization, alterations of the membrane potential were not different for cells plated onto the plastic dish or neat XCA (figure 6(A)), indicating that polymers do not affect the capability of neurons to form electrical synapses. Nevertheless, alterations of the membrane potential under KCl depolarization, measured as an increase in fluorescence of the lipid dye, doubled in comparison to neat XCA or plastic dish, when cells were seeded onto XCA/mag10S or XCA/mag1H scaffolds, indicating that the presence of magnetic nanoparticles in the scaffolds gave rise to neurons with higher responsiveness to electrical stimuli and supposedly increased synaptogenesis (figure 6(B)), as confirmed by immunostaining against the synapse-specific synaptophysin.

Immunofluorescence assay allowed to observe the formation of some macrostructures composed of neurons differentiated from cells seeded onto XCA/mag1H scaffolds (figure 7). These structures may resemble neuron bundles, suggesting that this scaffold is potentially interesting for the comprehension of nerve growth and differentiation.

Moreover, the scaffolds enabled cells to differentiate to both motor and sensory neurons, as seen by the immunostaining of ISL1, a transcription factor related to motor neuron differentiation (figure 8(A)), and Pax6, a transcription factor related to motor neuron differentiation (figure 8(B)). Fluorescence intensities of nuclear ISL1 and Pax6 were quantified and normalized using DNA staining intensity (figures 8(C) and (D)). The results clearly indicate that XCA/mag1H facilitated the ESC differentiation into sensory neurons, because Pax6 expression was increased in this condition.

The physical chemical properties of scaffolds, such as porosity, elasticity, hydrophilicity, and roughness, play an important role in the cell response. The main difference between XCA/mag and XCA/HA scaffolds is that the former has magnetic properties and the latter is diamagnetic. XCA/HA scaffolds were already successfully used as scaffolds for osteoblasts proliferation; however, the results in online supplementary material figure SI5 (stacks.iop.org/BMM/10/045002/mmedia) show that they are suitable for glial differentiation.

However, the effects of XCA/mag scaffolds during differentiation were specific for neuronal phenotypes because the proportion of neural precursor cells and glia cells were not affected.

Magnetite and maghemite nanoparticles are naturally present in human brain tissue [28, 29]. Their formation involves the ferritin protein complex, which is responsible for the storage and release of iron. Ferritin can oxidize Fe(II) to Fe(III) as ferrihydrite ($5\text{Fe}_2\text{O}_3 \cdot 9\text{H}_2\text{O}$), which is stored in the protein core. When it is overloaded, the protein loses its oxidative function and this situation might favor the formation of biogenic magnetite [28]. In brains with neurodegenerative disorders, biogenic magnetite particles were found in larger concentrations than in normal brains. Recently, Dadras and coworkers [30] observed conformational changes of tubulin, a precursor of microtubules, in the presence of large amounts of magnetite. The authors of this article proposed that the local magnetic field inherent of magnetite particles affects axonal microtubules, generating electromagnetic fields by the movement of electrons along the axons in normal brain function. Such induction of electron current along microtubules would be disrupted in the presence of a large amount of magnetite and the transport of axonal neurotransmitters affected, causing neuronal disorders [30]. Corroborating our data, an excess of magnetite can lead to cell disorders (death, malfunction), whereas lower concentrations present benefits to neural cell function.

In the present work neat XCA and XCA/mag loaded with less than 1 wt% iron were used successfully as scaffolds for neuronal cell adhesion, proliferation, and differentiation. The main results can be summarized as follows.

- Cells responded similarly to scaffolds with magnetization of 0.25 and 0.60 emu g⁻¹.
- The amounts of EBs adhered to XCA/mag10S and XCA/mag1H films were larger than those observed for neat XCA or plastic dish controls.
- Cells proliferated on XCA, XCA/mag, and commercial plastic dishes in a similar way.

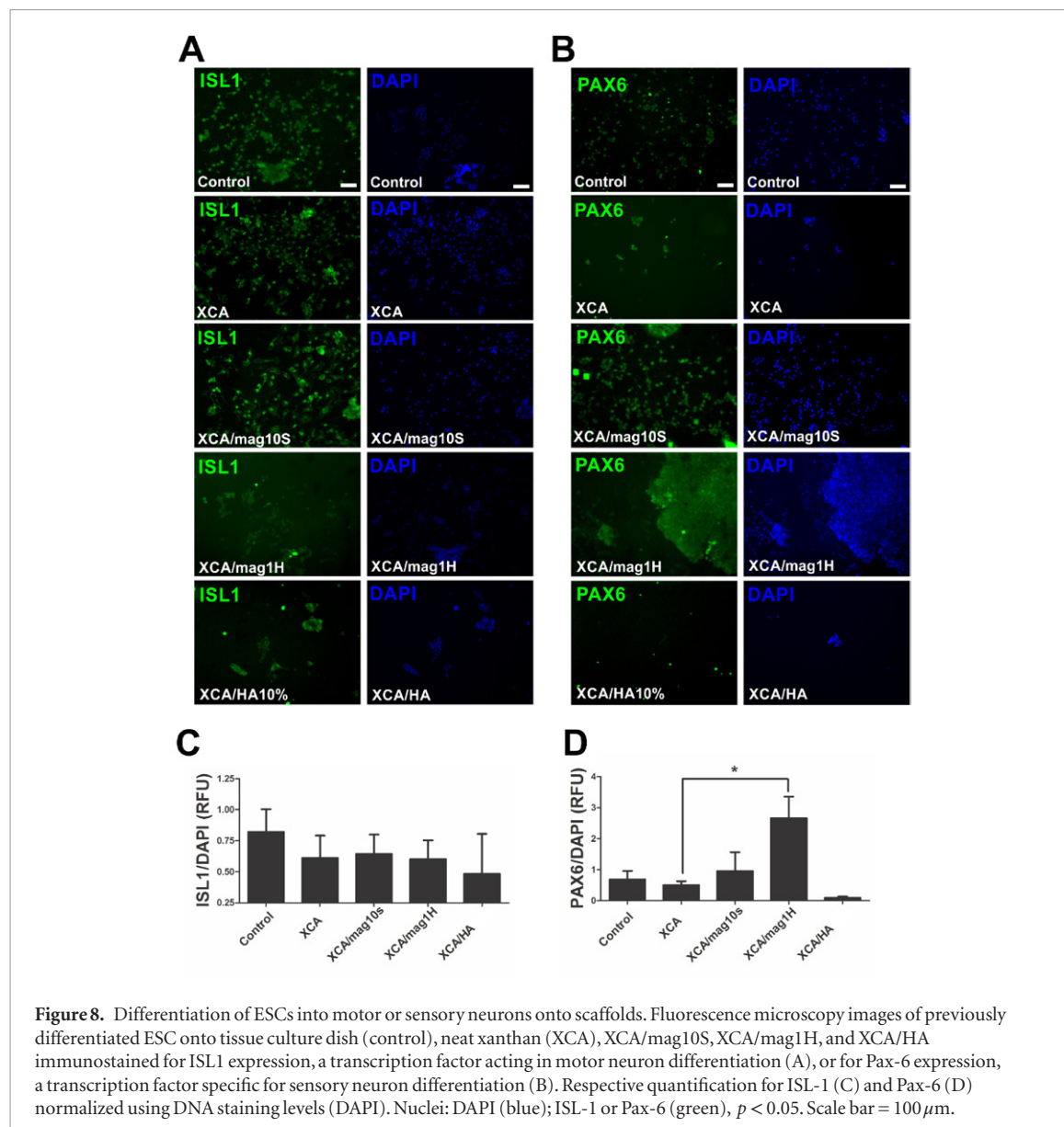


Figure 8. Differentiation of ESCs into motor or sensory neurons onto scaffolds. Fluorescence microscopy images of previously differentiated ESC onto tissue culture dish (control), neat xanthan (XCA), XCA/mag10S, XCA/mag1H, and XCA/HA immunostained for ISL1 expression, a transcription factor acting in motor neuron differentiation (A), or for Pax-6 expression, a transcription factor specific for sensory neuron differentiation (B). Respective quantification for ISL-1 (C) and Pax-6 (D) normalized using DNA staining levels (DAPI). Nuclei: DAPI (blue); ISL-1 or Pax-6 (green), $p < 0.05$. Scale bar = 100 μ m.

- The differentiation was expressed as the number of neurons grown on the scaffolds. The largest amount of neurons was observed on neat XCA and the smallest amount was observed on the commercial plastic dishes. XCA is a hydrogel with a high density of negative charge [18], which provides an electrical field for adequate differentiation.
- Neurons grown onto XCA/mag scaffolds responded better to electrical stimuli. Electrons of the local magnetic field, inherent of magnetic particles, are suggested to contribute to ion translocation along the plasma membranes of axonal microtubules.

4. Conclusions

XCA and XCA/mag scaffolds are easy to prepare, biocompatible, and of low cost. In comparison to commercial plastic dishes, these scaffolds offer a suitable environment for *in vitro* neuronal cell attachment, proliferation, and differentiation. The combination of highly charged polymer network (XCA) and magnetite

nanoparticles creates local electromagnetic fields, which stimulate these processes. Ultimately, such scaffolds might also benefit the delivery of the agents to speed the neuronal tissue regeneration processes.

Acknowledgments

This work was supported by research grants from Brazilian funding agencies São Paulo Research Foundation (FAPESP) Grants 2010/13034-2, 2010/51219-5, and 2012/50880-4; National Council for Scientific and Technological Development (CNPq) Grants 305178/2013-0 and 404663/2012-5 and Rede Nanobiotec CAPES; and Provost's Office for Research of the University of São Paulo, Grant number: 2011.1.9333.1.3 (NAPNA-USP), Brazil.

References

- [1] de Lau L M and Breteler M M 2006 Epidemiology of Parkinson's disease *Lancet Neurol.* **5** 525–35

- [2] Dunnett S B and Rosser A E 2014 Challenges for taking primary and stem cells into clinical neurotransplantation trials for neurodegenerative disease *Neurobiol. Dis.* **61** 79–89
- [3] Lindvall O and Bjorklund A 2004 Cell therapy in Parkinson's disease *NeuroRx* **1** 382–93
- [4] Lindvall O, Kokaia Z and Martinez-Serrano A 2004 Stem cell therapy for human neurodegenerative disorders-how to make it work. *Nat. Med.* **10** (Suppl.) S42–50
- [5] Nery A A, Nascimento I C, Glaser T, Bassaneze V, Krieger J E and Ulrich H 2013 Human mesenchymal stem cells: from immunophenotyping by flow cytometry to clinical applications *Cytometry* **83A** 48–61
- [6] Oliveira S L, Pillat M M, Cheffer A, Lameu C, Schwindt T T and Ulrich H 2013 Functions of neurotrophins and growth factors in neurogenesis and brain repair *Cytometry* **83A** 76–89
- [7] Park K I, Teng Y D, Snyder E Y 2002 The injured brain interacts reciprocally with neural stem cells supported by scaffolds to reconstitute lost tissue *Nat. Biotechnol.* **20** 1111–17
- [8] Murphy W L, McDevitt T C and Engler A J 2014 Materials as stem cell regulators *Nat. Mater.* **13** 547–57
- [9] Teng Y D, Lavik E B, Qu X, Park K I, Ourednik J, Zurakowski D, Langer R, Snyder E Y 2002 Functional recovery following traumatic spinal cord injury mediated by a unique polymer scaffold seeded with neural stem cells *Proc. Natl Acad. Sci. USA* **99** 3024–9
- [10] Carlberg, B, Axell M Z, Nannmark U, Liu J and Kuhn H G 2009 Electrospun polyurethane scaffolds for proliferation and neuronal differentiation of human embryonic stem cells *Biomed. Mater.* **4** 045004
- [11] Sensemig R, Sapir Y, MacDonald C, Cohen S and Polyak B 2012 Magnetic nanoparticle-based approaches to locally target therapy and enhance tissue regeneration *in vivo* *Nanomedicine* **7** 1425–42
- [12] Kim J J, Singh R K, Seo S J, Kim T H, Kim J H, Lee E J and Kim H W 2014 Magnetic scaffolds of polycaprolactone with functionalized magnetite nanoparticles: physicochemical, mechanical, and biological properties effective for bone regeneration *RSC Adv.* **4** 17325–36
- [13] Bock N, Riminucci A, Dionigi C, Russo A, Tampieri A, Landi E, Goranov V A, Mrcacci M and Dediu V 2010 A novel route in bone tissue engineering: magnetic biomimetic scaffolds *Acta Biomater.* **6** 786–96
- [14] Yamamoto Y, Ito A, Kato M, Kawabe Y, Shimizu K, Fujita H, Nagamori E and Kamihira M 2009 Preparation of artificial skeletal muscle tissues by a magnetic force-based tissue engineering technique *J. Biosci. Bioeng.* **108** 538–43
- [15] Petri D F S 2015 Xanthan gum: a versatile biopolymer for biomedical and technological applications *J. Appl. Polym. Sci.* **132** 42035
- [16] Reddy N and Yang Y Q 2010 Citric acid cross-linking of starch films *Food Chem.* **118** 702–11
- [17] Bueno V B, Bentini R, Catalani L H and Petri D F 2013 Synthesis and swelling behavior of xanthan-based hydrogels *Carbohydr. Polym.* **92** 1091–9
- [18] Bueno V B and Petri D F 2014 Xanthan hydrogel films: molecular conformation, charge density and protein carriers *Carbohydr. Polym.* **101** 897–904
- [19] Bueno V B, Bentini R, Catalani L H, Barbosa L R and Petri D F 2014 Synthesis and characterization of xanthan-hydroxyapatite nanocomposites for cellular uptake *Mater. Sci. Eng. C* **37** 195–203
- [20] Bueno V B, Silva A M, Barbosa L R, Catalani L H, Teixeira-Neto E, Cornejo D R and Petri D F S 2013 Hybrid composites of xanthan and magnetic nanoparticles for cellular uptake *Chem. Commun.* **49** 9911–13
- [21] Hooper M, Hardy K, Handyside A, Hunter S and Monk M 1987 HPRT-deficient (Lesch-Nyhan) mouse embryos derived from germline colonization by cultured cells *Nature* **326** 292–5
- [22] Fornazari M, Nascimento I C, Nery A A, da Silva C C, Kowaltowski A J and Ulrich H 2011 Neuronal differentiation involves a shift from glucose oxidation to fermentation *J. Bioenerg. Biomembr.* **43** 531–9
- [23] Strober W 2001 Trypan blue exclusion test of cell viability *Curr. Protoc. Immunol.* **21** A.3B.1–2
- [24] Glaser T, de Oliveira S L, Cheffer A, Beco R, Martins P, Fornazari M, Lameu C, Costa H M Jr, Coutinho-Silva R and Ulrich H 2014 Modulation of mouse embryonic stem cell proliferation and neural differentiation by the P2X7 receptor *PLoS One* **9** e96281
- [25] Lei L, Ling-Ling J, Yun Z and Gang L 2013 Toxicity of superparamagnetic iron oxide nanoparticles: Research strategies and implications for nanomedicin *Chin. Phys. B* **22** 127503
- [26] Xu H and Gu N 2014 Magnetic responsive scaffolds and magnetic fields in bone repair and regeneration *Frontiers Mater. Sci.* **8** 20–31
- [27] Yu D, Neeley W L, Pritchard C D, Slotkin J R, Woodard E J, Langer R, Teng Y D 2009 Blockade of peroxynitrite-induced neural stem cell death in the acutely injured spinal cord by drug-releasing polymer *Stem Cell* **27** 1212–22
- [28] Dobson J. 2001 Nanoscale biogenic iron oxides and neurodegenerative disease *FEBS Lett.* **496** 1–5
- [29] Kirschvink J L, Kobayashi-Kirschvink A and Woodford B J 1992 Magnetite biominerilization in the human brain *Proc. Natl Acad. Sci. USA* **89** 7683–7
- [30] Dadras A, Riazi G H, Afrasiabi A, Naghshineh A, Ghalandari B and Mokhtari F 2013 *In vitro* study on the alterations of brain tubulin structure and assembly affected by magnetite nanoparticles *J. Biol. Inorg. Chem.* **18** 357–69

Contents

Contributors	xi	2.3	Challenges and Opportunities of Neural Flow Cytometry	17
Foreword	xiii	2.4	Cell Sorting of Neural Cells—Step by Step	18
Preface	xv	2.5	Flow Cytometric Analysis of NSCs	20
1. Fundamentals of Neurogenesis and Neural Stem Cell Development		2.6	Flow Cytometry of Neurons	20
<i>Robert Beattie, Tanzila Mukhtar and Verdon Taylor</i>		2.7	Flow Cytometric Analysis of Glial Cell Types	22
1.1 Neurulation: Formation of the Central Nervous System Anlage	1	2.8	Conclusion	24
1.2 Neurulation and Neural Tube Formation	1		References	24
1.3 Regionalization of the Mammalian Neural Tube	2	3. CD36, CD44, and CD83 Expression and Putative Functions in Neural Tissues		
1.3.1 Molecular Basis of Regionalization	2	<i>Isaias Glezer, Serge Rivest and André Machado Xavier</i>		
1.3.2 Structural Organization of Cellular Compartments and Boundaries in the Developing Neural Tube	4	3.1	Introduction	27
1.4 Onset of Neurogenesis in the Telencephalon	4	3.2	The Putative CD36 Functions in the CNS: A Multifunctional Scavenger Receptor and Lipid Sensor	27
1.5 The Transition of the Neurepithelium to Neural Stem Cells	4	3.2.1	CD36 Structure and General Functions	27
1.5.1 Asymmetric versus Symmetric Cell Divisions	6	3.2.2	Cd36 Gene Expression Maps to Olfactory Relays and Reproductive Behavior-Associated Brain Regions	29
1.6 Progenitor Fate Commitment and Restriction	6	3.2.3	CD36 Functions in the Nervous System	29
1.6.1 The Common Progenitor Model	6	3.3	The Expression of CD44 Adhesion Molecule in Neural Cells	30
1.6.2 Multiple Progenitor Model	6	3.3.1	CD44 Structure and General Functions	30
1.7 Molecular Mechanisms of Neural Stem Cell Maintenance	7	3.3.2	Constitutive Murine Cd44 Gene Expression Maps to Intralaminar Nuclei of the Thalamus and Few Other Limited Nuclei of the CNS	31
1.7.1 Notch Signaling as a Key Regulator in Maintenance of NSCs	7	3.3.3	CD44 Glycoprotein Expression and Functions in the Nervous System	32
1.8 Interneuron Generation from the Ventral Telencephalon	8	3.4	The Glycoprotein CD83	33
1.9 Formation of the Cerebral Isocortex and Cortical Layering	9	3.4.1	CD83 Structure and General Functions	33
1.10 Oligodendrogenesis and Astrogenesis	9	3.4.2	Neuronal Cd83 Gene Expression is Widespread in Murine Brain, albeit Not Ubiquitous	34
1.10.1 Human Neocorticogenesis	10	3.4.3	Possible CD83 Functions in the Nervous System	34
References	11	3.5	Concluding Remarks	36
			References	36

4. Life and Death in the CNS: The Role of CD95

Si Chen, Robert Hermann, Enric Llorens-Bobadilla and Ana Martin-Villalba

4.1 Introduction	41
4.2 CD95 Expression in the Healthy and Diseased Brain	42
4.2.1 CD95 Expression in the Developing and Healthy Adult Brain	42
4.2.2 CD95 Expression after Brain Injury	43
4.2.3 CD95 Expression in Brain Tumors	43
4.2.4 Controversies Regarding CD95 Detection	43
4.3 Functions and Signaling of CD95 in the CNS	43
4.3.1 CD95-Mediated Neurite Growth in Neurons	43
4.3.2 Functional Relevance of CD95 in the Injured CNS	44
4.3.3 Role of CD95 in Neural Progenitors	45
4.3.4 Multifaceted Functions of CD95 in Brain Tumors	46
4.4 Conclusions	51
References	51

5. Role of Fundamental Pathways of Innate and Adaptive Immunity in Neural Differentiation: Focus on Toll-like Receptors, Complement System, and T-Cell-Related Signaling

Hélène Boudin and Antoine Louveau

5.1 Molecules from Innate Immunity	55
5.1.1 Toll-Like Receptors	55
5.1.2 Complement System	58
5.2 Molecules from Adaptive Immunity	59
5.2.1 Major Histocompatibility Complex Molecules	59
5.2.2 Costimulatory Molecules	60
5.2.3 CD3ζ	60
5.3 Conclusion	62
References	62

6. Neuropilins in Development and Disease of the Nervous System

Mathew Tata, Miguel Tillo and Christiana Ruhrberg

6.1 Introduction	65
6.2 Neuropilins Associate with Plexins to Mediate Semaphorin Signaling	65
6.3 Neuropilins and Plexins Cooperate to Confer Specificity to Semaphorin Signaling	66
6.4 Neuropilin-Mediated Repulsion in Axon Guidance	66

6.5 Neuropilins Can Mediate Attractive Responses by Axons to Semaphorins	67
6.6 Neuropilins Organize Axon Projections to Provide a Substrate for Migrating Neurons	67
6.7 Semaphorin Signaling through Neuropilins in Neurons Promotes Neuronal Migration	67
6.8 VEGF-A as an Alternative Neuropilin Ligand in the Nervous System	68
6.9 Differential VEGF-A Isoform Affinity for the Two Neuropilins	68
6.10 VEGF-A Signaling through Neuropilin 1	68
6.11 NRP1 in CNS Angiogenesis	70
6.12 VEGF-A/NRP1 Signaling Promotes Contralateral Axon Projection across the Optic Chiasm	70
6.13 VEGF-A Signals through NRP1 to Promote Neuronal Migration	70
6.14 Semaphorin Signaling through NRP1 Impairs CNS, but not PNS Regeneration	71
6.15 VEGF Signaling through NRP1 Promotes Survival of Developing Neurons	71
6.16 Neuropilin in Synaptogenesis and Plasticity	71
6.17 Outlook	72
References	72

7. Growth and Neurotrophic Factor Receptors in Neural Differentiation and Phenotype Specification

Talita Glaser, Ágatha Oliveira, Laura Sardà-Arroyo and Henning Ulrich

7.1 Introduction	77
7.2 Neurotrophins	77
7.3 Nerve Growth Factor	79
7.4 Brain-Derived Neurotrophic Factor	82
7.5 Neurotrophin-3	82
7.6 Epidermal Growth Factor	83
7.7 Fibroblast Growth Factor	83
7.8 Glial Cell Line-Derived Neurotrophic Factor	84
7.9 Insulin-like Growth Factor	85
7.10 Conclusion	86
References	86

8. Glycolipid Antigens in Neural Stem Cells

Yutaka Itokazu and Robert K. Yu

8.1 Introduction	91
8.1.1 Glycosphingolipids and Development	91
8.1.2 Gangliosides	91

8.2 Stage-Specific Embryonic Antigen-1 (CD15)	93	10. Comprehensive Overview of CD133 Biology in Neural Tissues across Species	
8.2.1 SSEA-1 in Early Embryogenesis	93	<i>József Jászai, Denis Corbeil and Christine A. Fargeas</i>	
8.2.2 SSEA-1 in Neural Stem Cells	94		
8.2.3 SSEA-1 and Integrin	94	10.1 Introduction	113
8.2.4 SSEA-1 and Notch Signaling	95	10.1.1 CD133	113
8.3 SSEA-4	95	10.1.2 Detecting Mammalian (Mouse and Human) CD133	115
8.4 GD3 Ganglioside	95	10.1.3 CD133: A Unique Cell Surface Antigen for Cell-Based Therapy and Tissue Engineering	117
8.4.1 GD3 as a Specific Marker for NSCs	95	10.2 Cell Biology of CD133 Protein in the Nervous System	117
8.4.2 GD3-Synthase-KO NSCs	95	10.2.1 CD133 ⁺ Membrane Particles	117
8.4.3 GD3 and Endocytosis	96	10.2.2 Symmetric versus Asymmetric Distribution of CD133	118
8.5 9-O-acetyl GD3	96	10.3 Compartmentalization of CD133 in Mammalian Neural Tissues	118
8.6 GM1 Ganglioside	96	10.3.1 Developing Mammalian Brain	119
8.6.1 GM1 and Its Epigenetic Regulation	96	10.3.2 Adult Mammalian Brain	119
8.6.2 Integrin–Focal Adhesion Kinase Signaling	97	10.4 CD133⁺ Neural Stem and Progenitor Cells across Species	120
8.7 The C-series Gangliosides	97	10.4.1 CD133 ⁺ Cells and Regeneration	122
8.8 GalCer and Sulfatide	97	10.4.2 CD133 and Neural Diseases	122
8.9 Sialosyl Galactosylceramide	97	10.4.3 CD133 and Photoreceptor Neuron Morphogenesis	123
8.10 Phosphatidylglucoside	98	10.4.4 Acknowledgments	124
8.11 Conclusions and Prospective Studies	98	10.4.5 References	124
Acknowledgments	99		
References	99		
9. NG2 (Cspg4): Cell Surface Proteoglycan on Oligodendrocyte Progenitor Cells in the Developing and Mature Nervous System			
<i>Akiko Nishiyama, Aaron Lee and Christopher B. Brunquell</i>			
9.1 Introduction	103	11. Fundamentals of NCAM Expression, Function, and Regulation of Alternative Splicing in Neuronal Differentiation	
9.2 The Structure of NG2	103	<i>Ana Fiszbein, Ignacio E. Schor and Alberto R. Kornblith</i>	
9.2.1 NG2 in Different Species	104		
9.3 Expression of NG2 in the Nervous System	105	11.1 Introduction	131
9.3.1 NG2 in the Central Nervous System	105	11.2 NCAM Gene and Alternative Splicing Isoforms	131
9.3.2 NG2 in the Peripheral Nervous System	106	11.3 Molecular Structure and Function of NCAM	133
9.4 The Role of NG2 in Cell Attachment and Migration	106	11.4 Alternative Splicing Regulation	134
9.5 The Role of NG2 in Axon–NG2 Cell Interactions	107	11.5 Chromatin Structure Regulates Alternative Splicing	135
9.5.1 NG2 and Developing Axons	107	11.6 Background in NCAM Alternative Splicing Regulation	136
9.5.2 NG2 and Axons in the Injured CNS	107	11.7 Regulation of NCAM Alternative Splicing by Chromatin Changes in Neuronal Differentiation	136
9.6 The Role of NG2 in Cell Proliferation	108	11.8 Conclusions	137
9.7 The Role of NG2 in Intracellular Signaling	109	11.9 Acknowledgments	138
9.7.1 Activation of Rho Family GTPases	109	11.10 References	138
9.7.2 Extracellular Signal-Regulated Kinase Signaling	109		
9.7.3 Akt Signaling	110		
9.8 Concluding Remarks	110		
References	110		

12. Role of the Clustered Protocadherins in Promoting Neuronal Diversity and Function	
<i>Takeshi Yagi</i>	
12.1 Introduction	141
12.2 The Cadherin Superfamily and the Clustered Pcdhs	141
12.3 Genomic Structures of the Clustered <i>Pcdh</i> Genes	142
12.4 Gene Expression of the Clustered <i>Pcdhs</i>	143
12.5 Gene Regulation of the Clustered <i>Pcdhs</i>	144
12.6 Cell Adhesion Activity of the Clustered Pcdhs	147
12.7 Cell Signaling Mediated by the Clustered Pcdhs	147
12.8 Roles of Clustered Pcdhs in the Nervous System	148
12.9 Conclusions	148
References	149
13. $\beta 1$-Integrin Function and Interplay during Enteric Nervous System Development	
<i>Sylvie Dufour, Florence Broders-Bondon and Nadège Bondurand</i>	
13.1 Introduction	153
13.2 Functions of the ECM and Integrins during ENS Development	154
13.2.1 ECM and Integrin Expression during ENS Development	154
13.2.2 Integrin Function during ENCC Migration and ENS Development	155
13.3 Effectors of the Integrin Signaling Pathway during ENS Development	156
13.3.1 Phactr-4 and Integrin Signaling	156
13.3.2 Role of Phosphatase and Tensin Homolog	157
13.3.3 Roles of Integrin-Linked Kinase and Pinch	157
13.3.4 Role of FAK	158
13.4 $\beta 1$ -Integrin CROSSTALK with ENS Genes and N-Cadherin during ENS Development	158
13.4.1 Interplay between $\beta 1$ -Integrins and SOX10	158
13.4.2 $\beta 1$ -Integrins and GDNF/RET Crosstalk	158
13.4.3 $\beta 1$ -Integrins and N-Cadherin Crosstalk	159
13.5 Control of Integrin Gene Expression	161
13.5.1 Organization of 5' Regions/Promoters	161
13.5.2 Control of Integrin Gene Expression by SP1 and Interacting TFs	161
13.5.3 Control of Integrin Gene Expression by other TFs	161
13.5.4 Posttranscriptional Control of Integrin Expression by MicroRNAs	162
13.6 Conclusion	162
References	162
14. Neural Flow Cytometry – A Historical Account from a Personal Perspective	
<i>Henry J. Klassen</i>	
14.1 Surface Markers on Neural Progenitor Cells	168
14.2 CD15	169
14.3 CD133	169
14.4 GD2 Ganglioside	169
14.5 Tetraspanins: CD9 and CD81	169
14.6 MHC	170
14.7 Fas/CD95	171
14.8 Retinal Progenitor Cells	171
14.9 Further Studies of Surface Markers	171
14.10 Conclusions	171
References	172
15. Multimarker Flow Cytometric Characterization, Isolation and Differentiation of Neural Stem Cells and Progenitors of the Normal and Injured Mouse Subventricular Zone	
<i>Krista D. Buono, Matthew T. Goodus, Lisamarie Moore, Amber N. Ziegler and Steven W. Levison</i>	
15.1 Introduction	175
15.2 Neural Stem Cells and Progenitors	175
15.3 Flow Cytometric Studies on Neural Precursors – Technical Considerations	176
15.4 Flow Cytometry Studies of the Fetal Mouse Forebrain	178
15.5 Studies Using Flow Cytometry on the Neonatal SVZ	178
15.6 Studies Using Flow Cytometry on the Adult SVZ	181
15.7 Using Flow Cytometry to Evaluate Effects of Cytokines and Growth Factors on Neural Precursors	182
15.8 Using Flow Cytometry to Evaluate Effects of Neurological Injuries and Diseases on Neural Precursors	183
15.9 Using Flow Cytometry to Better Understand Glioblastoma	184
15.10 Conclusion	184
References	185

16. Multiparameter Flow Cytometry Applications for Analyzing and Isolating Neural Cell Populations Derived from Human Pluripotent Stem Cells

Nil Emre, Jason G. Vidal, Christopher Boyce, Lissette Wilensky, Mirko Corselli and Christian T. Carson

16.1 Introduction	187
16.2 Methods for Neural Differentiation of Human Pluripotent Stem Cells	187
16.3 Cell Surface Signatures for Neural Cell Isolation from Pluripotent Stem Cells	188
16.4 Neural Applications for Multiparameter Flow Cytometry	190
16.4.1 Neural Fate Determination	190
16.4.2 In vitro Disease Modeling	190
16.5 Cell Transplantation	192
16.6 The Detection of Intracellular Antigens by Flow Cytometry	192
16.7 The Utility of Flow Cytometry for Analyzing Human PSC-Derived Neural Cells	193
16.8 Cell Surface Marker Screening Applications for Nonneural Stem Cell Populations	193
16.9 Pluripotent Stem Cells and Their Derivatives	194
16.10 Adult Stem Cells	195
16.11 Cancer Stem Cells	195
16.12 Conclusions and Future Considerations	196
References	196

17. Flow-Cytometric Identification and Characterization of Neural Brain Tumor-Initiating Cells for Pathophysiological Study and Biomedical Applications

Sujeivan Mahendram, Minomi K. Subapanditha, Nicole McFarlane, Chitra Venugopal and Sheila K. Singh

17.1 Introduction to Neural Stem Cells	199
17.2 Tumors of the Central Nervous System	199
17.2.1 Glioblastoma Multiforme	200
17.2.2 Medulloblastoma	200
17.3 Cancer Stem-Cell Hypothesis	201
17.4 Brain Tumor Initiating Cells	201
17.5 Identification of Neural Surface Antigens	201
17.5.1 CD133	201
17.5.2 CD15	202
17.5.3 CD271	202

17.5.4 High Aldehyde Dehydrogenase Activity	203
17.6 Flow-Cytometric Identification and Characterization	203
17.7 Limitations of Current CSC Markers	204
17.7.1 Hypoxia	204
17.7.2 Cell Dissociation Methods	205
17.7.3 Dynamic Growth	206
17.8 Applications of Functional BTIC Assays	206
17.8.1 Neurosphere Formation	206
17.8.2 In vivo Serial Transplantation	207
17.9 Conclusion	208
References	208

18. Using Cell Surface Signatures to Dissect Neoplastic Neural Cell Heterogeneity in Pediatric Brain Tumors

Tamra Werbowetski-Ogilvie

18.1 Cell Surface Markers to Distinguish Heterogeneity in the Neural Lineage Hierarchy	213
18.2 Medulloblastoma: An Example of Genomic, Molecular, and Cellular Heterogeneity	214
18.3 The CSC Hypothesis and Brain Tumors	214
18.4 In Search of New Markers: The Case for CD271/p75NTR	215
18.5 CD271: Its Role in Neurodevelopment and Progenitor/Stem Cell Function	216
18.6 Extending beyond CD133: Using High-Throughput Flow Cytometry to Identify Novel Markers of Neural Tumor Cell Phenotypes	217
18.7 Clinical Implications of Cell Surface Signatures in MB and Other Brain Tumor Pathologies	219
References	219

19. Synopsis and Epilogue: Neural Surface Antigen Studies in Biology and Biomedicine—What We Have Learned and What the Future May Hold

Jan Pruszak

19.1 Introduction	223
19.2 Progress in Neural Stem Cell and Cancer Biology Hinges Upon Understanding Cell–Cell Interactions	223
19.3 Neural Flow Cytometry and Cell Isolation Are Tricky, but Feasible	224
19.4 Neural Surface Antigens Are Critical Mediators of Cellular CROSSTALK in Neurobiology	224

x Contents

19.5 Expression of Even Some of the Better-Characterized Neural Surface Antigens Is Exceedingly Complex	225	19.8 What's Around the Corner?	226
19.6 Toward an Integrated View of Neural Surface Antigen Signaling	226	19.9 Conclusion	227
19.7 Neural Surface Antigens Serve as Valuable Markers for Cell Analysis and Cell Selection	226	Acknowledgments	227
		References	227
		Index	229

AUTHOR QUERY FORM

	Book: PRUSZAK-9780128007815 Chapter: 07	Please e-mail your responses and any corrections to: E-mail: neuralsurface@elsevier.com
---	--	--

Dear Author,

Any queries or remarks that have arisen during the processing of your manuscript are listed below and are highlighted by flags in the proof. (AU indicates author queries; ED indicates editor queries; and TS/TY indicates typesetter queries.) Please check your proof carefully and answer all AU queries. Mark all corrections and query answers at the appropriate place in the proof using on-screen annotation in the PDF file. For a written tutorial on how to annotate PDFs, click http://www.elsevier.com/_data/assets/pdf_file/0016/203560/Annotating-PDFs-Adobe-Reader-9-X-or-XI.pdf. A video tutorial is also available at <http://www.screencast.com/t/9OIDFhihgE9a>. Alternatively, you may compile them in a separate list and tick off below to indicate that you have answered the query.

Please return your input as instructed by the project manager.

Location in article	Query / remark
	No Queries

Chapter 7

c0007 Growth and Neurotrophic Factor Receptors in Neural Differentiation and Phenotype Specification

Talita Glaser, Ágatha Oliveira, Laura Sardà-Arroyo and Henning Ulrich

Departamento de Bioquímica, Instituto de Química, Universidade de São Paulo, S.P., Brazil

s0010 7.1 INTRODUCTION

p0010 During development, growth factors known to regulate the proliferation of nonneuronal cells can also promote the growth of neural stem and precursor cells (NPCs) [1]. Some examples are insulin-like growth factor (IGF) [2,3], fibroblast growth factors (FGFs) [4], the epidermal growth factor (EGF) family, platelet-derived growth factor (PDGF), and neurotrophins [5]. Furthermore, growth and neurotrophic factors including glial cell line-derived neurotrophic factor (GDNF), nerve growth factor (NGF), brain-derived neurotrophic factor (BDNF), and neurotrophins-3 and -4/5 (NT-3 and NT-4/5) participate in differentiation induction and phenotype determination of neural cells [6–8]. These growth factors function by binding and activating specific receptor tyrosine kinases, which then trigger a cascade of events that specify programs of gene transcription and epigenetic and particular cellular responses [6,8]. Tables 7.1 and 7.2 give an overview of the effects of growth and neurotrophic factors on proliferation, differentiation, and stem cell fates, which are further described in the following. Moreover, in this chapter we focus on describing the actions of growth factors and their intracellular signaling pathways in the processes of neurogenesis and neuromaturation during embryo development and neural stem cell differentiation (Figure 7.1 and 7.2).

s0015 7.2 NEUROTROPHINS

p0015 The discovery of the neurotrophin family (Figure 7.3) and their tyrosine kinase receptors by Rita Levi-Montalcini encouraged studies to identify a genetic system that contributes to the development and maintenance of the vertebrate nervous system, regulating neuronal survival, axonal growth and guidance, synaptic plasticity, and long-term

potentiation events [9–12]. This family includes BDNF, NT-3, and NT-4/5 [13–16]. Science has made tremendous progress in the identification and characterization of the intracellular signaling pathways triggered by neurotrophic factors. These signaling mechanisms support the elucidation of diverse cellular responses including proliferation, differentiation, and programmed cell death. Neurotrophic factor receptor stimulation usually activates cellular tyrosine kinases propagating signal transduction within cells [17–23], resulting in subsequent changes in gene expression [8,24–28]. NGF, BDNF, and NT-3 activate respectively the tropomyosin-related kinase receptors A, B, and C (TrkA, TrkB, and TrkC) [29–41]. A second neurotrophin, NT-4/5, also binds to the TrkB receptor [8]. The most described adaptor proteins for Trk receptors are the Src homology 2 domain-containing protein (SHC) and the FGF receptor substrate 2 (FRS2), initiating downstream phosphorylation cascades by activating the RAS/RAF/extracellular signal-regulated kinase (ERK) mitogen-activated protein kinase and the phosphoinositide 3-kinase (PI3K)/AKT pathways, which are widely attributed to classical Trk-promoted neuronal survival and differentiation. The tyrosine phosphorylation recruits phospholipase C- γ 1 (PLC- γ 1) protein, leading to the modulation of synaptic plasticity produced by the Trk system [12].

Neurotrophins can also bind to the p75 panneurotrophin receptor (p75NTR or CD271), a member of the tumor necrosis factor receptor family. This multiligand receptor is composed of an extracellular domain with four cysteine-rich regions that optimizes neurotrophin binding, a transmembrane portion, and an intracellular domain, the flexibility of which is responsible for the activation of intracellular signaling, because these receptors do not exhibit an enzymatic function induced by ligand binding, unlike Trk receptors [42].

p0020

t0010

TABLE 7.1 Effects of Neurotrophic and Growth Factors on Neural Differentiation

Model	Factors	Receptor	Differentiation Fate/Effect	References
SVZ-derived NPC	BDNF	TrkB	Neurite outgrowth	[83]
NSC	BDNF	p75	Neuroblast	[84]
NPC	BDNF	p75	Neuronal differentiation	[86]
In vivo rat hippocampal NSC	IGF-1	IGF-1R	Neuronal differentiation	[190]
NSC	IGF-1	IGF-1R	Oligodendrocytes	[191]
Human ESC	FGF-2	All	Maintenance of pluripotency	[150]
Mouse ESC	FGF-2	FGFR-1/3	Promotion of self-renewal	[151]
ESC	FGF-2	–	NSC	[152]
Mouse NSC	FGF-4	–	NPC	[153]
Human NSC	FGF-2/8 and 20	–	NPC	[153]
NPC	FGF-2 + EGF short-term removal	–	Neuron fate and neurite outgrowth	[124,125]
NPC	Low FGF-2 concentration	–	Neuronal differentiation	[126]
NPC	High FGF-2 concentration	–	Astrocyte	[126]
Telencephalic progenitors	FGF-8	–	Olfactory bulb neurons	[194]
Human ESC+mouse stromal cells	FGF-20	FGFR-1	Dopaminergic neurons	[195]
–	NT-3	TrkC and p75NTR	Neuronal differentiation	[95]
Cortical NPC	NT-3	TrkC	Neuronal differentiation	[96,199]
Cerebellar granule precursor cells	NT-3	TrkC	Increased neurite fasciculation	[7]
Striatal precursors	NGF+FGF-2	–	Proliferation	[68]
Different kinds of stem cell	NGF+BDNF	–	Neuronal and astroglial differentiation	[70,71]
Neural precursors	NGF	TrkA	Glutamatergic and sensory neuron differentiation, neurite outgrowth	[73,74,198]
NSC from subgranular zone	EGF	–	Proliferation	[78,193]
SVZ-derived NPC	EGF	–	Premyelinating and myelinating oligodendrocytes	[78,110]
Fetal telencephalon	EGF	–	Ventrolateral and radial migration	[78,111,113]
Enteric neural crest	GDNF	–	Migration, proliferation, differentiation, and survival to form enteric nervous system	[162,169]
Ventral mesencephalic neurons	GDNF	–	Differentiation and survival of TH-positive cells	[171,196,197]
Ventral mesencephalic neurons	GDNF	–	GABAergic neurons	[172]
NPC	GDNF	–	Survival and differentiation into TH-positive cells	[170]

TABLE 7.1 Effects of Neurotrophic and Growth Factors on Neural Differentiation—cont'd

Model	Factors	Receptor	Differentiation Fate/Effect	References
Multipotent astrocytic stem cells	Prolonged exposure to GDNF in vitro	–	Increased migration and neuronal differentiation	[173]
NPC	GDNF	–	Migration	[174]
Dentate gyrus-derived NPC	GDNF+retinoic acid	–	Astrocytes	[183]
ESC	GDNF+retinoic acids+other factors	–	Motor neurons	[177,178]

t0015

TABLE 7.2 Signaling Pathways Involved in Receptor Activation

Factors	Receptor	Signaling Pathways	References
NGF	TrkA	PI3K/AKT, PLC-γ/DAG/PKC	[64–66]
NGF	TrkA	RAS/RAF/ERK	[77]
NGF/proNGF	p75NTR	JNK/NF-κB	[61–63]
BDNF	TrkB	RAS/RAF/ERK, PI3K/AKT, PLC-γ/DAG/PKC	[80]
NT-3	TrkC	RAS/RAF/ERK, PLC-γ/DAG/PKC	[84]
NT-3	TrkC in Schwann cells	Cdc42–GEF/Dbl	[94]
EGF	EGFR	RAS/RAF/ERK, PI3K/AKT/mTOR, cAMP/PKA/CREB	[78,107,112]
FGF	FGFR	RAS/RAF/ERK, PI3K/AKT, PLC-γ/DAG/PKC	[116]
GDNF	GFR/RET complex	RAS/RAF/ERK, PI3K/AKT, PLC-γ/DAG/PKC	[141,142]
GDNF	GDNF/NCAM complex	RAS/RAF/ERK	[147,148]
GDNF	GFRα1	RAS/RAF/ERK, PI3K/AKT	[140,175]
IGF-1	IGF-1R	RAS/RAF/ERK, PI3K/AKT	[189]

p0025 Docked PLC-γ1 is activated through Trk-mediated phosphorylation and then hydrolyzes phosphatidylinositol 4,5-bisphosphate to generate inositol triphosphate (IP3) and diacylglycerol (DAG). IP3 formation results in Ca²⁺ release from cytoplasmic stores, whereas DAG stimulates activation of classical isoforms of protein kinase C (PKC). These signaling molecules activate intracellular enzymes including Ca²⁺-calmodulin-dependent protein kinases and other Ca²⁺-calmodulin-regulated targets. Moreover, PLC-γ1 stimulates PKC-δ, which is required for NGF-promoted activation of mitogen-activated protein kinase (MAPK) kinase (MEK) 1 and ERK1/2 [43], with subsequent expression and/or activity control of ion channels and transcription factors [44–47].

p0030 Evidence has shown that Trk may also modulate cancer growth such as neuroblastoma and medulloblastoma, whereas a rearranged Trk oncogene is often observed in nonneuronal neoplasms such as colon and papillary thyroid cancers [48]. However, further chapters of this book discuss this theme.

Between all existing neurotrophins, just four are expressed in mammals; these are NGF, BDNF, NT-3, and NT-4 [46]. We focus here on the effects of NGF, BDNF, and NT-3 in neural development and differentiation.

7.3 NERVE GROWTH FACTOR

In 1950, Levi-Montalcini and Hamburger observed neuron growth following mouse sarcoma transplantation into the chick embryo peripheral nervous system. By tissue culture techniques, they identified this tumor factor and named it nerve growth factor, the first identified member of the neurotrophin family (Figure 7.3) [49–51]. NGF exerts its functions on restricted target populations regulating axon guidance, synaptic function, and neuronal differentiation [11] and promotes survival of specific populations of sensory, sympathetic, and central nervous system (CNS) neurons. It is also involved in the maintenance of basal forebrain cholinergic neurons, which project to the hippocampus and are important for memory processes [52–55].

s0020

p0040

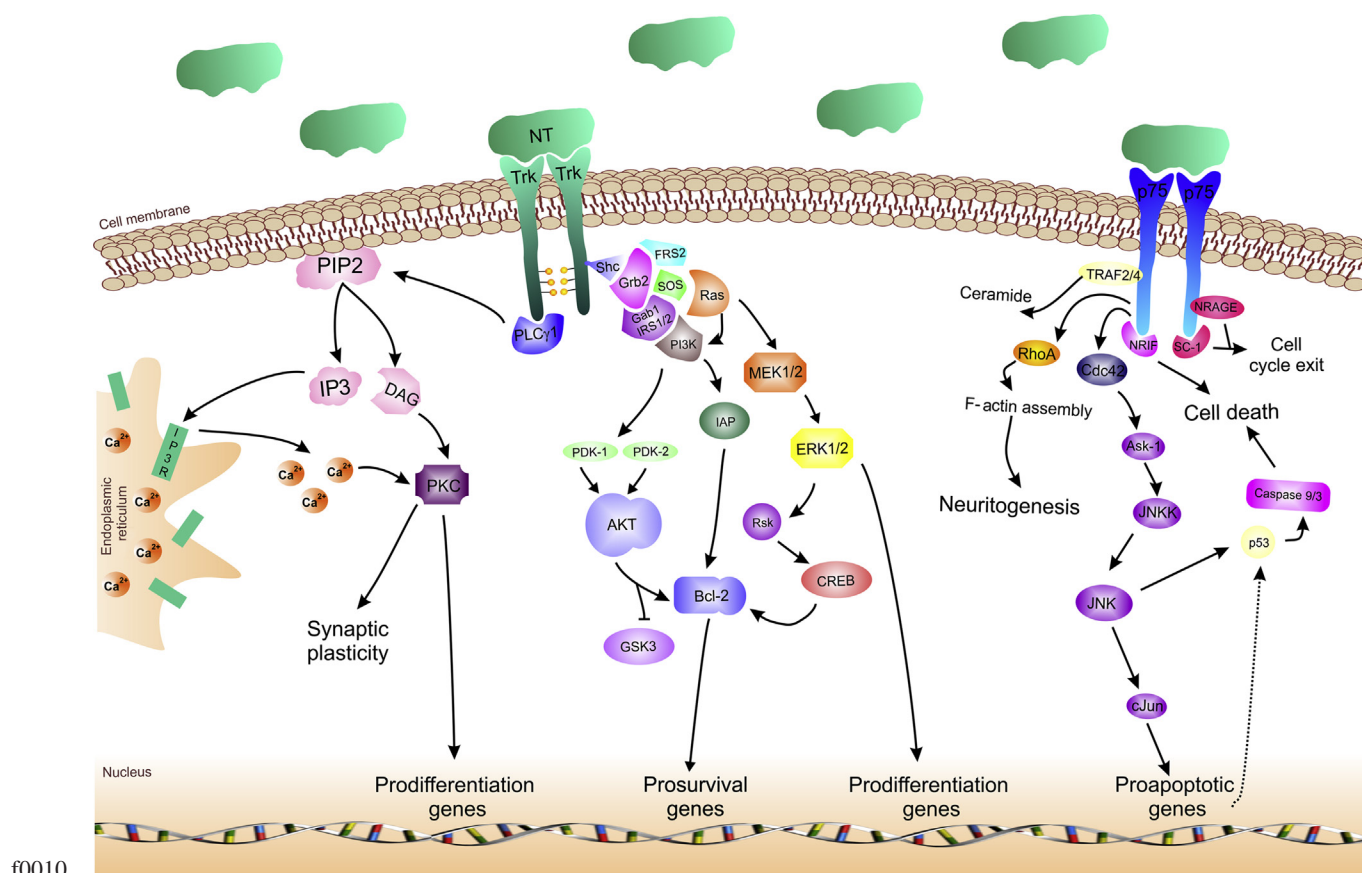


FIGURE 7.1 Neurotrophin signaling. This figure depicts the interactions of neurotrophins (NGF, BDNF, NT-3) with Trk and p75NTR receptors and major intracellular signaling pathways activated through each receptor. The p75NTR receptor triggers two major signaling pathways. One is RhoA activation resulting in F-actin assembly, promoting neuritogenesis and growth cone motility. The Jun kinase pathway controls the activities of several genes, with some of them promoting neuronal apoptosis. Proapoptosis actions of p75NTR appear to require the presence of sortilin, which functions as a coreceptor for neurotrophins. Sortilin is not depicted in this figure. Each Trk receptor controls three major signaling pathways. Activation of RAS results in activation of the MEK/ERK signaling cascade, which promotes neuronal differentiation including neurite outgrowth. Activation of PI3K through RAS or Gab1 promotes survival and growth of neurons and neuroblasts. Activation of PLC- γ 1 results in activation of Ca²⁺- and protein kinase C-regulated pathways that promote synaptic plasticity and differentiation of specific neuron subtypes. Each of these neurotrophin-activated signaling pathways also regulates gene transcription. Additional signaling proteins for p75NTR and Trk receptor pathways are not depicted for reasons of simplicity; however, these are described in more detail in the text.

Therefore, this neurotrophic factor is an important target for treating memory diseases such as Alzheimer disease.

NGF is initially synthesized as a large precursor protein called proNGF and is released in an activity-dependent manner as a precursor form (proNGF) into the extracellular space together with convertases and proteases, which cleave proNGF into its mature form (mNGF) and degrade free unbound mNGF [56]. This proteolytic cleavage has important roles during development and in the adult organism [57,58].

Mature NGF exerts its cellular effects preferentially through the activation of two different receptors, TrkA and p75NTR [11,59]. NGF triggers apoptosis in mistargeting conditions (binding to p75NTR) during neural development [60] and after nervous injury, inflammation, or stress conditions through p75NTR activation, increasing JNK and consequent NF-κB levels and inducing proapoptotic protein

synthesis [61–63]. ProNGF is more effective than mNGF at binding p75NTR and inducing this apoptotic process [62]. In addition to these proapoptotic events promoted by NGF–p75NTR interaction, NGF binds specifically to TrkA, and this activation usually promotes neuroprotective actions such as cell survival and differentiation.

Like TrkC, TrkA autophosphorylates at specific phosphotyrosine residues as soon as this neurotrophin binds to the activation site. The activated subunits turn into recruitment docking sites for signaling effectors, such as PI3K and PLC- γ and adaptor proteins SHC and FRS2 [64–66]. The main intracellular docking domains are Tyr490 and Tyr790 [59]. Consequently, these interactions trigger intracellular signal transduction cascades such as PLC- γ and others that will be further discussed. After prolonged activation, the receptor–ligand complex can be internalized into vesicles

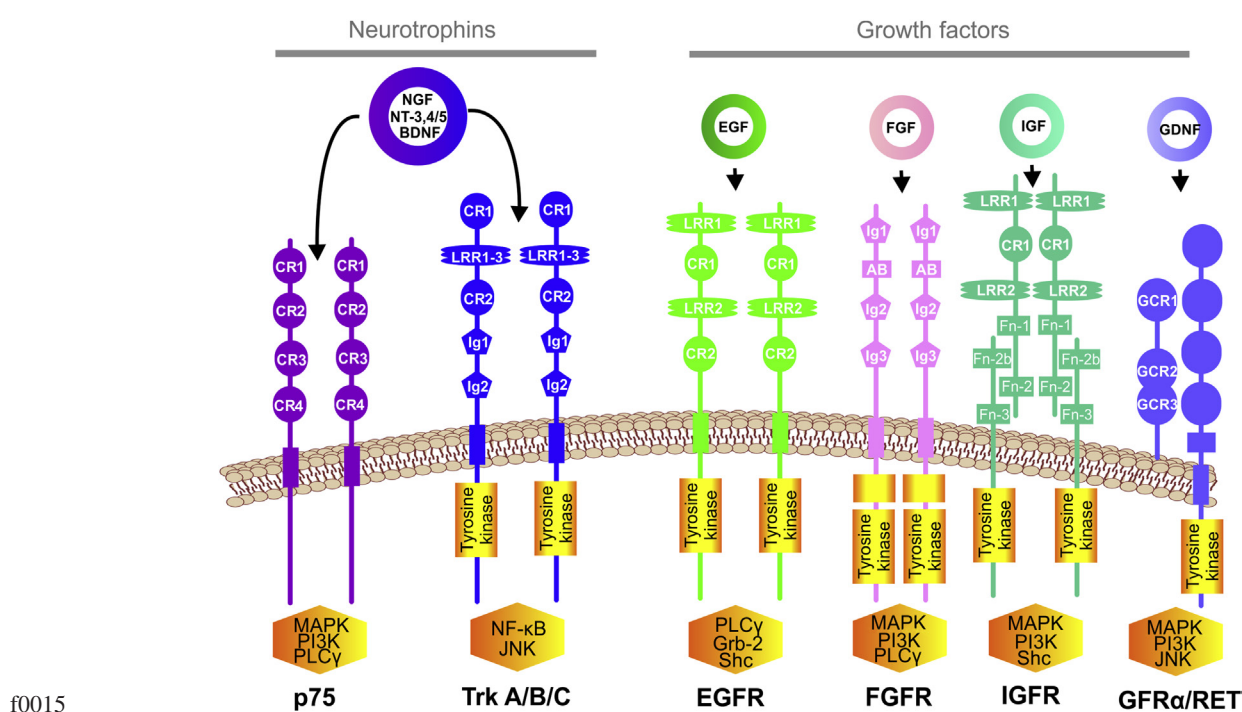


FIGURE 7.2 Structural domains of neurotrophin and growth factor receptors. This figure depicts the interactions of neurotrophins (NGF, BDNF, NT-3) with Trk and p75NTR receptors and major intracellular signaling pathways activated through each receptor and the interactions of growth factors (EGF, FGF, IGF, and GDNF) with their respective receptors (EGFR, FGFR, IGFR, GFR α /RET). Cysteine-rich domain (CR), leucine-rich-repeat domain (LRR), immunoglobulin-like domain (Ig), acid box (AB), fibronectin type III domain (Fn), and globular cysteine-rich domain (GCR). Additional structural domains are not depicted for reasons of simplicity; however, these are described in more detail in the text.

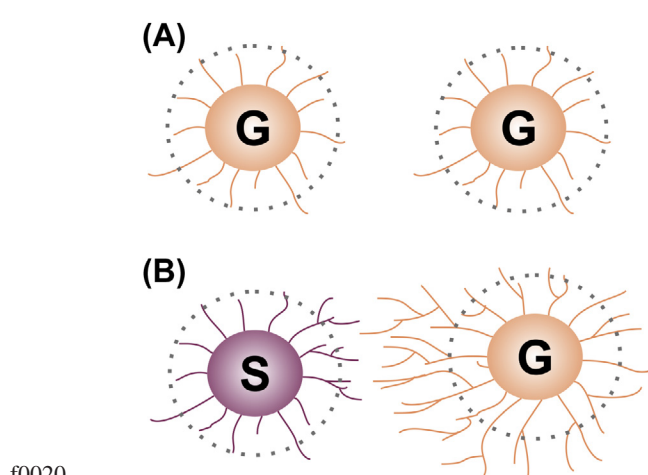


FIGURE 7.3 Nerve growth factor discovery. In 1950, Levi-Montalcini and Hamburger observed a huge innervation growth caused by mouse sarcoma 180 transplanted on the chick embryo peripheral nervous system. By tissue culture techniques they identified the chemical tumor factor as nerve growth factor, the first identified member of the neurotrophin family. (A) When a chick embryo sensory ganglion is cultivated in the presence of another ganglion there are many fibroblasts but few nerve fibers. (B) When a chick embryo sensory ganglion is cultivated in the presence of mouse sarcoma 180 there are many nerve fibers and few fibroblasts, showing the “halo” effect.

and kept activated for as long as the ligand remains associated with the receptor [67].

Some actions of NGF in cell differentiation were described by Cattaneo and McKay in 1990, who showed that NGF together with FGF-2 stimulates proliferation of striatal precursors [68]. Combined treatment with NGF/BDNF promotes neural and astroglial, but not oligodendrocyte, differentiation [69–72]. Furthermore, NGF promotes not only glutamatergic and sensory neuron differentiation but also neurite outgrowth from different neural precursors in a concentration-dependent manner [16,73,74]. A possible pathway resulting in differentiation through NGF activation is the downregulation of ATF5 [75] and upregulation of tissue inhibitor of metalloproteinases-2 expression [76].

NGF also activates the RAS-mediated induction of the MAPK pathway. This pathway is initiated through recruitment and activation of SHC, which leads to RAS activation through GRB-2 and SOS-1. The MAPK cascade includes RAF, MEK, and ERK. The downstream effectors of the RAS pathway include activation of c-Fos and Jun to form AP-1, activating genes through this transcription factor, leading to cell fate choice, synaptic plasticity, and also neoplastic transformation causing cancer [77].

EGR (early growth-response protein) and CREB (cAMP-response element-binding protein) are transcription

p0060

p0065

p0070

factors involved in NGF responses. The EGR family of transcription factors, as well as the MEK/ERK pathway, contributes to NGF-induced neurite formation, and the CREB family is involved in NGF-induced survival of sympathetic neurons. For instance, NGF treatment of PC12 cells induces continuous ERK activity, whereas EGF treatment provides a transient activation [78]. NGF-signaling mechanisms may be further studied to understand how modulation of NGF-induced responses can be exploited for the treatment of neurodegenerative diseases.

s0025 7.4 BRAIN-DERIVED NEUROTROPHIC FACTOR

p0075 Barde, Edgar, and Thoenen, in 1982, motivated by the fact that no molecule had yet been isolated from a tissue directly involved in nervous system development, purified “a neuronal survival factor” from pig brain, which later was named brain-derived neurotrophic factor [79].

p0080 BDNF is a neurotrophin that acts in neural development as well as in adult neurogenesis. BDNF is synthesized as a precursor isoform (proBDNF) that is proteolytically cleaved to produce its mature form (mBDNF). Like NGF, BDNF activates two classes of receptors: the selective TrkB and the aforementioned multiligand p75NTR [80]. mBDNF induces TrkB receptor dimerization and autophosphorylation of tyrosine residues, which induces various intracellular signaling pathways, such as the previously described RAS/MAPK, PI3K/AKT, and PLC- γ 1 pathways [81].

p0085 Secretion of BDNF and expression of its receptors by embryonic stem cells occur mainly during embryogenesis phases. The lack of this neurotrophin during development of mouse embryos results in a loss of neurons in the sensory ganglia and affects especially the developing thalamus, the substantia nigra, and the cerebellum, yielding poor motor coordination and body-balanced mice [82].

p0090 It is well known that TrkB activation by BDNF induces intracellular signaling pathways related to effects that are beneficial for the nervous system, by inducing long-term potentiation in the hippocampus. This physiological enhancement in signal transmission promotes proliferation, survival, and neuronal differentiation of neural stem cells (NSCs) and NPCs [1]. Furthermore, BDNF binding to TrkB is suggested to induce dendritic outgrowth of subventricular zone (SVZ)-derived NPCs in vitro [83]. However, BDNF per se is incapable of promoting proliferation and differentiation of NPCs derived from rat embryo telencephalon [78].

p0095 The primary function of p75NTR activation is the induction of apoptosis in some stages of development, though this receptor is expressed in a neurogenic area of the brain by mitotically active immature cells of the hippocampal SVZ, indicating a role in proliferation. Thus BDNF increases neuroblast generation and determines neuronal differentiation fate through activation of p75NTR during

development of dorsal root ganglia [84–86]. However, the mechanisms underlying the involvement of p75NTR in neuroblast generation by BDNF are not well understood and seem unlikely to affect NSC and NPC survival, but BDNF-promoted p75NTR activation through promotion of cell cycle progression and differentiation may have a role in final fate determination [84].

By exploring the neurogenic effects of BDNF in the CNS and combining it with cell therapy, novel strategies have been developed for treatment of neurological diseases. For example, mesenchymal stem cells (MSC) are known to secrete BDNF. In view of this, transplantation of these cells should increase BDNF levels and subsequently endogenous neurogenesis in diseases that causes neurodegeneration, such as Parkinson and Huntington diseases, stroke, and multiple sclerosis [87].

BDNF, as well as supplementation of the growth factors IGF-1 and EGF, facilitates the development of human embryonic stem cell (ESC) line derivation [88]. This is important, because of the obvious concerns with regard to the therapeutic use of ESCs obtained from fertilized embryos [40]. Accordingly, Lameu and coworkers showed that BDNF reverses the delay of neural differentiation of NSCs caused by inhibition of nitric oxide (NO) production together with upregulated p75NTR expression. As a possible mechanism, the lack of NO induces BDNF gene overexpression in these cells, probably in an attempt to compensate for deficient NO signaling and to maintain the progress of neural differentiation [89].

In addition to promoting cell differentiation, BDNF has neuroprotective properties that may sustain transplanted cells in cell therapy, because human MSCs (hMSCs) cultured in supernatant derived from ischemic brain extracts increased production of BDNF, NGF, VEGF, and hepatocyte growth factor. The capacity of these adult stem cells to increase expression of growth and trophic factors may be the key to the benefit provided by transplanted hMSCs in the ischemic brain [90].

7.5 NEUROTROPHIN-3

NT-3-induced dimerization of TrkC receptors results in receptor autophosphorylation and rapid generation of phosphorylated docking sites for adaptor cytoplasmic proteins as proteins containing phosphotyrosine-binding and/or Src homology 2 domains.

There are inactive splicing isoforms of TrkC presenting short cytoplasmic motifs without a tyrosine kinase domain that compete with the productive TrkC isoform for NT-3 binding, leading to a decreased bioavailability of NT-3 and subsequent TrkC activation [46]. Furthermore, a truncated isoform of TrkC associates with the postsynaptic density-95/discs large/zona occludens-1 domain of the scaffolding protein tamalin in the presence of NT-3, forming a complex with

ADP-ribosylation factor and guanine nucleotide-exchange factor (ARF-GEF) [91]. Therefore NT-3-mediated signaling through truncated TrkC results in activation of ARF6, which activates RAS-related C3 botulinum toxin substrate (Rac) and leads to membrane disturbance. Differential splicing of TrkC mRNA also results in expression of a TrkC isoform with an amino acid insert within the tyrosine kinase domain. This insert may modify the substrate specificity of this tyrosine kinase, inhibiting its activation for several substrates and interfering with its ability to promote neuronal differentiation [46].

p0125 Moreover, neurotrophins activate GTPases, such as cell division control protein 42 homolog (Cdc42) and Rac, through not yet elucidated mechanisms and pathways. Interestingly, neurotrophin effects on axonal growth and growth cone guidance depend on activity regulation of these G proteins [92]. In Schwann cells, stimulation of TrkC results in phosphorylation and activation of the Cdc42-GEF/Double's Big Sister (Dbl) signaling cascade [93] and activates other GEFs directly in neurons. Subsequent GEF-Son of Sevenless complex activity is regulated through phosphorylation by c-Abl and other tyrosine kinases [94].

p0130 NT-3 and BDNF stimulation of truncated TrkC receptors promotes differentiation into neurons only in the presence of p75NTR [95]. However, the p75NTR biological response to NT-3 versus BDNF can be quite different: NT-3 enhances neuronal differentiation of the cortical NPCs, whereas BDNF promotes their survival [96]. Similarly, cerebellar granule precursor cells express both TrkB and TrkC. In these cells BDNF promotes survival and enhances axonal elongation, whereas NT-3 increases neurite fasciculation [7,12].

s0035 7.6 EPIDERMAL GROWTH FACTOR

p0135 Cohen isolated and characterized EGF while trying to understand what made newborn mouse eyes open and teeth erupt precociously when treated with male mouse salivary gland extracts. Later he discovered that the EGF receptor is a ligand-activated tyrosine kinase protein using membranes from a human epidermoid carcinoma cell, a tumor that expresses high levels of EGF receptor (EGFR) [97,98]. Nowadays, there is plenty of information available on the structure of the EGFR [99], its relationship to oncogene products [100,101], and mitogenic responses induced by this receptor [102]. Recent investigations focus on second-messenger pathways that mediate biological responses to EGF.

p0140 The EGFR is composed of a single polypeptide chain of 1186 amino acid residues containing an N-linked oligosaccharide. A hydrophobic sequence separates an extracellular ligand-binding domain from a cytoplasmic domain that encodes an EGF-regulated tyrosine kinase. The organizational motif of the EGFR is similar to that of other growth

factor receptors (PDGF, insulin, IGF-1, colony-stimulating factor 1, and FGF) and its tyrosine kinase activity has a central role in the regulation of cell proliferation. EGF and EGF-like ligands bind with high affinity to the extracellular domain containing 10 or 11 N-linked oligosaccharide chains [103].

Usually this tyrosine kinase activity leads to activation p0145 of some intracellular signaling pathways such as the PI3K/AKT/mammalian target of rapamycin (mTOR) and ERK1/2 pathways [78]. Furthermore, activation of adenylate cyclase and inhibition of cAMP-specific phosphodiesterase activities may be induced by EGF, resulting in intracellular cAMP accumulation and protein kinase A (PKA) activation and consequent CREB stimulation [78]. Cells may migrate, proliferate, or differentiate depending on the pathway induced by EGFR activation. Distinct activation patterns in different cell types lead to a variety of signaling pathways, which in turn promote specific cell responses in specific cellular contexts as described below.

The EGFR has important functions in embryo development p0150 [104], including in the nervous system, by induction of proliferation and migration of neural stem cells during neural development (mouse embryonic day 10) and stimulating proliferation of neuroepithelial cells and NSCs from the SVZ (mouse embryonic day 14.5) [78,105,106]. The EGFR acts also during adult neurogenesis by promoting proliferation of NSCs of the SVZ through the cAMP/PKA/CREB pathway [107] and modulation of Sox2 and Pax6 (self-renewal markers) expression in NSCs and NPCs. The EGFR contributes to the maintenance of multipotency without disturbing the neurogenic potency, suggesting that EGFR might not promote differentiation [78,107–109]. Contradicting the hypothesis that EGFR functions are limited to NSC and NPC self-renewal, experiments *in vivo* showed that exogenous infusion of EGF into the SVZ induced NPC differentiation into pre-myelinating and myelinating oligodendrocytes after primary precursor proliferation and migration induction [78,110]. In line with this observation, migration during establishment of the developing nervous system occurs by EGF-stimulated ERK1/2 and PI3K/AKT pathways and focal adhesion kinase (FAK) activation [78,107,111–113]. This growth factor promotes ventrolateral migration of fetal telencephalon NPCs in the lateral cortical stream and radial migration in the direction of the cortical plate [78,111,113]. Furthermore, transit-amplifying precursor cells that later on differentiate into neuroblast cells are sensitive to stimulation by EGF and express high levels of EGFR [114].

7.7 FIBROBLAST GROWTH FACTOR

FGF is a polypeptide involved in several physiological processes, including paracrine signaling that modulates neural development and adult neurogenesis. It contains 23 isoforms (FGF-15 is not expressed in human tissue) and

s0040

p0155

activates five different tyrosine-kinase receptors (FGFRs) that are expressed in distinct patterns accordingly to the tissue type [115]. Receptor binding can induce the activation of several pathways including PLC- γ , PI3K, and ERK, which are regulated by the negative feedback of downstream transcriptional targets of these pathways [116]. Moreover, secreted FGF bioavailability can be modulated by its binding to extracellular heparin sulfate proteoglycans that prevents its degradation. When partially degraded, this complex releases FGF-glycosaminoglycan, an active FGFR ligand [117].

p0160 In the adult mammalian brain, FGF-2 is found in astrocyte cells of the SVZ and subgranular zone of the hippocampal dentate gyrus. However, proliferating NPCs express FGFR-1, -2, and -4, indicating that neurogenesis may be promoted by astrocytes releasing FGF-2 [118]. Functions of FGF in embryonic development are well established, and expression patterns of FGFR depend on the embryo stage. FGF-2 deficiency produces mice with a reduced number of neurons in the deep cortical layers. Moreover, mutations of the FGF-20 gene have been related to a predisposition for Parkinson disease development [115].

p0165 The importance of in vitro differentiation of stem cells has been recognized, keeping in mind possible therapeutic applications of cultured stem cells in neurological disorders. Thus, the modulation of stem cell fate during differentiation is currently a focus of study. FGF-2 is usually added to culture cell medium to maintain human ESC pluripotency by induction of multiple genes. Further, inhibition of the FGF signaling pathway causes human ESC differentiation [119]. It is noteworthy that mouse ESCs remain undifferentiated without FGF-2 supplementation in vitro, and leukemia-inhibitory factor and activin are enough to maintain the stem cell characteristics of pluripotency and self-renewal [120]. This can be promoted in rats in vivo by coactivating FGFR-1 and -3 along with higher concentrations of FGF-2 [121]. Beyond that, FGF-2 per se improves the commitment of ESCs to generate proliferative NSCs that can differentiate into all neural cell types [122]. Mouse stem cells can be induced to differentiation by FGF-4 as well as FGF-2, and human by FGF-2, -8, and -20 [123]. Once the neural fate of stem cells is established, proliferation can be induced by FGF-2 together with high concentrations of EGF. Short-term removal of these growth factors promotes neurogenesis and neurite outgrowth [124,125]. Moreover, inhibition of FGFR-1 activity reduces cell proliferation promoted by FGF-2 [118], and restriction of FGF-2 in the culture medium induces NSCs to differentiate into neurons, whereas at higher concentrations both neurons and astrocytes are obtained [126].

p0170 The presence of distinct FGF isoforms promotes differentiation into specialized neural phenotypes. For instance, FGF-8 induces telencephalic progenitors to differentiate into olfactory bulb neurons, whereas controlled FGF-2

treatment can induce cholinergic phenotype formation with motor-neuron characteristics, and FGF-20 has the ability to generate dopaminergic neurons from human ESCs when they are cocultured with mouse stromal cells [78].

7.8 GLIAL CELL LINE-DERIVED NEUROTROPHIC FACTOR

s0045

GDNF is a member of the neurotrophic factor family that p0175 was purified and characterized in 1993 from the supernatant of the B49 glial cell line based on its effects on the survival of midbrain dopaminergic neurons [127,128]. More recently, an increase in peripheral and central nervous system neurons was also related to GDNF-induced effects [129]. GDNF as well as other GDNF family ligands (GFLs) including neurturin, artemin, and persephin are part of the structurally related transforming growth factor- β superfamily. All GFLs possess enriched cysteine dimerization domains and are functional as homodimers [129].

Different from its suggestive name, GDNF is mainly p0180 expressed by neurons in some brain structures such as septum, striatum, and thalamus [130,131]. However, GDNF mRNA transcription has been detected in astrocyte and microglia cultures [132]. Several studies revealed that in pathological conditions such as inflammation, there is an increase in GDNF expression by astrocytes and microglia [133,134]. The GFLs have some signaling characteristics in common. They need the activation of two receptor types to exert their intracellular response: 1). the tyrosine kinase receptor RET, a single-pass transmembrane protein with an extracellular domain that transmits the signal to the cytoplasm; 2). the glycosylphosphatidylinositol-anchored coreceptor GFR α 1 (GDNF family receptor α 1), necessary for GDNF binding, containing an intracellular domain important for transmission of the intracellular signaling pathway [135,136]. RET, originally characterized by its functions as a proto-oncogene [137], is the most common receptor for all the GFLs, including GDNF [131,133,134,137–139].

As an agreed molecular mechanism of activation, p0185 canonical GDNF signaling is initialized by GDNF binding to GFR α 1, forming a homodimer [140], usually occurring at lipid rafts [129], followed by recruitment of RET receptors to these structures. Then, the GFR α 1-GDNF complex interacts with RET, which dimerizes and turns into the active tyrosine-phosphorylated form. In this state, various signaling pathways have been elucidated, including PI3K/AKT signaling for promotion of neural survival and transmission, activation of PLC- γ 1 as a regulator of neural transmission, and RAS/MAPK for cell survival and neurogenesis [141,142].

RET and GFR α 1 are differentially expressed in some p0190 regions of the CNS, as GFR α 1 is highly expressed when RET expression is almost undetectable [129,142]. There are

two explanations for this situation. First of all, it has been described that GFR α 1 can act in a non-cell-autonomous fashion, activating RET receptor *in trans* [143–145]. On one hand, GFR α 1 could act from the surface of other cells or be in a soluble form. On the other hand, GFR α 1 could signal through another kind of receptor in a fashion independent of RET. This hypothesis led to the discovery of neural cell adhesion molecule (NCAM; CD56) as an alternative signal receptor for GFR α 1 [146]. This pathway involving GFR α 1 and NCAM is called RET-independent signalization. Unlike RET, NCAM, specifically isoform p140^{NCAM}, can bind GDNF by itself, but in an inefficient way. In this situation GDNF interacts with two GFR α 1 receptor molecules to form a complex capable of interaction with NCAM [146]. This interaction produces a signal similar to that produced by homophilic NCAM–NCAM interactions. NCAM is associated in its intracellular domain with Fyn (a Src family member) [147], which becomes activated and recruits FAK, stimulating the MAPK pathway [148]. This GDNF–GFR α 1–NCAM pathway participates in migration, specification of neural morphology, and synaptogenesis [146,149–153].

GDNF is involved in physiological functions of various tissues including proliferation, migration, and differentiation of neural cells, as well as morphogenesis of the kidney; development of the enteric system; maintenance of sensory, parasympathetic, and enteric neurons; and maintenance and neuroprotection of dopaminergic and catecholaminergic populations [127,154–159]. In other words, GDNF participates in proliferation, migration, and differentiation of neural cells [129,160–163]. GDNF is essential for the formation of the enteric nervous system by regulating migration, proliferation, differentiation, and survival of enteric neural crest via RET–GFR α 1 signaling [160,162–169]. In vitro, GDNF acts on NPCs, promoting survival and differentiation into tyrosine hydroxylase (TH)-positive cells [170,171], and also on a subset of ventral mesencephalic neurons. It is able to generate, in addition to dopaminergic neurons, small-sized GABAergic cells [172].

In vitro studies of migration and differentiation of multipotent astrocytic stem cells show that GDNF added to the culture medium increases migration in prolonged exposure and most efficiently promotes neuronal differentiation compared to other neurotrophins [173]. Accordingly, some findings showed that GDNF acts as an attractant compound for neural precursors [174]. This neurotrophin at 50 ng/mL concentration promotes the differentiation and tangential migration of GABAergic neuronal precursors from the medial ganglionic eminence in a mechanism dependent on GFR α 1 and independent of RET and NCAM. This differentiation is promoted by activation of the MAPK pathway, by phosphorylation of the ERK1/2 kinases, and by moderate phosphorylation of AKT after 1 h of treatment [140,175].

In vitro protocols use a combination of GDNF and other factors after stimulus with retinoic acid and Sonic hedgehog for induction of neural differentiation of ESCs into motor neurons [176,177]. It has been shown that infusion of GDNF together with other neurotrophic factors contributes to the incorporation of predifferentiated motor neuron precursors into neural circuits [178–181]. In agreement with these findings, Garcia-Bennett and colleagues promoted, via delivery of mimetic growth factors through a mesoporous silica vehicle, specific differentiation of ESCs into motor neurons. Infusion of mimetic particles as well as of growth factor into the damaged area could be an alternative to the treatment of motor neurodegenerative disorders such as amyotrophic lateral sclerosis [182].

Depending on the context, GDNF may also favor glial differentiation. Boku and colleagues [183] showed that a 50 ng/mL GDNF treatment promotes an increase in the ratio of astrocyte-like glial fibrillary acidic protein-positive cells over Tuj1-positive cells after differentiation induction by *all-trans* retinoic acid. This astrogliogenic effect from neural precursors of the dentate gyrus is promoted by increasing the phosphorylation of STAT3, affecting neither proliferation nor apoptosis rates [183].

7.9 INSULIN-LIKE GROWTH FACTOR

The discovery of IGF goes back to 1963 when Froesch and coworkers observed that there was a serum factor similar to insulin, but its induced effects were not suppressed even in the presence of anti-insulin antibodies. Subsequent studies showed growth-promoting effects by IGF and the characterization of isoforms I and II [184]. The insulin-like growth factor family signaling system embraces two polypeptides (IGF-1 and IGF-2) and type 1 and 2 IGF receptors (IGF-1R, -2R). Both ligands can bind to IGF-1R with different affinities, triggering diverse biological responses [185].

IGF-1R is a class II tyrosine kinase receptor that, differing from TrkA, B, and C, is a heterotetramer composed of two extracellular α subunits containing the binding site and two β subunits that penetrate the membrane and include the tyrosine kinase domain [186]. This system also has IGF-binding proteins responsible for controlling the amount of free IGF-1 and -2 in the circulatory system, therefore modulating their binding to the receptors [185].

In the brain, IGF-1 and IGF-1R are expressed in similar areas, indicating an autocrine and/or paracrine action on this tissue. IGF-1 available in the CNS can be produced in peripheral tissues, being captured by the blood–brain barrier via specific receptors and reaching the hypothalamus and hippocampus. Evidence for a low synthesis of these peptides in the brain exists, although is not well defined [185].

IGF-1 signaling is present throughout development. The growth factor increases the number of embryos becoming

86 Neural Surface Antigens

blastocysts in normal and critical situations. For instance, IGF-1-mediated responses are directed against different types of stressors that could lead to a decreased survival ratio, such as toxicity, oxidative stress, and exposure to tumor necrosis factor- α . Although IGF-1 gene-knockout mice are viable, they show a retarded development of the CNS with loss of mass in several brain areas, especially involving the white matter [187]. Moreover, IGF is also related to cancer development, because cerebrospinal fluid samples from patients with glioblastoma multiforme show elevated IGF-2 levels and IGF-2-dependently stimulated stem cell proliferation [188].

p0235 In vivo studies endorse the importance of this growth factor in the cell fate of stem cells [189]. Hippocampal NSCs of rats submitted to IGF-1 infusion proliferate and differentiate in neurons [190]. Rat hippocampal NSCs can be stimulated in vitro to differentiate into oligodendrocytes in the presence of IGF-1 [71,191].

p0240 Furthermore, IGF-1 has antiapoptotic effects; this factor promotes cell survival of cortical neurons cultured on serum-free medium, in other words, medium that lacks essential nutrients for cell survival [192].

s0055 7.10 CONCLUSION

p0245 In summary, various intracellular pathways can be triggered depending on the expression patterns of growth and neurotrophic factors and their respective receptors in NSCs and NPCs. These signals, via subsequent modulation of transcription factors and gene expression, thereby determine stem cell fate, governing proliferation versus differentiation (see Table 7.1 for some examples).

p0250 Thus, as an oversimplified synopsis, whereas NT-3, BDNF, FGF, and GDNF mostly have implications for the progress of neurogenesis and neuronal phenotype determination, proliferation is favored in the presence of EGF and FGF. However, removal or combination or even different concentrations of these factors may lead to diverse effects by modulating NSC and NPC fate and neuronal and astroglial fate specification. Overall, the specific effects mediated by the discussed growth and neurotrophic receptors very much depend on the cellular context.

s0065 REFERENCES

- [1] Cho T, et al. Long-term potentiation promotes proliferation/survival and neuronal differentiation of neural stem/progenitor cells. *PLoS One* 2013;8(10):e76860.
- [2] LeRoith D, Roberts Jr CT. Insulin-like growth factors. *Ann NY Acad Sci* 1993;692:1–9.
- [3] LeRoith D, Roberts Jr CT. Insulin-like growth factors and their receptors in normal physiology and pathological states. *J Pediatr Endocrinol* 1993;6(3–4):251–5.
- [4] Reuss B, von Bohlen, Halbach O. Fibroblast growth factors and their receptors in the central nervous system. *Cell Tissue Res* 2003;313(2):139–57.
- [5] Hsu YC, Lee DC, Chiu IM. Neural stem cells, neural progenitors, and neurotrophic factors. *Cell Transplant* 2007;16(2):133–50.
- [6] Heldin CH. Dimerization of cell surface receptors in signal transduction. *Cell* 1995;80(2):213–23.
- [7] Segal RA. Selectivity in neurotrophin signaling: theme and variations. *Annu Rev Neurosci* 2003;26:299–330.
- [8] Segal RA, Greenberg ME. Intracellular signaling pathways activated by neurotrophic factors. *Annu Rev Neurosci* 1996;19:463–89.
- [9] Huang EJ, Reichardt LF. Neurotrophins: roles in neuronal development and function. *Annu Rev Neurosci* 2001;24:677–736.
- [10] Poo MM. Neurotrophins as synaptic modulators. *Nat Rev Neurosci* 2001;2(1):24–32.
- [11] Huang EJ, Reichardt LF. Trk receptors: roles in neuronal signal transduction. *Annu Rev Biochem* 2003;72:609–42.
- [12] Benito-Gutierrez E, Garcia-Fernandez J, Comella JX. Origin and evolution of the Trk family of neurotrophic receptors. *Mol Cell Neurosci* 2006;31(2):179–92.
- [13] Snider WD, Johnson Jr EM. Neurotrophic molecules. *Ann Neurol* 1989;26(4):489–506.
- [14] Eide FF, Lowenstein DH, Reichardt LF. Neurotrophins and their receptors—current concepts and implications for neurologic disease. *Exp Neurol* 1993;121(2):200–14.
- [15] Korschning S. The neurotrophic factor concept: a reexamination. *J Neurosci* 1993;13(7):2739–48.
- [16] Zhang L, et al. NGF and NT-3 have differing effects on the growth of dorsal root axons in developing mammalian spinal cord. *J Neurosci* 1994;14(9):5187–201.
- [17] Barbacid M, et al. The trk family of tyrosine protein kinase receptors. *Biochim Biophys Acta* 1991;1072(2–3):115–27.
- [18] Bothwell M. Tissue localization of nerve growth factor and nerve growth factor receptors. *Curr Top Microbiol Immunol* 1991;165:55–70.
- [19] Chao MV. Neurotrophin receptors: a window into neuronal differentiation. *Neuron* 1992;9(4):583–93.
- [20] Chao MV. Growth factor signaling: where is the specificity? *Cell* 1992;68(6):995–7.
- [21] Chao MV, Battleman DS, Benedetti M. Receptors for nerve growth factor. *Int Rev Cytol* 1992;137B:169–80.
- [22] Barbacid M. Nerve growth factor: a tale of two receptors. *Oncogene* 1993;8(8):2033–42.
- [23] Raffioni S, Bradshaw RA, Buxser SE. The receptors for nerve growth factor and other neurotrophins. *Annu Rev Biochem* 1993;62:823–50.
- [24] Cohen-Cory S, et al. Depolarizing influences increase low-affinity NGF receptor gene expression in cultured Purkinje neurons. *Exp Neurol* 1993;119(2):165–75.
- [25] Greenberg ME, Hermanowski AL, Ziff EB. Effect of protein synthesis inhibitors on growth factor activation of c-fos, c-myc, and actin gene transcription. *Mol Cell Biol* 1986;6(4):1050–7.
- [26] Greenberg ME, Ziff EB, Greene LA. Stimulation of neuronal acetylcholine receptors induces rapid gene transcription. *Science* 1986;234(4772):80–3.
- [27] Pincus DW, DiCicco-Bloom EM, Black IB. Vasoactive intestinal peptide regulates mitosis, differentiation and survival of cultured sympathetic neuroblasts. *Nature* 1990;343(6258):564–7.
- [28] Schwartz JP. Neurotransmitters as neurotrophic factors: a new set of functions. *Int Rev Neurobiol* 1992;34:1–23.
- [29] Berkemeier LR, et al. Neurotrophin-5: a novel neurotrophic factor that activates trk and trkB. *Neuron* 1991;7(5):857–66.

- [30] Cordon-Cardo C, et al. The trk tyrosine protein kinase mediates the mitogenic properties of nerve growth factor and neurotrophin-3. *Cell* 1991;66(1):173–83.
- [31] Glass DJ, et al. TrkB mediates BDNF/NT-3-dependent survival and proliferation in fibroblasts lacking the low affinity NGF receptor. *Cell* 1991;66(2):405–13.
- [32] Hempstead BL, et al. High-affinity NGF binding requires coexpression of the trk proto-oncogene and the low-affinity NGF receptor. *Nature* 1991;350(6320):678–83.
- [33] Kaplan DR, et al. The trk proto-oncogene product: a signal transducing receptor for nerve growth factor. *Science* 1991;252(5005):554–8.
- [34] Kaplan DR, Martin-Zanca D, Parada LF. Tyrosine phosphorylation and tyrosine kinase activity of the trk proto-oncogene product induced by NGF. *Nature* 1991;350(6314):158–60.
- [35] Klein R, et al. The trk proto-oncogene encodes a receptor for nerve growth factor. *Cell* 1991;65(1):189–97.
- [36] Klein R, et al. The trkB tyrosine protein kinase is a receptor for brain-derived neurotrophic factor and neurotrophin-3. *Cell* 1991;66(2):395–403.
- [37] Lamballe F, Klein R, Barbacid M. trkC, a new member of the trk family of tyrosine protein kinases, is a receptor for neurotrophin-3. *Cell* 1991;66(5):967–79.
- [38] Lamballe F, Klein R, Barbacid M. The trk family of oncogenes and neurotrophin receptors. *Princess Takamatsu Symp* 1991; 22:153–70.
- [39] Nebreda AR, et al. Induction by NGF of meiotic maturation of *Xenopus* oocytes expressing the trk proto-oncogene product. *Science* 1991;252(5005):558–61.
- [40] Soppet D, et al. The neurotrophic factors brain-derived neurotrophic factor and neurotrophin-3 are ligands for the trkB tyrosine kinase receptor. *Cell* 1991;65(5):895–903.
- [41] Squinto SP, et al. trkB encodes a functional receptor for brain-derived neurotrophic factor and neurotrophin-3 but not nerve growth factor. *Cell* 1991;65(5):885–93.
- [42] Chen Y, et al. Multiple roles of the p75 neurotrophin receptor in the nervous system. *J Int Med Res* 2009;37(2):281–8.
- [43] Corbit KC, Foster DA, Rosner MR. Protein kinase C δ mediates neurogenic but not mitogenic activation of mitogen-activated protein kinase in neuronal cells. *Mol Cell Biol* 1999;19(6):4209–18.
- [44] Klein M, Hempstead BL, Teng KK. Activation of STAT5-dependent transcription by the neurotrophin receptor Trk. *J Neurobiol* 2005;63(2):159–71.
- [45] Minichiello L, et al. Mechanism of TrkB-mediated hippocampal long-term potentiation. *Neuron* 2002;36(1):121–37.
- [46] Reichardt LF. Neurotrophin-regulated signalling pathways. *Philos Trans R Soc Lond B Biol Sci* 2006;361(1473):1545–64.
- [47] Toledo-Aral JJ, et al. A single pulse of nerve growth factor triggers long-term neuronal excitability through sodium channel gene induction. *Neuron* 1995;14(3):607–11.
- [48] Nakagawara A. Trk receptor tyrosine kinases: a bridge between cancer and neural development. *Cancer Lett* 2001;169(2):107–14.
- [49] Levi-Montalcini R, Angeletti PU. Nerve growth factor. *Physiol Rev* 1968;48(3):534–69.
- [50] Levi-Montalcini R, et al. In vitro effects of the nerve growth factor on the fine structure of the sensory nerve cells. *Brain Res* 1968;8(2):347–62.
- [51] Thoenen H, Barde YA. Physiology of nerve growth factor. *Physiol Rev* 1980;60(4):1284–335.
- [52] Chen KS, et al. Disruption of a single allele of the nerve growth factor gene results in atrophy of basal forebrain cholinergic neurons and memory deficits. *J Neurosci* 1997;17(19):7288–96.
- [53] Cuello AC. Trophic factor therapy in the adult CNS: remodelling of injured basalo-cortical neurons. *Prog Brain Res* 1994;100: 213–21.
- [54] Ebendal T. Function and evolution in the NGF family and its receptors. *J Neurosci Res* 1992;32(4):461–70.
- [55] Hefti F, Knusel B, Lapchak PA. Protective effects of nerve growth factor and brain-derived neurotrophic factor on basal forebrain cholinergic neurons in adult rats with partial fimbrial transections. *Prog Brain Res* 1993;98:257–63.
- [56] Bruno MA, Cuello AC. Activity-dependent release of precursor nerve growth factor, conversion to mature nerve growth factor, and its degradation by a protease cascade. *Proc Natl Acad Sci USA* 2006; 103(17):6735–40.
- [57] Fahnestock M, Yu G, Coughlin MD. ProNGF: a neurotrophic or an apoptotic molecule? *Prog Brain Res* 2004;146:101–10.
- [58] Fahnestock M, et al. The nerve growth factor precursor proNGF exhibits neurotrophic activity but is less active than mature nerve growth factor. *J Neurochem* 2004;89(3):581–92.
- [59] Chao MV, Rajagopal R, Lee FS. Neurotrophin signalling in health and disease. *Clin Sci (Lond)* 2006;110(2):167–73.
- [60] Majdan M, Miller FD. Neuronal life and death decisions functional antagonism between the Trk and p75 neurotrophin receptors. *Int J Dev Neurosci* 1999;17(3):153–61.
- [61] Dobrowsky RT, Carter BD. p75 neurotrophin receptor signaling: mechanisms for neurotrophic modulation of cell stress? *J Neurosci Res* 2000;61(3):237–43.
- [62] Lee R, et al. Regulation of cell survival by secreted proneurotrophins. *Science* 2001;294(5548):1945–8.
- [63] Roux PP, Barker PA. Neurotrophin signaling through the p75 neurotrophin receptor. *Prog Neurobiol* 2002;67(3):203–33.
- [64] Kaplan DR, Miller FD. Neurotrophin signal transduction in the nervous system. *Curr Opin Neurobiol* 2000;10(3):381–91.
- [65] Lemmon MA, et al. Independent binding of peptide ligands to the SH2 and SH3 domains of Grb2. *J Biol Chem* 1994;269(50):31653–8.
- [66] Lemmon MA, Schlessinger J. Regulation of signal transduction and signal diversity by receptor oligomerization. *Trends Biochem Sci* 1994;19(11):459–63.
- [67] Bergeron JJ, et al. Endosomes, receptor tyrosine kinase internalization and signal transduction. *Biosci Rep* 1995;15(6):411–8.
- [68] Cattaneo E, McKay R. Proliferation and differentiation of neuronal stem cells regulated by nerve growth factor. *Nature* 1990; 347(6295):762–5.
- [69] Levenberg S, et al. Neurotrophin-induced differentiation of human embryonic stem cells on three-dimensional polymeric scaffolds. *Tissue Eng* 2005;11(3–4):506–12.
- [70] Nakajima K, et al. Essential role of NKCC1 in NGF-induced neurite outgrowth. *Biochem Biophys Res Commun* 2007;359(3):604–10.
- [71] Choi KC, et al. Effect of single growth factor and growth factor combinations on differentiation of neural stem cells. *J Korean Neurosurg Soc* 2008;44(6):375–81.
- [72] Lachyankar MB, et al. Embryonic precursor cells that express Trk receptors: induction of different cell fates by NGF, BDNF, NT-3, and CNTF. *Exp Neurol* 1997;144(2):350–60.
- [73] Ernsberger U. Role of neurotrophin signalling in the differentiation of neurons from dorsal root ganglia and sympathetic ganglia. *Cell Tissue Res* 2009;336(3):349–84.

88 Neural Surface Antigens

- [74] Singh RP, et al. Retentive multipotency of adult dorsal root ganglia stem cells. *Cell Transpl* 2009;18(1):55–68.
- [75] Angelastro JM, et al. Regulated expression of ATF5 is required for the progression of neural progenitor cells to neurons. *J Neurosci* 2003;23(11):4590–600.
- [76] Jaworski DM, Perez-Martinez L. Tissue inhibitor of metalloproteinase-2 (TIMP-2) expression is regulated by multiple neural differentiation signals. *J Neurochem* 2006;98(1):234–47.
- [77] Hess J, Angel P, Schorpp-Kistner M. AP-1 subunits: quarrel and harmony among siblings. *J Cell Sci* 2004;117(Pt 25):5965–73.
- [78] Oliveira SL, et al. Functions of neurotrophins and growth factors in neurogenesis and brain repair. *Cytom A* 2013;83(1):76–89.
- [79] Barde YA, Edgar D, Thoenen H. Purification of a new neurotrophic factor from mammalian brain. *EMBO J* 1982;1(5):549–53.
- [80] Lu B, Pang PT, Woo NH. The yin and yang of neurotrophin action. *Nat Rev Neurosci* 2005;6(8):603–14.
- [81] Binder DK, Scharfman HE. Brain-derived neurotrophic factor. *Growth Factors* 2004;22(3):123–31.
- [82] Bartkowska K, Turlejski K, Djavadian RL. Neurotrophins and their receptors in early development of the mammalian nervous system. *Acta Neurobiol Exp (Wars)* 2010;70(4):454–67.
- [83] Gascon E, et al. Sequential activation of p75 and TrkB is involved in dendritic development of subventricular zone-derived neuronal progenitors in vitro. *Eur J Neurosci* 2005;21(1):69–80.
- [84] Young KM, et al. p75 neurotrophin receptor expression defines a population of BDNF-responsive neurogenic precursor cells. *J Neurosci* 2007;27(19):5146–55.
- [85] Pruginin-Bluger M, Shelton DL, Kalcheim C. A paracrine effect for neuron-derived BDNF in development of dorsal root ganglia: stimulation of Schwann cell myelin protein expression by glial cells. *Mech Dev* 1997;61(1–2):99–111.
- [86] Hosomi S, et al. The p75 receptor is required for BDNF-induced differentiation of neural precursor cells. *Biochem Biophys Res Commun* 2003;301(4):1011–5.
- [87] Paul G, Anisimov SV. The secretome of mesenchymal stem cells: potential implications for neuroregeneration. *Biochimie* 2013;95(12):2246–56.
- [88] Fan Y, et al. Improved efficiency of microsurgical enucleated tripronuclear zygotes development and embryonic stem cell derivation by supplementing epidermal growth factor, brain-derived neurotrophic factor, and insulin-like growth factor-1. *Stem Cells Dev* 2014;23(6):563–75.
- [89] Lameu C, et al. Interactions between the NO-citrulline cycle and brain-derived neurotrophic factor in differentiation of neural stem cells. *J Biol Chem* 2012;287(35):29690–701.
- [90] Chen X, et al. Ischemic rat brain extracts induce human marrow stromal cell growth factor production. *Neuropathology* 2002;22(4):275–9.
- [91] Esteban PF, et al. A kinase-deficient TrkC receptor isoform activates Arf6-Rac1 signaling through the scaffold protein tamalin. *J Cell Biol* 2006;173(2):291–9.
- [92] Yuan XB, et al. Signalling and crosstalk of Rho GTPases in mediating axon guidance. *Nat Cell Biol* 2003;5(1):38–45.
- [93] Blanke S, Jackle H. Novel guanine nucleotide exchange factor GEFmeso of *Drosophila melanogaster* interacts with Ral and Rho GTPase Cdc42. *FASEB J* 2006;20(6):683–91.
- [94] Sini P, et al. Abl-dependent tyrosine phosphorylation of Sos-1 mediates growth-factor-induced Rac activation. *Nat Cell Biol* 2004;6(3):268–74.
- [95] Hapner SJ, et al. Neural differentiation promoted by truncated trkB receptors in collaboration with p75(NTR). *Dev Biol* 1998;201(1):90–100.
- [96] Ghosh A, Greenberg ME. Distinct roles for bFGF and NT-3 in the regulation of cortical neurogenesis. *Neuron* 1995;15(1):89–103.
- [97] Cohen S. Origins of growth factors: NGF and EGF. *Ann NY Acad Sci* 2004;1038:98–102.
- [98] Cohen S. Origins of growth factors: NGF and EGF. *J Biol Chem* 2008;283(49):33793–7.
- [99] Needham SR, et al. Structure-function relationships and supramolecular organization of the EGFR (epidermal growth factor receptor) on the cell surface. *Biochem Soc Trans* 2014;42(1):114–9.
- [100] Burgess AW, et al. EGF receptor family: twisting targets for improved cancer therapies. *Growth Factors* 2014;32(2):74–81.
- [101] Tomas A, Futter CE, Eden ER. EGF receptor trafficking: consequences for signaling and cancer. *Trends Cell Biol* 2014;24(1):26–34.
- [102] Aasrum M, et al. The involvement of the docking protein Gab1 in mitogenic signalling induced by EGF and HGF in rat hepatocytes. *Biochim Biophys Acta* 2013;1833(12):3286–94.
- [103] Carpenter G, Cohen S. Epidermal growth factor. *J Biol Chem* 1990;265(14):7709–12.
- [104] Reinchisi G, et al. Sonic Hedgehog modulates EGFR dependent proliferation of neural stem cells during late mouse embryogenesis through EGFR transactivation. *Front Cell Neurosci* 2013;7:166.
- [105] Threadgill DW, et al. Targeted disruption of mouse EGF receptor: effect of genetic background on mutant phenotype. *Science* 1995;269(5221):230–4.
- [106] Kornblum HI, et al. Prenatal ontogeny of the epidermal growth factor receptor and its ligand, transforming growth factor alpha, in the rat brain. *J Comp Neurol* 1997;380(2):243–61.
- [107] Ciccolini F, et al. Prospective isolation of late development multipotent precursors whose migration is promoted by EGFR. *Dev Biol* 2005;284(1):112–25.
- [108] Hu Q, et al. The EGF receptor-sox2-EGF receptor feedback loop positively regulates the self-renewal of neural precursor cells. *Stem Cells* 2010;28(2):279–86.
- [109] Jia H, et al. Pax6 regulates the epidermal growth factor-responsive neural stem cells of the subventricular zone. *Neuroreport* 2011;22(9):448–52.
- [110] Gonzalez-Perez O, et al. Epidermal growth factor induces the progeny of subventricular zone type B cells to migrate and differentiate into oligodendrocytes. *Stem Cells* 2009;27(8):2032–43.
- [111] Caric D, et al. EGFRs mediate chemotactic migration in the developing telencephalon. *Development* 2001;128(21):4203–16.
- [112] Jiang Q, et al. EGF-induced cell migration is mediated by ERK and PI3K/AKT pathways in cultured human lens epithelial cells. *J Ocul Pharmacol Ther* 2006;22(2):93–102.
- [113] Burrows RC, et al. Response diversity and the timing of progenitor cell maturation are regulated by developmental changes in EGFR expression in the cortex. *Neuron* 1997;19(2):251–67.
- [114] Cesetti T, et al. Analysis of stem cell lineage progression in the neonatal subventricular zone identifies EGFR+/NG2– cells as transit-amplifying precursors. *Stem Cells* 2009;27(6):1443–54.
- [115] Itoh N, Ornitz DM. Fibroblast growth factors: from molecular evolution to roles in development, metabolism and disease. *J Biochem* 2011;149(2):121–30.
- [116] Lanner F, Rossant J. The role of FGF/Erk signaling in pluripotent cells. *Development* 2010;137(20):3351–60.

- [117] Ornitz DM, Itoh N. Fibroblast growth factors. *Genome Biol* 2001;2(3):REVIEWS3005.
- [118] Mudo G, et al. The FGF-2/FGFRs neurotrophic system promotes neurogenesis in the adult brain. *J Neural Transm* 2009;116(8):995–1005.
- [119] Vallier L, Alexander M, Pedersen RA. Activin/Nodal and FGF pathways cooperate to maintain pluripotency of human embryonic stem cells. *J Cell Sci* 2005;118(Pt 19):4495–509.
- [120] Daheron L, et al. LIF/STAT3 signaling fails to maintain self-renewal of human embryonic stem cells. *Stem Cells* 2004;22(5):770–8.
- [121] Maric D, et al. Self-renewing and differentiating properties of cortical neural stem cells are selectively regulated by basic fibroblast growth factor (FGF) signaling via specific FGF receptors. *J Neurosci* 2007;27(8):1836–52.
- [122] Guillemot F, Zimmer C. From cradle to grave: the multiple roles of fibroblast growth factors in neural development. *Neuron* 2011;71(4):574–88.
- [123] Kosaka N, et al. FGF-4 regulates neural progenitor cell proliferation and neuronal differentiation. *FASEB J* 2006;20(9):1484–5.
- [124] Schwindt TT, et al. Short-term withdrawal of mitogens prior to plating increases neuronal differentiation of human neural precursor cells. *PLoS One* 2009;4(2):e4642.
- [125] Schwindt TT, et al. Effects of FGF-2 and EGF removal on the differentiation of mouse neural precursor cells. *Acad Bras Cienc* 2009;81(3):443–52.
- [126] Gage FH, et al. Survival and differentiation of adult neuronal progenitor cells transplanted to the adult brain. *Proc Natl Acad Sci USA* 1995;92(25):11879–83.
- [127] Tomac A, et al. Protection and repair of the nigrostriatal dopaminergic system by GDNF in vivo. *Nature* 1995;373(6512):335–9.
- [128] Lin LF, et al. GDNF: a glial cell line-derived neurotrophic factor for midbrain dopaminergic neurons. *Science* 1993;260(5111):1130–2.
- [129] Airaksinen MS, Saarma M. The GDNF family: signalling, biological functions and therapeutic value. *Nat Rev Neurosci* 2002;3(5):383–94.
- [130] Pochon NA, et al. Neuronal GDNF expression in the adult rat nervous system identified by *in situ* hybridization. *Eur J Neurosci* 1997;9(3):463–71.
- [131] Trupp M, et al. Complementary and overlapping expression of glial cell line-derived neurotrophic factor (GDNF), c-ret proto-oncogene, and GDNF receptor-alpha indicates multiple mechanisms of trophic actions in the adult rat CNS. *J Neurosci* 1997;17(10):3554–67.
- [132] Saavedra A, Baltazar G, Duarte EP. Driving GDNF expression: the green and the red traffic lights. *Prog Neurobiol* 2008;86(3):186–215.
- [133] Bresjanac M, Antauer G. Reactive astrocytes of the quinolinic acid-lesioned rat striatum express GFR α 1 as well as GDNF in vivo. *Exp Neurol* 2000;164(1):53–9.
- [134] Hughes PE, et al. Activity and injury-dependent expression of inducible transcription factors, growth factors and apoptosis-related genes within the central nervous system. *Prog Neurobiol* 1999;57(4):421–50.
- [135] Treanor JJ, et al. Characterization of a multicomponent receptor for GDNF. *Nature* 1996;382(6586):80–3.
- [136] Jing S, et al. GDNF-induced activation of the ret protein tyrosine kinase is mediated by GDNFR- α a novel receptor for GDNF. *Cell* 1996;85(7):1113–24.
- [137] Takahashi M. The GDNF/RET signaling pathway and human diseases. *Cytokine Growth Factor Rev* 2001;12(4):361–73.
- [138] Durbec P, et al. GDNF signalling through the Ret receptor tyrosine kinase. *Nature* 1996;381(6585):789–93.
- [139] Trupp M, et al. Functional receptor for GDNF encoded by the c-ret proto-oncogene. *Nature* 1996;381(6585):785–9.
- [140] Pozas E, Ibanez CF. GDNF and GFR α 1 promote differentiation and tangential migration of cortical GABAergic neurons. *Neuron* 2005;45(5):701–13.
- [141] Sariola H, Saarma M. Novel functions and signalling pathways for GDNF. *J Cell Sci* 2003;116(Pt 19):3855–62.
- [142] Santoro M, et al. Minireview: RET: normal and abnormal functions. *Endocrinology* 2004;145(12):5448–51.
- [143] Ledda F, Paratcha G, Ibanez CF. Target-derived GFR α 1 as an attractive guidance signal for developing sensory and sympathetic axons via activation of Cdk5. *Neuron* 2002;36(3):387–401.
- [144] Paratcha G, et al. Released GFR α 1 potentiates downstream signalling, neuronal survival, and differentiation via a novel mechanism of recruitment of c-Ret to lipid rafts. *Neuron* 2001;29(1):171–84.
- [145] Worley DS, et al. Developmental regulation of GDNF response and receptor expression in the enteric nervous system. *Development* 2000;127(20):4383–93.
- [146] Paratcha G, Ledda F, Ibanez CF. The neural cell adhesion molecule NCAM is an alternative signalling receptor for GDNF family ligands. *Cell* 2003;113(7):867–79.
- [147] Beggs HE, et al. NCAM140 interacts with the focal adhesion kinase p125(fak) and the SRC-related tyrosine kinase p59(fyn). *J Biol Chem* 1997;272(13):8310–9.
- [148] Paratcha G, Ledda F. GDNF and GFR α a versatile molecular complex for developing neurons. *Trends Neurosci* 2008;31(8):384–91.
- [149] Iwase T, et al. Glial cell line-derived neurotrophic factor-induced signaling in Schwann cells. *J Neurochem* 2005;94(6):1488–99.
- [150] Ledda F, et al. GDNF and GFR α 1 promote formation of neuronal synapses by ligand-induced cell adhesion. *Nat Neurosci* 2007;10(3):293–300.
- [151] Nielsen J, et al. Role of glial cell line-derived neurotrophic factor (GDNF)-neural cell adhesion molecule (NCAM) interactions in induction of neurite outgrowth and identification of a binding site for NCAM in the heel region of GDNF. *J Neurosci* 2009;29(36):11360–76.
- [152] Niethammer P, et al. Cosignaling of NCAM via lipid rafts and the FGF receptor is required for neuritogenesis. *J Cell Biol* 2002;157(3):521–32.
- [153] Sjostrand D, et al. Disruption of the GDNF binding site in NCAM dissociates ligand binding and homophilic cell adhesion. *J Biol Chem* 2007;282(17):12734–40.
- [154] Arenas E, et al. GDNF prevents degeneration and promotes the phenotype of brain noradrenergic neurons in vivo. *Neuron* 1995;15(6):1465–73.
- [155] Gash DM, et al. Functional recovery in parkinsonian monkeys treated with GDNF. *Nature* 1996;380(6571):252–5.
- [156] Gerlach TH, Zile MH. Effect of retinoic acid and apo-RBP on serum retinol concentration in acute renal failure. *FASEB J* 1991;5(1):86–92.
- [157] Kordower JH, et al. Neurodegeneration prevented by lentiviral vector delivery of GDNF in primate models of Parkinson's disease. *Science* 2000;290(5492):767–73.
- [158] Pascual A, et al. Absolute requirement of GDNF for adult catecholaminergic neuron survival. *Nat Neurosci* 2008;11(7):755–61.
- [159] Ungerstedt U. 6-Hydroxy-dopamine induced degeneration of central monoamine neurons. *Eur J Pharmacol* 1968;5(1):107–10.
- [160] Young HM, et al. GDNF is a chemoattractant for enteric neural cells. *Dev Biol* 2001;229(2):503–16.

90 Neural Surface Antigens

- [161] Gianino S, et al. GDNF availability determines enteric neuron number by controlling precursor proliferation. *Development* 2003; 130(10):2187–98.
- [162] Natarajan D, et al. Requirement of signalling by receptor tyrosine kinase RET for the directed migration of enteric nervous system progenitor cells during mammalian embryogenesis. *Development* 2002;129(22):5151–60.
- [163] Taraviras S, et al. Signalling by the RET receptor tyrosine kinase and its role in the development of the mammalian enteric nervous system. *Development* 1999;126(12):2785–97.
- [164] Heuckeroth RO, et al. Neurturin and GDNF promote proliferation and survival of enteric neuron and glial progenitors in vitro. *Dev Biol* 1998;200(1):116–29.
- [165] Iwashita T, et al. Hirschsprung disease is linked to defects in neural crest stem cell function. *Science* 2003;301(5635):972–6.
- [166] Moore SW. The contribution of associated congenital anomalies in understanding Hirschsprung's disease. *Pediatr Surg Int* 2006; 22(4):305–15.
- [167] Pichel JG, et al. Defects in enteric innervation and kidney development in mice lacking GDNF. *Nature* 1996;382(6586):73–6.
- [168] Sanchez MP, et al. Renal agenesis and the absence of enteric neurons in mice lacking GDNF. *Nature* 1996;382(6586):70–3.
- [169] Uesaka T, Nagashimada M, Enomoto H. GDNF signaling levels control migration and neuronal differentiation of enteric ganglion precursors. *J Neurosci* 2013;33(41):16372–82.
- [170] Sun ZH, et al. GDNF augments survival and differentiation of TH-positive neurons in neural progenitor cells. *Cell Biol Int* 2004; 28(4):323–5.
- [171] Widmer HR, et al. Glial cell line-derived neurotrophic factor stimulates the morphological differentiation of cultured ventral mesencephalic calbindin- and calretinin-expressing neurons. *Exp Neurol* 2000;164(1):71–81.
- [172] Schaller B, et al. Effect of GDNF on differentiation of cultured ventral mesencephalic dopaminergic and non-dopaminergic calretinin-expressing neurons. *Brain Res* 2005;1036(1–2):163–72.
- [173] Douglas-Escobar M, et al. Neurotrophin-induced migration and neuronal differentiation of multipotent astrocytic stem cells in vitro. *PLoS One* 2012;7(12):e51706.
- [174] Cornejo M, et al. Effect of NRG1, GDNF, EGF and NGF in the migration of a Schwann cell precursor line. *Neurochem Res* 2010; 35(10):1643–51.
- [175] Perrinjaquet M, et al. MET signaling in GABAergic neuronal precursors of the medial ganglionic eminence restricts GDNF activity in cells that express GFR α 1 and a new transmembrane receptor partner. *J Cell Sci* 2011;124(Pt 16):2797–805.
- [176] Li XJ, et al. Specification of motoneurons from human embryonic stem cells. *Nat Biotechnol* 2005;23(2):215–21.
- [177] Marchetto MC, Winner B, Gage FH. Pluripotent stem cells in neurodegenerative and neurodevelopmental diseases. *Hum Mol Genet* 2010;19(R1):R71–6.
- [178] Li XJ, et al. Directed differentiation of ventral spinal progenitors and motor neurons from human embryonic stem cells by small molecules. *Stem Cells* 2008;26(4):886–93.
- [179] Rakowicz WP, et al. Glial cell line-derived neurotrophic factor promotes the survival of early postnatal spinal motor neurons in the lateral and medial motor columns in slice culture. *J Neurosci* 2002;22(10):3953–62.
- [180] Wichterle H, et al. Directed differentiation of embryonic stem cells into motor neurons. *Cell* 2002;110(3):385–97.
- [181] Zurn AD, et al. Combined effects of GDNF, BDNF, and CNTF on motoneuron differentiation in vitro. *J Neurosci Res* 1996;44(2):133–41.
- [182] Garcia-Bennett AE, et al. Delivery of differentiation factors by mesoporous silica particles assists advanced differentiation of transplanted murine embryonic stem cells. *Stem Cells Transl Med* 2013;2(11):906–15.
- [183] Boku S, et al. Tricyclic antidepressant amitriptyline indirectly increases the proliferation of adult dentate gyrus-derived neural precursors: an involvement of astrocytes. *PLoS One* 2013;8(11):e79371.
- [184] Rinderknecht E, Humbel RE. Polypeptides with nonsuppressible insulin-like and cell-growth promoting activities in human serum: isolation, chemical characterization, and some biological properties of forms I and II. *Proc Natl Acad Sci USA* 1976;73(7):2365–9.
- [185] Werner H, Leroith D. Insulin and insulin-like growth factor receptors in the brain: physiological and pathological aspects. *Eur Neuropsychopharmacol* 2014;1036(1–2):163–72.
- [186] Yarden Y, Ullrich A. Growth factor receptor tyrosine kinases. *Annu Rev Biochem* 1988;57:443–78.
- [187] O'Kusky J, Ye P. Neurodevelopmental effects of insulin-like growth factor signaling. *Front Neuroendocrinol* 2012;33(3):230–51.
- [188] Lehtinen MK, et al. The cerebrospinal fluid provides a proliferative niche for neural progenitor cells. *Neuron* 2011;69(5):893–905.
- [189] Annenkov A. The insulin-like growth factor (IGF) receptor type 1 (IGF1R) as an essential component of the signalling network regulating neurogenesis. *Mol Neurobiol* 2009;40(3):195–215.
- [190] Aberg MA, et al. Peripheral infusion of IGF-I selectively induces neurogenesis in the adult rat hippocampus. *J Neurosci* 2000;20(8):2896–903.
- [191] Hsieh J, et al. IGF-I instructs multipotent adult neural progenitor cells to become oligodendrocytes. *J Cell Biol* 2004;164(1):111–22.
- [192] Yamada M, et al. Differences in survival-promoting effects and intracellular signaling properties of BDNF and IGF-1 in cultured cerebral cortical neurons. *J Neurochem* 2001;78(5):940–51.
- [193] Tropepe V, et al. Distinct neural stem cells proliferate in response to EGF and FGF in the developing mouse telencephalon. *Dev Biol* 1999;208(1):166–88.
- [194] Eiraku M, et al. Self-organized formation of polarized cortical tissues from ESCs and its active manipulation by extrinsic signals. *Cell Stem Cell* 2008;3(5):519–32.
- [195] Correia AS, et al. Fibroblast growth factor-20 increases the yield of midbrain dopaminergic neurons derived from human embryonic stem cells. *Front Neuroanat* 2007;1:4.
- [196] Beck KD, et al. Mesencephalic dopaminergic neurons protected by GDNF from axotomy-induced degeneration in the adult brain. *Nature* 1995;373(6512):339–41.
- [197] Hou JG, Lin LF, Mytilineou C. Glial cell line-derived neurotrophic factor exerts neurotrophic effects on dopaminergic neurons in vitro and promotes their survival and regrowth after damage by 1-methyl-4-phenylpyridinium. *J Neurochem* 1996;66(1):74–82.
- [198] Zhang L, Jiang H, Hu Z. Concentration-dependent effect of nerve growth factor on cell fate determination of neural progenitors. *Stem Cells Dev* 2011;20(10):1723–31.
- [199] Ghosh A, Greenberg ME. Calcium signaling in neurons: molecular mechanisms and cellular consequences. *Science* 1995;268(5208):239–47.

PRUSZAK: 07

Non-Print Items

Abstract

In the developing and adult central nervous system there is a constant need for formation of neuronal networks. Although such networks are established during embryonic development, their full complexity is reached only in the adult. Moreover, brain plasticity and regeneration depend on the constant renewal of neuronal wiring as well as of a supportive glial network. We discuss here the implications of several pertinent examples of NGF, BDNF, NT-3, FGF, GDNF, and IGF in the processes of multipotency maintenance, self-renewal, and differentiation into distinct neural phenotypes. Most of these growth factors function by binding and activating specific receptor tyrosine kinases, which then trigger a cascade of events that specify programs of gene transcription for proliferation, differentiation, cell survival, or apoptosis. Integrative signaling pathways often require activation of more than one receptor type, and some divergent functions exerted by growth and neurotrophic factors can be understood in this context together with the microenvironment in which the activated stem cell is localized.

Keywords: BDNF; Embryonic stem cells; Growth factors; Neural stem cells; Neurotrophic factors; NGF; NT-3; NT-4; p75R; Phenotype specification; Receptor signaling; TrkA; TrkB; TrkC.

Metadata of the chapter that will be visualized online

Chapter Title	Intracellular Calcium Measurements for Functional Characterization of Neuronal Phenotypes
Copyright Year	2015
Copyright Holder	Springer Science+Business Media New York
Author	Family Name Glaser Particle Given Name Talita Suffix Division Department of Biochemistry, Institute of Chemistry Organization University of São Paulo Address Av. Prof. Lineu Prestes 748, São Paulo, Brazil
Author	Family Name Castillo Particle Given Name Ana Regina G. Suffix Division Department of Biochemistry, Institute of Chemistry Organization University of São Paulo Address Av. Prof. Lineu Prestes 748, São Paulo, Brazil
Author	Family Name Oliveira Particle Given Name Ágatha Suffix Division Department of Biochemistry, Institute of Chemistry Organization University of São Paulo Address Av. Prof. Lineu Prestes 748, São Paulo, Brazil
Corresponding Author	Family Name Ulrich Particle Given Name Henning Suffix Division Department of Biochemistry, Institute of Chemistry Organization University of São Paulo Address Av. Prof. Lineu Prestes 748, São Paulo, Brazil Email henning@iq.usp.br
Abstract	The central and peripheral nervous system is built by a network of many different neuronal phenotypes together with glial and other supporting cells. The repertoire of expressed receptors and secreted neurotransmitters and neuromodulators are unique for each single neuron leading to intracellular signaling cascades, many of them

involving intracellular calcium signaling. Here we suggest the use of calcium signaling analysis upon specific agonist application to reliably identify neuronal phenotypes, being important not only for basic science, but also providing a reliable tool for functional characterization of cells prior to transplantation. Calcium imaging provides various cellular information including signaling amplitudes, cell localization, duration, and frequency. Microfluorimetry reveals a signal summarizing the entire population, and its use is indicated for high-throughput screening purposes.

Keywords (separated by '-') Neuron - Differentiation - Stem cell - Calcium signaling - Phenotype - Neuronal receptors

Intracellular Calcium Measurements for Functional Characterization of Neuronal Phenotypes

4

5

Talita Glaser, Ana Regina G. Castillo, Ágatha Oliveira, and Henning Ulrich

6

Abstract

7

The central and peripheral nervous system is built by a network of many different neuronal phenotypes together with glial and other supporting cells. The repertoire of expressed receptors and secreted neurotransmitters and neuromodulators are unique for each single neuron leading to intracellular signaling cascades, many of them involving intracellular calcium signaling. Here we suggest the use of calcium signaling analysis upon specific agonist application to reliably identify neuronal phenotypes, being important not only for basic science, but also providing a reliable tool for functional characterization of cells prior to transplantation. Calcium imaging provides various cellular information including signaling amplitudes, cell localization, duration, and frequency. Microfluorimetry reveals a signal summarizing the entire population, and its use is indicated for high-throughput screening purposes.

8

9

10

11

12

13

14

15

16

Keywords: Neuron, Differentiation, Stem cell, Calcium signaling, Phenotype, Neuronal receptors

17

1 Introduction

18

The number of studies on the mechanisms of neural differentiation of embryonic stem cells (ESC), induced embryonic stem cells (iPSC), and their therapeutic potential in neurobiology, neuropathology, pharmaceutical research, and cellular therapy fields is increasing daily [1]. After establishment of neural lineage commitment of pluripotent ESC in vitro, a variety of differentiation protocols emerged trying to achieve greater efficiency and specificity. The majority of these protocols consist of the spontaneous origination of embryoid bodies (EB) by cultivating ESC in a feeder- and serum-free medium following supplementation with growth factors and other agents that induce neural differentiation [2].

19

20

21

22

23

24

25

26

27

28

29

Aiming at a homogeneous population at the endpoint of differentiation, an important challenge lies in the phenotypic characterization of possible intermediate cell types and neurons. Along differentiation, ESCs lose pluripotent markers while they gain specific lineage markers [3]. These changes can be tracked by immunocytochemistry, flow cytometry, and polymerase chain reaction among other methodological approaches. However, all of these

30

31

32

33

34

35

36

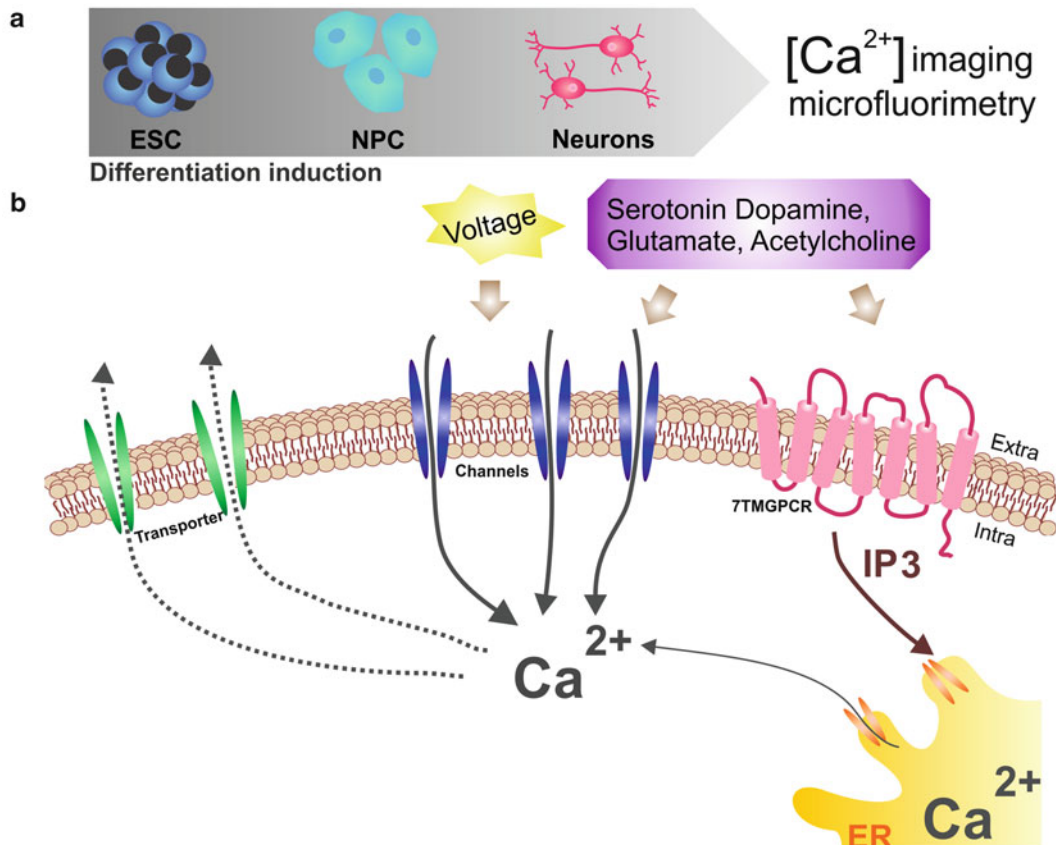


Fig. 1 Neuronal differentiation and calcium signaling in neurons. Depending on the neuronal phenotype obtained during neuronal differentiation, cells may be responsive to one or many neurotransmitters triggering intracellular calcium signaling pathways. (a) After neuronal differentiation induction, cells differentiate into different types of neurons and can be characterized by calcium imaging or calcium microfluorimetry. (b) Voltage-gated calcium channels can be triggered during membrane depolarization resulting in extracellular calcium entry. This can be achieved by adding 60 mM KCl. Furthermore, some neurotransmitters like serotonin, glutamate, acetylcholine, and dopamine can increase intracellular calcium concentration by activating ion channels or seven-transmembrane G protein-coupled receptors, by induction of release of inositol 1,4,5-trisphosphate (IP3) and consequently extrusion of calcium from the endoplasmic reticulum

methods verify the expression of some protein markers without evaluation of functional cellular activity.

Detailed information about the neuron phenotype can be obtained by its functional expression of neurotransmitters and their functional receptors (Fig. 1) using calcium imaging or microfluorimetry for measuring cytosolic calcium concentration during activation of these receptors after applying agonist/stimuli. Functional analysis of receptors confirms viability and functionality of differentiated cells, thus increasing reliability and reproducibility of differentiation protocols.

37
38
39
40
41
42
43
44
45
46

Cellular calcium signaling is a ubiquitous and extremely versatile system, once there are many ways to combine the molecular repertory for creating numerous signals with many temporal, spatial and calcium concentration level patterns [4–6]. At rest, many neurons reveal cytosolic free Ca²⁺ concentration ([Ca²⁺]_i) of 50–100 nM, and upon stimuli these values rise up to 100 times higher [4]. Transient oscillations of intracellular [Ca²⁺]_i, called intracellular calcium transients ($\Delta[\text{Ca}^{2+}]_i$), induce changes on expression and activity of several proteins, triggering many cellular processes including proliferation and differentiation [7]. Neurons have a highly developed calcium signaling system that is involved, among other processes in neurotransmitter release, synaptic transmission, cerebral rhythms, memory, and learning [8, 9].

Patterns of $\Delta[\text{Ca}^{2+}]_i$ change during neuronal differentiation according to timing and to neuronal phenotype in development [10–13]. Functional studies on neural lineages have shown calcium cascade signaling mediated by cholinergic, glutamatergic, serotonergic, dopaminergic, and purinergic receptors [14, 15].

Currently, there are many technologies available for calcium imaging analysis. Since the first appearance of equipment and calcium-binding bioluminescent proteins, development of new approaches in this area allowed detailed investigation of calcium signaling function [15]. The main rationale is to follow [Ca²⁺]_i levels through time using a calcium indicator that emits a fluorescence signal correlated to calcium concentration with an imaging microscope or fluorescence-microplate reader.

In this chapter, we describe briefly a protocol of pan-neural differentiation and two methods for intracellular calcium measurement commonly used for helping to monitor differentiation process of ESCs and final obtained phenotypes.

2 Materials

77

Prepare and store all reagents at 4 °C unless stated differently. All solutions should be prepared using ultrapure water and analytical grade reagents. All reagents and materials must be sterile.

80

2.1 Pan-Neural Differentiation of Feeder-Free Embryonic Stem Cells

2.1.1 Culture of Feeder-Free ES Cells

PBS 1×: Phosphate buffer saline (137 mM NaCl, 10 mM Na₂HPO₄, 2.7 mM KCl, 1.8 mM KH₂PO₄). Dissolve the reagents listed above in water. Adjust the pH to 7.4 with HCl. Dispense the solution into aliquots and sterilize them by autoclaving.

Gelatin from porcine skin solution: 0.2 % gelatin in PBS 1×. pH 7.4. Sterilize by autoclaving and store at 4 °C.

ES medium: Glasgow's modified Eagle medium or Dulbecco's modified Eagle medium high glucose, 15 % fetal bovine serum ES-QUALIFIED tested, 1× non-essential amino acids

86

87

88

89

90

(NEAA), 1 mM sodium pyruvate, 1000 U/ml ESGRO LIF.	91
pH 7.4. Sterilize by filtering through 0.22 µm pore size	92
membranes.	93
<i>Trypsin solution:</i> 0.25 % trypsin 1 mM EDTA (ethylenediaminetetraacetic acid). pH 7.4. Sterilize by filtering with 0.22 µm pore membrane.	94 95 96
<i>EB differentiation medium:</i> Glasgow's modified Eagle medium or Dulbecco's modified Eagle medium high glucose, 20 % fetal bovine serum, 1× NEAA, 1 mM sodium pyruvate. pH 7.4. Sterilize by filtering through 0.22 µm pore membranes.	97 98 99 100
<i>Neurobasal medium:</i> Dulbecco's modified Eagle medium/nutrient mixture F-12, 1 % Bottenstein's N-2 formulation, 100 ng/ml b-FGF.	101 102 103 106
2.2 Calcium Imaging	
<i>2.2.1 Calcium Indicator Incorporation</i>	
<i>Staining buffer:</i> Dulbecco's modified Eagle medium/nutrient mixture F-12 or extracellular medium without magnesium (140 mM NaCl, 3 mM KCl, 1 mM MgCl ₂ , 2 mM CaCl ₂ , 10 mM HEPES (4-(2-hydroxyethyl)-1-piperazineethanesulfonic acid), 10 mM glucose, pH 7.4), 5 µM Fluo-3 AM, 10 µl Me SO, 0.1 % pluronic surfactant F-127.	107 108 109 110 111 2 112
<i>2.2.2 Recording Data</i>	
<i>Time-lapse buffer:</i> Dulbecco's modified Eagle medium/nutrient mixture F-12.	114 115 116
<i>2.2.3 Equipment</i>	
<i>Hardware:</i> Inverted Research Microscope ECLIPSE-TiS (Nikon, Melville, NY) equipped with a 14 bit high-resolution CCD camera CoolSNAP HQ2 (Photometrics, Tucson, AZ).	117 118 119
<i>Software:</i> NIS-Elements Advanced Research (Nikon).	120 123
2.3 Microfluorimetry	
<i>2.3.1 Calcium Indicator Incorporation</i>	
<i>Probenecid Stock Solution:</i> Probenecid, 1 N NaOH, "Component B" buffer from FlexStation Calcium Assay Kit (Molecular Devices Corp.). To prepare 250 mM probenecid stock solution, mix properly until completely dissolved 77 mg probenecid with 500 µl of 1 N NaOH. Add 500 µl of "Component B" buffer from "FlexStation Calcium Assay Kit." Mix it properly again.	124 125 126 127 128 129 130
<i>Component B buffer with probenecid:</i> 1000 µl 250 mM Probenecid stock solution, "Component B" buffer of the FlexStation Calcium Assay Kit (Molecular Devices Corp.). Mix properly. This buffer can be used to make both your dye loading buffer and agonist dilutions.	131 132 133 134 135
<i>Staining buffer:</i> FlexStation Calcium 4 Assay Kit (Molecular Devices Corp.) containing 2.5 mM probenecid.	136 137
<i>Dish:</i> 96-well black microplate with clear bottom.	138
	139

2.3.2 Equipment	<i>Hardware:</i> FlexStation 3 (Molecular devices Corp.).	140
	<i>Software:</i> Softmax Pro (Molecular devices Corp.).	141
		142

3 Methods		143
------------------	--	-----

3.1 Pan-Neural Differentiation of Feeder-Free Embryonic Stem Cells	All reagents and materials must be sterile.	144
---	---	-----

3.1.1 Culture of Feeder-Free ES Cells	E14tg2a cell line: 129/Ola-derived HPRT-negative ES cells (Note 1).	145
		146

- *Gelatin coating* 147

All dishes, flasks, and plates should be gelatinized before use, if not otherwise mentioned. 148

1. Add gelatin from porcine skin solution. 150

2. Keep for 10 min at room temperature. 151

3. Aspirate thoroughly. 152

- *Splitting cells* 153

2 days after seeding with ES medium or when cells reach 80 % density confluence. 154

1. Aspirate medium and wash cells with PBS 1× once (Fig. 2a). 156

2. Add 1 ml trypsin solution. 157

3. Incubate at 37 °C for 3 min. 158

4. Add 3 ml of ES medium. 159

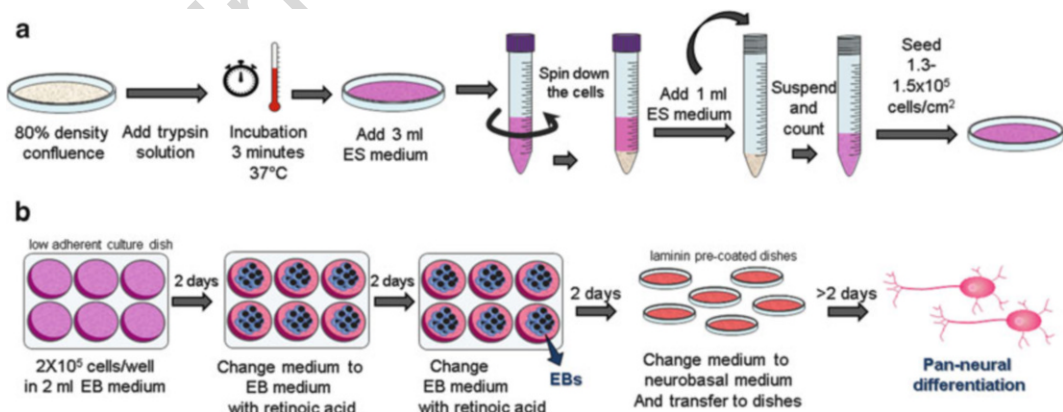


Fig. 2 Illustration of the embryonic stem cell maintenance (a) and neuronal differentiation (b) protocols (Note 11)

t.1 **Table 1**
Instructions for seeding cells

t.2	Seeding cell numbers	Flask/dish size	Medium volume
t.3	$3\text{--}4 \times 10^5$	25 cm ² small flask	5 ml medium
t.4	1×10^6	75 cm ² middle flask	15 ml medium
t.5	2×10^6	150 cm ² large flask	25 ml medium
t.6	1×10^5	60 mm dish	4 ml medium
t.7	5×10^5	90 mm dish	10 ml medium

5. Spin down the cells. 160
6. Discard the supernadant and suspend cells in 1 ml ES medium. 161
162
7. Count the number of cells. 163
8. Seed $1.3\text{--}1.5 \times 10^5$ cells/cm² (Table 1). 164
9. Number of cells usually reach 8–10 times higher than seeded ones. 165
166
- *Differentiation* 167
1. Seed $\sim 2 \times 10^5$ cells/well in 2 ml EB differentiation medium using 6-well low adherent culture dishes for induction of EB formation (Fig. 2b). 168
169
170
2. After 2 days of floating culture, sediment cells in a 15 ml conical tube, replace EB differentiation medium, and add 5 µM all-trans retinoic acid previously dissolved in DMSO (**Notes 2 and 3**). 171
172
173
174
3. After 2 more days of culture repeat **step 2**. 175
4. Following 2 further days sediment cells, replace EB medium by neurobasal medium, and seed EBs into laminin pre-coated dishes (as described below). 176
177
178
5. Replace neurobasal medium each 2 days until. 179[AU1]
6. Neurons are stable for more than 30 days in in vitro culture. 180
- *Laminin coating* 181
1. Add 50 µg/ml laminin to dish, and incubate 37 °C for at least 30 min. 182
183
2. Wash 3× with PBS 1×. 184
3. Dishes can be reused many times. 185
- 186

3.2 Calcium Imaging

3.2.1 Calcium Indicator Incorporation

1. After 8, 16, or 20 days since the first medium change to neurobasal medium (item IV of the above-described differentiation method), incubate EB for 45 min in staining buffer at 37 °C in cell culture incubator (water-saturated atmosphere, 5 % CO₂) (**Note 4**). 187
188
189
190
191

2. Wash cells twice with time lapse buffer and add 2 ml of this time-lapse buffer for subsequent calcium measurements. 192
193
3. Keep them in time-lapse buffer for 20 min to obtain complete deesterification of the acetoximethyl ester group (AM) of the fluorophore. 194
195
196
197

3.2.2 Live Imaging

1. Set parameters at Nis elements AR software for time-lapse measurements at *6D measurement* icon. Adjust to 2 frames/second and select FITC-band-pass filter. 198
199
200

2. Image cells for at least 5 s for basal fluorescence. 201
3. Apply 10× concentrated agonist in 200 µl volume while recording data of Δ[Ca²⁺]_i through changes of emitted fluorescence intensity (F) in sequential images. 202
203
204
4. After cells recover homeostasis (~1 min), apply 5 µM ionomycin (Ca²⁺ ionophore) to record maximum fluorescence intensity (F_{max}). 205
206
207
5. After 30 s, add 30 mM EGTA to measure minimum fluorescence intensity (F_{min}) (**Note 5**). 208
209
210

3.2.3 Data Analysis

1. First define elliptical regions of interest (ROI) for at least 40 cells (**Note 6**). 211
212
2. Set an ROI upon a region without cells and set as background ROI. 213
214
3. Measure the intensity of all ROIs. 215
4. Export numeric data from Nis elements program to the Excel sheet program. 216
217
5. Normalize raw data by subtracting background emitted fluorescence intensity (F_B). 218
219
6. Calculate F (peak height following stimulation by agonist solution) and mean values of F₀, F_{max}, and F_{min} for each cell. 220
221
7. Ratio F/F₀ is used for defining cells responding to agonist application. Values higher than 1.5 are considered as significant increase of Δ[Ca²⁺]_i (**Note 7**). 222
223
224
8. Use the following equation for calculating [Ca²⁺]_i peak values and kinetics: 225
226

$$[\text{Ca}^{2+}]_i = K_d \cdot \frac{[F - F_{\min}]}{[F_{\max} - F]}$$

9. where F_{min} is the fluorescence intensity of the indicator in the absence of calcium, F_{max} is the fluorescence of the calcium 227
228

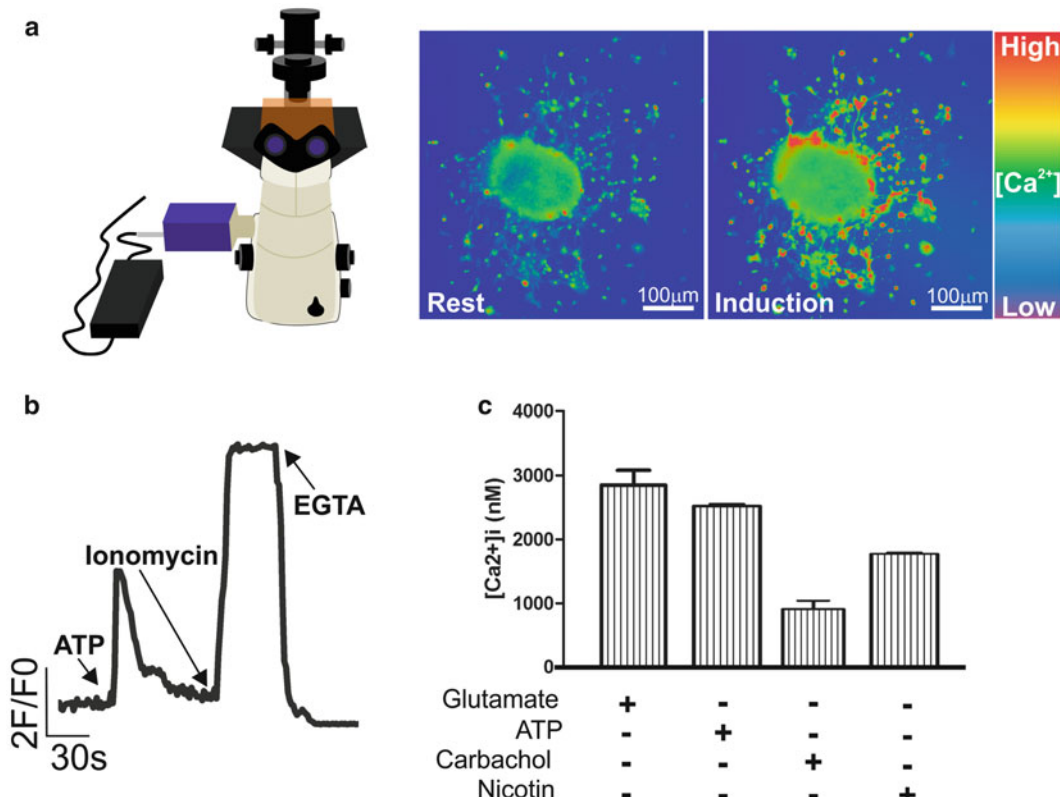


Fig. 3 Calcium imaging data plotting examples. After recording fluorescence intensities corresponding to $[Ca^{2+}]_i$, data can be usually plotted as density scale with rainbow mask (a), single-cellular normalized fluorescence traces (b), or amplitude graphs (c)

saturated indicator, and F is the emitted fluorescence intensity during $\Delta[Ca^{2+}]_i$. K_d is the dissociation constant for Fluo3 AM- Ca^{2+} binding, which is 325 nM (**Note 8**).

10. Another way is to plot variations in $[Ca^{2+}]_i$ as function of time relative to the basal (F_0 , $[Ca^{2+}]_i$ of resting cells) $[Ca^{2+}]$ determined from independent measurements (Fig. 3 and **Note 9**).

3.3 Calcium Microfluorimetry (FlexStation 3)

3.3.1 Calcium Indicator Incorporation

1. Remove the “FLIPR Calcium 4 Assay Dye” from the $-20^{\circ}C$ freezer and allow equilibrating for about 5 min to room temperature.

2. Add 10 ml of the Component B buffer with Probenecid to the “FLIPR Calcium 4 Assay Dye” vial and mix up and down several times until dissolved (It should look like cherry Kool-Aid).

3. Remove the cell plate from incubator. Using a multichannel pipettor, add 100 μl staining buffer to each well of the plate that already contains 100 μl of cell culture medium. Incubate for 1 h at $37^{\circ}C$.

229

230

231

232

233

234

235

236

237

238

239

240

241

242

243

244

245

246

Table 2
Parameter settings for calcium measurements using FlexStation 3
(molecular devices)

Excitation wavelength (nm)	485	t.2
Emission wavelength (nm)	525	t.3
Emission cutoff	515	t.4
Sensitivity readings	6	t.5
Sensitivity PMT	High	t.6
Run time	60 s	t.7
Run interval	~1,52 s	t.8
Pipettor height	225 µl	t.9
Sample volume	50 µl	t.10
Dispense speed	1	t.11

- 4. Meanwhile, prepare the compound dilution plate with the desired agonists and concentrations. 247
248
- 5. Make up a compound plate by applying the agonists on 96-well V-bottom plate with a multichannel pipettor (**Note 10**). 249
250
- 6. Set up the FlexStation equipment with the proper parameters and template info (Table 2). 251
252
- 7. Once the assay plate has incubated for an hour, place it in the FlexStation and click “Read.” 253
254
255

- 3.3.2 *Setting Parameters* Set parameters (Table 2). 256
257
- 3.3.3 *Data Analysis*
- 1. First in the reduction icon set kinetic reduction to Max-Min, and at baseline options choose % baseline. 258
259
 - 2. Then in the display icon choose reduced and display number. 260
 - 3. Select the plate and export to excel spreadsheet. 261
262

4 Notes 263

- 1. E14tg2a: 129/Ola-derived HPRT-negative ES cells. HPRT-minigene can be used as an additional option of selectable marker by combination with HAT selection. 264
265
266
- 2. Do not exceed 1 % of DMSO at final concentration, or cells may die. 267
268
- 3. EBs are already observed 2 days after the seeding. 269

4. Increasing signal to noise ratio: 30 min is enough to incorporate the dye for optimal calcium live imaging. You can diminished or increase this time according to the level of background imaging brightness. 270
271
272
273
5. For better results, keep cells dish in an isolated chamber at 37 °C, during the imaging acquisition. 274
275
6. The ROI must fit all cells and located upon brightest signal location. 276
277
7. It is important to recognize that the calcium-binding and spectroscopic properties of fluorescent indicators can vary quite markedly in cellular environments. For example, fluo-3 fluorescence in the nucleoplasm has been found to be twice that in the cytoplasm under conditions of normalized indicator and Ca²⁺ concentration. In addition, BAPTA-based indicators such as fluo-3 and fluo-4 bind various heavy metal cations. 278
279
280
281
282
283
284
8. To use this analysis the equipment should be calibrated using Molecular Probes' Calcium Calibration Buffer kit. 285
286
9. No calibration with known [Ca²⁺] solutions is needed. 287
10. Concentration must be 5× higher than the final desired concentration. 288
289
11. Some complementary studies direct differentiation to one cell type like dopaminergic, glutamatergic, motor, serotonergic, or GABAergic neurons [16–21]. 290
291
292

Acknowledgments

293

This work was supported by research grants from Brazilian funding agencies São Paulo Research Foundation (FAPESP), National Council for Scientific and Technological Development (CNPq), and Provost's Office for Research of the University of São Paulo, Grant number: 2011.1.9333.1.3 (NAPNA-USP), Brazil.

299 References

294

- 295 1. Gaspard N, Vanderhaeghen P (2010) Mechanisms of neural specification from embryonic stem cells. *Curr Opin Neurobiol* 20:37–43
- 296 2. Smith AG (2001) Embryo-derived stem cells: of mice and men. *Annu Rev Cell Dev Biol* 17:435–462
- 297 3. Calloni R, Cordero EA, Henriques JA et al (2013) Reviewing and updating the major molecular markers for stem cells. *Stem Cells Dev* 22:1455–1476
- 298
- 301 4. Berridge MJ, Lipp P, Bootman MD (2000) The versatility and universality of calcium signalling. *Nat Rev Mol Cell Biol* 1:11–21
- 302 5. Vanaman T, Carafoli E (2012) Introduction to thematic minireview series on calcium. *J Biol Chem* 287:31623
- 303 6. Parekh AB (2011) Decoding cytosolic Ca²⁺ oscillations. *Trends Biochem Sci* 36:78–87
- 304 7. Cheng H, Lederer WJ (2008) Calcium sparks. *Physiol Rev* 88:1491–1545
- 305 311
312
313
- 306 314
315
316
- 307 317
318
- 308 319
320

Ca^{2+} Measurements for Neuronal Phenotyping

- 321 8. Berridge MJ (2006) Calcium microdomains: 349
322 organization and function. *Cell Calcium* 350
323 40:405–412 351
324 9. Buonanno A, Fields RD (1999) Gene regulation 352
325 by patterned electrical activity during neural 353
326 and skeletal muscle development. *Curr Opin* 354
327 *Neurobiol* 9:110–120 355
328 10. Lin JH, Takano T, Arcuino G et al (2007) 356
329 Purinergic signaling regulates neural progenitor 357
330 cell expansion and neurogenesis. *Dev Biol* 360
331 302:356–366 361
332 11. Spitzer NC, Lautermilch NJ, Smith RD et al 362
333 (2000) Coding of neuronal differentiation by 363
334 calcium transients. *Bioessays* 22:811–817 364
335 12. Gu X, Spitzer NC (1995) Distinct aspects of 365
336 neuronal differentiation encoded by frequency 366
337 of spontaneous Ca^{2+} transients. *Nature* 367
338 375:784–787 368
339 13. Simpson PB, Challiss RA, Nahorski SR (1995) 369
340 Neuronal Ca^{2+} stores: activation and function. 370
341 *Trends Neurosci* 18:299–306 371
342 14. Strubing C, Ahnert-Hilger G, Shan J et al 372
343 (1995) Differentiation of pluripotent embryonic 373
344 stem cells into the neuronal lineage in vitro gives 374
345 rise to mature inhibitory and excitatory neurons. *Mech Dev* 57:969–978 375
346 15. Grienberger C, Konnerth A (2012) Imaging 376
347 calcium in neurons. *Neuron* 73:862–885 376

Author Query

Chapter No.: 271

Query Refs.	Details Required	Author's response
AU1	Please check the sentence "Replace neurobasal medium...." for completeness. ▲	

Uncorrected Proof